W. A. Davis, VA Tech

NATIONAL ACADEMIES OF SCIENCES AND ENGINEERING

NATIONAL RESEARCH COUNCIL

of the

UNITED STATES OF AMERICA

UNITED STATES NATIONAL COMMITTEE

International Union of Radio Science

National Radio Science Meeting

4–8 January 1999

Sponsored by USNC/URSI

University of Colorado
Boulder, Colorado
U.S.A.

NOTE:

Programs and Abstracts of the USNC/URSI Meetings are available from:

USNC/URSI
National Academy of Sciences
2101 Constitution Avenue, N.W.
Washington, DC 20418

at $5 for 1983–1998 meetings.

The full papers are not published in any collected format; requests for them should be addressed to the authors who may have them published on their own initiative. Please note that these meetings are national. They are not organized by the International Union, nor are the programs available from the International Secretariat.

MEMBERSHIP

United States National Committee
INTERNATIONAL UNION OF RADIO SCIENCE

Chair:	Susan K. Avery*
Vice Chair:	vacant
Secretary:	Gary Brown
Immediate Past Chair:	David C. Chang*

Members Representing Societies, Groups, and Institutes:

American Astronomical Society	T.J. Phillips
American Geophysical Union	George C. Reid
American Meteorological Society	vacant
IEEE Geosciences and Remote Sensing Society	Roger Lang
IEEE Microwave Theory and Techniques Society	Arthur A. Oliner

Members-at-Large:

Albin Gasiewski
John D. Mathews
Ronald Pogorzelski
Fritz Schuermeyer
W. Ross Stone
Jill Tarter
Roland T. Tsunoda
Edgeworth R. Westwater

Chairs of the USNC/URSI Commissions:

Commission A	John D. Norgard
Commission B	Donald R. Wilton
Commission C	David Thomson
Commission D	Robert Mattauch
Commission E	David J. Cohen
Commission F	Wolfhard Vogel
Commission G	Lewis Duncan
Commission H	Umran Inan
Commission J	Donald Backer
Commission K	James C. Lin

Officers, Chairs and Vice Chairs of Commissions of URSI residing in the United States:

President	Thomas B. A. Senior
Chair, Commission A	Motohisa Kanda
Vice Chair, Commission B	Chalmers Butler
Chair, Commission G	B. W. Reinisch
Vice Chair, Commission K	J. C. Lin

* Member of USNC/URSI Executive Committee

DESCRIPTION OF THE INTERNATIONAL UNION OF RADIO SCIENCE

The International Union of Radio Science is one of the world scientific unions organized under the International Council of Scientific Unions (ICSU). It is commonly designated as URSI (from its French name, Union Radio Scientifique Internationale). Its aims are (1) to promote the scientific study of radio communications, (2) to aid and organize radio research requiring cooperation on an international scale and to encourage the discussion and publication of the results, (3) to facilitate agreement upon common methods of measurement and the standardization of measuring instruments, and (4) to stimulate and to coordinate studies of the scientific aspects of telecommunications using electromagnetic waves, guided and unguided. The International Union itself is an organizational framework to aid in promoting these objectives. The actual technical work is largely done by the National Committee in the various countries.

The new officers of the International Union are:

President:	Thomas B. A. Senior (U.S.A.)
Past President:	Pierre Bauer (France)
Vice Presidents:	Peter J. B. Clarricoats (UK) Hiroshi Matsumoto (Japan) Joseph Shapira (Israel) Maria A. Stuchly (Canada)
Secretary-General:	Paul Lagasse (Belgium)
Assistant Secretary-General:	Peter Van Daele
Administrative Secretary:	Inge Heleu

The Secretary-General's office and the headquarters of the organization are located at Avenue Albert Lancaster, 32, B-1180 Brussels, Belgium. The Union is supported by contributions (dues) from 38 member countries. Additional funds for symposia and other scientific activities of the Union are provided by ICSU from contributions received for this purpose from UNESCO.

The international Union, as of the XXIVth General Assembly held in Kyoto, Japan, August 25–September 3, 1993, has ten bodies called Commissions for centralizing studies in the principal technical fields.

Every three years the International Union holds a meeting called the General Assembly The next is the XXVIth, to be held in August, 1999, in Toronto, Canada. The Secretariat prepares and distributes the Proceedings of the General Assemblies. The International Union

arranges international symposia on specific subjects pertaining to the work of one or several Commissions and also cooperates with other Unions in international symposia on subjects of joint interest.

Radio is unique among the fields of scientific work in having a specific adaptability to large-scale international research programs, since many of the phenomena that must be studied are worldwide in extent and yet are in a measure subject to control by experimenters. Exploration of space and the extension of scientific observations to the space environment are dependent on radio for their research. One branch, radio astronomy, involves cosmic phenomena. URSI thus has a distinct field of usefulness in furnishing a meeting ground for the numerous workers in the manifold aspects of radio research; its meetings and committee activities furnish valuable means of promoting research through exchange of ideas.

Steering Committee:

D. Cook	P. L. Jensen	D. Thorsen
R. Frehlich	J. McKie	

Technical Program Committee:

S.K. Avery, Chairperson

D. Backer	R. Frehlich	M. Kanda	D. Thorsen
G. Brown	R. Gardner	J. Lin	E. Westwater
L. Duncan	U. Inan	A. Mickelson	D. Wilton

Session A1, 1015-Mon., ECCR1B40
IDENTIFICATION OF BURIED TARGETS
Chairperson: Carl Baum (AFRL/DEHP)

A1-1
1020

BURIED ORDNANCE CLASSIFICATION USING POLARIZATIONS AND RESONANCES

Chi-Chih Chen
The ElectroScience Laboratory
1320 Kinnear Road
Columbus, OH 43212

The scattered fields from a buried unexploded ordnance (UXO) contain linear polarization and late-time resonance features. In the past, the resonance feature has been extracted from ground penetrating radar (GPR) to help classifying UXO's with reasonable success. The polarity feature, on the other hand, has not been fully utilized with GPR. It was found that the clutter caused by the scattering from inhomogeneous media and surface roughness were major problems in both UXO detection and classification. Since this type of clutter has quit different polarization behavior from most UXO's, it is possible to further improve signal to clutter and signal to noise ratios by utilizing multiple polarization data.

A new UXO classification approach proposed here is to collect both copolarization and cross-polarization data at various orientations by rotating the antenna sitting on top of a suspicious spot pre-selected from the field survey results. A good tool to locate suspicious spots has been found to be the magnetic sensor. Special processing technique is applied to extract the polarization and resonance features from this multiple-orientation data. Significant improvements in signal to clutter and signal to noise ratios were achieved. This also provides improved the radar sensitivity and the accuracy of the extracted resonances. A certain type of surface roughness, such as those caused by plowing or tire tracks, also creates linearly polarized scattered fields. But this type of scattering would not have resonant components. Therefore, the proposed new radar measurement and processing technique intends to utilize both linear polarity and resonance feature to achieve a better UXO classification technique.

A1-2
1040

MEASURES OF CROSS-POLARIZATION FOR SYMMETRICAL TARGETS

Carl E. Baum
Air Force Research Laboratory
AFRL/DEHP Bldg 909
3550 Aberdeen Avenue SE
Kirtland AFB NM 87117-5776

A radar signature of interest for certain symmetrical targets on or near (under) the earth surface is a null in the cross-polarization in the usual *h, v* measures of this cross-polarization in both narrowband and broadband/ transient contexts. These involve angles in the eigenvectors of the backscattering dyadic as well as norms of this dyadic and the cross-polarization part.

The measure of cross polarization in *h, v* coordinates is somewhat different for narrowband and broadband applications. In narrowband applications one can diagonalize $\overleftrightarrow{\Lambda}_b$ to find appropriate angles, except in the case of rotational scatterers. In broadband applications such angles are not appropriate except in cases where they do not rotate with frequency/ time. The use of norms, such as 2-norm and root span, can be applied in both domains.

The norms of the scattering dyadic which we have used are roll invariant. In the numerator of the norm-based measures we have a norm of $\widetilde{\Lambda}_{b_{h,v}}$. There can be errors in our estimation of the $\vec{1}_h$ direction. In particular the local earth near the target of interest may not be perfectly horizontal. In such a case it may be preferable to define horizontal by the earth near the target. This corresponds to a rotation of the *h, v* coordinates. In such a rotation one may observe a reduction of the cross-polarization. Of course, this applies for real rotation angles. If there is a complex angle ($\widetilde{\psi}_s$) in the scattering, then this comes from some other source (including a non-symmetrical target). There is also the problem of noise in the data.

A1-3
1100

WIDEBAND SYNTHETIC APERTURE RADAR FOR DETECTION OF BURIED MINES AND UXO

L. Carin, A. Sullivan and N. Geng
Department of Electrical and Computer Engineering
Duke University
Box 90291
Durham, NC 27708-0291
Email: lcarin@ee.duke.edu

M. Ressler and B. Merchant
Army Research Laboratory
AMSRL-SE-RU
2800 Powder Mill Road
Adelphi, Maryland 20783

The method of moments (MoM) is used to model three-dimensional scattering from unexploded ordnance (UXO) and mines buried arbitrarily in a layered soil environment. For the target depths of interest for buried UXO, the soil layering can become an important issue. The layered-medium Green's function is evaluated rigorously via the method of complex images, this allowing rigorous and efficient analysis of the ultra-wideband (UWB) problems of interest here. The results of the numerical modeling are compared with measurements taken with the Army Research Laboratory (ARL) synthetic aperture radar (SAR) system, which is implemented by placing four antennas atop a boom lift (the system is termed a "BoomSAR"). UWB BoomSAR data is collected at the Yuma Proving Ground (Yuma, AZ, USA) and at Eglin Air Force Base (FL, USA). The measurements are compared with the theoretical predictions, as a function of polarization and frequency.

After validating the theory, we use our theoretical expectations - as a function of target orientation, frequency, polarization and soil type - to build a UXO- and mine-detection algorithm for wide-area SAR surveillance. The algorithm is based on a Bayesian paradigm, in which we utilize rigorous models for the electromagnetic scattering from buried mines and UXO, with the nuisance parameters (target depth, orientation, and soil properties) handled via a statistical framework. In particular, we utilize a priori information to impose probability density functions on these parameters. Algorithm performance is quantified through consideration of the aforementioned Yuma Proving Ground and Eglin Air Force Base data base.

A1-4
1120

Modifications to the U. S. Army's Pulse-Induction Metal Detector (the AN/PSS-12) To Facilitate the Reduction of False Alarms Through Magnetic Singularity Identification (MSI)

L. S. Riggs, Jon E. Mooney, Larry Lowe, and Tom Barnett
Electrical Engineering Department 200 Broun Hall
Auburn University, Alabama

Low frequency scattering from permeable and highly conducting objects is characterized by natural frequencies that are negative and real. Equivalently, the time domain response is characterized by a sum of weighted exponentials. Unique correspondence between an object and its singularities forms the basis for identification and therefore clutter rejection. Aptly enough, the term Magnetic Singularity Identification (MSI) has been applied to techniques employing this identification methodology.

The authors have modified the U. S. Army's AN/PSS-12 hand-held metal detector so that the time domain signal available at the output of the receive coil can be captured and stored on a laptop computer. We show that the response of pule-induction metal detectors, like the AN/PSS-12, consist of two components; one due to the direct coupled signal from the transmit coil, and the other due to coupling from the metallic object. By proper design, the direct-coupled response can be made to decay rapidly enough so that, after some brief delay, only the object response will remain. As mentioned above, the decay rate of the object only response can be used as a means to discriminate among metallic objects.

Field experiments with our modified AN/PSS-12 will be described. Time domain data was collected with the sensor at Fort A. P. Hill Virginia over a grid of buried objects – some mines and some clutter. Decay rates extracted from the mine and clutter sets will be presented. Data was also collected over an x-y grid centered on the object. Since man made objects like mines usually exhibit symmetry, one might expect that the energy in the response as a function of position would be more symmetrical for mines than for clutter. We will examine the validity of this hypothesis. Other types of symmetry that may lead to reductions in false alarms will also be discussed.

A1-5
1140

Simulants (Decoys) for Low Metallic Content Mines Theory and Experimental Results

L. S. Riggs, Larry Lowe, Jon E. Mooney, and Tom Barnett
Electrical Engineering Department 200 Broun Hall
Auburn University, Alabama

A number of research teams in the U.S. and throughout the world are devoting substantial resources toward the goal of solving the ubiquitous and formidable landmine and unexploded ordnance (UXO) problem. The arsenal used to attack the problem includes electromagnetic, acoustic, chemical, biological, and nuclear based sensors. Electromagnetic based techniques may be further subdivided into metal detectors, ground penetrating radar (GPR), and infrared sensors (IR). Improvements in technology areas can only be assessed through objective testing leading to a requirement for standard targets.

This paper describes the development of standard test targets for metal detectors. Two sets of simulnat mines (SIMs) were manufactured: one made from a collection of small metal parts and a complementary set made from simple short-circuited loops of copper wire referred to as Inscoils. Each set of SIMs has seven elements, and state-of-the-art metal detectors can detect the lowest level member of the set at an average distance of around 4 cm and the highest level member at a distance of 20 cm.

A theory of simulants will be presented that is based on a simple circuit model for a metal detector. The circuit model is used to develop a transfer function between transmit and receive coil currents taking into account magnetic field coupling due to eddy currents excited in a nearby metallic object. We show that the step response is composed of two exponentially decaying terms. The decay rate of one term is fixed by receive coil parameters, and the other by metallic object parameters. The theory shows that a good simulant must have the same decay rate as the mine and should couple to the transmit and receive coil of the metal detector in the same way the mine does. A simple wire-loop simulant (Inscoil) is suggested and enjoys the property that, to first order, its decay rate and mutual coupling can be independently controlled. We show that the decay rate of the Inscoil depends on conductivity and wire diameter (gauge) while the mutual coupling depends on loop radius.

An experimental test apparatus is described that can be used to measure the pusle-induction signature of metallic objects. The equipment is used to design simulants by first recording the response of an arbitrary metallic object of interest (perhaps a mine). Then, the response of a candidate simulant is measured and compared to the response of the arbitrary metallic object until a match is achieved. Total energy, computed from the time-domain response, can be used as an alternative means of comparison and to rank the detectability of a set of metallic objects.

B/F1-1
0900

BACKSCATTER FROM MATURE FORESTS: UHF ATTENUATION AND SURFACE SCATTER EFFECTS

Roger H. Lang
The George Washington University
Washington, DC 20052
David M. Le Vine
NASA Goddard Space Flight Center
Greenbelt, MD 20771

Forest backscatter models focused on environmental remote sensing have been used to predict radar returns from forests at specific frequencies. These frequencies have been dictated to a large extent by aircraft and satellite system requirements. There exist large spectral regions between these discrete frequencies for which forest backscatter properties remain unexplored. It is the purpose of this paper to examine backscatter from mature forests over the UHF band, i.e., frequencies from 300 to 3000 MHz. The influence of forest attenuation and rough surface scatter on backscatter returns will be examined over the whole frequency band.

The discrete scatter model previously employed by the authors will be used in this study. Within this model tree trunks, branches and needles (leaves) are represented by a statistical distribution of cylinders (discs) with prescribed orientation statistics. A Distorted Born approach is used to calculate the backscatter taking coherent interactions between the scatterers and the ground into account. The resultant backscatter is represented in terms of direct or volume scatter from the tree components, trunk/branch interaction with the average ground surface, trunk interaction with the ground surface fluctuations and incoherent rough surface scatter. Model parameters will be obtained from ground truth measurements made at the Howland forest in Maine during the summers of 1989 and 1990. This data collection effort was closely coordinated with JPL AIRSAR measurements made at 440 and 1,250 MHz. These radar measurements will be compared with the model predictions.

B/F1-2
0920

A SIMPLE CONVOLUTIONAL MODEL FOR INCOHERENT PULSE SCATTERING FROM A VEGETATED ROUGH SURFACE

B. A. Davis* G. S. Brown
Electromagnetic Interactions Laboratory
Bradley Department of Electrical and Computer Engineering
340 Whittemore Hall, Virginia Tech
Blacksburg, VA 24061

When studying scattering from the combination of a foliage layer above a rough surface, one must deal with the scattering from the foliage, the rough surface, and the interaction between the two. Although the simulation of scattering from the foliage has been approached using many diverse methods, its primary implementation has been through radiative transfer. Historically, the level of detail encompassed within the radiative transfer models ranges from the use of a simple bulk scattering pattern to individual scattering patterns representing branches, twigs and various leaf shapes. In this study, we have chosen the former level detail in order to ensure the easy incorporation of measured data. The simulation of scattering from rough surfaces also has a large variety of implementations; again we choose a simple model.

Under the assumption of independently scattering objects and scattering from rough surfaces, it is possible to convert single-frequency models of the individual scattering cross sections (for the discrete objects) and the scattering cross section per unit area (for the extended surface) into models for the incoherent time-dependent average scattered waveform produced under pulse illumination. We have used this impulse response approach to characterize the return from a volume of vegetation and from a rough surface. In addition, the present implementation includes models of sufficient simplicity that the returned power waveform from both the surface and volume can be written in a convolutional form. This permits the rapid and efficient evaluation of the waveform using the FFT. Although the formulation of the model may be obtained through single scatter theory, the radiative transfer theory has been used to construct this model.

For strongly interacting individual scatterers, this impulse response model is not usually possible, the reason being that it is not sufficient to know that the scatterer is in a study volume because its location within the volume must also be known. Additional, more easily quantifiable restrictions include assumptions of a narrow-band signal and a narrow-beamwidth antenna pattern. Finally, implicit in this calculation is the assumption that there are no significant multiple interactions between the rough surface and the volume scattering components. This interaction as been studied to some extent and some estimates of when tis assumption is valid have been obtained.

Sample waveform results will be shown and some discussion of the separation of volume (foliage) and surface returns will be presented.

B/F1-3
0940

MODELING BACKSCATTERING FROM OBJECTS HIDDEN IN WOODS

Guoqing Sun[1] and K. Jon Ranson[2]

[1] Department of Geography, University of Maryland, College Park, MD, 20742, USA, Tel: (301)28602485, E-mail: guoqing@aspen.gsfc.nasa.gov
[2] Biospheric Science Branch, Code 923, Goddard Space Flight Center, Greenbelt, MD 20771,USA

ABSTRACT

A 3D radar backscatter model (Sun and Ranson, *IEEE TGRS*, 33, 372-382) was used in this study to model backscattering from objects hidden in a forest stand. Forest stem maps, which consist of position, species, dbh (diameter at breast height) of every trees, of a 150m by 200m area in Maine was used as the canopy structure to parameterize the radar backscatter model.

Figure 1 shows the simulated HH radar images of the test site with several hidden objects. Radar incidence angle is 45°. The pixel size of a) is one meter and b) is 12 meters, similar to the 4-look AIRSAR data. Upper-left image shows the positions of hidden objects - the two crosses at left and two crosses at right are 8-feet corner reflectors. The other two spots both have four metal top-hat reflectors (radius of 0.5 m and height 1 meter). Upper-right image is C band, lower-left is L band and Lower-right is P band. All are HH polarization. The hidden objects are not very distinct in the low-resolution images even though speckle does not exist in these simulated images.

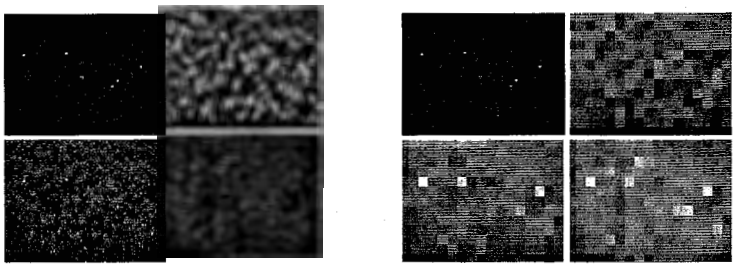

a) b)

Figure 1. Simulated HH radar images of a forest stand with several hidden objects.

B/F1-4
1000

MEASUREMENT AND MODELLING OF PROPAGATION OF MILLIMETRIC WAVES THROUGH VEGETATION.

A. Seville.
Radio Communications Research Unit,
Rutherford Appleton Laboratory,
Chilton, Didcot, U.K.

The use of the 38 GHz band for line of sight links between personal communications network base stations and the proposal of the Millimetrewave Video Distribution Systems at 42 GHz within the UK has led to a requirement for a knowledge of the propagation effects at millimetric frequencies. For the MVDS application in particular, where the signal is broadcast in an urban, suburban or rural region, the problem of attenuation by propagation through vegetation arises. A programme of study has been undertaken by the Radio Communications Research Unit to investigate such effects and this paper is intended to give an overview of these studies, and to present results of the measurements and modelling.

Measurements have been made of the attenuation of a 38GHz signal through trees of increasing depth, for the case of the trees in and out of leaf. These results have been compared with those presented by others at other frequencies (F. K. Schwering et al, *IEEE Trans. Geoscience and Remote Sensing*, 26, No. 3, 1978), (R. B. L. Stephens, and M. O. Al-Nuaimi, *Elec. Letters,* 31, No. 20, 1995). From these measurements a simple empirical model has been derived for the attenuation as a function of vegetation depth, frequency and the extent of the vegetation illuminated. A comparison of the modelled attenuation with that given from measured results from two sites at 38GHz is shown below.

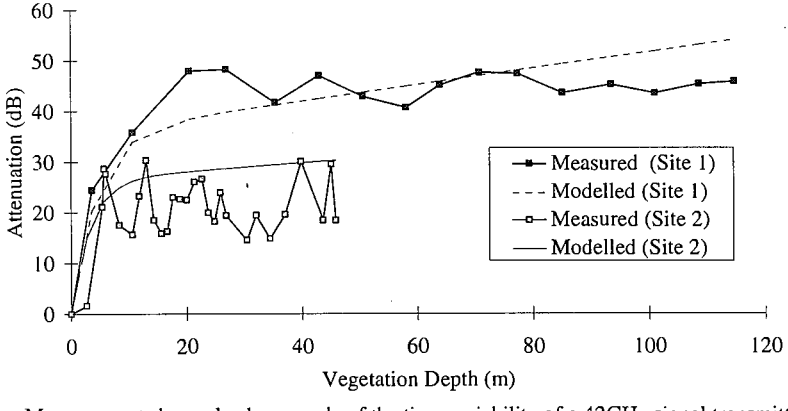

Measurements have also been made of the time variability of a 42GHz signal transmitted through vegetation, in different wind conditions. These effects may have a drastic influence on the feasibility of providing a service to homes in the presence of trees. For example it is relatively simple to conceive of locations where the mean signal is well within the system margin, but the short term variability due to scattering within the trees is sufficient to knock out the service for significant periods of time. In order to investigate these scattering mechanisms, attenuation measurements were made through three small trees in an anechoic. The trees were placed on a turntable, and the field propagated through them measured as they were rotated. The transmit-receive system was a vector network analyser, enabling the received field to be measured from 35-40GHz.

B/F1-5
1040

WIDEBAND SCATTERING FROM TREE TRUNKS ON SLOPPED TERRAIN

N. Geng
Universitaet Karlsruhe
Institut fuer Hoechstfrequenztechnik und Elektronik
Kaiserstrasse 12
D-76128 Karlsruhe, Germany

A. Sullivan, J. He, and L. Carin
Department of Electrical and Computer Engineering
Duke University
Box 90291
Durham, NC 27708-0291

An important form of clutter encountered in foliage penetrating (FOPEN) synthetic aperture radar (SAR) is produced by dihedral scattering by large tree trunks. While this phenomenon is widely appreciated, there is little detailed information in the literature on the dependence of tree-trunk scattering on polarization, frequency, incidence angle, soil properties, and tree type. Here we perform a detailed study of these issues by employing a rigorous method of moments (MoM) analysis, which accurately accounts for all relevant wave physics. The MoM analysis employs the half-space Green's function, which is evaluated efficiently via the method of complex images.

In addition to considering tree-trunk scattering for flat soil, we address this phenomenon for sloped terrain, the slope complicating the associated dihedral scattering. Our goal is to develop a sound understanding of the underlying phenomenology for such a scattering scenario, for better interpretation of FOPEN SAR imagery as well as for improved development of automatic-target-detection (ATD) algorithms.

Finally, we use our rigorous MoM algorithm to consider wideband scattering from conducting targets concealed behind single and multiple tree trunks. The underlying phenomenology so elucidated is critical for understanding FOPEN SAR imagery as well as for ATD development. The tree trunk will be modeled as a body of revolution (BoR) while the target will be of arbitrary shape. To rigorously account for the interaction between these disparate targets, the target and tree trunk are modeled separately, with interactions handled via an elegant iterative procedure. In addition to yielding very accurate results, this procedure has memory and run-time requirements that are significantly less than required of a brute-force MoM solution. This latter issue is particularly important for the problem of interest here, since the tree trunks and targets are generally electrical large (many wavelengths in dimension).

B/F1-6
1100

FOREST FLOOR CONDITIONS OBSERVED FROM MULTIFREQUENCY SAR AND RADAR BACKSCATTER MODELING

K. Jon Ranson[1] and Guoqing Sun[2]

[1] Biospheric Science Branch, Code 923, Goddard Space Flight Center, Greenbelt, MD 20771,USA, Tel: (301)286-4041, E-mail: jon@taiga.gsfc.nasa.gov
[2] Department of Geography, University of Maryland, College Park, MD, 20742, USA

ABSTRACT

In retrieval of forest parameters from radar images, one of the major concern is the forest floor condition (surface roughness, moisture contents, and understories). These conditions may significantly change the backscattering characteristics of the forest stand. Both forest classification and biomass estimation results were affected by these factors (K. J. Ranson et al., *IEEE TGRS*, 33, 867-876, 1995). The objective of this study is to investigate the wavelength and incidence angle dependence of these factors on radar backscattering by polarimetric radar data analysis and radar backscatter modeling.

SAR images at C, L and P bands over boreal and northern forest areas (Maine, USA and Prince Albert, Canada) with significantly different floor conditions were compared in this study. These include jack pine stands with/without understories and hemlock-spruce stands with dry and snow-melting surfaces. The results from these studies show that due to different forest canopy penetration and relative roughness at different frequencies, the effect of the forest floor condition on radar backscattering is distinct at different radar wavelength/incidence angle configurations.

Radar backscatter models (Sun et al., *IEEE TGRS*, 29, 639-650; Sun and Ranson, *IEEE TGRS*, 33, 372-382) were used in this study to understand the backscatter observed in radar imagery. Forest stem maps, which consist of position, species, dbh of every trees, of a 150m by 200m area in Maine and a 100m by 100m area in Prince Albert were used as the canopy structure to parameterize the radar backscatter models. The modeling results were consistent with the observations from radar imagery.

The results from this study will guide our future projects on forest mapping and physical parameter retrieval from SAR images.

B/F1-7
1120

THE INFORMATION CONTENT OF MULTIBASELINE POLARIMETRIC RADAR INTERFEROMETRY

R. N. Treuhaft*
Jet Propulsion Laboratory, MS 300-227, California Institute of Technology, 4800 Oak Grove Drive, Pasadena, CA 91109
B. E. Law
Dept. of Forest Science, Oregon State University, Corvallis, OR
P. R. Siqueira
Jet Propulsion Laboratory, MS 300-227, Pasadena, CA

Remote sensing of vegetated land surfaces is the estimation of vegetation and surface parameters from some combination of remote sensing observations. This paper presents candidate simple models $\mathbf{M}$ which express multibaseline polarimetric radar interferometric observations in terms of vegetation and surface parameters to be estimated. The estimation of a vector of vegetation and surface parameters, $\vec{V}$ from remote sensing observations $\vec{O}$ can be schematically represented as

$$\vec{V} = \mathbf{M}^{-1}\vec{O} \qquad (1)$$

For fixed-baseline (as opposed to repeat-pass) fully polarimetric interferometry, which will soon be available at C-band on the JPL TOPSAR system (H. A. Zebker et al., *IEEE Trans. Geosc. and Remote Sensing*, **30**, 933-940, 1992), $\vec{O}$ will consist of the interferometric phases and amplitudes, for all polarization combinations at each end of each baseline, along with the usual, zero-baseline radar polarimetry (e.g. W. M. Boerner et al., *IEEE Trans. Ant. and Prop.*, **AP-29**, 262-271, 1981). The quantities estimated in the parameter vector $\vec{V}$ will depend on the model being used to construct $\mathbf{M}$. For example, for scalar (nonpolarimetric) interferometry, for a homogeneous, single-layer, horizontal, randomly-oriented volume model (R. N. Treuhaft et al., *Rad. Sci.*, **31**, 1449-1485, 1996), the elements of $\vec{V}$ are vegetation height, extinction coefficient, and underlying topography; the elements of $\vec{O}$ are the correlation amplitude and phase of one or more baselines at a single polarization. The more extensive $\vec{O}$ of multibaseline polarimetric interferometry enables extraction of much more information, by estimating a more accurate, complete, and realistic $\vec{V}$.

This paper explores the information content of multibaseline polarimetric interferometry by augmenting the randomly-oriented volume model with surface-reflection and oriented-volume returns. The program of the paper will be 1) show the parameter sets for each of the above model augmentations, 2) show that adding zero-baseline polarimetry to single-polarization multibaseline interferometry does not improve parameter estimation performance, 3) show that multibaseline polarimetric interferometry does improve parameter estimation, and 4) show first-generation multibaseline interferometric data taken over central Oregon.

Session E1, 0855-Mon., ECCR155
SPECTRUM MANAGEMENT OF WIDEBAND EMISSIONS
Chairperson: David Cohen (Univ. of Maryland)

E1-1
0900

DESIGN AND APPLICATION OF A BROADBAND INTERFERENCE SOURCE

Robert B. Stafford
Institute for Telecommunication Sciences
Mail Code ITS.S2
U. S. Department of Commerce
325 Broadway
Boulder, CO 80303-3328

A system which can accurately simulate various types of broadband interference waveforms and couple them into a radio receiver is described. This system uses one or more arbitrary waveform generators (AWGs) to supply complex modulating and control waveforms to various combinations of mixers, modulators, and voltage-controlled-oscillators to simulate in a controlled fashion interference sources which may be intermittent in nature or may be difficult to procure in any other way. It is used to evaluate the effects of known sources such as military and commercial radar systems on existing or proposed wireless installations, as well as to evaluate the susceptibility of those installations to future interference threats. The signals produced can be radiated into the target receivers through various different types of transmitting antennas or can be directly coupled to the target system.

This system, which can be reprogrammed in the field if necessary, is currently being used to simulate the waveforms produced by a sophisticated naval radar. In this capacity it produces a frequency hopping spread spectrum signal which covers a 400 MHZ bandwidth in the 3.1 GHz to 3.5 GHz region of the radio spectrum. This signal is phase encoded using derivative phase shift keying and is also pulse width modulated. The system has also been used in interference studies to produce gaussian distributed noise in bandwidths up to 8 MHZ about the GPS L1 frequency (1575.42 MHZ) and to simulate pulsed radar signals in the PCS bands. This paper discusses the design of this system and gives a detailed discussion of the applications mentioned.

E1-2
0920

TIME MODULATED ULTRA-WIDEBAND RADIO MEASUREMENT & SPECTRUM MANAGEMENT ISSUES

Paul Withington
Time Domain Systems
6700 Odyssey Drive
Huntsville, Alabama 35806

Time Domain Corporation has developed an ultra-wideband radio technology. The technology uses sub-nanosecond pulses, noise coded time-hopping, and pulse position modulation to create noise-like signals with bandwidths nearly equal to their "center" frequencies. The spectral characteristics of the signal will be discussed.

Time Domain is incorporating the technology into communications applications. Because the technology achieves very high processing gains, e.g., 50+ dB for a 32 kbps link, the technology can be used to create very high performance in-building and cluttered environment data links. In-building propagation measurements will be presented. Additionally, when a time modulated ultra-wideband link is operational, the radios' clocks are synchronized to better than 40 ps RMS. Thus, extremely high precision ranging measurements are possible.

Time Domain is also incorporating the technology into radar applications where the technology's high resolution at low operating frequencies allows tomographic imaging of buildings. Some images will be presented.

This technology creates many definitional, measurement, and spectrum management issues:
- What are the "center frequencies" of such emissions?
- What measurement techniques properly characterize these emissions?
- How well do spectrum analyzers measure these signals?
- How can such signals be allocated operating bands?
- What approaches might be taken to allow introduction of products using the technology?

These issues will be discussed, as will some additional issues, such as the emissions from "unintentional" radiators such as electric razors, hair driers, and kitchen blenders.

E1-3
0940

A DISCUSSION OF WIDEBAND EMISSIONS IN THE SPECTRUM

William A. Luther
Chief, Radiocommunication Policy Branch
International Bureau
Federal Communications Commission
2000 M Street, NW.
Washington, D.C. 20554

Wideband and "ultra-wideband" radio emissions are being studied by radio engineers on an expedited basis for several purposes:

First, the world is developing unwanted emission standards of wideband signals for possible inclusion in a global standard comprising a technical recommendation of the International Telecommunication Union (ITU). Stemming from this work is also the possibility of inclusion within the ITU treaty-based, international Radio Regulations, of specific requirements addressing limitations on unwanted emissions for wideband signals, and specifically for the first time, definition of "wideband" emissions. This presentation describes the studies that are underway within the ITU, examines the direction of tentative conclusions that have been reached within the context of preparations for the year-2000 ITU World Radiocommunication Conference where the issue will be debated and considered, and discusses the conclusions in the light of contemporary application of wideband signals.

Second, the civilian telecommunications authority of the United States is exploring the application of national regulatory provisions for ultra-wideband (UWB) radio systems. UWB radio systems typically use extremely narrow pulse (impulse) modulation or swept frequency modulation that employs a fast sweep over a wide bandwidth. Because of the type of modulation employed, the emission bandwidths of UWB emitters generally exceed one gigahertz and may be greater than ten gigahertz. UWB technology can be employed for radar systems, permitting the precise measurement of distances, the detection of objects within a defined range of distances, or high resolution imaging of objects that are behind or under other surfaces. When combined with appropriate modulation techniques, UWB devices may also be used for communications purposes, such as the transmission of voice, control signals, and data. Such signals are not easily detected or intercepted. For UWB signals, this presentation characterizes electromagnetic parameters, indicates the status of relevant current studies, and addresses the course of regulatory developments.

E1-4
1000

INVESTIGATION OF AGGREGATE INTERFERENCE FROM UNLICENSED (PART 15) RADIO DEVICES

Gerald F. Hurt
NTIA, Room 6725
U.S. Department of Commerce
1401 Constitution Ave., N.W.
Washington, DC 20230

An increasing number of low power radio devices are being authorized by the Federal Communications Commission (FCC) on an unlicensed basis under the FCC Part 15 Regulations. Since the emitted power is often quite low, e.g., -70 dBW/MHz, calculating the potential interference from a single unlicensed device to a licensed radio service is relatively straight forward. However, a methodology for evaluating the potential aggregate effects from these devices has not been clearly defined. This paper examines a general Monte Carlo simulation methodology to develop interference statistics from a random environment of unlicensed devices and applies the method to a variety of potentially interfered-with radio services including radio astronomy, radiolocation, and fixed services. While this method appears to be valid for narrow and wide band unlicensed devices that operate solely within a given allocated frequency band, it may not be applicable for very wideband devices that cover multiple allocated bands.

The starting point for this investigation is a methodology described in a Recommendation developed by the International Telecommunication Union (ITU-R Rec. M.1316) addressing aggregate interference from Mobile Earth Stations to radio astronomy. In that document a random (uniform) geographic distribution of interferers with random transmit times is simulated and account taken of the long integration times of the radio astronomy receivers. That methodology has been generalized for application to other radio services and expanded to consider other statistical variables including emitter heights, receiver antenna parameters, and radio propagation. A computer model was developed to apply the methodology for various radio services providing several output results including the cumulative interference to noise and signal to (noise plus interference) ratios versus probability of occurrence. These values are compared with established interference criteria where available.

E1-5
1040

BROADBAND SPECTRUM SURVEY AT BOULDER, CO TABLE MOUNTAIN RADIO QUIET ZONE

Frank H. Sanders
Institute for Telecommunication Sciences
Mail Code ITS.S2
U.S. Dept. of Commerce
325 Broadway
Boulder, CO 80303-3328

The United States Department of Commerce maintains a radio-quiet zone at Table Mountain, north of Boulder, CO. The Code of Federal Regulations, Part 47 (CFR 47), defines restrictions on radio transmitter assignments (excluding mobile transmitters) in the vicinity of the quiet zone. Within the boundaries of the quiet zone, the received signal levels from such assignments are limited by CFR 47 to values between 1 and 30 mV/m in the authorized bandwidth of service, the limit being defined as a function of frequency. Historically, the received signal levels at the quiet zone have been periodically checked only for individual signals that were known to be close to quiet zone limits. To more completely characterize the overall electromagentic environment at this location, the National Telecommunications and Information Administration (NTIA) Institute for Telecommunication Sciences (ITS), as part of a cooperative effort with the National Institute of Standards and Technology (NIST), performed a broadband (30 MHz to 19.7 GHz) spectrum survey at the quiet zone in 1998.

The most significant results of the ITS broadband spectrum survey are as follows: Comparison of the overall radio spectrum environment to other measured environments in the United States (Sanders, Lawrence, and Ramsey, Broadband Spectrum Survey at Denver, Colorado, NTIA Report 95-321; ibid, Broadband Spectrum Survey at San Diego, California, NTIA Report 97-334; and ibid, Broadband Spectrum Survey at Los Angeles, Claifornia, NTIA Report 97-336) demonstrates that the spectrum-occupancy density and amplitudes of signals are reduced in the fixed bands relative to the occupancy densities and amplitudes in metropolitan areas. However, in mobile bands (e.g., air traffic control between 118-136 MHz) and some radionavigation bands (e.g., 960-1215 MHz) the measured occupancy levels are essentially identical. The impact of new technologies, such as personal communication systems (PCS) and digital television transmitters (DTV) are discussed as they relate to the quiet zone.

E1-6
1100

SPECTRUM MEASUREMENTS OF THREE ULTRA-WIDEBAND DEVICES

Brad Ramsey*
Institute for Telecommunication Sciences
Boulder, CO 80303

United States federal spectrum managers are investigating the interference potential of recently introduced ultra-wideband radar and communication devices. The National Telecommunication and Information Administration's Institute for Telecommunication Sciences and the Laboratories of the Federal Communications Commission conducted a series of measurements on three such devices. These devices emit waveforms with bandwidths ranging up to 2 GHz, and spectra extending beyond 3 GHz.

At such large emission bandwidths, these devices radiate across a wide range of bands, including those allocated for communication, radiolocation, radionavigation, and radio astronomy systems. Because of the low duty cycle and low average power emitted by these devices, the manufacturers are seeking commercial licensing under Title 47, Part 15 of the Code of Federal Regulations.

The measured devices include a ground penetrating radar (GPR), a radio location device designed to locate in-wall objects such as wiring and and plumbing, and a multi-purpose system which combines radio location with a communication capability. Two of the devices incorporate spectrum spreading techniques to reduce the emitted spectral density. The measurements were conducted both in a Gigahertz Transverse Electromagnetic Field Cell (GTEM) and in an open laboratory setting at the Federal Communication Commission's Laboratories in Columbia, Maryland. The measurements were performed using the Institute for Telecommunication Sciences' Compact Radio Spectrum Measurement System.

The difficulty of measuring the peak power of ultra-wideband devices with conventional test equipment is addressed and the measured power spectra of these devices are presented. Comparisons are made between different detection modes and measurement system bandwidths. Several measurement techniques are discussed and illustrated.

E1-7
1120

SPECTRUM MANAGEMENT APPROACHES TO SUPPORT WIRELESS WIDEBAND COMMUNICATIONS

David J. Cohen
Information and Telecommunication Studies
University of Maryland, University College
University Blvd at Adelphi Road
College Park, MD 20742

An emerging telecommunication requirement is wireless delivery of high bit rate information such as video and high speed data (e.g. Internet traffic). These information sources will utilize bit rates of 2 Mb/s and greater. Even with higher level modulations wideband communication systems will be needed to support these bit rates. This paper addresses three spectrum utilization methods the wireless industry is considering to support wideband communications. These are channelization, spectrum etiquette and specialized packet access. Each of these methods will be discussed.

Channeling Plans: Generally, in the past the regulatory community has been responsible for developing and adopting channeling plans. Recently, in an emerging "user/industry" responsible spectrum management era it is the wireless industry developing and instituting the channeling methods. An example is the PCS band where a variety of channeling methods and medium access methods has been developed for both narrowband and wideband systems. The proposed alternative channeling methods for broadband wireless will be explained.

Spectrum Etiquette: The FCC has allocated the unlicensed bands 5150-5250 MHz, 5250-5350 MHz, and 5725-5825 MHz for wideband short-range systems. These bands are more commonly known as the NII bands. The FCC has made the allocation and specified certain technical parameters such as power levels and antenna gains. However, the wireless industry has the responsibility to develop the spectrum utilization methods (i.e. "spectrum etiquette") for the band. The alternative methods under consideration by the wireless community will be explained.

Packet Access: Dynamic spectrum resource assignments may prove advantageous for wireless wideband packet transfer. The goal is make the most efficient use of the spectrum resource while avoiding packet collisions and interference. Several packet multiple access schemes will be described including that which will eventually be utilized by the Teledesic "Internet in the sky" system.

E1-8
1140

ANALYSIS OF RECEIVER RESPONSE TO ULTRA WIDEBAND DEVICES

Edmund A. Quincy
National Telecommunication and Information Administration
Institute for Telecommunication Sciences
325 Broadway
Boulder, CO 80303-3328

Interest by the private sector in the potential application of ultra-wideband devices has stimulated measurement and analysis programs to determine the effect of these devices on generic receivers. This paper provides new interference analysis through simulation that is compared, where available, with measurements and analytic predictions. Our parametric results show the effect of receiver bandwidth on peak power. Bit error analysis was performed (R.A. Scholtz , MILCOM '93 Conf. Rec, 2, 447-450, 1993) for a similar multiple access system with time-hopping impulse modulation as a function of the number of users and bit rate.

The simulated ultra wideband system transmits a psuedo-periodic, very low duty cycle pulse train where narrow pulses were shaped with a Gaussian derivative filter and dithered slightly according to a psuedo-noise code. These operations produce a noise-like, spread spectrum that enables the system to operate as a low-power radar imaging or communication system. Typical parameters for the system simulated are: a pulse repetition frequency of 10 MHz, a pulse width (before Gaussian derivative shaping) of 0.5 ns, a duty cycle of 0.5%, a shaping filter center frequency of 2 GHz, and a 3 dB bandwidth of 2 GHz.

In our simulation we show the time and frequency characteristics of the shaping filter, the pulse train before and after shaping and dithering, and the transmitted spectrum. Assuming an ideal propagation channel, the received spectrum and average power are provided and the corresponding received time waveform as a function of bandwidth is also given. Received peak power is calculated from the time domain pulse trains and shown as a function of receiver bandwidth.

E1-9
1200

DESIGN CONSIDERATIONS FOR ROBUST SPECTRUM MEASUREMENT SOFTWARE

Brad Ramsey*
Institute for Telecommunication Sciences
Boulder, CO 80303

The Institute for Telecommunication Sciences has a twenty-five year history of making computer automated spectrum measurements. Over this time, engineers at the institute have built three generations of the Radio Spectrum Measurement System (RSMS) and are in the early implementation stages of the fourth generation. These systems have evolved from collections of one-of-a-kind devices requiring intensive training and support to our present system, which makes use of commercially available test equipment and software tools to form a user-friendly, robust spectrum measurement facility.

Despite the dramatic changes in the capabilities of successive generations of measurement system hardware, computing power, and user interfaces, many tenets of software system design have remained constant, albeit refined, throughout the history of the RSMS. These include hardware fault detection, combined measurement parameter and data storage, system response characterization via noise diode, support for scheduling and unattended operation, and scalability to include new measurement devices and algorithms.

By continuously refining and improving these features, the RSMS and similar systems designed by ITS are among the most full featured and user friendly spectrum measurement systems available. The system no longer requires a staff of engineers for maintenance and operation, and the data products are more numerous and varied than ever before.

The design criteriâ for computer controlled spectrum measurement systems are discussed, with examples from the RSMS and the Federal Aviation Administration's Radio Frequency Interference Monitoring System (RFIMS). The software's ability to report and tolerate faults, adapt to changing equipment availability, and be scaled to perform large and distributed measurement tasks will be shown.

Session G/H1, 0855-Mon., ECCR265
IONOSPHERIC HEATING (I)
Chairperson: Mike Sulzer (Arecibo Obs.)

G/H1-1
0900

SPECTROGRAPHIC OBSERVATIONS OF O (557.7 NM) AND N_2 MOLECULAR BANDS IN HF-HEATED SPORADIC-E LAYER

J.A. Gardner, A.L. Broadfoot (AFRL/VSBM)

G/H1-2 0920

ASPECT ANGLE DEPENDENCE OF O AND Z MODE HF-ENHANCED INCOHERENT BACKSCATTER

B. Isham (1)* M. T. Rietveld (2) T. Hagfors (3) C. La Hoz (4) E. Mishin (3) W. Kofman (5) T. B. Leyser (6) A. P. van Eyken (7)
(1) Interamerican University, Bayamón, PR 00957
(2) EISCAT Scientific Association, Tromsø, Norway
(3) MPAE, Katlenburg-Lindau, Germany
(4) University of Tromsø, Tromsø, Norway
(5) CEPHAG, Grenoble, France
(6) Swedish Institute of Space Physics, Uppsala, Sweden
(7) EISCAT Scientific Association, Longyearbyen, Norway

The EISCAT Observatory in northern Scandinavia, the Arecibo Observatory in Puerto Rico, and the Institute of the Ionosphere in Kharkov, Ukraine, are the only three locations worldwide where an incoherent scatter (IS) radar is co-located with a powerful HF ionospheric interaction facility. EISCAT has two IS radars, at 224 (VHF) and 931 (UHF) MHz, its HF transmitter possesses more that a GW in effective radiated power, and the geomagnetic field angle is offest from vertical by just 13 degrees. In experiments carried out on 26 November and 1 December 1997, we explored the effect of EISCAT's geomagnetic geometry on the plasma instabilities which have been observed during previous HF interaction experiments at EISCAT and Arecibo (Stubbe et al., *J. Geophys. Res.*, **97**, 6285–6297, 1992; Kohl et al., *J. Atmos. Terr. Phys.*, **55**, 601–603, 1993; Isham and Hagfors, *J. Geophys. Res.*, **98**, 13605–13625, 1993; Sulzer and Fejer, *J. Geophys. Res.*, **99**, 15035–15050, 1994) and searched for evidence of the generation, propagation, and decay of Z mode HF waves (Mishin et al., *J. Geophys. Res.*, *102*, 27265–27269, 1997).

During the experiments the pointing of the EISCAT UHF radar was varied in a predetermined and repeating cycle between azimuth angles of 90 and 77.2 degrees south, that is, between vertical and geomagnetic field aligned. The HF transmitter duty cycle was intentionally kept to a low value, either 2% (200 ms every 10 s) or 2.85% (114 ms every 4 s), in order to minimize the effects of ionospheric irregularities. Here we report on the variations in the intensity of the enhanced incoherent scatter ion and plasma lines observed during the experiments. The intensity of the enhanced lines observed with the UHF radar was clearly correlated with pointing angles between the Spitze angle and field aligned, and bottomside and topside F region enhanced lines were seen with both radars. No correlation between the intensity of the lines observed with the scanning UHF radar and the vertically pointing VHF radar was observed.

G/H1-3
0940

ION DYNAMICS OBSERVED WITH MULTIPLE DIAGNOSTICS DURING HAARP/HIPAS CAMPAIGN

A. Y. Wong* R. F. Wuerker J. Pau P. Y. Cheung P. Kidd
G. Rosenthal
UCLA, Los Angeles, CA 90095-1547
M. McCarrick and H.Zwi
APTI, Washington, DC 20037

Ion dynamics are predicted to occur during ionospheric heating. Both parametric decay and collapse processes must involve ion motion. Such ion motion can be observed as the asymmetric sidebands of the reflected skywave, monitored by SEE diagnostics. The motion of the resonant layer in ion time scale, as a result of heating by HAARP irradiation, can be measured by the Doppler diagnostic which has been developed at HIPAS.

Three ion resonances are dominant in the auroral ionosphere, the ion acoustic resonance, the lower hybrid resonance and the electrostatic ion cyclotron waves. Using multiple diagnostics at both HAARP and HIPAS sites we would like to observe these resonances. Previous observations at HIPAS have demonstrated that preconditioning has a dramatic effect on the subsequent power required for the nonlinear excitation (Cheung *et al.*, Phys. Rev. Lett. 80, 4891, 1998). We will discuss similar experiments at HAARP. The experiment consists of a sequence of two pulses. The high-power long duration pulse of 2 min sets up the pre-conditioning while subsequent pulses of 10 s will interrogate the ionosphere to find out if nonlinear excitation can occur. Nonlinear excitation is represented by the asymmetric spectrum of the skywave return observed by SEE.

In the case of ion cyclotron resonance we will monitor the ELF detectors located at HAARP, HIPAS and UA-GI. The resonance occurring at the ionosphere will be observed by a dip at the ELF receiver at the ion cyclotron resonance. The difference frequency will be swept between 21-52 Hz, corresponding to the ion cyclotron frequencies of Calcium and oxygen respectively (Wong *et al.*, Ionospheric Modification and Environmental Research in the Auroral Region in Plasma Science and the Environment, ed. by W. Manheimer, L. Sugiyama, and T. Stix, AIP Press, Woodbury, NY, ch. 3, pg. 41-75, 1997). When HIPAS heater is used the diagnostics will be correlated with the Lidar observations by Wuerker et al wherever possible, especially when there is matching of the excitation signal matching with the plasma resonance at the E layer.

G/H1-4
1000

KINETIC EFFECTS IN LANGMUIR TURBULENCE MODELING

K.Y. Sanbonmatsu* H.X. Vu D. F. DuBois B. Bezzerides
Los Alamos National Laboratory, Los Alamos, NM 87545

Two new and complementary simulation models have been developed, which have domains of quantitative agreement, for the self consistent evolution of the electron velocity distribution and the Langmuir turbulence. Our goal has been to incorporate kinetic electrons and ions in simulations which resolve Langmuir decay cascades and cycles of Langmuir collapse which are experimentally observed but usually not resolved in previous particle simulations. The reduced description particle-in- cell (RPIC) simulation model has been employed in which a two time scale approach for the electrostatic fields, familiar in the Zakharov modeling, is used. The particle ions respond only to the low frequency field resulting in a large decrease in noise which usually plagues particle simulations. Langmuir decay cascades and Langmuir collapse cycles are then seen for the first time in particle simulations. In our quasilinear Zakharov (QLZ) model the electron velocity distribution, which determines the Landau damping, is evolved along with the Langmuir turbulence using a quasilinear model. The quasilinear evolution equation for the electron distribution function contains the quasilinear diffusion, determined by the instantaneous Langmuir wave spectrum, plus a Cerenkov emission loss term and a boundary term accounting for the loss of hot electrons streaming out of the system and the inflow of cold electrons. Cerenkov noise also enters as a driving term in the first Zakharov equation for the Langmuir fluctuations. Fourier spectra of fluctuations and modified electron velocity distributions from the two simulation methods agree quantitatively in weak driving, high background noise, domains where agreement is expected. Preliminary 1D simulation results from the QLZ method for regimes of hf heating will be presented.

G/H1-5
1040

ALTITUDE DEPENDENCE OF EARLY TIME ISR SPECTRA IN HF HEATING: THEORY VS OBSERVATION

D. F. DuBois* D. Russell
Lodestar Research Corporation, Boulder, CO 80301
P. Y. Cheung
UCLA Department of Physics, Los Angeles, CA 90095
M. P. Sulzer
Arecibo Observatory, Arecibo, PR 00612

Recent observations by Sulzer and Cheung of ISR spectra, using the upgraded Arecibo heater at very low duty cycles, have revealed new details of the altitude distribution of Langmuir turbulence in the undisturbed ionosphere. Among these are the first unambiguous observations of the decay lines at the predicted altitudes in the unmodified ionospheric electron density profile. New numerical simulations based on the equations of strong Langmuir turbulence theory will be reported which agree with many details of these observations. These simulations indicate that the Langmuir turbulence spectrum spreads in k space with increasing heater power so that at the higher heater power now available at Arecibo the decay Langmuir waves can be viewed by the radar at a relative angle of about 42 degrees. At higher altitudes near reflection the familiar down-shifted caviton continuum and the-upshifted free mode features can be seen in the ISR spectra. The strength of the free mode line relative to that of the caviton continuum is seen in simulations to increase with decreasing altitude below reflection. Nearest to reflection altitude the free mode is very weak and may be unobservable, a new result of theory and observation. Below reflection the caviton continuum weakens and the free mode appears to stand alone. The ISR spectra during the decay of the turbulence after heater switch off has been studied. One result is that the caviton continuum decays faster than the free mode. The role of "clutter' inherent in the coded-long-pulse observational technique (Sulzer 1986) must be taken into account in making comparisons of theory and experiment. The absence of a critical (reflection) density in some observations may allow an extended free mode line, resulting from a strongly driven decay cascade, to be seen well below the decay matching altitude.

G/H1-6
1100

NEW OBSERVATIONS OF THE *F* REGION RESPONSE TO LARGE HF-INDUCED ELECTRON-TEMPERATURE ENHANCEMENTS

F. T. Djuth[1], P. A. Bernhardt[2], M. P. Sulzer[3], J. H. Elder[1], and C. Brown[4]
[1]Geospace Research, Inc., 550 N. Continental Blvd., Suite 110, El Segundo, CA 90245
[2]Plasma Physics Division, Naval Research Laboratory, Washington, DC 20375
[3]Arecibo Observatory, P. O. Box 995, Arecibo, PR 00614
[4]Brown Computer Company, P. O. Box 13381, Research Triangle Park, NC 27709

Measurements of large (1000 - $\gtrsim$2500 K) HF-induced electron temperature enhancements and associated large-scale electron density depletions (10 -25%) were first made at Arecibo Observatory between 1985 and 1988. Significant (> 30 Rayleigh) enhancements in the 630.0 nm nightglow emission from (O^1D) are correspondingly detected. Major ionospheric modifications of this nature are readily achieved in the winter, nighttime ionosphere when radio waves having frequencies between 3 and 4 MHz (O-mode polarization) reflect near ~300 km altitude with f_0F_2 ~ 3.2-4.0 MHz.

Physically, heat initially deposited by the HF wave in the bottomside *F* layer is rapidly spread by electron gas conduction over an altitude interval of the order of a neutral scale height. For the low (~1×10^5 cm^{-3}) electron densities present in the ionosphere during these experiments, local Coulomb collisions with ions are inadequate to confine the electron temperature (T_e) enhancements; T_e then increases until heat conduction by the electron gas carries the locally deposited heat to heat sinks well above and below the deposition height. When electron energy loss to ions and thence neutrals is small near the heat source region, very large electron temperature enhancements develop before thermal conduction (dependent on T_e gradients) is sufficiently great to carry away locally deposited heat. In this environment ion temperatures rise $\gtrsim$100 K above ambient values. Electron density depletions form primarily because of increased recombination rates caused by an elevation in the vibrational temperature of N_2.

New Arecibo results were obtained during a campaign conducted from 19 January - 29 January 1998. Approximately twice the HF power available in previous experiments was used for modification of the *F* region. This led to major increases in 630.0 nm and 557.7 nm airglow and gave rise to significant restructuring of the *F* region plasma. Very large HF-enhanced ion-lines were detected, and extremely large asymmetries were noted between the amplitudes of the two ion-acoustic sidebands. The upshifted sideband was usually found to be dominant. As the temperature of the electron gas increased, measurements of stimulated electromagnetic emissions revealed that a strong downshifted maximum tends to widen and merge into a cascade starting at the modification frequency. The added deposition of heat in the *F* region appears to drive the plasma into a highly nonlinear state. Enhanced electron temperatures greatly lower the collisional damping of Langmuir oscillations and significantly reduce the ion-wave damping decrement. As a result, ponderomotive instabilities are driven approximately five times harder than normal, and this may account for the large observed increases in airglow.

G/H1-7
1120

PRODUCTION OF LARGE AIRGLOW ENHANCEMENTS VIA WAVE-PLASMA INTERACTIONS IN SPORADIC E

F. T. Djuth[1], P. A. Bernhardt[2], C. A. Tepley[3], J. A. Gardner[4], M. C. Kelley[5], A. L. Broadfoot[6], L. M. Kagan[5], M. P. Sulzer[3], J. H. Elder[1], B. Isham[3], C. Brown[7], and H. C. Carlson[8]
[1]Geospace Research, Inc., 550 N. Continental Blvd., Suite 110, El Segundo, CA 90245
[2]Plasma Physics Division, Naval Research Laboratory, Washington, DC 20375
[3]Arecibo Observatory, P. O. Box 995, Arecibo, PR 00614
[4]Air Force Research Laboratory, VSBM, Hanscom Air Force Base, MA 01731
[5]Department of Electrical Engineering, Cornell University, Ithaca, NY 14853
[6]Lunar and Planetary Laboratory, University of Arizona, Tucson, AZ 85721
[7]Brown Computer Company, P. O. Box 13381, Research Triangle Park, NC 27709
[8]AFOSR/CA, Bolling Air Force Base, Washington, DC 20332

In the past there has been great interest in monitoring enhanced 557.7 nm O(^{1}D) emissions from the thermosphere in connection with high-power, high-frequency (HF) radio wave modification of the *F* region ionosphere. These emissions are considered to be evidence that the HF-modified electron distribution function is non-Maxwellian because a significant flux of ~4-5 eV electrons is required to produce the airglow. The suprathermal tail is believed to develop as a result of nonlinear plasma processes. Past *F* region observations of 557.7 nm airglow have yielded only a few Rayleighs of enhanced emissions. Recently, airglow enhancements were monitored in sporadic *E* above Arecibo Observatory, Puerto Rico. Surprisingly, these experiments yielded ~55 Rayleighs of enhanced 557.7 nm airglow and the first observations of emissions from the N_2 first positive molecular bands. The observations imply that a large flux of energetic electrons between 4 and 10 eV is generated as part of the wave-plasma interaction in sporadic *E*.

It is highly likely that ponderomotively driven instability processes are responsible for the generation of the suprathermal electrons. The physically meaningful quantity that characterizes the driving of ponderomotive processes is

$$W_o \equiv \left\langle |E|^2 \right\rangle / 8\pi n_o T_e,$$

where E is the HF electric field amplitude at the first maximum in the standing wave pattern, and T_e is the background electron temperature. One finds that $W_o \sim 1.5 \times 10^{-2}$, which is 12-16 times greater than that encountered in the *F* region prior to the Arecibo HF facility upgrade. Additionally, $\nu_t / \omega_o \sim 2 \times 10^{-4}$, and $W_o/(\nu_t / \omega_o) \sim 75$, which is large enough for an absolute instability to develop in the plasma. Our near-term goal is to develop viable estimates of the electron energy spectrum required to produce the 557.7 nm and N_2 emissions, and thereby set boundary conditions for the plasma physics. A self-consistent description of the electron acceleration process represents a major theoretical challenge.

G/H1-8
1140

HF EXCITATION OF LANGMUIR TURBULENCE: COMPARISON OF F-REGION AND SPORADIC-E HEATING**

D. L. Newman* M. V. Goldman
Center for Integrated Plasma Studies, Campus Box 390,
University of Colorado, Boulder, CO 80309
F. T. Djuth
Geospace Research, Inc., El Segundo, CA 90245
P. A. Bernhardt
Naval Research Laboratory, Washington, DC 20375

Modification of the ionosphere by 5.1 MHz heater radiation at Arecibo usually excites Langmuir waves near the reflection altitude in the F-region where the ionospheric plasma frequency equals the heater wave frequency. These Langmuir waves are thought to evolve nonlinearly and then transfer their energy to hot nonthermal electrons which, in turn, propagate out of the heated region and excite oxygenic airglow at lower altitudes. The density scale length in the F-region is very long ($\sim$ 20–50 km). Thus, the ionospheric plasma is usually treated as *locally homogeneous* when studying the parametric excitation of Langmuir waves and their subsequent nonlinear evolution.

During recent modification experiments at Arecibo with a 3.175 MHz heater, an unusual situation was found where Langmuir waves were excited at lower altitudes in association with a sporadic-E event with a short ($\sim$ 500 m) density scale length. This observation was accompanied by copious 557.7 nm (green line) airglow simultaneous with suppression of 630.0 nm (red line) emission. Theoretical interpretation of this event—as constrasted with F-region heating—must take into account both the higher normalized heater intensity ($W_0 = E_0^2/16\pi n_e T_e$) at the lower sporadic-E altitude, and the steeper density gradient. The higher intensity is due to a larger heater electric field, E_0, as well as to a lower electron density, n_e, and temperature, T_e. The steeper density gradient increases the role of WKB *steering* of Langmuir waves and results in heightened parametric-instability thresholds. In light of the above differences between F-region and sporadic-E heating, it is necessary to determine whether the higher instability thresholds are able to limit Langmuir-wave growth given the higher effective pump intensity associated with the sporadic-E event.

For parameters characteristic of the new sporadic-E observations,[1] the heater is determined to be well above the gradient-elevated threshold for parametric decay—consistent with the airglow measurements. However, the role of the modulational instability, which is often invoked in descriptions of F-region modification, is found to be greatly reduced by the density gradient.

** Work supported by NSF Atmospheric Sciences Division

J1-1
0900

THE SQUARE KILOMETER ARRAY - SCIENCE WITH THE NEXT GENERATION TELESCOPE FOR RADIO ASTRONOMY

P. E. Dewdney
Dominion Radio Astrophysical Observatory
Box 248
Penticton, B.C.
Canada V2A 6K3
A. R. Taylor*
University of Calgary
Physics and Astronomy
2500 University Dr. N.W.
Calgary, Alberta
Canada T2N 1N4

Moving toward the beginning of the next millenium, we stand poised to make a major leap forward in observational radio astronomy. Over the past few years an international effort has been developing to solve the technical challenges required to realize a giant radio telescope with a collecting area of one square kilometer. The Square Kilometer Array (SKA) will have a hundred times more collecting area than our most powerful existing radio telescopes, providing sensitivity of a few tens of nano-Jansky in the centimeter wavelength continuum.

Such a telescope will be needed to meet upcoming scientific challenges presented by telescopes in the optical, infrared and high-energy bands. The Square Kilometer Array will be able to detect emission from the atomic and molecular gas at extreme redshifts, allowing study of the "Dark Ages" of the Universe before, and during, the transition phase when the initial stars formed and reionization occured. By combining sensitivity, wide field of view and inteferometer baselines as high as several hundred kilometres the interstellar media of galaxies will be detected and imaged to great distances. Measurements of atomic hydgrogen emission and continuum emission from galaxies will trace the star formation history of the Universe from the present to very early epochs. In our own Galaxy star formation processes and phenomena in the gaseous ISM will be studied on linear scales down to a few A.U. Millions of stars will be detected as radio sources, allowing, for example, the initial mass function of massive stars in our own and nearby galaxies to be measured, the surface of red giant stars to be directely imaged, and the detection of solar-type phenomena on hundreds of nearby stars.

J1-2
0920

OBSERVATIONS OF EXTENDED SUPERNOVA REMNANTS WITH THE SKA

John R. Dickel*
Astronomy Department
University of Illinois at Urbana-Champaign
Urbana IL 61801

Understanding how cosmic rays and relativistic electrons are accelerated in supernova remants requires high sensitivity and high resolution polarimetric radio observations of these objects at several wavelengths. Variations in the spectrum of the observed synchrotron radiation in different parts of a remnant can identify the sites of particle acceleration and indicate how diffusion mechanisms operate. Polarimetry can map the magnetic fields and elucidate their role in both confinement and acceleration processes. Currently, for most SNRs, the resolution of aperture-synthesis radio telescopes is limited by low sensitivity which requires convolving the emission over several arcseconds to obtain a detection. Optical observations of one radio feature often show several sub-arcsec filaments. With the great sensitivity of the SKA we can realize the same resolution at radio wavelengths and see the detailed relation of the morphology and other physical properties of the SNR. The high sensitivity is even more important for polarimetric observations as polarized intensities are typically 1 - 10% of the total intensities.

Another serious concern for SNRs is that generally over 80% of the emission is in a smooth component which can extend over an area larger than the primary beam pattern. How is this major component of the emission related to the bright fine scale structure? It is clear that we will not have a complete picture unless this smooth emission is measured as well. This need to include the smooth emission requires that good sensitivity be available for short spacings as well as long ones and that there be complete coverage of the intermediate spatial frequencies between those covered by a single element of the array and those between individual elements. A "superelement" of some kind should be included in the array. In addition, the instrument must be quickly steerable to allow mosaic observations for large fields of view.

Many of these requirements are also needed for observations of thermal Galactic radio sources and the continuum emission from other galaxies.

J1-3
0940

SQUARE KILOMETER ARRAY: ORGANIZATIONAL ISSUES

Harvey Butcher
Netherlands Foundation for Research in Astronomy
P.O. Box 2
7990 AA Dwingeloo
Netherlands

Observation of the early Universe including the formation of the first galaxies is now with the reach of our technology. For those phenomena that can best or only be studied at radio frequencies a new generation of instruments is required having roughly a hundred times the sensitivity of current large radio telescopes. Essential to understanding the history of the Universe will be observations of neutral hydrogen in galaxies as a function of redshift, a requirement that argues directly for a telescope having a collecting area of a million square meters and maximum sensitivity in the range 150 to 1500 MHz. The need for similar gains for other studies have promoted discussions of a frequency coverage from 30 MHz to 20 GHz. Around the world astronomers have begun to think about how one or more "Square Kilometer Array" radio telescopes – SKA for short – might be built. Eight institutes in six countries have formally agreed to coordinated R&D efforts that should lead to a choice of technical concept(s) in the first years of the new decade.

A growing interest world-wide, the expected large cost as well as the demographics of the next generation of radio astronomers, make it likely that the SKA project will be an international endeavor. No obviously suitable international organization exists to adopt the project, however, so a structured and well organized effort either to create an appropriate organization or to adapt an existing one is in order. Radio astronomers should see this situation as an opportunity to obtain the kind of organization we want.

This talk will review the current international situation, note the pre-conditions for a successful project, discuss the options for organizational forms, and comment on issues relating to timescales and to financing.

J1-4
1000

THE ONE HECTARE ARRAY

John W. Dreher*
SETI Institute
2035 Landings Drive
Mountain View, CA 94043

The One Hectare Array (1hT) is a joint project of the SETI Institute and the Radio Astronomy Laboratory of the University of California at Berkeley. The 1hT will consist of a large array of small parabolas with a total collecting area of $10^4 m^2$ (larger than the VLA) and a continous RF frequency range of at least 1-10 GHz. The location is not yet decided, but the existing site at Hat Creek is a strong possibility.

The research and development phase of this project has already begun. Prototypes of the elements are expected in late 1999, with a prototype array to follow, and full-scale construction to begin early in the next decade.

A variety of element designs in the diameter range 3-10 m are being studied. Cryogenic InP low noise amplifiers will be used, exploiting the recent availability of inexpensive 80 K coolers. The full RF bandwidth will be brought to a central signal processing facility using analog optical fibers. A wide range of backends are anticipated. For work on known targets, several simultaneous wideband beams will be available within the pattern of the elements. It is expected that the number of such beams will grow over time to reach hundreds, creating a powerful instrument for survey work. For imaging, a (relatively) narrow-band cross-correlator is also being planned, supporting of order 10^5 to 10^6 baselines.

The primary purposes of the 1hT will be to provide 1) a dedicated SETI facility, 2) a novel and powerful radio astronomy system, 3) a prototype for a possible station design for the Square Kilometer Array, and 4) a test bed for RFI suppression schemes.

J1-5
1040

THE LARGE ADAPTIVE REFLECTOR FOR THE SQUARE KILOMETER ARRAY

P. E. Dewdney*
Dominion Radio Astrophysical Observatory
A. R. Taylor
University of Calgary

Over the past few years the astrophysical argument has been made on the international scene for a next-generation telescope with a collecting area of 10^6 m^2, noting that radio astronomers have now done almost everything possible to improve sensitivity without adding significantly to collecting area. The resolution of a radio telescope no longer presents fundamental problems of design - aperture synthesis telescopes can be designed so that resolution is well "matched" to the sensitivity and the astrophysical problems. The greatest question in the development of such a telescope is exactly how to build it - costs of implementation using current technology are high, making it implausible, if not impossible, to consider its financing. Another major design issue is the wavelength coverage of the telescope. In addition to sensitivity and resolution, the question of whether the Square Kilometer Array will be a general purpose successor to the present generation of radio telescopes depends mainly upon its wavelength coverage. If the SKA can be designed to cover the range from about 1 m to 1 cm, then it will succeed as a general purpose telescope.

We have proposed an antenna design, called the Large Adaptive Reflector (LAR), which potentially permits the construction of large parabolic reflectors as elements of the SKA. The LAR is a long focal-length parabolic reflector that requires an air-borne platform to support the focal receiver. A very large, nearly flat active reflecting surface brings incoming radiation to a focus on the airborne platform. The long focal length permits the reflector to present a very flat profile. The reflector is active - made up of panel segments whose height and angle to the vertical can be adjusted, but the reflector itself does not need to be mechanically tilted as in the traditional design. The shape of the reflector can be chosen to provide a focus anywhere on the sphere above a "horizon limit", which is determined by the allowable range of movement of the panels and the "cosine foreshortening" of the reflector. The telescope is pointed by moving the focus (airborne platform), while simultaneously adjusting the shape of the surface. Antenna diameters of about 200 m are being considered for the SKA. The airborne platform is the most unusual and exacting requirement of the LAR. At present a multi-tethered aerostat (balloon) is being considered as the airborne platform. The LAR concept exchanges the fundamental problem of gravitational loading encountered with large traditional designs for problems that may be amenable to high technology solutions (e.g. advanced control systems).

J1-6
1100

THE DEEP SPACE NETWORK AND THE SQUARE KILOMETER ARRAY

G. M. Resch* T. B. H. Kuiper J. G. Smith
Jet Propulsion Laboratory
Pasadena, CA 91109

The evolution of the NASA Deep Space Network is driven by the telecommunications needs of the current and future NASA spacecraft that are sent to explore the solar system. Undoubtedly, if the SKA existed and could operate at our telecommunications wavelengths (2.1, 8.4, and 32 GHz), there will be special situations in which the DSN would want to use the SKA. Historically, the DSN has turned to interagency arraying to do things like boost the data return during the Voyager encounter with Neptune or support the Galileo spacecraft during the tour of the Jovian satellites. However, that kind of interest is difficult to predict and does not elicit strong support either politically or financially from NASA/DSN until some kind of emergency is apparent.

We will outline the way the DSN views its evolution in the coming decade, based largely on what it perceives to be the long range strategy for NASA missions. This perception is based on the number and types of spacecraft that are expected to be launched during the coming decade as well as the reluctance to make additional investment in expanding the number of 34 meter antennas in the DSN. We will attempt to outline the strategy by which decisions are made and to speculate on the ways that the SKA can impact these decisions. Our objective is to begin a dialogue between the various developers of the SKA and DSN management that will make it possible for the DSN to be a partner in this enterprise rather than an interested spectator.

J1-7
1120

WIDEBAND FEEDS FOR THE SQUARE KILOMETER ARRAY

W. J. Welch and G. Engargiola
Radio Astronomy Laboratory
University of California
Berkeley, CA 94720

An important option for the Square Kilometer Array is continuous operation over a wide band of frequencies. This capability will be essential for a variety of scientific programs. It is enabled by the very low noise, wideband HFET amplifiers which are now available. The challenge is to build antennas for the array that are also wide band. The specific need is for a wideband feed for a parabolic reflector, implemented with as few moving parts as possible. In addition to full frequency coverage, the primary spillover must be kept small in order that thermal noise pick up from the ground be minimized. Good input match to the amplifier and small ohmic losses are also critical. We discuss some promising designs based on log-periodic arrays. These feeds are being studied with the aid of E-M simulation software and will be prototyped in the coming year. This particular implementation, based upon a single feed and two amplifiers for dual polarization holds the promise of being inexpensive and requiring minimal maintenance. Printed circuit board technology may be used for feed production. The development of small, inexpensive cryo-coolers for computer applications may provide the affordable cooling for the HFET amplifiers, required to achieve a low system temperature. For the Square Kilometer Array, the goal is to cover a frequency band of at least 0.3 GHz to 10 GHz, with an overall system temperature $\leq$ 50K.

J1-8
1140

RFI DIRECTION FINDING AND SUPPRESSION USING AN ADAPTIVE ARRAY: FIELD RESULTS

S. W. Ellingson* R. S. Dixon
The Ohio State University
Columbus, OH 43212

As part of our "Argus" omnidirectional radio telescope project, we recently built a four-element adaptive array for 220 MHz. The purpose was to test the ability of the Minimum Variance Distortionless Response (MVDR) algorithm (J. Capon, *Proc. IEEE*, **57**(8):2408-18, 1969; R.T. Lacoss, *Geophysics*, 36:661-75, 1971) to locate and suppress radio frequency interference (RFI) in field conditions.

The 220 MHz band was selected because it is well known to us from other field projects. Each element of the array was a commercially-available vertically-polarized monopole. As a tradeoff between maximizing aperture and preventing direction-of-arrival ambiguity, the elements were arranged in an "L" shape with $\lambda/2$ spacing. Signals from the antenna array were downconverted and digitized, yielding a 2-MHz-wide digital signal centered at 1.25 MHz. Quadrature downconversion, calibration, and additional filtering were performed in software.

For this study, a typical data set consisted of a block of 32,768 snapshots (6.5 ms). An FFT of data from one element of the array revealed two strong sources (approximately -75 dBm and -90 dBm) plus many much smaller signals. The two strong sources were known to us as commercial utility broadcast towers which are several miles away from our test site and separated by about 120° degrees. Using Capon's method we were able to clearly identify these signals and estimate bearing with accuracy on the order of $\pm 3°$.

We then tested our ability to suppress these signals using the MVDR beamformer, which is derived from Capon's method. We used a sidelobe canceling constraint with one element as the quiescent pattern. This prevented MVDR from simply zeroing the array output to achieve suppression. Adaptive array theory suggests that this approach should be able to place deep nulls on three signals. In our experiment, we found that the strongest signal could be suppressed by 25 dB, and the other strong signal by about 12 dB. The discrepancy between theoretical and observed performance is attributable to various "real world" problems such as multipath, limited integration time, and linearity.

In a large array telescope, this method could be used "as is" with an MVDR constraint to define the desired beam. For multibeaming or omnidirectional telescopes, a better approach may be to use this information to design a "spatial whitening filter" in the form of a matrix transform which excises RFI from snapshots but leaves them in vector form suitable for subsequent processing.

J1-9
1200

RESULTS OF THE R&D PROGRAM ON ARRAY ANTENNA SYSTEMS AT NFRA

A. van Ardenne
Netherlands Foundation for Research in Astronomy
P.O. Box 2
7990 AA Dwingeloo
The Netherlands

After many years of relative consolidation, the radio astronomy community has embarked upon the development of antenna concepts that will allow the reception of faint radio signals with 2-3 orders of magnitude increase in collecting area compared with current radio telescopes. The aim is to reach nJansky sensitivity using up to a million square meters, distributed over up to 50 locations and a non-instantaneous bandwidth of several decades (from 0.02 - 20 GHz in two polarizations).

Several concepts can, in principle, support this next generation of radio telescopes. These range from the use of large Arecibo type dishes (with a diameter of about 300m) to (combinations of) tens of thousands of small dishes with 3-5m diameter that can be fabricated through cheap mass production techniques. Adaptive (planar) array techniques can also be used to cover the decade wide mid-frequency range. The electronic beamforming capability allows a huge increase in scientific merit using advanced levels of functional integration and data processing techniques.

In 1995 NFRA, embarked on a technical R&D program aimed at the development of wide band adaptive array technologies with the capability of operating in an RFI-"polluted" environment. The 5 year program involves the prototyping of arrays with increasing size and complexity. Each prototype is to be built over a 1.5 year period, in parallel with a number of research programs with longer time horizons. The first step - a small 8-element array that includes digital beamforming - has been completed, and some results will be presented. Early results will also be shown from the second (100-element) array and we introduce the next step: a 1000-element array. Results from the parallel programs will also be discussed. So far, we have not encountered problems that might block the realisation of a large telescope early in the next century.

Session B/H1, 1335-Mon., ECCR150
NUMERICAL METHODS IN ELECTROMAGNETICS AND PLASMAS
Chairperson: Glenn Joyce (Naval Research Lab.)

B/H1-1
1340

PHYSICAL MODELING OF M-I COUPLING: GLOBAL SCALE ISSUES

J. J. Sojka and R. W. Schunk
Center for Atmospheric and Space Sciences
Utah State University
Logan, UT 84322-4405

With a much improved understanding and modeling capability of the solar wind-magnetosphere interaction in response to solar wind variability, it is now possible to simulate ionospheric weather that results from these interactions. Studies have been carried out using the Utah State University time-dependent ionospheric model (TDIM) to simulate these responses from inputs that were generated by the Naval Research Laboratory MHD model of the magnetosphere-solar wind interaction. Such studies not only give insight into geophysical dynamics, but also highlight shortcomings in the present stage of M-I modeling. On the positive side, such simulations generate ionospheric structures that are consistent with observations. This includes the tongues of ionization (TOI), polar holes, and mid-latitude trough features. They have also generated new discoveries that await observational validation, e.g., the F-regions reverse tongue of ionization. A reverse TOI is generated under extreme northward IMF conditions and is associated with a sunward convection over the polar cap in winter. However, shortcomings are also evident, especially at low auroral to mid-latitudes where MHD boundary conditions need to be imposed. As a result, phenomena such as the Storm Enhanced Density (SED) positive phase of a geomagnetic storm is not reproduced. This feature, in particular, is known to extend from high (75Λ) to low (35Λ) latitudes in the afternoon sector and appears to be associated with the ring current shielding during the most dynamic phases of storm events. These topics will be discussed in the context of the status of M-I coupling on a global scale using physical models.

B/H1-2
1400

A PERFECTLY-MATCHED-LAYER BOUNDARY CONDITION FOR USE IN FDTD MODELING OF PULSE PROPAGATION IN THE EARTH-IONOSPHERE WAVEGUIDE

M. W. Chevalier* U. S. Inan T. F. Bell
STARLab
Stanford University
Stanford, CA 94305

The Finite-Difference Time-Domain (FDTD) technique is applied to model the propagation of extremely low frequency (ELF) pulses, launched by lightning discharges, into the earth-ionosphere waveguide. Because the ground , the troposphere, and the ionosphere are stacked very much like dielectric slabs, the Berenger Perfectly Matched Layer (PML) serves as the foundation for a boundary condition to terminate the FDTD space. The reason for this is that the PML, with good results, has been used to terminate FDTD spaces modeling lossless dielectric waveguides. In the case of the earth-ionosphere waveguide, because the ground and the D-region of the Ionosphere are highly lossy, the original PML does not accurately absorb electromagnetic energy as it exits the model space. This is because the original PML was derived to match lossless materials. We modify Berenger's equations in order to match general dielectric materials. The derivation yields a frequency independent spatial-decay function, similar to that derived by Berenger for lossless dielectrics. The new boundary condition is tested in both 1D and 3D. We model the earth-ionosphere waveguide and compare results with a validated frequency domain waveguide model, the Long Wave Propagation Capability (LWPC) code. The two different techniques yield similar accuracies. The major advantage of the FDTD code is that it is a time domain code so that the transient behaviors can be studied. Another advantage of the FDTD technique is that complex geometries and spatial inhomogeneities, such as local conductivity changes in the ionosphere due to sprites and blue elves, are easily modelled.

B/H1-3
1440

EFFECTS OF A SUDDENLY CREATED PLASMA MEDIUM ON TURNED-ON WAVES

V. R. Goteti
Department of Electrical Engineering
Alabama A&M University, Normal, AL 35762

The effects of an isotropic transient plasma medium on a wave that is in the process of propagation are analyzed in this paper. A plane wave is assumed to be set in propagation at time $t = -t_1$ in the positive z-direction and at time $t = 0$ the entire space is suddenly converted to a plasma medium. The entire space is free-space for time $t < 0$ and plasma for time $t > 0$. Thus the original wave is assumed to exist over a certain extent in space when the plasma is switched on. The problem is solved using one sided Laplace transform with respect to the time variable and two sided Laplace transform (C.D.McGillem, and G.R.Cooper, *Continuous and Discrete Signal and System Analysis,* Holt, Rinehart and Winston, New York, 1974, 253-264) with respect to the space variable. Propagation of an impulsive plane wave has been discussed by the author earlier (V.R. Goteti, and D. Kalluri, *1987 IEEE International Conf. on Plasma Science,* Buffalo, NY, 46). The problem is solved here for a general wave and special cases of an impulsive wave, a step wave and a harmonic wave are discussed.

The newly created electrons are assumed to be at rest at time $t = 0$ and are set in motion only for $t > 0$. This assumption makes it possible to impose the conditions of continuity of the tangential components of the fields at $t = 0$. Analytical expressions for the fields are obtained for the specific cases in terms of convolution integrals involving Bessel functions.
Inversion of the two sided Laplace transforms makes it possible to identify the direction of propagation of the resulting waves. It is found that in the case of a harmonic wave, new waves propagating in both positive z-direction and negative z-direction are obtained. These are identified as transmitted waves and reflected waves. The frequency of both these waves is $(\omega_o^2 + \omega_p^2)^{1/2}$ where ω_p is the plasma frequency and ω_0 is the frequency of the original wave.

The salient features of the proposed solution are a description of the fields for time $t > 0$ in terms of composite Laplace transforms, leading to a simple way by which the general solution can be applied to specific cases of an impulsive wave, a step wave and a harmonic wave. Further, the relation between the impulsive wave solution and the solution of the other types of original wave makes it possible to describe a 'transfer function' for the set up.

B/H1-4
1500

MODELING THE NEUTRAL COMPONENT OF THE UPPER ATMOSPHERE

Tim Fuller-Rowell
CIRES, University of Colorado and NOAA, SEC
325 Broadway
Boulder, CO80303

Many of the features seem in ionospheric plasma arise from interaction with the neutral atmosphere, which is the dominant component even at the altitudes of the ionospheric layers in the upper atmosphere. It is important, therefore, to model both the neutral and ionized species, in order to furnish an accurate understanding of the changes observed in the plasma domain. Modeling the neutral upper atmosphere, i.e. the thermosphere, requires solution of the time-dependent, equations of momentum, energy, and composition. The time scale of processes such as diffusion and advection require that the thermospheric equations are solved at least every one minute. Diffusion times are greatest at the high altitudes where molecular diffusion dominates due to the long mean free path of the particles. The advection time-scales are short due to the high velocity winds that can be driven by the magnetospheric forcing, sometimes exceeding 1 km/s. These speeds transport material across the grid spacing in a matter minutes. For global modeling, the resolution limits are set by the width of the auroral oval and ion convection channels, and by the ability to capture large-scale gravity waves. The latter are the cause of the travelling ionospheric disturbance (TID), one of the characteristic features seen in the ionosphere. The other key neutral parameter is the composition of the thermosphere. Ionospheric recombination rates are controlled to a large extent by the ratio of the atomic oxygen and molecular nitrogen species. The numerical methods are required to handle the range of physical process at a computation speed sufficient to simulate many days of the global system.

B/H1-5
1540

NUMERICAL METHODS USED IN THE LYON-FEDDER-MOBARRY GLOBAL MHD CODE TO MODEL THE MAGNETOSPHERE

M. Wiltberger*
Department of Astronomy
University of Maryland
College Park, MD 20742
J. G. Lyon
Department of Physics and Astronomy
Dartmouth College
Hanover, NH 03755

The Lyon-Fedder-Mobarry (LFM) global MHD code is one of the leading codes used to simulate the coupled solar wind - magnetosphere - ionosphere system. This talk concentrates on the numerical techniques used to solve the MHD equations and how this solution is coupled to the ionospheric simulation.

The code uses the Partial Interface Method (PIM) to solve the MHD equations. PIM is a modern shock capturing technique that uses the Partial Donor Method (PDM) as an upwind limiter to maintain a total variation diminishing solution to the MHD equations. In addition PIM utilitizes a staggered mesh, with magnetic fluxes through the cell interfaces and electric fields along the cell edges, to maintain magnetic field which remains divergence free. We present the results from one and two dimensional test problems that illustrate the robustness and strength of this technique.

The LFM uses a specially designed grid to model the magnetospheric and solar wind plasma. The distorted spherical grid was created to place maximal resolution in regions known a priori to be important, eg bow shock, magnetopause, magnetotail, and ionosphere. However the grid remains logically rectangular so that determination of nearest neighbors and the application of an finite volume method is relatively straight forward to implement.

The inner boundary condition on the magnetospheric plasma is determined from the ionospheric simulation. The plasma parameters are used with an empirical model to determine the anisotropic conductivity tensor. Once this tensor is known the application of current conservation between the field aligned currents (FAC) at the magnetospheric boundary and the ionosphere leads to a electrostatic potential equation that is solved by with an ICCG method.

This talk concludes with two examples of event studies conducted using the LFM. On March 9, 1995 a series of two substorms occurred and have been reproduced with surprising qualitative and quantitative agreement by the code. We have also used the LFM to simulate the over 36 hours that composed the magnetic cloud event of January 10-11, 1997. This event is the longest known magnetospheric simulation and comparison to data remains strong through out the entire event.

B/H1-6
1600

PHYSICAL MODELING OF THE IONOSPHERE USING SELECTED MEASUREMENTS AS ADDITIONAL CONSTRAINTS

P. G. Richards
Computer Science Department,
The University of Alabama in Huntsville,
Huntsville, Alabama, 35899
USA

Until recently, physically based ionospheric models have produced results that are more qualitative than quantitative because there are a large number of basic inputs with potentially large uncertainties. Our approach has been to develop algorithms that employ measurements as constraints on the physical models. Horizontal neutral winds are a very important input because of their direct effect on the ionospheric peak density, yet they are highly variable and there are few measurements available. In fact, without accurate information on neutral winds, truly quantitative electron density modeling is not feasible. The plasma temperatures also play an important role in the altitude distribution of the electron density but there are considerable uncertainties in the electron heating rate, especially in the plasmasphere. Uncertainties in the thermospheric neutral densities are an additional source of ionospheric uncertainty, particularly during magnetic storms. Other lesser uncertainties involve the chemical reaction rates and solar EUV fluxes. Our first algorithm uses the fact that neutral winds are, to a good approximation, linearly related to the ionospheric peak height which is readily obtained from measurements. Our algorithm continually adjusts the wind input so as to accurately reproduce the measured peak height. Other algorithms constrain the model electron and neutral temperatures based on particular measurements. By constraining the model with measured electron temperatures in the topside ionosphere, we are able to deduce the heat flux from the plasmasphere. With all of these constraints in place, we are able to perform more quantitative modeling of diurnal, seasonal, magnetic storm, and solar cyclical electron density variations in the ionosphere. This paper will show the capability of these algorithms to improve our understanding of ionospheric variability.

B/H1-7
1620

DISCOUNTINUITY EFFECTS DUE TO SUDDENLY IMPOSED BOUNDED PLASMA MEDIUM ON WAVE PROPAGATION

V. R. Goteti* and S. Kapoor
***Department of Electrical Engineering**
Alabama A&M University, Normal, AL 35762

The dispersive effects of an isotropic transient plasma medium on a plane wave are analyzed in this paper. Transient plasmas are characterized by a number density that rises rapidly to a final value and decays slowly due to recombination and other effects. Generally such plasmas are confined to a finite region in space. Thus a temporal discontinuity as well as a spatial discontinuity in the properties of the medium are involved in this problem. It is necessary to examine the individual contribution of these discontinuities to the fields of the resulting waves.

The basic effects of such a plasma on wave propagation can be analyzed by approximating the plasma as a suddenly created plasma half-space. In this analysis, a plane wave is assumed to be propagating in the positive z-direction and at time $t = 0$ the $z > 0$ half-space is suddenly converted to a plasma medium. Some work has been done in this regard earlier (D. K. Kalluri, *IEEE Trans. on Plasma Sci.*, **AP-16 (1)**, 1988, 11-16) In this paper, a complete solution for fields in the $z < 0$ free-space as well as in the $z > 0$ plasma medium is obtained. The solution is arranged such that the effects of temporal discontinuity and spatial discontinuity and transient effects resulting from the creation of the plasma are clearly identified. Results are compared with a steady state solution to the problem which is derived independent of the transient solution.

The problem is formulated as an initial value problem in time domain and a boundary value problem in space domain. A solution is obtained using Laplace transforms with respect to time variable and solution of ordinary differential equations with respect to the space variable. The solution contains Laplace transforms of Bessel like functions and terms having simple poles on the $j\omega$ - axis. It is known that temporal discontinuity results in the conservation of the wave number and a shift in the wave frequency. Spatial discontinuity conserves the frequency of the waves. Based on this, the terms containing poles that correspond to the upshifted frequency are identified as caused by the temporal discontinuity effects. Terms containing poles that correspond to the original wave frequency are identified as caused by the spatial discontinuity effects. The remaining terms in the Laplace transforms are attributed to purely transient terms that die out in the steady state.

The salient feature of this investigation is thus a clear identification of the discontinuity effects, frequency and fields associated with the waves in the two media, identification of pure transient terms, and identification of any other fields that are not evident from the steady state solution. The pure transient terms behave essentially like Bessel functions with respect to time. Specifically, Laplace transform for the magnetic field in the $z > 0$ plasma medium is found to contain a pole at the origin. Therefore this term does not yield the magnetic field of a traveling wave. It is found that the response due to the pole at $s = 0$ has one term that varies harmonically with the space variable, z, and a second term that decays exponentially with z.

Numerical solution at various values of the initial wave frequency confirmed the identification of the discontinuity effects when compared to the steady state solution

B/H1-8
1640

DEVELOPMENT AND RESULTS OF A NEW LOW-LATITUDE IONOSPHERE MODEL: SAMI5.2

G. Joyce* J.D. Huba
Plasma Physics Division
Code 6790
Naval Research Laboratory
Washington, DC 20375

A new low-latitude ionosphere model is under development at the Naval Research Laboratory. The model solves the continuity, momentum, and energy equations for ions along a field line from hemisphere to hemisphere. The electron energy equation is also solved. Seven ion species are considered: H^+, He^+, N^+, O^+, N_2^+, NO^+, and O_2^+. The corresponding neutral species are also considered and the MSIS86 and HWM93 models are used to obtain neutal densities and winds. The daytime photodeposition is based upon the solar EUV model of *Richards et al.* (1994) (Richards et al., *J. Geophys. Res. 99*, 8981, 1994); the nighttime photodeposition is based upon that of *Strobel et al.* (Strobel et al., *Planet. Space Sci. 28*, 1027 1980). The new code is similar in scope to the Field Line Interhemispheric Plasma model (FLIP) developed by Richards and Torr, but uses a different numerical scheme. Preliminary results from the latest version of the code (SAMI5.2) will be presented. SAMI was originally developed at NRL by *Oran et al.* (Oran, E. S., T. R. Young, Jr., D. V. Anderson, T. P. Coffey, P. C. Kepple, A. W. Ali, and D. F. Strobel, *NRL Memorandum Report 2839*, 1974) as a midlatitude ionosphere model. The numerical methods, geometry, photodeposition model, chemistry, and neutral inputs have been upgraded from the original work. The field lines are treated with the offset tilted dipole model. The ion density equation is treated as an advection-diffusion equation. The advection terms of the equation are differenced using the donor cell method. The diffusion terms are treated by implicit differencing. The coupling of the various ions in the ion density equation is handled by iterating the solution among the seven ion species at each time step until the solution converges. After the first few time steps, the solution converges in after three to four iterations. The ion temperature equation is also treated as an advection-diffusion equation. At present, there is a single ion temperature used for all the species.

Research supported by ONR, and a grant from the DoD HPC Shared Resource Centers CEWES and NAVO.

B/H1-9
1700

DUSTY PLASMA SIMULATIONS

M. Horanyi*
Laboratory for Atmospheric and Space Physics
University of Colorado
Boulder, CO 80309-0392

The study of dusty plasmas bridges traditionally separate subjects: celestial mechanics and plasma physics. Dust particles immersed in plasmas and UV radiation collect electrostatic charges and respond to electromagnetic forces in addition to all the other forces acting on uncharged grains. Simultaneously they can alter their plasma environment. Dust particles in plasmas are unusual charge carriers.They are many orders of magnitude heavier then any other plasma particles and they can have many orders of magnitude larger (negative or positive) time dependent charges. Dust particles can communicate non- electromagnetic forces (gravity, drag, radiation pressure) to the plasma that can represent new free energy sources. The Jovian magnetosphere shows a number of dusty plasma phenomena. The ring/halo region close to the planet, allows for the remote sensing of the fields and particles environment of the inner most regions of the magnetosphere. The dust streams, seen by Ulysses and Galileo, put constraints on the plasma properties of the Io torus, for example. The magnetosphere sculpts the size and spatial distribution of the small grains often resulting in capture, transport, energization and ejection of the dust particles. In this talk The analysis of the observations of the Galileo Dust Detector System (DDS) requires extensive computer simulations for the interpretation of the data. These simulations require a detailed description of the fields and particles environment and provide a unique consistency test of our models of the jovian magnetosphere.

The DDS observations indicate at least 3 different populations of dust grains in the jovian magnetosphere: 1) very small and very fast stream particles, 2) prograde big grains related to satellites and 3) big grains unrelated to satellites, some on retrograde orbits. In addition to the analysis and interpretation of these DDS observations we will also provide numerical models of the jovian ring/halo region. The SSI and NIMS observations provide detailed new information on the spatial structure and size distribution of small dust particles in this region. These observations will be used to infer the plasma conditions near Jupiter where no measurements are available.

C1-1
1340

WAVELET ANALYSIS OF HIGH ALTITUDE TEMPERATURE DATA

C. Y. Chen, M. C. Kelley
School of Electrical Engineering,
Cornell University, Ithaca, NY

D. L. Walters
Department of Physics,
Naval Postgraduate School,
Monterey, California

David Fritts, Denis Riggin
Colorado Research Associates,
3380 Mitchell Lane,
Boulder, Colorado

In this paper, and a companion paper that follows (Chen et al, *in preparation,* 1998), we apply wavelet transforms to analyze high-resolution balloon measurements of atmospheric temperature. Our goals are several. In this paper we use the wavelet method to isolate features in the data stream which are highly localized in space and which have very high wavenumber components due to the edge-like features, known among the laboratory turbulence community as ramp-cliff structures (e.g., Antonia et al, *J. Fluid Mech., 84* , 561-580, 1978; Mestayer, *J. Fluid Mech., 125* , 475-503, 1982; Sreenivasan et al, *Phys. Fluids, 20,* 1986-1988, 1977). Wavelets have the advantage over Fourier analysis of defining in an optimum way both the scale size and location of the edge dominated features. Once the edge dominant features are isolated, the residual signal can be interpreted for evidence of quasi-homogenous turbulence (Alcala et al, *In preparation,* 1998a; Alcala, *In preparation,* 1998b; Mallet and Zhong, *IEEE Trans. Pat. Anal. Machine Intel., 14,* 710, 1992). We show that these structures dominate the small-scale and possibly isotropic turbulent portion of the data stream and lead to a power spectra with a spectral index whose absolute value is larger than 5/3. Our goal is to extract information about the edges in the data to determine their contribution to the scatter power received by the radar.

C1-2
1400

NOVEL MULTIDIMENSIONAL OPTIMAL GRID TRANSFORMATION FOR DYNAMIC MEDIA

Ashok K Gupta
SIGCOM Company
10 Wheeler Road
Westborough, MA 01581

This paper analyzes multidimensional optimal grid transformation technique (- Emistical dynamic mapping, E. Gupta, Appendix 1 and 2, A. K. Gupta, Proc. Of National Radar Conf., Dallas, TX, May 1998), with applications to variable super high speed data transfer and chip resolution, to simulate deterministic and ripple (- "colored" and white noise) media and its rotational Gama dynamics, rather than previously published specular, diffusive and anisotropy. Furthermore, this paper analyzes multichannel multidimensional process graph via grid and optimal grid (-edge) transformation, for data split and/or media split and its process dynamics (including chaos and growth , J. Gupta, Appendix 3, Proc. Of National Radar Conf., Dallas, TX, 1998).Such process results in different weather patterns and arbitrary system dynamics including irreversible media shift and intermittency patterns in media and/or nodal network (e.g. meteor-burst channels).

In the proposed grid transformation, the multidimensional media is represented as H= T A P F D, where A-amplitude, P-phase, F-frequency, D-space (direction), T-transformation (including time). In general, each domain matrix can be represented by a coded system matrix (time variable or random). Note that with this grid, the discrete multidimensional output data set is a linear (or non-linear or functional optimally) combination of discrete multidimensional input data set. Therefore, Y=H U, U is deterministic, networked, random etc.. In the process graph, the multidomain signal S=T A P F D U. In many general signals and mediums, any or all domains can be coupled , in terms of rate of change, e.g. dP/dF, dP/dT etc., which can be split by a canonical transformation as an input U-output S process graph. Interpretation of matrix transformation (in terms of nonoverlap beams)and the analysis of fluctuations in phase domain is yet to be done. Known structure density is proposed in this paper to analyze or synthesize phase ripple.

Previously known analytical media simulation methods are: Partial differential equations, distortion analysis, state variables, delay line, polynomials. Past data synthesis methods are: complex exponential data fit for EKG in 60's, differential equations for cardiovascular system in 60's, time-series statistics, linear prediction (and its matched filter in 1978). This author in 1974 MS thesis synthesized system spectrum (amplitude and phase) and phase pole- zero approximation (delay approximation in s-domain) model for specified input-output blood pressure BP signals at Tufts University, Mass..Digital data transfer function (for nonlinear source) was found to be noisy. Therefore techniques to split fluctuations are of interest.

The optimal mapping for any random media (layered and/or concatenated) and data as linear or non-linear functionals (such as Emistical growth model proposed in this paper by Vanderpole nonlinear equation with piece-wise + - dynamic slope conductance's) and loss control for deterministic component (possibly by new " high conductor" materials) are of future interest. The dynamic relationship between vanderpole equation and infinite potential well Schrodinger equation is of continued interest.

C1-3
1420

ITS ADVANCED ANTENNA TEST-BED

Kenneth C. Allen
Institute for Telecommunication Sciences
U.S. Dept. of Commerce, ITS.S, 325 Broadway
Boulder, CO 80303-3328

The Institute for Telecommunication Sciences of the National Telecommunication and Information Administration, U.S. Department of Commerce, has established a test-bed for promoting the development of adaptive antenna technology for mobile communications. The ITS Advanced Antenna Test-Bed makes it possible for the performance of adaptive antennas used for mobile communications to be compared for real-world urban, suburban, and rural environments.

The test-bed is located in Boulder, CO where the proposed air-interface standards for PCS were tested by the T1/TIA Joint Technical Committee. The test-bed consists of several antenna sites of various heights and locations within and around Boulder. Instrumentation has been developed that allows the simultaneous sampling and digitization of the signal from each element of a multiple element or array antenna. Up to 40 mega-samples per second on each of four channels is currently possible. Several mobile units transmitting pseudo-random noise codes up to 10 mega-chips per second can be operated. This allows the simultaneous and repeated measurement of the channel impulse response to each antenna element as frequently as once every 51 s. In addition, arbitrary waveforms or real mobile communication system waveforms can be transmitted.

Several applications of the test-bed are possible to advance adaptive antenna technology. One, that is in progress, is to create a data base of signals sampled from the elements of various antennas while mobile units transmit direct sequence spread spectrum signals. This data will be made available to other researchers for realistic simulation, testing, and comparison of adaptive antenna algorithms, ranging from diversity combining to digital beam forming. This data can potentially be used to determine the dynamic channel impulse response to each antenna element so that adaptive antenna simulations can be made for any potential system waveform.

Particular antenna designs may be used or tested by the above method. In addition, complete adaptive antenna/ mobile communication systems can be tested in a real-world environment for which the fading and delay spread statistics have been well characterized. This is particularly important for the comparison of the actual performance of the wide variety of adaptive antenna technologies in development.

Results from initial measurements in the 1900 MHz, unlicensed, PCS band are presented.

C1-4
1440

MATCHED AND ADAPTIVE SUBSPACE DETECTORS

Louis L. Scharf Shawn Kraut*
Department of Electrical and Computer Engineering
Campus Box 425
University of Colorado
Boulder, CO 80309-0425

Matched subspace detectors are used for detection of a deterministic signal vector in Gaussian noise, under the various problem scenarios of known and unknown signal phase, and known and unknown noise power. Known noise power scenarios require coherent and non-coherent versions of the matched-filter. Unknown noise power scenarios require coherent and non-coherent versions of a scale-invariant, beta-distributed "cosine" statistic. The four detectors in this class have been shown to be Uniformly-Most-Powerful invariant (L. L. Scharf, *Statistical Signal Processing*, chapter 4, Addison-Wesley, 1991) and GLRT (Generalized Likelihood Ratio Tests) (L. L. Scharf and B. Friedlander, Matched Subspace Detectors, *IEEE Trans. Signal Processing*, **42**(8):2146-2157, 1994).

We will present a comprehensive summary of the adaptive versions of these detectors, for unknown noise covariance, which employ a sample covariance estimate based on training data. The *adaptive subspace detectors* are obtained from a GLRT formalism, from maximizing the joint likelihood ratio of both training and test data, with the noise covariance as a additional unknown parameter set.

When the noise power is assumed to be constant between training and test data, the detectors obtained are the well-known GLRT of Kelly (E. J. Kelly, An Adaptive Detection Algorithm, *IEEE Transactions on Aerospace and Electronic Systems*, **22**(1):115-127, 1986), and its coherent version. When the noise power is not not constrained be constant between training and test data, we have shown that the "cosine" statistic is GLRT; remarkably, this scale-invariant detector is GLRT under both the non-adaptive and adaptive scenarios.

We will compare the appropriate operating regimes and performance of these detectors, using our method of "stochastic representations" (S. Kraut, L. T. McWhorter, and L. L. Scharf, A canonical Representation for Distributions of Adaptive Matched Subspace Detectors, in *Proceedings of the 31st Annual Asilomar Conference on Signals, Systems, and Computers*, 1997). We have shown that each adaptive detector can be paired with a statistically equivalent expression of five independent scalar random variables, three of which account for the random fluctuations in the sample covariance matrix. These expressions are insightful, and greatly simplify several computational analysis tools.

C1-5
1500

PASSIVE INTERMODULATION MEASUREMENT ROUND-ROBIN FOR U.S. WIRELESS INDUSTRY

Jeffrey A. Jargon and Donald C. DeGroot
National Institute of Standards and Technology
325 Broadway, Mail Stop 813.01, Boulder, CO 80303 USA
Tel: (303) 497-3596 | Fax: (303) 497-3970 | E-Mail: jjargon@nist.gov

Passive intermodulation (PIM) is a form of signal distortion that occurs whenever signals at two or more frequencies conduct simultaneously in a passive device, such as a cable or connector, which contains some non-linear response. The non-linear behavior produces spurious signals whose frequencies are linear combinations of the frequencies of the original signals. Odd-ordered intermodulation (IM) products (eg. $f(IM_3) = 2*f_1-f_2$) are usually the most problematic in the wireless industry since they have the highest potential of falling within the receive band, or up-link, of a base-station and creating rf interference in the receiver. Although frequency allocations are specifically designed to guard against this phenomenon, collocation of two or more base-station transceivers at a single site substantially increases the risk of PIM interference (M. Lang, *Microwave Journal*, 20-28, May 1995).

Base stations built for mobile communications systems such as PCS 1900, AMPS, GSM, and DCS 1800, use DIN 7-16 and Type N coaxial connectors to handle the high transmit power requirements. At these high power levels (above 1 Watt), nonlinearities present in coaxial connectors become apparent and measurable. There are many possible causes of intermodulation in coaxial connectors and cables including poor mechanical contact, dissimilar metals in direct contact, ferrous content in the conductors, debris and dust within the connector, poor surface finish, corrosion, vibration, and temperature variations (J. S. Petit and A. D. Rawlins, *Proceedings Third ESA Electronic Components Conference*, 45-49, Jul. 1997).

At the request of several base station equipment manufacturers, the National Institute of Standards and Technology (NIST) has begun a PIM measurement comparison for the U.S. wireless industry. The goal is to determine the level of agreement in PIM measurements made by participating companies for currently deployed communication bands. Two sets of artifacts were obtained for the comparison, one to be used as control standards by NIST, and the other to be circulated among the participants. Each set contains four two-port artifacts with DIN 7-16 connectors and varying levels of passive nonlinearity (on the order of –100 dBm).

For this comparison, the power of the third-order IM products of each artifact are measured with two cw signal sources, each measuring +43 dBm (20 Watts) at the test ports, following the International Electrotechnical Commission's guidelines (IEC Technical Committee 46, Working Group 6). Each artifact is measured within the receive (up-link) band of any or all of the four communications bands when the two +43 dBm signals are tuned to fall within the corresponding transmit (down-link) band. The minimum required data from each participant is a single third-order intermodulation power in one communication band. Participating companies who have the ability to make swept frequency measurements are encouraged to make additional measurements at specified frequencies.

At the end of the comparison, we will present each of the participants with a report showing how their measurements compared with everybody else's, keeping the other companies' identities confidential. In this presentation, we will present preliminary results of the comparison. Due to the small number of data sets collected to date, we will only show the spreads at each of the data points without reporting average measured values in order to avoid biasing future results. Only after a significant number of participants have reported their data, will we publish average values.

C1-6
1540

AVERAGE CYCLE PHASE RELATION BETWEEN TWO QUAZIPERIODIC SERIES - A NONSPECTRAL APPROACH

Samuel J. Haimov*
Atmospheric Science Department
University of Wyoming
P.O.Box 3038
Laramie, WY 82072

Richard K. Moore
Radar Systems and Remote Sensing Laboratory
University of Kansas
2291 Irving Hill Road
Lawrence, KS 66045

In this presentation we will discuss a new approach of studying radar backscatter modulation by the long gravity waves. Here is the idea: 1) Use a finite autoregressive parametric model to model long ocean waves (surface elevations and/or wave slopes). 2) Determine instantaneous wave quasi periods for the predominant waves (maximum energy in 0.1 to 0.4 Hz frequency range). 3) Transform the single cycle decomposition of the surface elevation (or wave slope) to phase series. 4) Compute ocean radar backscattered power phase distribution.

The essence of this technique is to obtain a stable estimate of a time series phase distribution. For that we require time series to be a narrow band random process with a single or multiple spectral peaks. We than can use the dominant frequency of each cycle and its initial phase to map the amplitudes of the individual cycles (not necessarily sinusoidal) into the phase space. All individual cycles are then averaged in the phase domain to form the phase distribution.

Results from simulated time series and actual measurements of ocean surface elevation show minimal phase error for the simulation and tolerable mean phase error (less than 3 deg) for the wave-height series. The standard deviation of the phase error depends on the number of averaged cycles and for more than 50 individual cycles it is less than 5 deg.

Finally we use this technique to derive the long wave phase distribution of the ocean radar backscatter.

C1-7
1600

ON THE USE OF SPIRAL ANTENNAS FOR TARGET LOCATION ESTIMATION

Robert Penno* and Krish Pasala
Department of Electrical and Computer Engineering
University of Dayton, 45469-0226

Abstract: Multi-mode, single aperture antennas, such as the N-arm spiral antenna, have been useful in the estimation of the direction of arrival of an electromagnetic source. Typically, the terminal outputs of the multi-arm spiral are connected to a modeformer. Comparison of the phases of the modeformer outputs yields the azimuth of the incident radiation. This work describes the development of closed form representations of the modeformer outputs and how these explicit expressions are useful in obtaining azimuth and elevation information from a single spiral antenna. Furthermore, super resolution techniques, such as the Maximum Likelihood Approach (MLA) and the MUSIC algorithm, are employed to provide improved angle estimates, especially in areas where the phase comparison method fails.

Physical arguments are employed to argue that the radiation corresponding to the m^{th} mode at the output of the modeformer emanates from an active circular region on the spiral whose circumference is $m\lambda$. This active region, induced by θ- or ϕ-polarized incident fields, supports a traveling current wave which result in modeformer outputs described by:

$$M_{\theta}^{n} = E_0 I_n \left(\frac{n\lambda}{2\pi}\right) \pi j^n e^{-jn\phi_0} \left[\cos\theta_0 \left(J_{n-1}(n\sin\theta_0) + J_{n+1}(n\sin\theta_0)\right)\right]$$

$$M_{\phi}^{n} = E_0 I_n \left(\frac{n\lambda}{2\pi}\right) \pi j^{n+1} e^{-jn\phi_0} \left[\left(J_{n+1}(n\sin\theta_0) - J_{n-1}(n\sin\theta_0)\right)\right]$$

where $J_n(x)$ is the Bessel's function of the first kind of n^{th} order, and the elevation and azimuth angles of the source are given by (θ_o,ϕ_o).

The closed form expressions given above lead to explicit representations of the steering vectors of the multi-mode spiral. The availability of these steering vectors makes it possible to implement the super resolution techniques, i.e. the MLA and the MUSIC algorithm. The angle estimates from a moving platform obtained using these two approaches are compared with those provided by the phase comparison method by using a non-linear, least squares estimator to determine the location of the source. Results obtained from the computer model which compare the effectiveness of these three methods will be presented and discussed.

C1-8
1620

A MORE ROBUST METHOD FOR UNWRAPPING IN THE PRESENCE OF DENSE FRINGE PATTERNS

M. Costantini
Jet Propulsion Laboratory
MS 300-235
4800 Oak Grove Drive
Pasadena, CA 91109
E-mail: mc@ampersand.jpl.nasa.gov

Phase unwrapping is the problem of reconstructing a function on a grid given its values modulo 2π. Phase unwrapping problems occur in many fields, and a number of techniques have been developed for Phase Unwrapping.

In this work, we examine an interesting phase unwrapping problem arising in Synthetic Aperture Radar (SAR) differential interferometric measurements of fast glacier motion. In contrast to most other applications, these phase data can present areas characterized by very dense (close to one per pixel) fringes and by very distinct phase patterns (Moiré and bull-eyes patterns). More precisely, the absolute value of the "discrete partial derivatives" (i.e. the neighboring pixel differences) of the phase function to be reconstructed exceed π in extended regions, which contradict the starting assumption of classical phase unwrapping algorithms. Moreover, an approximating function for the phase surface to be reconstructed is not usually known that can be used to modify the original data to have the above hypothesis fulfilled almost everywhere. In order to circumvent this problem, in the proposed phase unwrapping method we do not make use of this classical assumption, but we exploit a regularity hypothesis on the "discrete partial second derivatives." This approach allows to extend the region which can be successfully unwrapped.

The proposed phase unwrapping method is applied to data sets that include ERS SAR differential interferometric measurements of glacier motion in Greenland and Antarctica. Comparison with the results obtained by using the classical approach shows that significant improvements are achieved in the areas characterized by the above underlined phenomena of very dense fringes, while consistent results are obtained in the other cases.

C1-9
1640

SOLAR EFFECTS ON CELLULAR PHONE SYSTEMS

David J. Thomson*
Mathematics Research
2C-360
Bell Laboratories
Murray Hill, NJ 07974

Many cellular phone systems drop calls at a higher rate in summer than in winter and also have larger day-to-day fluctuations than can be reasonably expected from known causes. In this talk I describe some time-series analysis that has been done to try and identify the causes of this problem. The cellular phone data is corrected for hour-of-day and day-of-week changes in usage, and missing observations in the radio data are estimated with an EM version of Wiener interpolation. The coherence between the series is then calculated by multiple window methods. These are jackknifed over windows to obtain non-parametric confidence intervals. Much of this problem can thus be attributed to tropospheric ducting and related effects, but a significant fraction is related to solar effects. Although solar activity is quite coherent with all the dropped call indicators, direct solar radio noise seems to be a minor part of the problem, while solar effects coupling to climate variables seems stronger.

Estimates of the coherence between the daily fraction of calls dropped for interference and the USAF's 1415 Mhz solar flux measured at Sagamore, MA from Jan. 1, 1996 to July 31, 1997 show highly significant levels, above the 99 percent level, at a series of discrete frequencies. The same frequencies, from 1.1 to 5.26 microHertz, have been identified in other solar phenonema, such as particle fluxes observed by *Ulysses*, and are believed to represent discrete solar modes, although whether the modes are g, gravity, or r, convection, types is presently unknown. Some of these modes are observed in both 10.7 cm flux and also in long series of daily temperature observations. These show that the frequencies remain stable within a few nHz over a span of 200 years, suggesting that they are g modes.

The phase of the coherence at the modal frequencies shows that the radio flux leads the dropped calls by two or three days, implying that solar wind effects are primarily responsible; again the mechanism is unknown.

E2-1
1340

STATISTICAL ANALYSIS AND MODELING OF LOW-FREQUENCY RADIO NOISE AND IMPROVEMENT OF LOW-FREQUENCY COMMUNICATIONS

Douglas A. Chrissan* Antony C. Fraser-Smith
Space, Telecommunications and Radioscience Laboratory
Department of Electrical Engineering
Durand Bldg., Rm. 202
Stanford University
Stanford, CA 94305-9515

We present work on the statistical characterization and modeling of atmospheric radio noise in the range 10 Hz – 60 kHz (denoted *low-frequency* noise), with the specific goal of improving communication systems operating in this range. The statistics analyzed include seasonal and diurnal variations, amplitude probability distributions (APDs), impulse interarrival time distributions, background noise statistics, and power spectral densities; the analyses are based on many thousands of hours of measurements made by the Stanford ELF/VLF Radio Noise Survey.

A number of noise models which accurately represent low-frequency noise APDs are compared, and two of the simplest models (*i.e.*, each with only two parameters) are found to give extremely good performance in general. These are the Hall and alpha-stable (or α-stable) models, both of which approximate the Rayleigh distribution for low amplitude values but decay with an inverse power law for high amplitude values. It is concluded that the Hall model is the optimal choice in terms of accuracy and simplicity for locations exposed to heavy sferic activity, and the α-stable model is best for locations relatively distant from heavy sferic activity.

Based on the statistical characteristics of the noise data, a new clustering Poisson atmospheric noise model is developed. This model is based on several previously known statistical-physical models, but in addition takes into account the clustering of sferic impulses. It is shown that the clustering model accurately predicts the statistical features found in low-frequency radio noise data.

Finally, the bit error rate (BER) performance of receivers specifically designed for α-stable noise is compared with the BER performance of conventional low-frequency receivers. The communication signal formats examined are quadrature phase shift keying (QPSK) and 16 point quadrature amplitude modulation (16QAM). Hundreds of simulations using time-series data from various times and locations and at various center frequencies and bandwidths are performed, and the following results are found uniformly: for QPSK signals, virtually no performance improvement is gained when using an α-stable receiver instead of the best conventional receiver, but for 16QAM signals, an improvement of several dB is gained by using an α-stable receiver.

E2-2
1400

THE EFFECTIVE ANTENNA NOISE FIGURE F_a FOR A VERTICAL LOOP ANTENNA AND ITS APPLICATION TO ELF/VLF ATMOSPHERIC NOISE

Antony C. Fraser-Smith* Frankie Y. Liu
STAR Laboratory
Stanford University
Stanford, CA 94305

Expressions tabulated for the effective antenna noise figure F_a usually assume an electric-field antenna, since most measurements of radio noise are made on the electric field of the noise. In addition, the International Radio Consultative Committee (CCIR) noise model predictions for F_a are made only for electrically short, grounded, vertical monopoles located over a perfect ground. However, at frequencies lower than those traditionally used for communications, i.e., at extremely-low frequencies (ELF; frequencies in the range 3 Hz to 3 kHz) and very-low frequency frequencies (VLF; frequencies in the range 3–30 kHz), it is common for magnetic-field loop antennas to be used, and the CCIR tabulated expressions for F_a for short monopoles do not apply.

This paper reports the derivation of an expression for F_a as measured by a small vertical magnetic-loop antenna and its subsequent application to ELF/VLF radio noise measurements made at a variety of locations around the world. There is good agreement between the F_a values derived from these measurements (using the new expression for F_a) and estimates of maximum and minimum F_a values for the ELF/VLF range published by Spaulding and Hagn in 1978 (Spaulding, A. D., and G. H. Hagn, *Proceedings: Effect of the Ionosphere on Space and Terrestrial Systems*, 117–182, 1978), and summarized for the CCIR in 1982 (CCIR, *Report 670*, 184–196, 1982), but an improved fit to the measurements can be obtained by making moderate adjustments to the maximum and minimum values at both the low (10–100 Hz) and high (8–32 kHz) frequency limits of the ELF and VLF bands, respectively.

E2-3
1420

VHF SPORADIC E - A SIGNIFICANT EMI FACTOR

Ernest K. Smith
ECE Department
University of Colorado
Boulder, CO 80309-0425

Sporadic E, or or Es, is an ionospheric propagation mode which is useless for service, but is crucial for estimating interference at the low end of the VHF band. It has played a determining role in spectrum allocations for FM and TV. Es is particularly important in Asia where temperate-latitude sporadic E has its summer and yearly peaks.

While sporadic E was studied from ionograms starting in the 1930s the first systematic studies of oblique-incidence sporadic E were not published until 1944 in the United States (FCC Docket No. 6651, Sept. 28, 1944) and until 1954, at least in English, in Japan (T. Kono, Y. Uesugi, M. Hirai and G. Abe, *J. Radio Research Lab.., Tokyo,* **1**, 1, 1954). It was the comparison of these two studies that first led to the recognition of the longitudinal peak in temperate-latitude sporadic E over Asia (E.K. Smith, NBS Circular 582, March 15, 1957). Radio amateurs operating at 50 MHz have since provided a wealth of data.

Our understanding of sporadic E had progressed considerably in the 1950s (see the survey by J.A.Thomas and E.K. Smith, *J. Atmos. & Terr. Phys.*, **13**, 295-314, 1959) but took an impressive leap forward in 1960 with the advent of the windshear theory of formation of sporadic E. As a consequence the 1960s were a time of active sporadic-E research (see the survey by J.D. Whitehead *Rev. Geophys. & Space Phys.* **8**, 85, 1970).

The European Broadcast Union made extensive VHF Es measurements in the late sixties and early seventies. These results and others were utilized by the CCIR of the International Telecommunications Union in an extensive study by Interim Working Party 6/4, under the chairmanship of Dr. Kenichi Miya, resulting, in 1978, in an internationally-approved prediction method for estimating VHF field strength due to sporadic E (now to be found as Recommendation 534-3 of Study Group III, ITU-R) .

The method adopted in Rec. 534-3 melds the VHF oblique-incidence data with ionogram data to provide a world-wide method for predicting duration and field-strength of temperate-latitude sporadic E. The technique involves extrapolating semi-log hourly values of vertical critical frequency (fEs) from observed occurrence values of fEs > 7 MHz and fEs > 10 MHz. The current study, undertaken with the collaboration of Kyoshi Igarashi of the Communications Research Lab. (Tokyo), tests the accuracy of the CCIR/ITU-R prediction method for the Japanese chain of ionospheric vertical sounding station for prediciting fEs > 15 MHz. The agreement is found to be surprisingly good. These results were first presented at the Beijing 1997 Symposium on Electromagnetic Compatibility, in a paper jointly authored by Smith and Igarashi. Examples of interference to Chinese TV reception from Japan were given and seen to be substantial.

E3-1
1440 **Time Domain Characterization of Antennas with TEM Feeds**

Everett G. Farr*, Carl E Baum†
*Farr Research Inc., 614 Paseo Del Mar NE, Albuquerque, NM, 87123
†U.S. Air Force / DEHP , 3550 Aberdeen Ave., Kirtland AFB, NM 87117

We provide here a clear accounting of how to relate the source voltage from a 50 Ω source, through a transmitting and receiving antenna, into a 50 Ω load. Transmission coefficients at impedance mismatches are handled explicitly. A relationship is provided between the area under the antenna's impulse response and the line dipole moment of the aperture.

We also show that the antenna equations are simplified considerably by normalizing voltages and electric fields to the local characteristic impedance. In doing so, we introduce a universal time domain antenna parameter, $h_N(t)$. When the antenna equations are expressed in terms of $h_N(t)$, the equations take on a number of useful simplifications. First, the transmission coefficients between the feed cable and antenna impedance are eliminated. Second, the impedance of the antenna is eliminated. Normally an assumption has to be made that the antenna impedance is a constant, but it does not appear in our formulation. Third, the normalized impulse response applies to both transmission and reception equations. Fourth, the expressions in transmission and reception are as simple as one can imagine that they will ever get. Finally, by writing our equations in this manner, we are able to tie the theory back to measurements that are routinely made on transient antennas. The process of normalizing voltages to the local characteristic impedance is reminiscent of S-parameters in circuit theory.

E3-2
1500

DESIGN AND MEASUREMENT OF A CONICAL COAXIAL TRANSMISSION LINE-FED COAXIAL BEAM-ROTATING ANTENNA

C. Courtney*
Voss Scientific
418 Washington St, SE
Albuquerque, NM 87108
C. E. Baum R. Torres
Air Force Research Laboratory / DEHP
3550 Aberdeen Dr. SE, Kirtland AFB, NM 87117-5776

The fundamental principles and characteristics of the Coaxial Beam-Rotating Antenna (COBRA) have been presented (C. Courtney et al, Sensor and Simulation Note 395, Air Force Research Laboratory, 1996), and the design and measured performance of a second prototype have also been reported (C. Courtney et al, EUROEM98, Tel Aviv, Israel, 1998). This paper describes the design and measurement of a third type of COBRA antenna. The COBRA III prototype antenna is cassegrain with a paraboloidal main reflector, a hyperboloidal subreflector, and a novel feed geometry that is bolt-on compatible with many High Power Microwave (HPM) sources (K. Hendricks et al, IEEE Trans. Plasma Science, vol. 26, no. 3, June 1998). The COBRA III feed begins as a circular coaxial transmission line and converts to a conical transmission line that has its vertex coincident with that of the paraboloidal reflector. The center conductor attaches directly to the subreflector. The line launches a quasi-spherical wavefront onto the subreflector, which reflects it back into the main reflector. To prevent it from intercepting the wave reflected from the subreflector, the outer conductor of the conical transmission line feed is truncated at a point short of the total length of the center conductor, and folded back to act as a guide for the wave reflected from the subreflector.

In addition, a design procedure to optimize the subreflector size as a function of the transmission feed line electric field mode and main reflector size is presented. The dimensions of the optimum subreflector are computed for the transmission line field distribution, and the dimensions of the conical transmission line are determined. Also, since a main application of the COBRA designs will be as antennas for HPM sources, a calculation of the optimum coaxial transmission line impedance is presented. This optimum value will minimize the peak electric field for a given power level. Finally, a summary of the complete COBRA III prototype design is given and some measured data indicative of the antenna input impedance, far-field pattern, gain and bandwidth will be shown.

E3-3
1540

A SYMMETRY RESULT FOR AN ANTENNA ON A GROUND PLANE

Carl E. Baum
Air Force Research Laboratory
AFRL/DEHP Bldg 909
3550 Aberdeen Avenue SE
Kirtland AFB NM 87117-5776

In some applications it is desirable to mount an antenna on a finite-size or truncated ground plane which is separated from other nearby scatters (e.g., the earth surface). One class of such applications concerns the matching of single-ended sources producing transient waveforms to a single-ended antenna, the truncated ground plane being the "ground" or reference potential for the source. Examples of interest are the half reflector impulse radiating antenna (IRA) and the half lens IRA (TEM horn with lens). The alternate to this approach is a differential source driving a differential (symmetric) antenna, or a single ended source matched to a differential antenna via a balun, a difficult task for extremely high powers and extreme bandwidth pulses.

For an observer on the reference plane (infinite) on which the ground plane lies, one can use symmetry considerations (partial symmetry) to analyze and simplify the results. Considering the radiation of a transient pulse, for a time window of width t_g (ground-plane-contour clear time) the fields are precisely ½ the fields for the antenna plus image, a symmetrical configuration. This and other considerations influence the choice of ground-plane size and shape for best antenna performance.

From a low-frequency point of view one can consider the transmitting antenna as characterized by electric and/or magnetic dipole moments. (The reflector IRA, for example, can have both. A relevant questions concerns how close these moments are to ½ those for the antenna plus image (differential mode for addition with $2V$ excitation). One can also make a similar comparison of the input impedances. With no (or negligible) structures attached below the ground plane, as one makes the ground plane larger in all directions on the reference plane this ideal factor of ½ is asymptotically approached. How large one should make the ground plane can be estimated based on calculations for appropriate canonical geometries.

E3-4
1600

COMPREHENSIVE TIME-DOMAIN FIELD MAPPING OF A HALF-IMPULSE RADIATING ANTENNA

J. Scott Tyo* Jon S. H. Schoenberg
AFRL/DEHP
3550 Aberdeen Ave SE
Kirtland AFB NM 87117

A comprehensive field mapping of a half-impulse radiating antenna (HIRA) has been performed to determine its near, intermediate, and far zone radiation patterns when driven by a fast-rising step function. The HIRA is a wideband focused aperture antenna, the design principles of which is presented by Farr and Sower (E. G. Farr and G. D. Sower, *Sensor and Simulation Notes,* **390**, 1995). The antenna under consideration consists of one-half of a 1-meter diameter parabolic reflector mounted on a truncated ground plane illuminated by two 200 Ω TEM horn feed arms. The apeces of these feed arms meet at the antenna focal point on the ground plane, presenting a 100 Ω impedance to a single-ended source. The feed arms are terminated at the reflector edge in their characteristic impedance. The source drives the HIRA with a 15 ps risetime, 4 ns step function. Various sensor antennas were used. Near-field measurements were accomplished with a EG&G D-dot probe and a single-ended TEM horn sensor manufactured by Farr Research. Intermediate and far field measurements were performed with a replicating TEM horn with a balanced differential input designed by the Air Force Research Laboratory. Data was collected with a Tektronix 11801B digital sampling oscilloscope and SD-24 20 GHz bandwidth sampling head.

Numerous measurements were performed to determine the elevation and azimuthal patterns, beam spot size, and 3 dB cutoff frequency of the radiated waveform as a function of range from the HIRA. Extensive measurements in the intermediate field were accomplished, where theoretical predictions are less established. For free field measurements, special care was taken to prevent the reception of multipath signals during the desired acquisition time window. The free field measurements show that the beam width initially broadens in the intermediate range, then narrows as the far-field is approached. High frequency content becomes relatively more prominent as far-field is approached. The effect of ground-bounce signals on the received signal is found to be a strongly dependent on the range and height above and conductivity of the conducting earth.

E3-5
1620

EXACT TRANSIENT EM LENS DESIGN

Carl E. Baum
Air Force Research Laboratory
DEHP, Kirtland AFB
Albuquerque, NM 87117-5776
Alexander P. Stone*
University of New Mexico
Department of Mathematics and Statistics
Albuquerque, NM 87131-1141

Transient lenses may be thought of as transition regions between various types of transmission lines. They may be used for a number of purposes, such as redirecting TEM waves on coaxial waveguides from one direction to another (bending lens). Another important application is in the specification of a lens Impulse Radiating Antenna (IRA). This is basically a TEM horn with a lens at the aperture to straighten out the spherical TEM wave on the conical transmission line into a plane wave at the aperture. Transient lenses used for purposes such as these are quite different from narrowband (optical or microwave) lenses. Ideally in our lens synthesis procedures the TEM wave is to be transmitted from one region to another with no distortion or reflection as the wave goes through an interface. The synthesis of such devices is usually accomplished by either a differential-geometric scaling procedure or by matching impedances at interfaces and requiring that transit times through the lens region are preserved for various ray paths. The latter method has frequently been utilized in the design of approximate lenses, while the former approach has been applied in the synthesis of certain exact lenses. Some recent results, obtained for exact lenses, concern generalized inhomogeneous TEM plane waves which are specialized to the cases of bipolarized and unipolarized waves. As a consequence an additional degree of freedom in specifying acceptable coordinate systems is obtained and leads to specific lens designs. In particular, examples of purely dielectric lenses (spatially variable permittivity and constant permeability) are described.

E3-6
1640

FIELD MEASUREMENTS OF AN ULTRA-WIDEBAND LINEAR ARRAY OF PHOTOCONDUCTIVE SEMICONDUCTOR SWITCHED SOURCES

Jon S. H. Schoenberg*
AFRL/DEHP
3550 Aberdeen Ave SE
Kirtland AFB NM 87117
M. D. Abdalla M. C. Skipper
ASR Corporation–Federal Division
7817 Bursera Drive NW
Albuquerque, NM 87120

Field measurements from an array of ultra-wideband (UWB) pulse radiators is presented. Each array element consists of a parallel-plate blumlein driving a matched, low impedance impulse radiating antenna (IRA). Each blumlein is charged with the same pulse power conditioner and each is independently commuted with a lateral photoconductive semiconductor switch (PCSS). Switching is achieved by illuminating each lateral PCSS gap with a compact, low power solid-state laser diode array and driver module. Low timing jitter of all devices used in the switching process enabling precise timing of each element for array beam forming and beam steering control. Each of the array IRAs is a tapered flat-plate rectangular TEM horn with 4:1 width-to-height aspect ratio, resulting in a 70 Ω aperture impedance. Four elements are inter-connected and stacked in the electric field plane (E-plane) so that their fields constructively add in the far field. The size of the entire array aperture is 30.5 cm on a side.

Electric field measurements were accomplished in the intermediate and far field of the array using a replicating TEM horn sensor and a Tektronix SCD-5000 transient digitizer. Measurements were made on two types of E-plane tapers for the TEM horn elements: linear and exponential. The results are compared to a frequency-domain numerical analysis using the hybrid finite element method.

E3-7
1700

Tailoring of the Transmitted Waveform from a Spark Gap via System Geometry

Jane M. Lehr and Carl E. Baum

Air Force Research Laboratory
Directed Energy Directorate
Kirtland AFB, NM

Abstract

A spark gap is a high power switch consisting of a set of electrodes separated by an insulating media. Switching occurs when a streamer discharge develops in the insulator, resulting in a minimal voltage between the two electrodes and the switching action is said to be complete when the current becomes circuit limited. Generally, features desirable for the switch initiation mechanism, such as electric field enhancement, overvoltage, delay time and switch jitter, dominate spark gap design. For the switching of pulses of microsecond length and submicrosecond duration, many geometry dependent parameters, such as capacitance, were not relevant at that timescale compared to more dominant quantities, such as spark gap inductance. Thus, rarely was consideration given to either the electromagnetic wave propagation through the spark gap, or even to its equivalent circuit model. However, as switching speeds are pushed to their fundamental limits, the wave propagation, as well as the equivalent circuit model, aspects of high power spark gaps need to be addressed.

Moreover, the output of the spark gap switch is generally of more interest for applications. A circuit model of the spark gap is introduced for an analytical solution, and bounds are placed on the circuit parameters that reflect the physical geometry of the spark gaps. A full circuit synthesis has been performed on a spark gap that is both fed and terminated in a transmission line. The transmitted waveforms are calculated from the model, and related back to the physical geometry of the system.

E3-8
1720

REQUIREMENTS FOR PHYSICAL MODELS IN LIGHTNING

Robert L. Gardner
Spectral Synthesis Labs
6152 Manchester Park Cir.
Alexandria, VA 22310
Carl E. Baum
Air Force Research Laboratory/DEHP
3550 Aberdeen SE
Kirtland AFB, NM 87117.5776

There are many models of the lightning return stroke in the literature. These models have different purposes. For example, "engineering" models may be designed to quantify, in an approximate sense, the fields from lightning that might be used to state a threat that an engineer must design a product to withstand. A "physics" model may be designed to predict, from first principles, an observable of the lightning, like its electromagnetic fields. The "physics" model also may predict that connection between certain physical quantities such as the connection between current and brightness. We would like as much physics as practical in the "engineering" models and the "physics" models should predict the quantities important to the engineers.

Systems designers require current waveform envelopes or estimates to properly design systems that are hard to direct lightning strikes. It is difficult to measure the currents directly, but it is relatively easy to measure the distant fields that are related to the lightning currents through the Green's function. This process of determining the currents from the fields is an ill-posed inverse problem. It is ill-posed because the solution for the currents in not unique for a given far field value. That lack of uniqueness exists even for a simple dipole model of the lightning current. One way of treating such a problem is to impose a means of regularization on the lightning currents. For example, the lightning community often uses a double or triple exponential with an exponential decay with height with parameters available to specify the components and the decay rate.

In this paper we will examine several approaches to regularization of the lighting currents used in the inverse problem and consider the resulting loss of information with the regularization. Since there are also physics models in the literature, the regularized models can be compared directly to the physical models. Neither the physical models nor the regularized models is exact so the effectiveness of the model can be determined by how well the model can predict available data. Such data include fields and currents as well as currents and brightness.

F1-1
1340

ACCURACY OF TURBULENT DISSIPATION RATES MEASURED BY WIND PROFILERS

Earl E. Gossard
NOAA/ETL
325 Broadway
Boulder, CO 80303

An experiment at Vandenburg AFB is described that compares the profiles of turbulent dissipation rate measured by a 449 MHz wind profiler from A) Doppler spectral line broadening and B) from spectral analysis of time series of vertical velocity sensed in the vertically pointing mode. The experiment was conducted with a 449 MHz wind profiler at 147 m above sea level. The profiler was a five-beam system with 120 m gate spacing. The beamwidth was 3.3 degrees. The vertical beam data were collected every 7.5 seconds with 512 sec coherent averaging. In addition to comparing (A) and (B), the effects of velocity resolution in the Doppler spectrum on the accuracy of method (A) and the effects of averaging spectral realizations over long dwell times are evaluated, and a theoretical correction for the averaging is proposed based on an assumption that the larger scales in the turbulent ensemble lie within the inertial subrange. It is found that good resolution in the Doppler spectrum (< 0.1 m/s) is required to get good agreement between (A) and (B). The line broadening caused by long dwell times was substantial, amounting to at least a factor of two for 100 sec averages. The proposed correction of the spectral width for long dwell time provides a good estimate of the true spectrum. The data collected in this experiment are compared with earlier measurements of profiles of turbulent dissipation rate and with tower measurements. Errors and caveats are discussed and recommendations for profiler systems of the future are given.

F1-2
1400

ANALYSIS AND IMPROVEMENT OF MICROWAVE RADIOMETER TIPPING-CURVE CALIBRATIONS

Yong Han and Ed R. Westwater
CIRES, University of Colorado/NOAA
Environmental Technology Laboratory
325 Broadway, Boulder, Colorado

One factor that determines the accuracy of the water vapor and cloud liquid measurements with ground-based microwave radiometers is the absolute calibration of these instruments. A technique, often called tipping-curve calibration, which utilizes the atmosphere as the calibration source, has been applied extensively in routine operations and field experiments. However, in recent years, comparisons of tipping-curve performances among different radiometer systems and comparisons of radiometer-derived water vapor with that measured by other sensors revealed unexpected tipping-curve calibration uncertainties; thus there is a need to investigate and improve this technique. In this presentation we report results from our recent investigation and the methods we have developed to improve the calibration.

The uncertainties of tipping-curve calibrations are controlled by a number of factors, including atmospheric conditions, uncertainties in the mean radiating temperatures, effect of radiometer antenna beam width, and errors in radiometer pointing angles. These factors are evaluated in detail with models and data simulations. Methods to reduce the calibration uncertainties are developed and evaluated using both the simulated and experimental data. The experimental data were taken during the 1997 Water Vapor Intensive Operating Period (WVIOP97) at the Department of Energe's Atmospheric Radiation Measurement (ARM) Program's Cloud and Radiation Testbed (CART) site in North Central Oklahoma. A large portion of our investigation is devoted to explain the bias of about 2 mm between the integrated water vapor derived from the ARM dual-channel microwave radiometer and that measured by other remote and in situ sensors during the WVIOP97. Possible causes are identified and the bias is almost completely removed with the re-calibrations of the radiometer data, in which the developed methods are applied.

F1-3
1420

REMOTE SENSING OF WATER VAPOR BY MICROWAVE RADIOMETERS AND GPS DURING THE 1997 WATER VAPOR INTENSIVE OPERATING PERIOD: RECENT RESULTS

E. R. Westwater and Y. Han,
CIRES
University of Colorado/NOAA
Environmental Technology Laboratory
325 Broadway, R/E/ET1
Boulder, Colorado
80303-3228 USA

Seth I. Gutman
NOAA
Forecast Systems
Laboratory
325 Broadway, R/E/FSL
Boulder, Colorado
80303-3228 USA

During September 15 to October 5, 1997, an intensive experiment to measure atmospheric water vapor was conducted at the Department of Energy's Atmospheric Radiation Measurement (ARM) Program's Cloud and Radiation Testbed (CART) site in North Central Oklahoma. This experiment was called the 1997 Water Vapor Intensive Operating Period (WVIOP'97). Among the goals of WVIOP'97 was the comparison of different methods of measuring integrated precipitable water vapor (PWV). This paper focuses on the intercomparison of water vapor measurements by ground-based microwave radiometers (MWR) , Global Positioning System - Integrated Precipitable Water instruments (GPS-PWV), and by radiosondes. For this experiment, Vaisalla HUMICAP sensors were deployed on 3-hourly radiosondes for in situ measurements of water vapor; in addition, radiosondes from different calibration lots were analyzed.

Microwave radiometric measurements of water vapor in the zenith direction were made by three independent radiometers. The first was the ARM operational radiometer that operates routinely at the CART site; it produces PWV and cloud liquid path from brightness temperature T_b measurements at 23.8 and 31.4 GHz. The second and third radiometers were operated by the Environmental Technology Laboratory and operate at the frequency pairs of (20.6, 31.65 GHz) and (23.87, 31.65 GHz). The calibration of the instruments was achieved by the so-called "tip cal" method. The microwave radiometer data were also compared with two independent GPS-PWV instruments that were also operated; one was located at the CART site, while the other was located at Lamont, Oklahoma, about 9-km from the Central CART Facility. After careful recalibration of the ARM radiometer, all retrievals of PWV agreed to within about 1 mm rms over a total range of 5 to 50 mm.

Using quality-controlled radiosonde data that were obtained during clear conditions, we also compared forward model calculations of brightness temperatures with the calibrated radiometer data. The two models that we used were those of Liebe (H. J. Liebe, Int. J. Infrared Millimeter Waves, 10, 631-650,1989) and Rosenkranz (P. W. Rosenkranz, Radio Science, 33 ,919-928 ,1998). The slope (brightness temperature/optical depth vs PWV) and the intercept (at zero PWV and due to the wings of the oxygen absorption band) are compared for all of the radiometric channels used during the experiment.

F1-4
1440

NADIR SENSITIVITY OF MILLIMETER AND SUB-MILLIMETER FREQUENCIES TO CLEAR AIR TEMPERATURE AND WATER VAPOR VARIATIONS – STATISTICAL RESULTS.

M. Klein[1] and A. J. Gasiewski[2]
[1]CIRES, NOAA/ETL, R/E/ET1, 325 Broadway, 80303 Boulder, Colorado
[2] NOAA/ETL, R/E/ET1, 325 Broadway, 80303 Boulder, Colorado

There are several motivating factors for vertical sounding of temperature and moisture using microwave channels that are higher in frequency than currently employed on satellites (i.e., ~200 to ~1000 GHz). First, water vapor lines in this higher frequency range are generally stronger than below 200 GHz and it is thus possible to sense at altitudes above the middle troposphere. Second, for diffraction limited antennas of a given size improved spatial resolution can be obtained since the spot area decreases with the square of the frequency. This is particularly important for geosynchronous microwave sounding of the atmosphere. Third, the scattering coefficient α_S for spherical Rayleigh ice cloud particles varies as f^4, where f is frequency, thus facilitating cirrus cloud water path estimation.

A sensitivity study of the tropospheric to stratospheric sounding capabilities for the significant water vapor and oxygen absorption lines in the frequency range from ~10 to 1000 GHz has been performed. The TOVS Initial Guess Retrieval (TIGR) atmospheric profiles database (Chedin, A. et al., J. Clim. Appl. Met., 24, 128-143, 1985) was used to obtain seasonal and latitudinal variations in observed brightness temperatures. Several parameters, including the effective sensing height and its standard deviation, brightness temperature variations due to the natural variations in temperature and water vapor, the naturally available bandwidth for sounding at particular height and frequency, and the minimum required integration time for sensing such variations using a total power radiometer will be presented. Two extreme atmospheric conditions (summer low latitude and winter high latitude) are considered.

F1-5
1500

MILLIMETER-WAVE SPECTRAL OBSERVATIONS OF CLOUDS AND PRECIPITATION FROM AIRCRAFT AND SPACECRAFT

F. W. Chen* J. W. Barrett W. J. Blackwell P. W. Rosenkranz
M. J. Schwartz D. H. Staelin
Research Laboratory of Electronics
Massachusetts Institute of Technology
Cambridge, MA 02139-4307

Detection of clouds and precipitation using passive microwave imagery at millimeter wavelengths requires removal of most effects of surface emissivity, temperature profile, and humidity profile variations. The general approach studied here involved four steps: 1) principal-components analysis of observed microwave spectra over diverse cloud-free regions, 2) removal of the first 1-3 principal components from all data, 3) principal-component analysis of filtered data containing variable clouds and precipitation, and 4) choice of a cloud-detection metric in the multi-dimensional space of this second group of principal components.

The data employed to test this method were obtained from two passive microwave instruments: (1) the NPOESS Aircraft Sounder Testbed - Microwave Temperature Sounder on the NASA ER-2 high-altitude aircraft, which has eight channels in the 50-56 GHz oxygen band and eight double-sideband channels distributed symmetrically within +-4 GHz around the oxygen absorption line at 118.75 GHz, and which measures brightness temperatures with spatial resolution of approximately 5 km; (2) the Advanced Microwave Sounding Units-A/B on the NOAA-15 polar-orbiting satellite, with 15 channels and spatial resolution of approximately 50 km in the 23-89 GHz band, and 5 channels with spatial resolution of approximately 16 km in the 89-190 GHz band.

Overpasses of thunderstorms in central Florida show distinctive signatures of absorption and scattering by hydrometeors. When channels having similar gaseous opacities are compared, the perturbations to the clear-air brightness temperatures are, as expected, larger in the 115-123 GHz band than in the 50-56 GHz band; these perturbations are related to the altitude, size distribution, and liquid/ice phase of the hydrometeors.

F1-6
1540

POLARIMETRIC SCANNING RADIOMETER – PSR/A – ANALOG CORRELATOR AND CALIBRATION SYSTEM

V. Ye. Leuski[1], A. J. Gasiewski[2], A. J. Francavilla[2], M. Klein[1],
J. R. Piepmeier[3], I. S. Corbella[4]
[1]CIRES, NOAA/ETL, R/E/ET1, 325 Broadway, 80303 Boulder, Colorado
[2] NOAA/ETL, R/E/ET1, 325 Broadway, 80303 Boulder, Colorado
[3]School of Electrical and Computer Engineering, Georgia Institute of Technology, Atlanta, GA 30332-0250
[4] Polytechnic University of Catalonia, 08034 Barcelona, Spain

The NOAA Environmental Technology laboratory recently rebuilt the Polarimetric Scanning Radiometer/Digital (PSR/D) scanhead for the NASA Third Convection and Moisture Experiment (CAMEX-3). The new scanhead (PSR/A, analog) consists of a set of five polarimetric radiometers operating at 10.7, 18.7, 21.5, 37.0, and 89.0 GHz housed within a gimbal-mounted scanhead drum and using analog correlators to obtain measurements of the third and fourth Stokes' parameters.

The 10.7, 18.7, 21.5 GHz radiometers are direct detection receivers utilizing high electron mobility transistors (HEMT) low noise front-end amplifiers, while the 37 and 89 GHz receivers are double sideband super-heterodyne receivers. The 18.7 and 21.5 GHz channels use a broad band (18.6-21.6 GHz) antenna and front-end components, including waveguide ferrite switches and low noise HEMT amplifiers. The polarization correlators are of the analog adding correlator type and use quadrature hybrid arrays to obtain the necessary in-phase and quadrature-phase signals. This system allows measurements of the four Stokes' parameters with the direct detection receivers at 10.7 and 18.7 GHz and the first three Stokes' parameters at 37 and 89 GHz. In addition to the standard hot- and ambient-external calibration targets are semiconductor noise generators used for subinterval calibration. The hot external calibration target consists of a canted array of iron epoxy pyramids over an aluminum core.

The scanhead drum is rotatable by the gimbal positioner so that the radiometers can view any angle within 70° elevation of nadir and at any azimuthal angle, as well as the external hot and ambient calibration targets. Antennas are of the lens/corrugated feedhorn type and are dual orthogonal-linear polarized with grooved rexolite lenses. The 10.7 and 37 GHz radiometers utilize a common dual-band antenna.

Details of the radiometer design, correlation circuitry, calibration hardware and preliminary results from CAMEX-3 will be presented.

F1-7
1600

OCEAN SURFACE WIND FIELD MEASUREMENT BY PASSIVE POLARIMETRIC MICROWAVE REMOTE SENSING

J. R. Piepmeier*
School of Electrical and Computer Engineering
Georgia Institute of Technology
Atlanta, GA 30332-0250
A. J. Gasiewski
NOAA/ETL, R/E/ET1, 325 Broadway
Boulder, CO 80303

During the last several years, both satellite and aircraft measurements and modeling efforts have been made to assess the geophysical origin of passive microwave ocean wind vector signatures. The results of these efforts were directed toward the development of a geophysical model function (GMF) for the polarimetric microwave emission from a wind-driven ocean surface. An accurate GMF is required for any physically-based wind vector remote sensing system; however, the question remains as to how best to perform the retrieval. In this investigation, we examine the utility of the maximum likelihood (ML) estimator for retrieving ocean surface wind direction from passive polarimetric microwave imagery obtained using the Polarimetric Scanning Radiometer/Digital (PSR/D). The PSR/D is the first airborne imaging radiometer to obtain multiband polarimetric microwave brightness imagery of the ocean surface. The PSR/D was designed to measure the first three Stokes parameters (T_v, T_h, T_U) at 10.7, 18.7, 37, and 89 GHz.

The PSR's conical-scan imaging capabilities were used to measure the azimuthal dependence of brightness temperature over the ocean during the Labrador Sea Deep Convection Experiment in March 1997. The full conical scanning mode enabled the collection of high resolution (less than 1 km footprint size) two-look microwave imagery of the ocean surface during cold Arctic air outbreaks over the Labrador Sea. By comparing brightness measurements with a geophysical model function for emission, the ocean surface wind direction can be inferred. The maximum likelihood (ML) estimation technique is well suited to this problem since a statistical model is needed only for the radiometer measurements and not for the geophysical parameter being estimated. Applying the ML estimator to the wind vector retrieval problem results in a least-squares minimization problem that is useful for multi-look, multi-frequency, and multi-polarization microwave brightness temperature measurements. The accuracy of this retrieval technique as it is affected by radiometer sensitivity, frequency channel selection, footprint size, and atmospheric attenuation will be presented.

F1-8
1620

OCEANIC WIND DIRECTION USING POLARIZED MICROWAVE RADIOMETERS- THEORY AND MEASUREMENT

Mark D. Jacobson
NOAA/ERL/ETL, R/E/ET1
325 Broadway
Boulder, CO 80303

Winds over the ocean create rough surfaces consisting of a variety of waves and foam. Therefore, the microwave emissivity of the ocean surface is a function of sea skin temperature, salinity, surface roughness and foam distribution. A sensitive microwave radiometer can measure the surface emissivity (brightness temperature) variations and therefore infer the near-surface wind vector (speed and direction). This paper examines the theoretical and measured wind direction signatures inferred by microwave radiometers over the ocean.

An expression for the total brightness temperature observed by an airborne radiometer viewing the ocean is derived. The effects of the cosmic background radiation, the atmosphere, and the rough ocean surface are included. Atmospheric emission is calculated by a Radiative Transfer Equation (RTE) algorithm developed at the Environmental Technlology Laboratory (ETL) of the National Oceanic and Atmospheric Administration (NOAA). The rough ocean surface is modeled as a two-scale surface. The large-scale features include an upwind/downwind asymmetric surface slope profile. The small-scale features are averaged over the slope distribution of the large scale surfaces (S. H. Yueh, IEEE TGRS, 35, 1400-1418, 1997). Scattering calculations from these surfaces are performed using the second-order small perturbation method (S. H. Yueh et al., Radio Sci., 29, 799-814, 1994).

The Coastal Ocean Probing Experiment (COPE) was conducted off the Oregon coast during September-October 1995. An airship (blimp) was used as a platform for a microwave dual-frequency radiometer (23.9 GHz-vertically polarized and 31.7 GHz- horizontally polarized) and a microwave polarimeter (37 GHz-first three Stokes parameters). The radiometric sensitivities were about 0.05-0.1 K at 1 s integration time. The air and sea temperatures, wind speed and direction, and several other sea and atmospheric quantities were made from the FLoating Instrument Platform (FLIP) at a fixed point about 24 km from the shoreline at a depth of about 150 m. The in-situ wind direction measurements are compared with the theoretical and measured brightness temperature results. These results show promise of retrieving the near-surface wind direction over the ocean with microwave radiometers.

G1-1
1340

GPS DATA ASSIMILATION

D. S. Coco* G. S. Bust C. Coker T. L. Gaussiran
Center for Ionospheric Research
Applied Research Laboratories, The University of Texas at Austin
P.O. Box 8029, Austin, TX 78713
dcoco@arlut.utexas.edu

GPS ionospheric TEC data presents some unique challenges in data assimilation due to the satellite orbits, the irregular spacing of the ground stations, and the diverse scales of structures in the ionosphere. In this presentation, several different techniques that have been developed by a number of research groups for assimilating GPS into ionospheric models or grids will be discussed and compared. The advantages and limitations of these techniques will also be discussed. Examples of ionospheric specifications generated from several assimilation techniques will be presented.

The objective of most GPS ionospheric applications is to use GPS measurements to characterize the ionosphere over a specified region so that auxiliary systems can be calibrated or ionospheric phenomena can be investigated. A variety of techniques has been developed to assimilate the GPS data because no single technique can possibly address the diverse needs of all applications. These assimilation techniques include those that ingest GPS measurements into existing ionospheric models and also those that convert GPS measurements to TEC maps directly. The spatial extent of these techniques range from a limited region overhead a single station to the global ionosphere. In some assimilation techniques, GPS data is the only data type used as input whereas in other techniques, GPS data is combined with other data types to produce an enhanced view of the ionosphere.

Each assimilation technique depends on a set of assumptions about ionospheric behavior that only holds true under certain conditions. In addition, each technique is capable of mapping ionospheric structures within only a limited range of scale sizes. It is important the user understand the ionospheric assumptions and the structure scale size limitations of the technique, especially when applying the technique to an application other than that for which it was developed. In this presentation, these issues will be discussed and examples will be presented. Finally, the issue of how GPS TEC measurement errors are propagated into the final ionospheric specification will be discussed.

G1-2
1400

MULTIPOINT SPACE-BASED GPS MEASUREMENTS OF IONOSPHERIC STRUCTURES

Brian E. Gilchrist*
Space Physics Research Laboratory
University of Michigan
Ann Arbor, MI 48109
George Hajj
Jet Propulsion Laboratory
Pasadena, CA 91109-8099

The use of GPS radio signals as an efficient limb scanning scientific measurement tool from space is now well established. Here we intend to present a new space-based measurement concept of using at least two GPS receivers separated vertically over distances of a few to ten's of kilometers using space tethers to provide the separation. This can be understood as follows. In the limb scanning geometry, GPS TEC and phase measurements are most sensitive to small-scale vertical wavelength. With a single GPS occulting receiver, large horizontal wavelengths can be determined by correlating observations from nearby occultations, however, small horizontal scales (¡200 km) are averaged out. On the other hand, when we have two nearby GPS occulting receivers, small-scale horizontal wavelengths can be resolved when the GPS satellite is sufficiently out of the orbital plane.

Such a measurement capability would be appropriate for detecting, for example, traveling ionospheric disturbances (TIDs) as the occulted rays sample the ionosphere horizontally. TIDs arise from atmospheric internal gravity waves generated near the planet surface by seismic, tsunami, volcanic, meteorological, and other atmospheric and geophysical events which are amplified as they rise through conservation of energy flux. Depending on the relative geometry of the occulting link and the satellites, the two GPS links would provide information that is orthogonal in time or space to the information provided by the motion of each individual receiver. This orthogonality can be exploited to detect the gravity wave motions in the lower atmosphere and trace their effects up to ionospheric heights and the generation of TIDs.

Details of this measurment concept as applied to detecting greater detail in ionospheric structures will be presented.

G1-3
1420

SURFACE REFLECTED GPS SIGNALS AS POTENTIAL DATA SOURCE FOR SATELLITE ALTIMETER IONOSPHERIC DELAY CORRECTIONS

Attila Komjathy,* George Born, Penina Axelrad
Colorado Center for Astrodynamics Research
Department of Aerospace Engineering
Campus Box 431
University of Colorado at Boulder
Boulder, CO 80309

The Global Positioning System (GPS) signals reflected from the ocean surface and acquired by a GPS receiver onboard an altimetry satellite can potentially be used to compute the ionospheric delay present in the altimeter measurements. One method of accomplishing this is to ingest the total electron content (TEC) information obtained from the reflected GPS signals into ionospheric models such as IRI-95 or PRISM to improve their performance.

The objective of this study is to quantify the potential accuracy of the line-of-sight TEC computations from spacecraft altitude based on surface reflected GPS signals as a function of GPS satellite visibility, elevation angle, geographic location and solar activity conditions.

As the data source we used TEC from simulated surface reflections computed from GPS-derived global ionospheric maps. To compute the accuracy of altimeter ionospheric corrections from surface reflection TEC data, we compared the simulated surface reflection TEC and independent TOPEX TEC measurements at the sub-satellite points and found a daily RMS agreement of 3.3 TECU at a typical 40 degree elevation angle for low solar activity conditions.

We will discuss the possibility and limitations of ingesting ionospheric data from GPS surface reflections into the IRI-95 model to produce better spatial and temporal coverage especially over oceans where the global ionospheric models are generally less accurate than over land. We will also describe the algorithm we developed to update the IRI-95 model's CCIR/URSI coefficient sets from ionospheric data such as that can be inferred from GPS surface reflected signals.

G1-4
1440

RESOLVING IONOSPHERE AND PLASMASPHERE CONTRIBUTIONS TO GPS ERROR

N. Lunt
University of Wales, Department of Physics
Aberystwyth, SY23 2JA, UK
A. J. Mazzella
NorthWest Research Associates
Bellevue, WA 98009, USA
G. J. Bailey
Department of Applied Mathematics, University of Sheffield
Sheffield, S10 2TN, UK
G. J. Bishop*
Air Force Research Laboratory/VSBP, 29 Randolph Road
Hanscom AFB, MA 01731-3010, USA
L. Kersley
University of Wales, Department of Physics
Aberystwyth, SY23 2JA, UK

Propagation effects, arising from the total electron content along the ray path through the ionized atmosphere, present an important limitation to the accuracy of single frequency GPS systems. It is well-known that even simple models can with some success simulate the major contribution from the ionospheric F layer. However, the effects arising from the long propagation paths through the hydrogen-dominated plasma of the high plasmasphere or protonosphere are largely unknown, and not yet accounted for in GPS error estimation.

In the present study, the Sheffield University Plasmasphere Ionosphere Model (SUPIM) has been used to estimate the total electron contents along ray paths from constellations of GPS satellites. In this fashion, specifications of the protonospheric electron content have been determined, by differencing the contribution along the ionospheric ray path below 1100 km from the total, for a wide range of mid-latitude station geometries and covering complete diurnal cycles for all seasons at both solar minimum and maximum.

In addition, the estimated electron content results from SUPIM have been used to provide input data to the Self-Calibration of Range Errors (SCORE) process used to estimate TEC from GPS measurements. It is shown that it is possible, by appropriate modification to the use of SCORE, to compensate for the geometrical effects arising from the protonospheric ray paths, thus improving the estimate of the TEC determined from GPS measurements at mid-latitude stations.

Results are also presented of empirical measurements of protonospheric TEC, obtained by comparison of GPS and NNSS observations at stations in the UK.

G1-5 1500 EQUATORIAL IONOSPHERIC MODELING FOR SPACE SURVEILLANCE

S. M. Hunt, S. Close
MIT Lincoln Laboratory
244 Wood Street
Lexington MA, 02173

The Arpa Long Range Tracking and Instrumentation Radar (ALTAIR) fulfills high-volume launch support and satellite catalog maintenance for US Space Command. Real-time atmospheric modeling is executed to produce accurate positional measurements for the purpose of immediate orbit determination. ALTAIR's equatorial location and operating frequencies (160 MHz and 422 MHz) present a particularly difficult real-time modeling problem. Since 1983, a number of ionospheric modeling techniques have been developed to support space surveillance operations and have been executed at ALTAIR with varying results.

During the last peak of the solar activity cycle, the spatial and temporal variations of the equatorial ionosphere at Kwajalein Missile Range (KMR) significantly impacted ALTAIR's measurement accuracy due to unmodeled ionospheric range and elevation angle bias errors. The requirement to bring ALTAIR's real-time measurement accuracy back to within the required specification has motivated an ionospheric data collection and modeling effort, which began near the peak of the last solar activity cycle. The Ionospheric Error Correction Model (IECM) was the result of said effort, and is used in conjunction with an Ashtech ZY-12 GPS receiver to resolve ionospheric model accuracy shortcomings experienced during periods of increased solar activity. The major component of IECM, the Parameterized Electron Content Model, consists of a climatological ionospheric model that is adjusted to agree with ionospheric data taken in near real time (R. Daniell et al, *Radio Sci.*,Vol 30, 1499-1510, 1995). This paper provides an assessment of the IECM while using real-time Global Positioning System (GPS) Total Electron Content (TEC) data to scale the model to match actual local conditions. GPS TEC and radar calibration data are presented to characterize the system accuracy. A brief overview of the previously existing ALTAIR ionospheric model is also presented to contrast the features of the IECM/GPS system.

Prepared for the Department of the Army under Air Force Contract F19628-95-C-0002. Opinions, interpretations, conclusions, and recommendations are those of the authors and are not necessarily endorsed by the United States Air Force or Army.

G1-6
1540

A COMPARISON OF TEC FLUCTUATIONS AND SCINTILLATION AT ASCENSION ISLAND

K. M. Groves* S. Basu J. Quinn H. Kuenzler G. Bishop
Air Force Research Laboratory
29 Randolph Road
Hanscom AFB, MA 01731
P. Doherty
Boston College
Newton Center, MA 02159
P. Ning
27 Irving Street
Brookline, MA 02445

With increasing reliance on space-based platforms for global navigation and communication, concerns about the impact of ionospheric scintillation on these systems have become a high priority. Recently the Air Force Research Laboratory (AFRL) conducted a study comparing simultaneous observations of total electron content (TEC) and scintillation at Ascension Island during March-April 1998. Ascension Island is located in the South Atlantic at approximately 16 deg N lat under the nominal location of the equatorial anomaly crest. TEC data from the NASA Jet Propulsion Laboratory's (JPL) GPS receiver at Ascension was compared with GPS (L-band) and VHF scintillation data collected by AFRL. The JPL TEC values are recorded every 30 secs from phase data smoothed over a 10 sec period. Given typical drift velocities of 100 m/sec near the equator, the time series of data thus recorded effectively provides information on fluctuations with scale lengths of 6 km or more, smoothed over a 1 km interval. GPS scintillations, on the other hand, result from irregularities with scale lengths of only a few hundred meters. Preliminary results indicate that there is a strong correlation between the relatively large scale TEC fluctuations and GPS scintillation events. The quantitative relationship between these two quantities, however, proves to be quite noisy. A discussion of the utility of TEC fluctuations as an indicator of both L-band and VHF scintillation activity will be presented.

G1-7
1600

IONOSPHERIC MODELING FOR WADGPS AT NORTHERN LATITUDES – INITIAL RESULTS

Peter J. Stewart and Richard B. Langley

Geodetic Research Laboratory,
Department of Geodesy and Geomatics Engineering,
University of New Brunswick,
Fredericton,
New Brunswick E3B 5A3
CANADA

email: pstewart@unb.ca and lang@unb.ca

The FAA-sponsored Wide Area Augmentation System (WAAS) has been designed to provide en-route through Category I precision approach capabilities to suitably equipped aircraft operating within the Contiguous United States (CONUS). If WAAS is to be made available for these phases of flight outside the CONUS region, evaluation of the error modeling scheme at different locations is required. As part of a contract awarded by Nav Canada (the not-for-profit corporation which recently took over the provision of air traffic control services from the Canadian Federal Government), the University of New Brunswick has been charged with evaluating the proposed WAAS ionospheric modeling scheme in Canadian airspace over the full intensity range of solar and geomagnetic activity.

In the WAAS scheme, a network of continuously observing GPS receivers at precisely known locations provide dual frequency carrier phase and pseudorange observations to one or more central processing facilities where the delay imparted along the line of sight from each receiver to each satellite is measured. Interpolation of these measurements to a previously defined set of grid nodes (the Ionospheric Grid Points (IGPs)) on an ionospheric "shell" located at an latitude of 350km provides a series of vertical ionospheric delay estimates which are transmitted to the user. Estimated along with the grid ionospheric delay is the Grid Ionospheric Vertical Error (GIVE), a bound on the postcorrection ionospheric vertical error at each of the grid nodes. The user is then required to interpolate these grid node vertical delays and GIVE values to provide a slant range correction and slant range correction error at each intersection of the line of sight to a satellite with the grid shell defined by the IGPs.

Our work focuses on the evaluation of the techniques described above for use in Canadian airspace. Due to the influence of the auroral zone, Canada is uniquely located for the study of solar and geomagnetic effects on high precision GPS navigation. The flip side of this is that account must be taken of the high ionospheric variability at northern latitudes in order for systems such as WAAS to provide the accuracy and integrity for which they are proposed. Initial test results will be presented, outlining the work done using data from the network of dual frequency GPS receivers in Canada from which data is readily available through the International GPS Service (IGS), as well as various "receivers of opportunity". Proposed modifications to the WAAS ionospheric modeling technique to take account of the higher spatial and temporal variability of ionospheric delay encountered over the Canadian land mass are outlined, along with results showing their effect on the bottom line – navigation accuracy and integrity.

G1-8
1620

ANALYSIS OF IONOSPHERIC ERRORS OVER A LOCAL AREA NETWORK

A. J. Coster, B. P. Burke, M. M. Pratt, and P. N. Misra
M.I.T. Lincoln Laboratory, Millstone Radar, 244 Wood Street, Lexington, MA 02420-9108; e-mail: coster@ll.mit.edu

GPS carrier phase measurements can provide centimeter-level estimates of relative position if the integer ambiguities are resolved. Recent studies have shown that these integer ambiguities may be resolved in real-time with GPS L1-L2 measurements from a single epoch provided that the errors in the double differences are kept small (less than 5 cm). This error bound includes contributions of all error sources: ionospheric and tropospheric differences at the two receivers, ephemeris errors, and multipath.

This paper specifically looks at the modeling of ionospheric errors over a local area network. One of the primary goals of this research is to develop a real-time model of the atmospheric errors. Such a model is required to set baseline integers for a satellite as it rises. GPS data were collected over a period of several months from a network of four GPS L1-L2 receivers located within 25 km of each other. The GPS observations are analyzed to determine the residual unmodelled double-difference errors.

The primary ionospheric contribution to the error budget is associated with traveling ionospheric disturbances (TIDs). TIDs are short-term variations in the total electron content (TEC) that have typical periods ranging from a few minutes to over an hour, and typical amplitudes of only a few percent of the background TEC. The use of the network data allows for estimation of the magnitude and propagation direction of the TIDs. These observations are then correlated with time of day, geomagnetic events, and other atmospheric data. Early analysis shows that during quiet geomagnetic conditions, the largest errors associated with TIDs occur in the early afternoon, corresponding to the peak daytime values in the TEC. During geomagnetically disturbed conditions, peak errors due to TIDs can be observed at any time, including nighttime.

G1-9
1640

OVAL MONITORING USING TWO GPS STATIONS

Clayton Coker*
Center for Ionospheric Research
Applied Research Laboratories, The University of Texas at Austin
P.O. Box 8029, Austin, TX 78713
ccoker@arlut.utexas.edu

Gregory J. Bishop
Air Force Research Laboratory/VSBP
29 Randolph Road, Hanscom AFB, MA 01731

GPS data from two stations, Tromso and Ny Alesund, are used to monitor the location of the equatorward boundary of the oval in the Scandinavian sector. Intersecting F-region lines-of-sight from the two stations are examined to resolve the altitude of small scale total electron content (TEC) variations observed in the GPS data. Small-scale TEC variations are attributed to E-region irregularities in the oval and F-region irregularities in the polar cap. Two days of GPS data are processed for oval detections — January 9 and 10, 1997, a quiet day and a moderately disturbed day, respectively. The oval detection algorithm utilizes a highpass filter on the phase-derived relative TEC data to identify variations under 10 minutes in duration. The equatorward-most edge of the variations is used to estimate the equatorward boundary of the oval. Variations detected poleward are often attributed to polar cap irregularities. Comparisons are made with ionosonde data, TIROS particle precipitation data, and a model of the oval. Significant sporadic-E observations on ionosondes at Lycksele, Kiruna, and Ny Alesund confirm times when E-region irregularities were present over these stations. TIROS passes through the region confirm the location of the oval at selected times during the day. The oval model shows the generally expected location of the oval boundary as a function of the magnetic index Kp. Each confirms, to within accuracy limits, the location of the oval as determined by the GPS detections. Some of the advantages and limitations of using GPS for oval monitoring are discussed, as are the limitations specific to these two GPS stations.

G1-10
1700

CALIBRATION OF GPS SCINTILLATION MEASUREMENTS USING SIMULATED SIGNALS

D. S. Coco* C. Coker
Center for Ionospheric Research
Applied Research Laboratories, The University of Texas at Austin
P.O. Box 8029, Austin, TX 78713
dcoco@arlut.utexas.edu
G. J. Bishop
Air Force Research Laboratory/VSBP
29 Randolph Road, Hanscom AFB, MA 01731
A. J. Mazzella, Jr. E. J. Fremouw
Northwest Research Associates, Inc.
14508 NE 20th St, Bellevue, WA 98007
D. Howell
Air Force Research Laboratory/SNAR
2241 Avionics Circle, Wright Patterson AFB, OH 45433

High speed (20 Hz) GPS scintillation measurements have been calibrated and evaluated using signals from a specialized GPS signal simulator. The simulated signals were produced using a modified version of the Antenna WaveFront Simulator which generated simulated GPS signals perturbed at a 250 Hz rate with user specified phase and amplitude scintillation scenarios. These scenarios were designed to simulate three levels of real world ionospheric scintillation (low, moderate, and severe) for both phase and amplitude scintillation. An off-the-shelf Ashtech Z-12 GPS receiver was used to collect data at a 20 Hz rate using a high speed data acquisition mode. The measured data were analyzed and compared to the simulated input data.

The high speed measurements used in our analysis include carrier phase (L1, L2) and carrier-to-noise signal amplitude (L1) measurements (C/N0). The L1 and L2 carrier phase measurements were combined to generate differential phase measurements. The differential phase and C/N0 measurements were used to generate the σ_ϕ and S4 parameters which characterize phase and amplitude scintillation, respectively. Frequency spectra for the differential phase and C/N0 measurements were also produced. The measured data were compared to the simulated input data to provide a measure of the GPS receiver's capability to measure scintillation.

Using the results of this calibration, a discussion of the potential for using GPS for ionospheric scintillation measurements is presented. The results indicate that off-the-shelf GPS receivers have the capability of providing useful information about both carrier phase and amplitude scintillation. The limitations of using GPS to measure ionospheric scintillation will also be discussed, including behavior during severe scintillation events, the effects of multipath, and data acquisition challenges.

G1-11
1720

REAL-TIME GPS SCINTILLATION MEASUREMENTS

R.G. Caton* W.J. McNeil
Radex Incorporated
3 Preston Court
Bedford, MA 01730
K.M. Groves M. Smitham P. Sultan S. Basu
AFRL/VSBI
Hanscom AFB
Bedford, MA 01731

GPS L-band scintillation measurements are available in real-time with the Air Force Research Laboratory (AFRL) Scintillation Network Decision Aid (SCINDA). SCINDA is a prototype operational tool designed to help the warfighter mitigate the impacts of both UHF and L-band ionospheric scintillation in real-time on communication and navigation systems. Systems at the highest risk are those which transmit and receive signals between 250 and 2000 MHz, including the NAVSTAR GPS constellation of satellites which are relied upon extensively by US tactical commanders for navigational purposes. Any loss of this capability could significantly degrade operational effectiveness.

Ionospheric scintillation disturbances are routinely observed near the equatorial belt and the poles. During the next solar maximum period from 1999 to 2002, signal fades as much as 25 dB will not be uncommon for L-band systems. Although SCINDA is specifically designed to monitor equatorial scintillation, with monitoring stations located in Chile, Peru, and Guam, a link to the High Frequency Active Auroral Research Program (HAARP) site in Alaska has recently been added.

SCINDA receives data in real-time from ground based UHF and L-band receivers generating 2D and 3D displays of communication outages. L-band signals from the NOAA GOES satellite and the GPS constellation over South America are displayed concurrently producing a composite image of the real-time scintillation in the region. DMSP data is also collected in real-time from a receiver in Guam and processed to calculate a scintillation warning index, based on plasma density asymmetry measurements, predicting the probability ionospheric instabilities leading to scintillation. This information is displayed graphically in SCINDA along with NovAtel GPS scintillation data from Guam.

Data from an individual GPS satellite is displayed in SCINDA as a sphere (in 3D) or a circle (in 2D) located at the satellite's ionospheric penetration point above the local receiver. The sphere/circle is colored based the five-minute averaged S4 measurement and the user selected threshold levels for operational impact on their system. The scintillation structures detected by the GPS receivers appear to be extremely localized. Initial comparisons of GPS data with the L-band measurements from the NOAA GOES-8 satellite and DMSP scintillation warning index predictions have proven to give a consistent composite representation of the equatorial scintillation region.

G/H2-1
1400

EARLY TIME LANGMUIR TURBULENCE RESULTS FROM ARECIBO

M. P. Sulzer*
Arecibo Observatory, Arecibo, PR 00612
P. Cheung
UCLA, Los Angeles, CA 90095

We describe the results of two experiments conducted in July and August of 1997 concerning the behavior of Langmuir turbulence in the time shortly after the pump wave has reached the ionosphere. The Arecibo HF Facility had recently undergone an extensive upgrade. The most significant part of this upgrade was the replacement of most of the transmission lines, originally constructed from open wires in the form of cages simulating coax, with true coax constructed from aluminum irrigation pipe. These new lines eliminate about 3 db of loss, thus doubling the effective power of the facility, increasing the pump field, and thus affording new opportunities to observe plasma instabilities.

One purpose of the experiment was to observe very early time heating by the use of short HF pulses repeated with a very low duty cycle. These experiments were similar to ones conducted in 1992. A specific goal was to look at the spectrum of the return near the matching height with the purpose of observing the parametric decay instability just after the turn on of the heater. Previously, only the below threshold spectrum had been observed at early times, but it seemed possible that the higher power level would excite the instability. This did occur on some occasions, but the most striking observation was of extremely intense scatter occurring near and below the matching height along the free mode dispersion line. The scatter is significantly stronger than that observed in very low duty cycle heating experiments in the past.

Another purpose was to study the evolution of the free mode feature, in particular its fading and broadening in relationship to the duration of the heater pulse and heating duty cycle. Also the density profile modification, tempatature changes, and the generation of fast electrons were explored.

A third purpose of these experiments was to characterize the development of irregularities with the new higher power; that is, to examine the conditions determining when the "cold start" ionosphere is lost. Preliminary analysis shows that this occurs at a very low duty cycle with the higher power, but it is difficult to make comparision with half power experiments because the high power spectra are quite different.

G/H2-2
1420

ON THE HEAT FLUX INSTABILITY EFFECT UPON NON-LINEAR THERMAL SELF-FOCUSSING INSTABIITY

E. Mishin * T. Hagfors
Max-Planck-Institut für Aeronomie
D-37191 Katlenburg-Lindau
Germany

The numerical simulation (P. Guzdar et al., *Paper GH1-4*, National Radio Science Meeting, Boulder, 1997) has shown that an absolute thermal filamentation instability may develop inside the critical layer of the heater wave. As a result, the hot filaments are created with the shortest scale-lengths perpendicular to the magnetic field of the order of the electron skin depth while the longitudinal size grows up to several km. The time scale for the evolution and formation of these filaments was of the order hundreds milliseconds to seconds depending on the heater power. An important role in the formation of those filaments belongs to the thermal electron flux that is assumed to be determined by electron collisions. That is, the electron thermal conductivity is proportional to the ratio of the electron mean free path over the temperature gradient scale.

However, D. Forslund, (*J. Geophys. Res.*, **75**, 17, 1970) has shown that if this ratio exceeds $\sqrt{m/M}$, "skewing" of the electron distribution function becomes sufficient to yield the development of ion acoustic or ion cyclotron instability. This results in the suppression of the heat conductivity (E. Mishin, *Astrophys. Space Sci.*, **27**, 367, 1974) quite similar to the well known problem of anomalous resistivity. As the electron mean free path increases with the temperature as T_e^2, the hotter a filament, the more probable is the heat flux instability. The characteristic growth rate of the instability accounting for the narrowness of the filaments perpendicular to the magnetic field is evaluated at different stages of the filamentation instability. The value of "anomalous" thermal conductivity in a saturated state is defined in terms of weak turbulence theory. Possible effects of the heat flux instability upon the filamentation instability are discussed.

G/H2-3
1440

STUDY OF HF HEATER WAVE-INDUCED LARGE-SCALE IONOSPHERIC PLASMA TURBULENCE AT ARECIBO

M.C. Lee*
Plasma Science and Fusion Center
Massachusetts Institute of Technology
Cambridge
MA 01239

Ionospheric plasma heating experiments were conducted at Arecibo in the summer of 1997, using the newly upgraded HF heater and 430 MHz radar. Large-scale ionospheric irregularities, generated by O-mode heater waves, have been found for the first time to have "sheet-like" structures [Lee et al., GRL, 25, 3067, 1998]. It is deduced, from sequential measurements of radar backscatter power, that these irregularities have scale lengths ranging from a few hundred meters to a few kilometers. The wave vectors of these O-mode-excited irregularities are predominantly perpendicular to the meridional plane, as the model of thermal filamenation instabilities predicts. These sheet-like iregularities were associated with reduced radar backscatter power, indicating that hot spots coexisted with density depletion on the O-mode-generated irregularity sheets. Continuous heating of a stationary ionosphere results in further plasma depletion along the Earth's magnetic field, producing a large-scale plasma turbulence. The depleted magnetic flux tube can subsequently drift upward as a "rising ionospheric plasma bubble" [Lee et al., GRL, 25, 579, 1998]. The HF heater wave-induced large-scale ionospheric density inhomogeneities can enhance the source mechanisms, which cause the natural spread F phenomenon. Furthermore, our conjugate whistler wave propagation experiments show that ionospheric ducts can be modified by HF heater waves to support ducted radio wave propagation with less transit time [Lee et al., GRL, 1998].

G/H2-4
1500

INVERSION OF SUBIONOSPHERIC VLF MEASUREMENTS TO DETERMINE D-REGION DENSITY AND TEMPERATURE PROFILES

M. K. Demirkol* T. F. Bell U. S. Inan
Star Laboratory
Stanford University
Stanford, CA, 94305

Electron density and temperature changes in the D region are sensitively manifested in changes in the amplitude and phase of subionospheric Very Low Frequency (VLF) signals propagating beneath the perturbed region. Both localized and large scale disturbances (either in electron density or temperature) in the D region significantly cause scattering of VLF waves propagating in the earth-ionosphere waveguide leading to measurable changes in the amplitude and phase of VLF waves. Large scale auroral disturbances, associated with intensifications of the auroral electrojet, as well as ionospheric disturbances produced during relativistic electron enhancements cause characteristic changes over relatively long time scales that allow the assessment of the 'ambient' ionosphere. Localized disturbances are routinely produced by powerful HF transmitting facilities such as the High Power Auroral Stimulation (HIPAS) facility and the High frequency Active Auroral Research Program (HAARP) and also by lightning discharges. Amplitude and phase changes of VLF waveguide signals scattered from artificially heated ionospheric patches are known to be measurable [Barr et al., 1985; Bell et al., 1995]. In this paper, we describe a new inversion algorithm to determine altitude profiles of temperature and electron density within such a localized disturbance by using the measured amplitude and phase of three different VLF signals at three separate receiving sites. For this purpose a new optimization algorithm is developed which is primarily based on the recursive usage of the three dimensional version of the Long Wave Propagation Capability (LWPC) code used to model the subionospheric propagation and scattering of VLF signals in the earth-ionosphere waveguide in the presence of ionospheric disturbances.

G/H2-5
1540

EISCAT OBSERVATIONS TO DETERMINE THE LOCATION OF THE HF EXCITATION OF ENHANCED ION ACOUSTIC AND LANGMUIR WAVES

B. Isham, Arecibo Observatory, Arecibo PR
T. Hagfors,* E. Mishin, M. Rietveld
Max-Planck-Institut für Aeronomie, Germany
C. LaHoz, Auroral Observatory, Tromsø, Norway
W. Kofman, CEPHAG, St. Martin d'Heres, France
T. Leyser, Uppsala Ionospheric Observatory, Uppsala, Sweden

EISCAT ionospheric HF modification experiments have shown evidence that features such as the the outshifted plasma line, an enhancement of plasma oscillations at a frequency higher than the heater frequency by hundred to several hundred kHz, some times occurs at a height well above the normal reflection level. An explanation in terms of coupling to the O-mode to a Z-mode at the O-mode reflection level, a decay of this Z-mode wave into Bernstein and lower hybrid waves at the level of reflection of the Z-mode, with associated electron acceleration has been advanced. This type of decay can only take place provided the heater frequency is near a multiple of the gyro-frequency a requirement for Bernstein waves to exist.

In a series of experiments conducted in November and December 1997 the UHF (933 MHz) incoherent scatter radar was scanned between vertical and field aligned in order to detect the height of occurrence of the enhanced plasma oscillations and a possible dependence of the enhancements on the angle of incidence of the heater wave. The VHF (224 MHz) was kept pointing vertically at all times. Ample evidence was found to show that there is coupling through the ionosphere of the heater wave creating enhanced plasma and ion oscillations on the topside of the ionosphere, presumably due to Z-mode propagation. In these experiments we detected little convincing evidence of a decay of the Z-mode into lower hybrid and Bernstein modes.

The excitation of plasma waves at the topside is observed with the VHF radar and the observation of ion-acoustic waves at the topside is commonly observed at UHF. At UHF the excitation of ion-acoustic waves at the bottom of the ionosphere is strongest in a region near field aligned pointing. The excitation at the top of the ionosphere occurs over a wide angular range, which is surprising in view of the narrow window expected to exist for efficient coupling of the O- and the Z-modes. The height where ion-acoustic waves are excited is the lowest where the UHF beam is aligned with the magnetic field. The ion line appears to originate near the critical level when the UHF beam is pointed vertically, but below this height when field aligned. In the few cases where a UHF plasma line is observed the origin appears to be below the height of the ion line oscillation by several km. The data is still under analysis at the time of this writing.

G/H2-6
1600

ENERGY BALANCE STUDIES OF THE LOWER TOPSIDE IONOSPHERE USING THE ARECIBO ISR AND HEATING FACILITIES

S. A. González* M. P. Sulzer
Arecibo Observatory, Arecibo, PR 00612

Electron temperature enhancements have been frequently observed when high power radio waves are injected into the ionosphere. Under special conditions (near winter solar minimum when FoF_2 is low during the night) these can be accompanied by significant ion temperature enhancements. Before the Arecibo heater was upgraded these enhacements had been observed to be of the order of 50-200 K (F. T Djuth, *Adv. Space Res.*, *9*, 123–131, 1989). Recently the Arecibo HF Facility has undergone an extensive upgrade effectively doubling the power of the facility and thus larger temperature increases should be expected.

We describe the results of an experiment in the lower topside ionosphere using the incoherent scatter radar and the heating facility at Arecibo with the primary objective of the heating the F-region ionosphere to observe the temperatures inside the heated volume and also along the magnetic field as the heat is conducted away. The experiments were conducted on the nights of February 3 and 4, 1998. We will show the major parameters measured by the radar including H^+ number density T_e, T_{O+} and T_{H+} (Sulzer and González, *Geophys. Res. Letters*, *23*, 3235–3238, 1996) at various altitudes along the field lines that map down to the heated volume. Essentially, the radar was pointed at the heated volume and the aziumth and zenith were varied to track the field tubes at succesively higher altitudes. For example the field tube that crosses over the HF facility near 300 km altitude can be intersected near 500 km altitude by pointing the ISR near 18° off zenith and 166° azimuth. At the higher altitudes the H^+ concentration increases and any increase in T_{H+} is caused by the hot electrons. We will show the gradients in electron temperature caused by the heater, estimate heat conduction along the field and study the transfer of energy form the hot electrons to the ions (both H^+ and O^+).

G/H2-7
1620

COMPUTERIZED IONOSPHERIC TOMOGRAPHY (CIT) IMAGING OF AN HF-HEATED IONOSPHERIC VOLUME

P. Bernhardt C. A. Selcher*
Naval Research Laboratory
Washington, DC 20375
G. Bust T. Gaussiran J. Holmes S. White
Applied Research Laboratory
Austin, TX 78713
F. Djuth
Geospace Research, Inc.
El Segundo, CA 90245
C. Tepley M. Sulzer
Arecibo Observatory
Arecibo, PR 00614

Tomographic techniques use line integral measurements to reconstruct local values of the measured parameter. These techniques have recently been applied to the ionosphere by using radio transmissions to measure the integral of electron density between a satellite and a chain of ground-based receiving stations. The resultant reconstructions form a 2-dimensional map of the electron density in the plane of the satellite / receiver chain (Jeffrey R. Austen, et al, *Radio Science*, **23**, 299-307, 1988). These reconstructions are nonunique due to limited angle considerations or possible nonoptimal receiver placement which may be required by geographic constraints. The limited angle problem can be alleviated by making use of alternative data sources which provide information on the electron density vertical structure, such as incoherent scatter radars (ISR). The nonoptimal receiver placement problem can be resolved through the use of sophisticated reconstruction algorithms (Paul A. Bernhardt, et al., *Phys. Plasmas*, **5**, 2010-2021, 1998).

During the January 1998 Arecibo heating campaign, an array of CIT receivers was deployed on the island of Puerto Rico, forming a three by three matrix. This arrangement allows for three reconstruction planes and provides information on the evolution of the HF heater induced density cavities. Measurements of Total Electron Content (TEC) using the differential Doppler technique were made, during both heater on and heater off periods. To supplement this closely-spaced data set, the Applied Research Lab (ARL) of the University of Texas at Austin made available the data from a chain of CIT receivers deployed throughout the Caribbean region. Vertical electron density profiles were obtained by use of the ISR at Arecibo Observatory, and were used to form empirical initial conditions for the reconstructions. Reconstructions generated using code developed at the Naval Research Laboratory (NRL) will be presented, and will demonstrate the applicability of CIT to the imaging of HF heated volumes.

G/H2-8
1640

THEORY AND PRACTICE OF USING GROUND AND IONOSPHERIC REFLECTIONS TO DETERMINE RADIO EMISSION SOURCE HEIGHTS AND IONOSPHERE VIRTUAL HEIGHTS

D. A. Smith* R. S. Massey X. M. Shao K. C. Wiens
Space and Atmospheric Science Group
MS D466
Los Alamos National Laboratory
Los Alamos, NM 87545

Measurement of the differential times of arrival (DTOAs) of distinct waveform features by multiple, spatially separated recording stations provides a powerful means of locating the source of the waveforms. For many decades, DTOA techniques have been utilized to determine the locations of lightning strokes in two dimensions (latitude and longitude) or three dimensions (2-D plus altitude).

A powerful extension of lightning DTOA location techniques has recently been developed and applied to the geolocation of events within a distinct class of thunderstorm electrical discharges. The discharges are singular, isolated events that occur at altitudes between 7 and 20 km and produce very powerful, very brief broadband radio emissions. In addition to receiving groundwave or line-of-sight signals from these sources, VLF/LF recording stations and HF recording stations have often recorded clear reflections of the emissions from the ionosphere and surface of the earth. The relative delays of the reflections provide a means of determining both the height of the source that produced the emissions (h) and the virtual reflection height of the ionosphere (H). The technique requires that multiple stations record one-hop reflections or that a single station record multiple-hop reflections. It is also possible to determine h and H when one-hop reflections are received by a single station and the range to the source (r) is known a priori. Some challenging aspects of the technique include the assignment of time tags to the reflected signals after their distortion by the ionosphere and distinguishing the reflections from other lightning transients.

This technique for radio emission source geolocation was utilized to analyze data acquired in 1996 by an array of electric field change meters (LF/VLF instruments) and an array of broadband HF receivers. During 1998 the technique has been refined and used to study data acquired by the Los Alamos National Laboratory sferic array, a quartet of electric field change meters that began operation in May of 1998 in New Mexico in support of the acquisition of VHF lightning emissions by the FORTE satellite.

J2-1
1340

POST-UPGRADE PULSAR OBSERVING WITH THE ARECIBO TELESCOPE

K. M. Xilouris*
Arecibo Observatory
HC3 Box 53995
Arecibo, PR 00612

The upgraded Arecibo telescope recovered pointing and tracking capabilities in early May 1998. This marked the beginning of the post-upgrade commissioning phase. Following the establishment of satisfactory pointing models for both the Gregorian Dome receivers and the 430-line feed a series of commissioning tasks were performed evaluating the performance of the telescope and of the available data-taking processors. The results from this evaluation, relevant to pulsar observing, are summarized in this work. In particular, the zenith-angle dependence of the telescope-gain and system temperature at various frequencies as well as the beam shape and polarization purity are presented.

The new computer-controlled signal distribution is presented with emphasis on a development which allows signal sharing among different backends that operate at different IFs. The simplicity of configuring as many as five different pulsar backends is shown. This configuration led to coordinated pulsar-timing observations among five groups, restricting in this way the role of instrumentation in such experiments and also optimizing telescope time. Among the processors used is the Observatory's fast-dump spectrometer (AOFTM) with a programmable number of channels and time resolution. The performance of this processor is presented.

NAIC plans to construct a modular postdetection-signal processor based on 64 of the NAIC 1024-lag correlator chips, covering up to 800 MHz bandwidth in each of two polarizations. An overview of the processor is presented here. Initially, a prototype 16-chip *Unit* will be built providing:

- a) 50 MHz bandwidth, full Stokes, 9 levels – one frequency chunk
- b) 50 MHz bandwidth, dual polarization, 9 levels – two frequency chunks
- c) 100 MHz bandwidth, full Stokes, 3 levels – one frequency chunk
- d) 100 MHz bandwidth, dual polarization, 3 levels – two frequency chunks
- e) 100 MHz bandwidth, single polarization, 3 levels – four frequency chunks

This initial Unit will go on the air while the remaining 3 Units are constructed.

J2-2
1400

NRAO SYSTEMS FOR THE GBT

M. M. McKinnon
National Radio Astronomy Observatory
Green Bank, WV 24944

The Green Bank Telescope (GBT) is a 100-meter diameter offset parabolic reflector that is currently under construction at the National Radio Astronomy Observatory in Green Bank, West Virginia. The telescope will be equipped with actuators beneath the reflector surface panels to correct for deformations in the surface and thus maintain high aperture efficiency over the full range of telescope elevation angles. Precise locations of the surface panels and other parts of the telescope structure will be measured with a system of laser rangefinders. The rangefinder data will be used to optimize the shape of the reflector surface and refine the pointing of the telescope.

The initial suite of GBT receivers consists of a prime focus receiver which can cover frequencies ranging from 290 MHz to 1200 MHz and a set of eight receivers at the Gregorian focus which are spaced throughout a frequency range of 1.2 GHz to 52.0 GHz. The data recording instruments available on the GBT include the NRAO spectral processor, a digital continuum receiver, a holography receiver, and a VLBA data acquisition system.

The most impressive backend for the GBT is the new GBT spectrometer which can support a variety of observational configurations in both spectral line and pulsar observing modes. For example, in one of its spectral line configurations, the spectrometer can accept up to eight IF inputs of 800 MHz bandwidth each with 2048 frequency channels across each band. Another spectrometer configuration consists of a single IF input of 50 MHz bandwith with 262144 frequency channels. The machine could also be used in a pulsar search mode by bypassing its long term accumulators and recording the raw lags on tape or disk.

J2-3
1420

PULSAR SEARCHING: MULTIPLE BEAMS, GLOBULAR CLUSTERS, AND ALL THAT...

Fernando Camilo
University of Manchester, Jodrell Bank
Cheshire SK11 9DL, UK

Thirty-one years after the discovery of the first pulsar, the number of radio pulsars known now surpasses 1000.

The present rate of discoveries is such that fully a quarter of all known pulsars have been discovered in the past year. Follow-up studies of most of these objects have hardly begun, but we may safely expect to be surprised by some of the discoveries among such a bounty of pulsars.

I review the status of various search projects currently underway, including:

- *Multibeam Survey*: using a 13-beam receiver system at a wavelength near 21 cm mounted on the ATNF Parkes telescope, this survey of the Galactic plane has a sensitivity to long-period pulsars of about 0.15 mJy, improving by a factor of seven on previous 21 cm surveys. To date the collaboration has discovered more than 200 pulsars, with at least 500 expected when completed.

- *Globular Cluster Searches*: after a hiatus of several years, new results are now available from continuing searches of the globular cluster system. At least one new pulsar has been discovered in Terzan 5, and seven in 47 Tucanae, all spinning with periods of a few milliseconds. In most instances these searches employ new hardware, and data are reduced with the unknown period *and* acceleration of the target pulsar taken into account.

- *(Re-)Joining of Searches by Large Telescopes*: while conducting surveys near 21 cm, both the MPIfR Effelsberg and the Nançay radio telescopes have recently discovered their first pulsars. The NAIC Arecibo telescope, long a prime instrument for pulsar studies, is now back in operation following a complex upgrade, and has already detected a score of new pulsars.

J2-4
1440

THE NEUTRON STAR/SUPERNOVA REMNANT CONNECTION

V. M. Kaspi*
Department of Physics and Center for Space Research
37-621
MIT
Cambridge, MA 02139

The intimate relationship between supernova remnants and neutron stars, was suggested as long ago as the 1930's: neutron stars are hypothesized to be born in supernova explosions of massive stars that leave behind expanding nebulous remnants. This has been verified conclusively in at least one case, the famous Crab Nebula, which houses the young, energetic 33 ms radio pulsar PSR B0531+21. Since then, the focus has been mainly on the radio pulsar population as representative of neutron stars in general. Numerous additional examples of young radio pulsar/supernova remnant associations have been proposed in the literature over the years, with varying degrees of conclusiveness. Along the way, however, fundamental questions regarding the neutron star/supernova remnant connection have been raised. These include the possibility that not all neutron stars are born in supernova explosions. Equally intriguing, some or maybe most neutron stars formed in supernovae are not observable as radio pulsars, or even exhibit no radio pulsar mechanism at all. These questions challenge the very basis of our understanding of the fate of massive stars and the nature of the stellar compact object population.

It has become increasingly clear that radio observations alone are insufficient to address these issues. Mounting evidence from observations across the spectrum, some of which has been uncovered only very recently, suggests strongly that the radio pulsar population is but a member of a larger young neutron star population; young pulsar phase space may be far bigger than has been imagined.

In this talk, I review the observational status of young neutron star astrophysics. I argue that, today, combining radio observations with studies in other regions of the spectrum, particularly X-ray, is a necessity for finding definitive answers to the question of the nature of the young neutron star population.

J2-5
1500

EMISSION CHARACTERISTIC OF MILLISECOND PULSARS

M. Kramer*
University of California
Berkeley, CA 94720-3411

The discovery of millisecond pulsars (MSPs) opened new ways to study the still not understood emission mechanism of pulsars. Although pulse periods and surface magnetic fields are several orders of magnitude smaller than those of slowly rotating pulsars, the same emission process might work in both types of objects and thus for an extremely large parameter space. The probable origin of MSPs from a recycling process might also lead to different magnetic field structures in the emission regions, possibly affecting the observed radiation. A systematic study of the emission properties of MSPs and a comparison of the results with characteristics of normal pulsars can thus lead to new important insight in the emission physics of pulsars.

We recently conducted such observations (Kramer et al. 1998, 1999a,b, Xilouris et al. 1998, 1999) investigating the spectra, luminosity, beam structure and polarisation of MSPs. The obtained results can be combined with those recent ones by Sallmen (1998), Stairs (1998) and Toscano et al. (1998), providing a detailed picture of the emission properties. We find that the emission process of MSPs and 'normal' pulsars seems to be identical although distinct differences can also be observed: The polarisation angle swing, usually interpreted geometrically, is much flatter for MSPs than for normal pulsars, while however the beam radius is also much smaller than expected. A multi-frequency study of MSPs including frequencies up to 5 GHz does not support the existence of magnetic multipoles in the emission region, which might however be very compact. An increasing sample of MSPs is discovered, which does not show the so far expected (and observed) stability of MSP pulse profiles. These pulse shape changes seem to be different than the 'mode-changing' phenomenon long known for normal pulsars and can severely affect the timing stability of these objects. An apparent narrow band variation of the pulse shape found for one such source points to a propagation effect in the compact magnetosphere of MSPs as the origin of this effect.

The future long-term goals are certainly single pulse observations of MSPs done simultaneously at different frequencies, which will require the collaboration of several observatories.

J2-6
1520

THE ORTHOGONAL MODES OF POLARIZATION IN PULSAR RADIO EMISSION

M. M. McKinnon*
National Radio Astronomy Observatory
Green Bank, WV 24944
D. R. Stinebring
Department of Physics
Oberlin College
Oberlin, OH 44074

The observed position angle of the linear polarization of pulsar radio emission can switch between two values that are separated by 90°. These orthogonal modes of polarization are found in the radio emission from many pulsars and are best studied with polarization observations of a pulsar's individual pulses. The single pulse observations show essentially random fluctuations in the polarization properties of the emission, suggesting that one should adopt a statistical approach when interpreting the observations. The observations also suggest that the two orthogonal modes occur simultaneously because both the average and the instantaneous linear polarization are very low when the modes occur with nearly equal frequency. Some locations within the pulse are highly polarized, and, since the simultaneous interaction of the two modes depolarizes the emission, the individual modes must also be highly, if not completely, polarized.

We have developed a statistical model for the polarization of pulsar radio emission that is based upon these observed properties of the emission's polarization. The model assumes that the Stokes parameters of the emission are determined by the simultaneous interaction of two, completely polarized, orthogonal modes. The flux densities of the modes are assumed to be random variables to account for the statistical nature of the emission's polarization properties. With our model, we can compute mode-separated pulse profiles and compare the statistical properties predicted by the model with the observed ones.

Our model is quite different from previous work on the topic of the orthogonal modes, which has assumed that the modes occur separately or disjointly. We do not believe that the observations support a disjoint mode assumption. We compare the mode-separated pulse profiles of PSR B0525+21 that are computed using disjoint and superposed models. The profiles produced by the two models are distinctly different and their interpretation can lead to different conclusions regarding the underlying properties of the emission.

J2-7
1600

RECENT RESULTS WITH BERKELEY PULSAR PROCESSORS

D. C. Backer*
University of California
Berkeley, CA 94720-3411

Over the past several years two designs of Berkeley Pulsar Processors have been installed at Green Bank, Effelsberg, Nançay and Arecibo observatories. A testbed unit of both designs operates in our lab in Berkeley. The original design is a 112-MHz coherent dispersion removal system that channelizes orthogonally polarized signals into 32 bands, removes dispersion within each channel with a full custom VLSI chip using the time convolution technique, and detects the dedispersed voltages for signal averaging synchronous with the apparent pulse period. A second design divides its 168-MHz bandwidth into 96 channels. Each is detected, smoothed and passed over a high speed interface to a SUN workstation for recording on magnetic tape (exabyte or DLT7000). In both cases the full bandwidths quoted can be reduced in steps of $\sqrt{2}$ to match the dispersion of a known, or desired, signal. Full Stokes parameter capability is either available or under development for the two systems. Monitor, control and data acquisition of the incoherent system was built upon the 'PSPM' code described in the Anderson *et al.* paper. Part of the processors is described by Backer *et al.* in (1997) PASP, **109**, 61. Various documents of description are available at http://astro.berkeley.edu/~mpulsar.

The Green Bank and Effelsberg coherent processors were used by Sallmen in her Ph.D. thesis study 'Millisecond Pulsars : Decoding Magnetospheres'. She offers an explanation for the small slopes of linear polarization position angle with respect to rotational longitude. The Green Bank processor is now used daily to monitor short period pulsars at 327 MHz and 610 MHz using an 85ft telescope. The Crab pulsar has been particularly active: a swarm of glitches (Wong *et al.* 1998, in preparation), large amplitude variations of dispersion and scattering, and curious 'echoes' that are probably the result of multiple imaging in intervening plasma. The Green Bank system was used at 610 MHz while T. Hankins & D. Moffet used their system at the VLA at 1420 MHz to study the spectrum of Crab pulsar giant pulses (Sallmen *et al.* 1998 *ApJ*, submitted). The amplitudes of the giant pulses are strongly correlated between the two frequencies. The Arecibo coherent system has been used for polarization studies, a 'Shapiro delay' experiment on PSR J1713+0747, and a 'time transfer' experiment joint with Effelsberg.

In addition to those named above I want to acknowledge the Berkeley Radio Astronomy Laboratory, S. Anderson, B. Cadwell, R. Bosel, M. Dexter, R. Foster, A. Jessner, M. Kramer, S. Kulkarni, J.-F. Lestrade, S. Lundgren, M. Pukish, P. Ray A. Somer, J. Valanju R. Wielebinski & A. Wolszczan for their effort or support.

J2-8
1620

NANÇAY GALACTIC PLANE PULSAR SURVEY WITH THE NBPP

B. J. Cadwell* R. S. Foster P. S. Ray
Naval Research Laboratory
Washington, DC, 20375, USA
D. C. Backer
University of California
Berkeley, CA 94720, USA
J.-F. Lestrade I. Cognard
Observatoire de Paris-Meudon
92 195 Meudon Cedex, FRANCE

We are conducting a high frequency pulsar survey of approximately 1170 square degrees of the Galactic plane using the large steerable reflecting radio telescope at the Nançay Observatory. Our project goal is to survey the Galactic plane between -15 < l < 180 degrees, |b| <3, covering a region from 17h to 5.5h in right ascension. Observations centered near 1400 MHz represent a good trade-off between the requirements of low frequency, for stronger pulsar signal due to their intrinsic steep spectrum nature, and high frequency for limited pulse smearing by high dispersion measures in the Galactic Plane. Using the half power beam width of the Nançay telescope (4'x 22') or 41 beams/square degree, the entire survey will require nearly 50,000 individual pointings. We have completed all of the observations, processed approximately 50% of the data, and can report the discovery of 2 new pulsars.

The Naval Research Laboratory in conjunction with the U.S. Naval Observatory and the University of California at Berkeley has built a pulsar processor for observations over large bandwidths (170 MHz) at frequencies above 1 GHz. The primary limitation to these observations is the availability of a backend processor with the necessary time and frequency resolution for both pulsar searching and timing. The Navy/Berkeley Pulsar Processor (NBPP) instrument is a dual polarization 96 channel device with a nominal frequency resolution of up to 1.7 MHz per channel adjustable downward in bandwidth. A single 9U-VME crate is capable of processing 170 MHz of total bandwidth in six independent 28 MHz bands.

The majority of the the data processing is taking place at the Naval Research Laboratory, utilizing Department of Defense supercomputer resources. Efforts have concentrated on solving the problems associated with processing the massive 4 Terrabyte database and dealing with the extensive radio frequency interference (RFI) that permeates the data. The data are transfered from tape to a 40 Terrabyte multi-resident file server, accessible by a variety of computers over the local network. Analysis is proceeding on a 64 processor SGI Origin 2000 distributed shared memory computer at a peak rate of about one beam every 60 minutes. We have developed a system for excising the majority of the RFI from the data while maintaining sensitivity to weak sources ($f_{1400\ MHz} \geq 3$ mJy) with sub-millisecond periods.

J2-9
1640

THE S2 BASEBAND PROCESSING SYSTEM FOR PHASE-COHERENT PULSAR APPLICATIONS

R. Wietfeldt
Jet Propulsion Laboratory, Pasadena
W. Van Straten
Swinburne University of Technology, Australia
D. Del Rizzo
Dominion Radio Astrophysical Observatory
N. Bartel
York University, Ontario
A. Novikov* W. Cannon
Space Geodynamics Laboratory, Ontario

The S2 baseband processing system (S2-BPS) is designed for a variety of pulsar measurements such as ultrafast signal fluctuations and pulse timing. Its key features are: the S2 recorder; the S2 Tape-to-Computer Interface (S2-TCI) which provides an efficient high data rate transfer from S2 tapes to computer; and the tightly coupled control interface to the computer which enables automated data transfer and processing.

Originally S2 recorder was designed for VLBI applications (Wietfeldt R.D., Baer D., Cannon W.H. et al., *IEEE TIM*, **45**, No. 6., 923, 1996) at the Institute for Space and Terrestrial Science (ISTS) (now Centre for Research in Earth and Space Technology - CRESTech) at York University. S2 recorder design is based on the use of commercial VHS tape transports (VCR's), modified for use in digital high density, high data rate applications. A single S2 recorder "tape-set" of eight SVHS tapes provides up to 500 GBytes of data storage, and an unattended operating time of up to 8.5 hours at the maximum data rate of 128 Mbits/s or 16 MBytes/s, corresponding typically to 16 MHz bandwidth in two circular polarizations at 2-bit quantization, which generates a data rate of up to 1 GByte/min. For more challenging applications, multiple S2's may be used.

In this paper, we describe a phase-coherent baseband processing system for radio pulsar observations. We give an overview of the S2 baseband processing system. Then we discuss considerations for the design of the Tape-to-Computer Interface (S2-TCI), a system designed to transfer S2 recorded data from tape to computer memory (RAM) via direct memory access (DMA). Computer data may be processed immediately, transferred to other media such as disk or alternate tape device with subsequent processing in the "local" computer, or sent to a more powerful "remote" computer, such as a super computer, for processing. The software control system of the S2-TCI is described. We demonstrate first results of the first observations of Vela pulsar recordings at Parkes in September 1995 with using the S2 baseband processing system. Finaly we derive our conclusions and present future prospects for baseband processing systems.

J2-10
1700

THE PENN STATE PULSAR MACHINES

S. B. Anderson B. A. Jacoby
Caltech
Pasadena, CA 91125
B. J. Cadwell
NRL
Washington, DC 20375
A. Wolszczan*
Penn State University
University Park, PA 16802

We have designed and constructed two analog filterbank–based pulsar backends, the Penn State Pulsar Machines PSPM–1 and PSPM–2.

The PSPM–1 is a 2 × 128 × 60 kHz portable filterbank equipped with a digital interface and a data acquisition/analysis computer. It has been designed to conduct ultra-fast sampled (80 μs) pulsar surveys and high precision timing observations (12 μs sampling) at decameter wavelengths. The PSPM–1 parameters have been specifically chosen to maximize its performance, when observing nearby (d < 1–2 kpc) millisecond pulsars. Extra emphasis has been placed on designing the PSPM–1 as a truly remote pulsar backend to ensure its efficient utilization.

The PSPM–1 has been installed at the Arecibo Observatory in June 1994 and became the first "user–owned, Observatory–maintained" backend at Arecibo, under a formal agreement with the National Astronomy and Ionosphere Center. This status makes the PSPM–1 a public access device, available to all successful applicants for the telescope time.

The architecture of PSPM–2 closely follows that of PSPM–1 with the number of filters (2 × 64) and the filter width (3 MHz) chosen to meet total bandwidth and resolution requirements for pulsar search and timing observations at frequencies above 1 GHz. This design was motivated by the fact that, because of the intrinsic timing noise and pulse instabilities, the use of very large telescopes is not required to reach a $\sim$ 1 ms level of timing precision in observations of many reasonably strong pulsars. Consequently, a medium–size, frequently available radio telescope and a specialized backend hardware designed to maximize the system sensitivity are quite sufficient to conduct very valuable, long–term timing measurements of many pulsars.

The PSPM–2 has been installed at the Toruń 32–m radiotelescope in Poland in June 1996 and begun its service in a long–term program of the weekly timing of over 100 "normal" pulsars.

K1-1
1540

DEATH BY MAGNETIC FIELD?—A SHOCKING THEORY ABOUT LIGHTNING

Howard Wachtel
University of Colorado-Boulder

Abstract:

Every year in the United States, lightning kills about 100 people and injures several thousand others. It might be expected that those who are killed suffer more severe physical damage (burns, etc.) than those who survive—but this is not always the case. Many of the fatalities—as well as those survivors who owe their lives to cardio-pulmonary resuscitation—show no outward manifestations of lightning current having entered or exited the body (such as burn marks or "ferning" lesions on the skin). In some instances, and in groups of people are "struck" by the same lightning bolt, those that survive are severely burned while those who are killed (as a result of cardiac arrest) have no marks on their body.

Lightning fatalities have been thought to be attributable to three possible pathways for current entry into the body: a direct strike (which could cause massive burning over the entire body), a side flash from the main bolt (which would also leave distinct current entry or exit wounds), and ground current (which would usually enter one leg and leave through the other). These three pathways seem to account for the majority of lightning injuries—it is also possible, however, to induce current in the body by magnetic field coupling, and this would not involve current entry or exit. The issue, though, is to determine how much current could be generated and what the plausible effect—particularly on the heart—would be.

Lightning "bolts" have very high peak currents (100,000 Amps or more) that rise in a few microseconds and decay more slowly. A person standing a meter or so from such a bolt would therefore experience a dB/dt on the order of 10,000 Tesla per second during the rising phase. If parts of the heart are approximately 10 cm off the torso center axis, this can result in an induced current on the order of 1000 A/m^2—however, this current would only last for a few μsecs. The heart is particularly vulnerable to "fibrillation" over a short portion of the cardiac cycle (the T-wave of ECG) during which it is plausible that a brief pulse of lightning-induced current could be lethal. Thus victims would incur two improbabilities concurrently—1) they would have to be pretty close to a lightning bolt and 2) they would have to be in the ventricular repolarization phase of their cardiac cycle at the instant the lightning arose. However, this concomitance would also apply to other mechanisms for fatal electrocution by brief pulse.

K1-2
1600

MAGNETIC FIELD INTERACTIONS WITH BIOMAGNETIC PARTICLES

Ron B. Goldfarb
National Institute of Standards and Technology
325 Broadway
Boulder, Colorado 80303

Magnetic particles are of broad interest in biology and medicine. Naturally occurring biomagnetic particles, such as the iron-storage molecule ferritin, have unusual properties that arise from their small size and the nature of their magnetic order (R.A. Brooks, J. Vymazal, R.B. Goldfarb, J.W.M. Bulte, and P. Aisen, *Magn. Res. Med., 40,* 227-235, 1998). Because of their magnetic properties, ferritin deposits in the brain can distort contrast in magnetic resonance images.

Magnetic particles may be used in medical experiments and therapeutics. Iron oxides and carbides have been proposed as drug carriers, able to be guided by external magnetic fields to their targets. However, to be useful, particle size, composition, and magnetic properties must be tailored for small hysteresis and remanent magnetization, and large permeability and saturation magnetization.

Magnetic particles may be accelerated by pulsed magnetic field gradients. Specially coated iron particles in an aqueous medium may be used to ballistically insert foreign DNA into living cells without damage to the cell walls.

In addition to these applications, the talk will discuss the physics of the size dependence of the magnetic properties of particles and different magnetic measurement techniques.

K1-3
1620

HYPOTHETICAL BASIS FOR BIOEFFECTS OF STATIC MAGNETIC FIELDS

Frank Barnes
University of Colorado-Boulder

Abstract:

Recent work has shown that large DC magnetic fields with large gradients can suppress pain and inflammation [on the order of 0.1 T and 1 T/cm] (1-BEMS Abstract, June 1998). In this paper we will calculate the forces on diamagnetic and paramagnetic materials involving iron such as hemoglobin, feritin and magnetite and then speculate on how they may affect pain and inflammation. The paramagnetic materials are attracted to the magnetic while diamagnetic materials are repelled. Thus oxygenated hemoglobin—which is diamagnetic—is repelled, and hemoglobin—without oxygen, and which is paramagnetic—is attracted by a magnet with a force which is proportional to the magnetic flux B times the gradient (dell) B. It has been shown that the spin polarization in a magnetic field changes the resistance of a channel, and this may provide a mechanism for static magnetic fields to influence cell function. Static magnetic fields also affect chemical reaction rates and are very sensitive to the distance of the electrons from stable orbits of both the initial reactants and the final compound. Shifts in the position of the electrons from stable orbits of as little as a few tenths of an Angstrom may reduce the size of the magnetic field required to change the direction of a spin from tens of Tesla to tens of microtesla. (2-R. S. Wadas "Biomagnetism" Ellis Horwood, 1991) Additionally, fields of a few millitesla have been shown to change the lifetimes of free radicals by reducing the probability of immediate recombinations and this, in turn, may increase the free radical concentrations in biological systems. (3-U. E. Steiner and Ulrich, *Chem. Rev.* 89, 51-147, 1989 and 4-C. Eichwald and J. Wallenczek, *Biophysical Journ.* 71, 623-631 Aug 1996)

K1-4
1640

ENVIRONMENTAL MAGNETIC FIELD TRANSIENTS, A RED HERRING?

Ed Leeper
Monitor Industries, Boulder, CO 80302

Abstract:

Low-level magnetic field transients arising from various kinds of power switching have been suggested as a possible cause of certain adverse biological effects—a hypothesis broached independently or as possibly "explaining" associations that have been observed between bioeffects and certain other non-ionizing, non-thermally-potent electromagnetic exposures that might be concomitant with the presence of transients—such as sub-microtesla 60-Hz magnetic fields. This has been discussed for most of a decade, with little actual research being done. Largely that has been due to uncertainty about where and how to get started with exposure assessment, or even with measuring the "size" of a given transient. The difficulties and some possible answers will be discussed, with a plea made for any suggestions as to how the bioelectromagneticists might get off square one, toward either accepting or rejecting admittedly implausible hypotheses.

Fundamental difficulties include: (1) The wide variability in shape, speed, and prevalence of what might come under the heading of "transient" (i.e., too many degrees of freedom). (2) The wide spatial and temporal variability of transient field strength, complicating exposure assessment for epidemiology. (3) The usual problem of assessing historical exposures, for retrospective epidemiology. (4) The inadequately-addressed problems of repeatability associated with the entrenched biolectromagneticists' habit of using 24-hour time-weighted-average dosimetry as the ultimate answer for any exposure-assessment quandary.

K1-5
1700

USING GIS METHODS TO ASSESS COMMUNITY EXPOSURE TO EMF AND OTHER RELATED FACTORS

Robert L. Pearson
Radian International LLC
707 17th Street, Suite 3400
Denver, Colorado 80202

Geographic information systems (GIS) have recently evolved to become powerful tools for the assessment of environmental exposure patterns over large areas such as cities. For instance, community exposure to electric and magnetic fields (EMF) from various sources can be displayed geographically and analyzed using GIS techniques. Data in a GIS format are now commonly available for street layouts, topographic features, census socioeconomic and population profiles, tax assessor records and many other types of spatial factors.

We have used GIS techniques to compute and analyze the geographic pattern of population exposure to a surrogate for 60 Hz magnetic fields from electric power lines. This magnetic field surrogate, wire code, has previously been associated with childhood cancer occurrence. Wire code is computed from the size and function of the power line conductors and the distance from the conductors to nearby residences. We obtained from Public Service Company of Colorado, a detailed GIS database of their electric power distribution and transmission system in the Denver-Boulder metropolitan area. We constructed a map of wire code buffers along each neighborhood power line for the entire city. We also used residence specific tax assessor data to compute wire codes for each of 238,000 residences in the city.

We have also used the GIS tool to display a surrogate metric for traffic air pollution based on distance weighted traffic density (DWTD) for streets in this area. DWTD was computed by using a Gaussian curve to weight the traffic density on a street by the distance to a nearby home. This was done for each of the residences for which wire code was previously determined. We also have evaluated other spatially distributed factors on a house by house basis throughout the city including rental status, and the likelihood of children living in the home.

This GIS tool could conceivably be extended to analyzing cumulative population exposures to radio frequency EMF from cellular telephone and broadcast television and radio signals by superimposing antenna radiation patterns over population census data. The conduct of such a study would necessitate the involvement of a wider range of electromagnetic scientists.

K1-6
1720

ELECTROMAGNETIC RADIATION ON LOOKOUT MOUNTAIN

Adam Bechtel
Mark Crossman
Bjorn Eriksen
Alex Lee
2080 W 10th Ave #106
Broomfield, CO 80020

Lookout Mountain in Golden, Colorado is one of the most complex electromagnetic environments in the country. More than 600 transmitters are located in this mountainous region. Lookout Mountain is also one of the most intense electromagnetic environments in a residential area. Some residents live within a few hundred meters of antenna farms. Due to the varying elevation, others residents live in direct line-of-sight of television and radio broadcast antennas. Non-ionizing electromagnetic radiation exposure on Lookout Mountain is continuous for many people living there.

In March of 1998, a citizens group in Jefferson County, Colorado petitioned the FCC to lower the Maximum Permissible Exposure (MPE) level in an uncontrolled area from 200.00 microwatts per centimeter squared to 0.01 microwatts per centimeter squared. Initial testing on county roads near the Lookout Mountain antenna farms found hotspots up to 4.4 times the current MPE for an uncontrolled area.

Four students at the University of Colorado investigated the electromagnetic radiation at Lookout Mountain. Radio and television broadcast antennas are the primary contributors of the electromagnetic radiation in this area. The FCC has mandated that digital television broadcast be provided by 2006. Applications for digital broadcast antennas have already been submitted to Jefferson County. In the transition stage from analog to digital, many stations will transmit both signals. As a result, the existing significant electromagnetic radiation levels at Lookout Mountain will increase. Using a software model, we have developed current and forward looking radiation patterns for the Lookout Mountain area. This paper discusses the current and potential situations for this area, as well as strengths and weaknesses of the model.

K1-7
1740 RECENT ACTIVITIES IN HUMAN EXPOSURE STANDARDS DEVELOPMENT

J.C. Lin (Univ. of Illinois)

0830-Tues, MATH 100
PLENARY SESSION

Session A2, 1355-Tues., ECCR1B40
EM MEASUREMENTS
Chairpersons: M. Kanda (NIST), J. Norgard (UCCS)

A2-1
1400

FREE-SPACE CHARACTERIZATION OF THE PERMITTIVITY AND PERMEABILITY OF A MATERIAL USING MULTIPLE TRANSMISSION MEASUREMENTS

Michael Havrilla* Andreas Kurtz Dennis Nyquist
Department of Electrical Engineering, 2120 Engineering Building
Michigan State University, East Lansing, MI 48824

In the free-space characterization of materials, the scattering parameters S_{11} and S_{21} are commonly measured to determine the permittivity and permeability of a dielectric/magnetic sample. If the sample is thin or prone to warping or bending, it can be supported via attachment to a known substrate layer or placement within a multi-layered configuration. The S_{11} reflection measurement suffers a drawback in that it is highly sensitive to the physical location of the sample with respect to the transmit/receive antenna. This error will be compounded for a multi-layered environment. The S_{21} transmission measurement, on the other hand, is location independent and is therefore more reliable. The purpose of this paper is to discuss how two independent transmission measurements can be used to determine the constitutive parameters, ϵ and μ, for the general case of an unknown material embedded in a known multi-layered environment.

The multi-layered sample structure is studied by developing wave-transmission parameters (A-parameters) immersed in a free-space environment. The theoretical expression for the transmission coefficient of the entire layered structure, $S_{21}^{t}(\omega, \epsilon, \mu)$, is determined by multiplying the A-parameters of the individual layers (where an initial guess for ϵ and μ of the unknown layer must be provided) and then using the general relation $S_{21} = 1/A_{11}$. The permittivity and permeability of the unknown material can be experimentally found if two independent transmission measurements, $S_{21}^{e1}(\omega)$ and $S_{21}^{e2}(\omega)$, are performed. Possible measurement scenarios include two different aspect angles (aspect-angle method), two separate sample thicknesses (thickness method) or two independent layered configurations (layered method). Equating the above theoretical and experimental transmission coefficients leads to

$$S_{21}^{t1}(\omega, \epsilon, \mu) - S_{21}^{e1}(\omega) = 0$$
$$S_{21}^{t2}(\omega, \epsilon, \mu) - S_{21}^{e2}(\omega) = 0$$

This set of coupled equations can be iteratively solved using a two-dimensional Newton's method root search. If the sample is non-magnetic, only a single transmission measurement is required, resulting in a one-dimensional root search.

A theoretical analysis will be presented and experimental results given for various materials. The aspect-angle, thickness and layered methods will be compared and the calibration and measurement procedure (believed to be new) will be discussed.

A2-2
1420

NONDESTRUCTIVE PERMITTIVITY MEASUREMENTS WITH A SPLIT-CYLINDER RESONATOR

Michael D. Janezic* James Baker-Jarvis
National Institute of Standards and Technology
NIST MS813.08
325 Broadway
Boulder, CO 80303

The split-cylinder resonator method has emerged as a nondestructive method for measuring the complex permittivity of low-loss dielectric materials. In this technique, a sample is placed in the gap between the two shorted cylindrical waveguide sections. A TE_{011} resonance is excited, and from measurements of the resonant frequency and the quality factor, one determines the complex permittivity of the sample.

Kent, in his original model of the split-cylinder resonator (G. Kent, *IEEE Trans. Microwave Theory Tech.*, **36**, 1451-1454, 1988), correctly recognized that neglecting the fields in the region of the sample outside of the waveguide sections would lead to a systematic error in the measured permittivity. He initially proposed a correction to the measured permittivity based on a perturbation calculation. Later, Kent and Bell developed an improved approximation to correct the initial theoretical model (G. Kent, *IEEE Trans. Instrum. Meas.*, **45**, 102-106, 1996) (G. Kent and S. Bell, *IEEE Trans. Instrum. Meas.*, **45**, 98-101, 1996).

Unfortunately, this approximation still leads to systematic errors in the measured permittivity. This paper presents a full-wave analysis of the split-cylinder resonator which removes this systematic error by properly taking into account the fringing fields in the sample region outside of the cylindrical waveguide sections. This model includes the TE_{011} resonant mode plus evanescent TE_{on} modes in the cylindrical waveguide regions. These modes must be included to properly satisfy the boundary conditions at the boundaries between the sample and waveguides. A resonance condition is derived by applying a Hankel transform with respect to the radial coordinate, reducing the problem to one dimension.

Using this theoretical model we calculated the complex permittivity for four low-loss ceramic materials from measurements of the resonant frequency and quality factor. For comparison, we measured the same samples in a cylindrical resonator and found good agreement between the two sets of measurements. In addition, we identified the largest sources of error in the complex permittivity measurement and performed an uncertainty analysis.

A2-3
1440

CHARACTERIZATION OF WEAK, ELECTRICALLY SMALL EMITTERS FROM TEM-CELL MEASUREMENTS

David A. Hill and Kenneth H. Cavcey
Radio Frequency Technology Division
National Institute of Standards and Technology
Boulder, CO 80303-3328

Electrically small emitters (with dimensions much less than a free-space wavelength) can be characterized by their electric and magnetic dipole moments. Measurement methods using three orthogonal loop antennas (M. Kanda and D.A. Hill, *IEEE Trans. Electromag. Compat.*, 34, 1-3, 1992) or transverse electromagnetic (TEM) cells (I. Sreenivasiah et al., *IEEE Trans. Electromag. Compat.*, 23, 113-121, 1981) have been implemented and applied to electromagnetic compatibility (EMC) problems. The purpose of this paper is to describe a variation of the above TEM-cell method that is simpler and more sensitive in characterizing weak emitters.

The previous TEM-cell method required the sum and difference of the outputs of the two ports to determine one component of the electric dipole moment and one component of the magnetic dipole of the unknown emitter to be characterized. Our method uses a one-port measurement with the opposite port either open or short circuited. When the opposite port is open circuited, the cell functions as a shielded capacitor which responds to one component (normal to the center septum) of the emitter's electric dipole moment. When the opposite port is short circuited, the cell functions as a shielded inductor which responds to one component (transverse to the axis and parallel to the center septum) of the magnetic dipole. In both cases, the sensitivity of the method is enhanced by the unity, in-phase reflection from the open-circuited or short-circuited port. Lorentz reciprocity is used to provide a quantitative theory for the output voltage in terms of the particular dipole moment. This method has a smaller bandwidth than the sum-and-difference method because the length of the cell must be small compared to the free-space wavelength.

This method has been demonstrated on a weak, low-frequency emitter in a TEM cell of length 0.73 m. Both the time-domain waveform and the frequency-domain spectrum have been measured for three orthogonal orientations of the emitter.

A2-4
1500

PRACTICAL TWO-PORT SCATTERING PARAMETER MEASUREMENT TECHNIQUE FOR LARGE SIGNAL APPLICATIONS

J. B. Call
Motorola Semiconductor Products Sector
Wireless Infrastructure Systems Division
Mail Drop E102
5005 East McDowell Road
Phoenix, AZ 85008
W. A. Davis
The Bradley Department of Electrical Engineering
Virginia Polytechnic Institute and State University
Blacksburg, VA 24061-0111

An innovative microwave measurement technique is described that facilitates two-port large signal microwave measurements which have traditionally been regarded as being beyond the safe operating limits of laboratory instruments. Calibration of the measurement system is achieved using readily constructed standards and a one-way Reflect-Thru-Line (RTL) calibration method (W. A. Davis, et. al., National Radio Science Mtg., Jan. 1993). The RTL calibration method provides the convenience of the familiar TRL calibration available on high-end network analyzers with a system measurement topology that can be easily adapted to high power or novel measurement applications where it may not be prudent or possible to directly stimulate the second port. Using the RTL measurement method, port 2 measurements can be made with an RF input on port 1 and two independent load terminations. The measurement system can readily accommodate additional attenuation in the measurement path without affecting the input and output power levels of the device under test (DUT). The unique capability of obtaining port 2 measurements by driving port 1 allows for true two port measurement of devices operating in class B. This system has been used successfully to safely measure RF power transistors at input and output levels well beyond the typical upper limit for standard microwave test equipment. The instrumentation can be safely isolated from the direct signal path so that unforeseen catastrophic events, such as DUT instability, will not have adverse effects on sensitive equipment. An additional benefit of this measurement system is that the load is always known as a result of the measurement process. With slight modifications the system has been used as a low-cost platform for load-pull measurements without requiring precision tuners.

A2-5
1540

Non-Ideal Ground Return Path Measurements and Modeling

Andrew Byers, Melinda Piket-May
Department of Electrical and Computer Engineering
Campus Box 425, University of Colorado, Boulder,CO 80309
byersa@maori.colorado.edu
mjp@colorado.edu

Steve Hall
Intel Corp.
Platform Architecture Labs
stephen.h.hall@intel.com

Non-ideal ground return path issues can pose several significant problems for high-speed system designers. In an ideal system, the return current travels through the ground plane directly beneath the transmission line. A non-ideal ground return path occurs when there is a discontinuity in the ground plane, such as a hole or a slot, that causes the return current to diverge away from the ideal path. Occurring in many different forms, non-ideal return path problems can cause detrimental effects such as ground bounce, timing pushouts, signal disruption, and electromagnetic incompatibility. The purpose of this study is to quantify through measurements the timing and signal quality impacts of a transmission line passing over a slot in the ground plane. Additionally, modeling techniques were developed to predict these timing and signal integrity impacts.

To evaluate the impact of this ground return path problem, a test board was built that consists of two parallel microstrip lines traversing a slot in the ground plane. Time domain reflectometry (TDR/TDT) was used to measure the effects of the gap on flight time and signal quality as a function of the ground current divergence path. Simulation techniques using FDTD algorithms, as well as traditional HSPICE and QUAD simulators, were then developed and compared to the measurements. The study highlights the three major problems associated with this specific non-ideal return path: a large inductive disruption in the signal, a degradation of the edge rate at the receiver, and an unusually high coupling coefficient between lines that are traversing the same gap. Detailed descriptions of these problems will be presented, along with an analysis of their causes. Since any type of non-ideal return path will introduce additional timing uncertainties into the system and degrade timing budgets, the ability to identify and model the specific mechanisms that contribute to the performance degradations is vital. This study quantifies the performance degradation caused by a specific ground return path discontinuity, explores several different modeling techniques and gives insight into the performance impact trends that can be expected for other return path problems. Finally, a rudimentary set of design guidelines is presented that will help designers mitigate the effects of ground return path problems in future designs.

A2-6
1600

AZIMUTHAL SCATTERING PATTERN OF MOTOR VEHICLES

Ram M. Narayanan and Scott R. Klawitter
Department of Electrical Engineering
Center for Electro-Optics
University of Nebraska-Lincoln
Lincoln, NE 68588-0511

The azimuthal scattering characteristics of typical motor vehicles were measured at C-band and X-band frequencies (5 GHz to 12 GHz in 1 GHz steps). The vehicles investigated were: Honda Civic DX (small car), Ford Mustang (mid-size car), Nissan Pick-up (light truck), and Jeep Wrangler (utility vehicle). Normalized radar cross section (NRCS) measurements for all four polarization combinations were made using the HP 8720B Network Analyzer configured as a short range radar system, using appropriate antennas for each frequency band. Antennas were physically rotated by 90 degrees to achieve different polarization combinations. Measurements were made on vehicles placed on a rotating turntable in the parking lot of a local car dealer. The distance between the antennas and the vehicles was approximately 4 meters, and the illuminated spot size was within the range of 0.9-1.5 meters over the frequency range. Calibration was performed using a direct 8-meter transmit link for the VV and HH polarizations before and after each measurement.

Our measurements indicate that the azimuthal scattering pattern shows significant lobing characteristics, with peak-to-null ratios of the order of 20 dB. As expected, the azimuth-averaged NRCS for the like-polarized, i.e., VV and HH, backscatter is higher than for the cross-polarized, i.e., VH and HV, backscatter by about 5-10 dB. There does not appear to be a strong dependence of the backscatter on vehicle type. However, the data reveal that in the C-band frequency range, especially at 6 GHz, all of the vehicles studied show significantly higher VV-polarization NRCS values (of the order of +10 dB) over a broad angular range when viewed from the rear. This indicates that the C-band frequency range is well-suited for developing low-cost rear-end collision avoidance radar systems.

A2-7
1620

MICROWAVE HOLOGRAPHIC MEASUREMENTS OF THE GEORGIA TECH WOODBURY RESEARCH FACILITY

Wonchalerm Chalodhorn* David R. DeBoer Paul G. Steffes
School of Electrical and Computer Engineering
Georgia Institute of Technology
Atlanta, GA

The Georgia Tech Woodbury Research Facility, built in mid-1970's for use as a satellite communications station, consists of a pair of 30-meter Cassegrain antennas located 65 miles south of Georgia Tech's Atlanta campus (DeBoer *et al.*, *SPIE Tele scope Control Systems III*, **3351**, 157-164, 1998). Though abandoned in the early 1980's the facility still provides a potential resource for radio astronomy and satellite communications research and was acquired by Georgia Tech in 1992. One of the tw o antennas has been fully upgraded and was used as part of SETI Institute's Project Phoenix in the past two years.

To characterize the performance of this refurbished antenna, the microwave holography technique (Rahmat-Samii, *IEEE A&P Trans.*, **AP-33**, 1194-1203, 1985) has been performed at C-band (4.2 GHz). Both the antenna under test and the reference ante nna (a ten-foot focal reflector antenna) receive the satellite telemetry beacon from a geostationary satellite and are coherently downconverted to a baseband frequency of 10 kHz. Both signals are then digitized using a 200 kHz sampling frequency and store d on a PC. To improve the accuracy, those sampled signals are then modeled using the Steighlitz-McBride signal modeling algorithm, which is based on iteratively minimizing the mean square error. The regenerated signals from the models are significantly le ss noisy in comparison to the incoming signals. Finally by correlating those signals over several periods, the phase difference can be obtained.

Besides the measurement noise, several external effects are found to affect the accuracy of the holographic measurement. The temperature variation between day and night can cause substantial phase drift between two signals and since the measurement will t ake a substantial amount of time (about 90 hrs), the movement of the satellite as well as the instrumental gain and phase drift must be taken into account. Therefore instead of collecting data consecutively, the antenna under test is repointed to the sate llite periodically to calibrate the relative amplitude and phase (*ibid.*). The data rate of the telemetry beacon also has a large impact on the rms noise level of the measurement.

A2-8
1640

USE OF MICROWAVE LABORATORY DEMONSTRATIONS AT THE UNIVERSITY OF ARIZONA

S. L. Dvorak* K. L. Virga R. W. Ziolkowski D. G. Dudley
Department of Electrical and Computer Engineering
The University of Arizona, Tucson, AZ 85749

Since electromagnetics (EM) is one of the more mathematical, and possibly more abstract areas of electrical engineering, the faculty in the Department of Electrical and Computer Engineering (ECE) at the University of Arizona have encountered numerous unprepared and disinterested students in the undergraduate EM courses. In order to help address this problem, we have developed various techniques that both stimulate interest in EM and demonstrate the relationship between EM theory and physical phenomenology. There are three methods used to achieve this goal. First, we regularly bring physical components into our undergraduate and graduate microwave course lectures in order to provide students with a better feeling for the applications of the theory that is being discussed. Example "show and tell" components include antennas, waveguiding structures, couplers, cavities, tuners, etc. Such devices can be used to emphasize that high-frequency design techniques are very different from the standard circuit techniques used at lower frequencies.

We have also designed a "hands-on" Microwave Measurements course (ECE 481), which has been offered since 1968. Because of the unavailability of state-of-the-art, high-frequency measurement equipment within the ECE department, this course was taught off-campus at Hughes Missle Systems Company (now Ratheyon) from 1984 to 1992. In 1992, a gracious gift from Hughes and Hewlett Packard was used together with Departmental funds to purchase the modern measurement equipment necessary to bring ECE 481 back on campus in 1993.

The Microwave Measurements course has consistently received high marks from the students that take the course. Unfortunately, equipment availability limits the class size to approximately twenty students. Therefore, we felt that it was also necessary to expose the rest of the students in the ECE program to high-frequency measurement techniques and practical microwave devices. Thus, we offer students in our other EM courses the opportunity to attend optional microwave laboratory demonstrations. These demonstrations include some of the more interesting experiments taken from the Microwave Measurements course (ECE 481). Included in the demonstrations are slotted-line measurements; network analyzer measurements for various loads, waveguides, tuners, and antennas; spectrum analyzer measurements showing AM and FM modulation; and time-domain reflectometry measurements. These demonstrations have had a positive impact on our program. By exciting the students, it not only improves their performance in the theoretical classes, but it also encourages the students to take additional microwave courses as their technical electives. The details of these lab demonstrations will be discussed in greater detail in this presentation.

B1-1
1420

CONFINED, CLASSICAL, CAUSAL PULSES PRODUCED BY FINITE-ENERGY SOURCES IN A BOUNDED VOLUME

A. D. Yaghjian
AFRL/SNH, Hanscom AFB, MA 01731, USA

The magnetic and electric fields along the central z axis of a circular disk of uniform surface current with radius a and arbitrary time dependence $\mathbf{K}(t)$ is given by (Blejer, Wittmann and Yaghjian, 285-292 in Ultra-Wideband, Short-Pulse Electromagnetics, NY: Plenum, 1993)

$$\mathbf{H}(z,t) = -\frac{1}{2}\hat{\mathbf{z}} \times \left[\mathbf{K}\left(t-\frac{z}{c}\right) - \frac{z}{\sqrt{z^2+a^2}}\mathbf{K}\left(t-\frac{\sqrt{z^2+a^2}}{c}\right)\right] \tag{1}$$

$$\mathbf{E}(z,t) = -\frac{1}{2}\sqrt{\frac{\mu}{\epsilon}}\left[\mathbf{K}\left(t-\frac{z}{c}\right) - \frac{z^2+\frac{a^2}{2}}{z^2+a^2}\mathbf{K}\left(t-\frac{\sqrt{z^2+a^2}}{c}\right) + \frac{1}{2}\frac{ca^2}{(z^2+a^2)^{3/2}}\int_{-\infty}^{t-\sqrt{z^2+a^2}/c}\mathbf{K}(t')dt'\right] \tag{2}$$

where $c = 1/\sqrt{\mu\epsilon}$ is the speed of light, and μ and ϵ are the permeability and permittivity of free space.

In principle, a pulse can be sent to infinity with finite or even infinite energy through a finite area. For example, equations (1) and (2) show that a current source with delta-function time dependence on a circular disk radiates two pulses (forming an "electromagnetic missile") with infinite energy to an indefinitely large distance in the direction of the z axis, which is normal to the center of the disk.

In general, however, one can argue that a current source of finite energy in a bounded volume cannot radiate an electromagnetic missile with nondecaying energy to an infinitely large distance from the source (Wu, J. Appl. Phys., 57, 2370-2373, 1985). The argument goes as follows. Because a source pulse of finite bandwidth cannot generate an electromagnetic missile, any electromagnetic missile must maintain itself on the energy in the increasingly higher frequencies. If the total energy radiated by the sources is finite, the energy in the frequency spectrum at frequencies higher than any finite value must approach zero.

Nonetheless, finite energy current sources are mathematically possible that will produce a pulse that travels without decay of the energy to a finite distance arbitrarily far from the source region. To see this, let the surface current $\mathbf{K}(t)$ on a current disk of fixed radius a have a time dependence given by the function

$$\mathbf{K}(t) = \hat{\mathbf{x}}\begin{cases} \dfrac{1}{\sqrt{t_1}}, & 0 < t \le t_1 \\ 0, & t \le 0 \text{ and } t > t_1 \end{cases} \tag{3}$$

with $t_1 > 0$. This current radiates a finite energy because $\int_0^{t_1} |\mathbf{K}(t)|^2 dt = 1$. Now equations (1) and (2) show that this current will radiate two separate nondecaying finite-energy pulses to the far field along the z axis provided $a^2/(2cz) \ge t_1$. In other words, the pulses will travel with finite nondecaying energy to a distance z given by $z = a^2/(2ct_1)$. Since, in principle, t_1, the width of the current pulse, can be made arbitrarily small, the excited pulses can be made to travel arbitrarily far along the z axis without any loss in energy. Moreover, it can be shown that the significant transverse area of the pulses is approximately equal to the area (πa^2) of the current disk. Of course, for a fixed nonzero value of t_1, the energy in the pulse will begin to decay beyond the distance $z = a^2/(2ct_1)$. Also, since the frequency spectrum of the current pulse has the extremely slow decay of $\sin(\omega t_1/2)/\omega$ as $\omega \to \infty$, these classical, fixed-energy, nonspreading pulses cannot be generated in the laboratory (today or in the foreseeable future).

B1-2
1440

LC CHARACTERISTICS OF A SINGLE LOOP INDUCTOR INSIDE A PEC SHELL

John C. Young* Chalmers M. Butler
Department of Electrical and Computer Engineering
Clemson University
Clemson, SC 29631-0915

In the design of LC circuits for broadband antennas, it is desirable to reduce the size of the LC circuits as much as possible so that deployment in antennas is feasible. These circuits typically consist of a coil inside a metal cylindrical shell, often with an additional structural member which with the shell forms a capacitor. The goal of this study is to devise a means of significantly reducing the physical size of the circuit without altering the values of LC or increasing its weight. Of interest are the factors which contribute to inductance and capacitance and which have a bearing on size and weight. In this study, we analyze a single loop inductor inside a cylindrical shell and determine what effect the presence of the conducting shell has on L. For the purpose of this initial investigation, we assume a filamentary loop inside a perfectly conducting cylindrical tube of infinite length. The radius of the metal shell is taken to be much much smaller than a wavelength. Under these assumptions, the shell acts as a waveguide well below cutoff so the field created by the wire loop decays very rapidly as a function of axial displacement in the tube. Therefore, the simple model of a single wire loop inside an infinite cylindrical PEC is a convenient one on which to base a study of the design tradeoffs between the circuit's size and its LC characteristics. To better understand the effect of the shell on the inductance of the wire loop, the inductance of a wire loop without a shell is first calculated. The effects of the PEC shell on the inductance of the loop is then analyzed by calculating the inductance of the loop-shell combination for varying values of shell radius. These results show that, as the shell radius approaches that of the wire loop, the inductance of the circuit rapidly approaches zero. The capacitance between the wire loop and the shell is then calculated and is seen to be negligible compared to the inductance at frequencies of interest. The capacitor in a prototype circuit is created by overlapping the end of the metal shell with part of the antenna itself. To achieve a significant capacitance value either the distance between the antenna member and the shell must be made small or the overlapped area must be large. Our analysis shows that, if the distance between the shell and the antenna member is made small enough to increase the capacitance significantly, the inductance becomes very small. Hence, the overlap and shell radius must be larger than desired. To validate the analytical results, measurements are performed on a simple laboratory model.

B1-3
1500

EXACT RADIATION AND SCATTERING FROM A METAL ELLIPTIC CYLINDER AT THE INTERFACE BETWEEN TWO ISOREFRACTIVE HALF SPACES

P. L. E. Uslenghi
Dept. of EECS, University of Illinois at Chicago
Chicago, Illinois 60607-7053

A perfectly conducting elliptic cylinder at the interface between two isorefractive half-spaces is considered. Two configurations are examined: the case of a cylinder whose elliptical cross-section has the major axis in the plane interfacing the two media, and the case in which the minor cross-sectional axis lies in the interface plane. In either case, the primary source is a plane wave (TE or TM polarized), an electric or magnetic line source parallel to the elliptic cylinder axis, or an arbitrarily located and oriented electric or magnetic dipole.

All the above boundary-value problems are solved exactly by separation of variables followed by the imposition of boundary and radiation conditions. The solutions are in terms of series (and, for dipole sources, integrals) of Mathieu functions. They are of interest because they constitute new canonical solutions, and because they provide test cases for computer codes developed for penetrable structures.

In the limit case in which the cross-section of the conducting cylinder has eccentricity equal to one, the cross-section becomes that of a metal strip. The first configuration then involves boundary-value problems for a metallic strip located at the interface between two isorefractive half-spaces. A comparison between this case and the complementary case of a slit in a conducting screen separating two isorefractive half-spaces leads to an extension of Babinet's principle. The second configuration yields a metallic strip normal to the interface between two isorefractive half-spaces, and extending an equal distance into both half-spaces.

B1-4
1540

EXACT RADIATION AND SCATTERING FROM A SLOTTED SEMIELLIPTICAL CHANNEL FILLED WITH ISOREFRACTIVE MATERIAL

P. L. E. Uslenghi
Dept. of EECS, University of Illinois at Chicago
Chicago, IL 60607-7053

A semielliptical channel flush mounted to a perfectly conducting ground plane and open along the strip connecting the two foci of the semielliptical cross-section is considered. The channel is filled with isorefractive material and the half-space above the channel is free space. Isorefractive material means that the product of relative permittivity and relative permeability of the material filling the channel is equal to that of the free space above it, i. e. unity; thus, the refractive index of two materials isorefractive to each other is the same, whereas the intrinsic impedances of the two materials are different.

The boundary-value problems involving the scattering of an incident TE or TM plane wave, the radiation from an electric or magnetic line source parallel to the channel, and the radiation from an electric or magnetic dipole arbitrarily located and oriented are solved exactly by separation of variables and imposition of the boundary and radiation conditions. The solutions involve series and, for dipole sources, integrals of Mathieu functions. In the particular case of a channel filled with air and incident TE plane wave, the solution reduces to one previously obtained by the author (P.L.E. Uslenghi, *Proc.IEEE-APS Int. Symp.,* Chicago, Illinois, July 1992). Considerations involving low- and high-frequency analyses are developed.

When the channel extends to infinity in transverse dimensions, the problem of a slot in a perfectly conducting screen separating two isorefractive half-spaces is solved, as a particular case. All these solutions are important for two reasons: first, they enrich the catalog of available canonical solutions, and second, they provide validation test cases for computer codes involving penetrable structures.

B1-5
1600

NEW CHARACTERIZATIONS OF NONRADIATING CURRENT DISTRIBUTIONS

Edwin A. Marengo* Richard W. Ziolkowski
Department of Electrical and Computer Engineering
1230 E. Speedway
The University of Arizona
Tucson, AZ 85721

Current distributions which do not radiate (referred to as nonradiating (NR) sources) have been studied since the early days of electromagnetic theory. Interest in such a class of sources appears to have originated from their possible connection with questions of radiation-reaction and models of charged particles (D. Bohm and M. Weinstein, *Phys. Rev.*, **74**, 1789-1798, 1948). In more recent years, most of the (renewed) interest in NR sources has been linked to their role in inverse source and inverse scattering theories (where they arise as the null space of the mapping from the source (scatterer) to the field) (N. Bleistein and J.K. Cohen, *J. Math. Phys.*, **18**, 194-201, 1977).

We report new descriptions of time-dependent NR current distributions based on recently derived time-dependent plane-wave and multipole expansions for electromagnetic fields (E.A. Marengo and A.J. Devaney, *J. Math. Phys.*, **39**, 3643-3660, 1998). The results are corroborated and developed further by using the time-dependent scalar and vector potentials $\phi(\mathbf{r}, t)$ and $A(\mathbf{r}, t)$ in both the Lorentz and Coulomb gauges. The general results derived for arbitrary time-dependence are then found to reduce to well known results derived for sources and fields having time-harmonic time-dependence. In particular, the characterization of NR current distributions from the points of view of time-dependent plane-wave and multipole expansions is seen to reduce to that derived by Devaney and Wolf (A.J. Devaney and E. Wolf, *Phys. Rev.*, **8**, 1044-1047, 1973) for time-harmonic sources and fields.

By using a Radon transform representation of the time domain radiation pattern, NR sources are found to be analogous to the so-called ghost (invisible) objects of computerized tomography (A.K. Louis, *SIAM J. Math. Anal.*, **15**, 621-633, 1984). A procedure is derived for constructing rather arbitrary time-dependent piecewise continuous (spatially and temporally) sources confined within a specified region of support. The time-harmonic counterpart of the procedure is examined in detail. We use spherical harmonics and a Fourier-Bessel series to derive complete sets for all monochromatic continuous NR sources that are confined within a spherical volume $V : r \leq a$ and for the fields they produce.

B1-6
1620

GREEN DYADICS FOR SELF-DUAL BI-ANISOTROPIC MEDIA

I.V. Lindell, F. Olyslager*
Electromagnetics Lab., Helsinki University of Technology
PO Box 3000, FIN-02015 HUT, Espoo, Finland
* Department of Information Technology, University of Ghent
Sint-Pietersnieuwstraat 41, B-9000 Ghent, Belgium

The most basic problem of electromagnetics related to any particular linear electromagnetic medium is to find the field created by a vector point source (an electric and/or magnetic dipole) in the homogeneous medium filling all space. Such a field created by a point source of unit magnitude and isotropic direction (a dyadic source) is called the Green dyadic. Knowledge of the Green dyadic in analytic form allows one to formulate a wide variety of electromagnetic problems associated to the medium in question in terms of integral equations. This is why it is of prime importance to find analytic formulations for Green dyadics for as many different media as possible. The effort so far has been limited to a small number of media.

In this paper, the Green dyadic problem is solved for a class of linear and bi-anisotropic media, labeled as self-dual media, whose material parameter are defined in terms of two independent dimensionless dyadics $\overline{\overline{\alpha}}$ and $\overline{\overline{\kappa}}_r$ in the form

$$\begin{pmatrix} \mathbf{D} \\ \mathbf{B} \end{pmatrix} = \begin{pmatrix} \epsilon\overline{\overline{\alpha}} & \sqrt{\mu\epsilon}(\chi_r\overline{\overline{\alpha}} - j\overline{\overline{\kappa}}_r) \\ \sqrt{\mu\epsilon}(\chi_r\overline{\overline{\alpha}} + j\overline{\overline{\kappa}}_r) & \mu\overline{\overline{\alpha}} \end{pmatrix} \cdot \begin{pmatrix} \mathbf{E} \\ \mathbf{H} \end{pmatrix}.$$

The class of self-dual media can be defined as consisting of linear and bi-anisotropic media satisfying any of the following three conditions:
(1) The media are invariant in duality transformation,
(2) The media allow factorization of the second-order dyadic Helmholtz operator in terms of two first-order dyadic operators,
(3) The media allow decomposition of fields and sources in two independent electromagnetic problems in a way that is an extension of the Bohren decomposition well known for isotropic chiral media.

It is shown that the Green dyadic can be solved in closed analytic form for any self-dual bi-anisotropic medium and its general expression is given in terms of the self-dual decomposition. This generalizes previous results where special cases of self-dual media were considered.

C/D1-1
1400

HIGH-SPEED, MIXED-SIGNAL COMPONENTS FOR ADVANCED DIGITAL COMMUNICATION SYSTEMS

Ruai Yu* Neng-Haung Sheng Jeff Liu Brian Sung Vincent Ho Paul van der Wagt Kevin Cheng Gary Gutierrez Pete Zampardi
Rockwell Science Center
1049 Camino Dos Rios
Thousand Oaks, CA 91360

Currently most military and space communication, radar, and EW systems use a separate set of hardware for a given system function. As a result, systems incorporating many of these functions are bulky, heavy, power-hungry, and expensive to make and maintain. Recently, advanced digital receiver concepts were proposed where the entire signal spectrum of interest is digitized, and powerful digital signal processing techniques can then be used to perform channel selection. Consequently, a single set of hardware can be used for many different system functions because the system functions are now determined with software/digital circuitry and can be easily reconfigured for different system needs. However, success of such system concepts hinges upon practical realization of analog-to-digital converters (ADCs) capable of digitizing a wide instantaneous frequency bandwidth (tens of Megahertz to a few Gigahertz) with high resolution (8–16 bit) and high sampling frequencies. The same can be said about broadband transmitters where different waveforms need to be generated for different system functions. High-speed, high-resolution digital-to-analog converters (DACs) and direct digital synthesizers (DDS) are the key components for such transmitters.

With more than a decade of research and development of high-speed, high-resolution mixed-signal circuits, Rockwell Science Center has established unique expertise in this area and has demonstrated numerous state-of-the-art results in ADCs, DACs, and DDS. For example, we have successfully developed 6–10 bit, 1–6 GS/s Nyquist ADCs and both low-pass and band-pass Sigma-Delta modulators; we have demonstrated > 1 GS/s, 12-bit DACs and > 1.7 GHz DDS with > 60 dB SFDR. Some of these devices are now commercially available to serve the needs of both commercial and defense industries. In this presentation, we will review our recent results on these devices and discuss their implications on future military and commercial communication, radar, and EW systems based on DSP techniques.

This work is funded in part by DARPA/NRaD, AFWPL, NASA, ONR.

C/D1-2 1440

MILITARY RECEIVER TECHNOLOGY

Dr. James Tsui
Air Force Research Laboratory
Sensors Directorate
AFRL/SNRP, Wright Patterson AFB, OH 45433
tsuijb@sensors.wpafb.af.mil

This talk will cover wide band and narrow band military receivers. These receivers are mainly used for electronic warfare (EW) applications. Wide band receivers are used to intercept radar signals. Narrow band receivers are used for intercepting communication signals. The requirements of the wide band receivers are high sensitivity and dynamic range with the capability of processing simultaneous signals. The requirements of the narrow band receiver are high sensitivity and versatility. The present approaches to build these receivers are through digital technology. The input signals are digitized as close to the antenna as possible. Digital signal processing is used to obtain the desired information. For the wide band receiver, the desired information is the carrier frequency, pulse width, pulse amplitude, time of arrival and angle of arrival. For the narrow band receiver, the desired information is the modulation type, chip rate, hopping rate and protocol of digital message. At present time the wide band receivers are built through digital channelization. There are two approaches to perform digital channelization. One is to use the multirate digital signal processing and the other way is to use monobit approach. The multirate approach produces coarse channelization but with high instantaneous dynamic range. The monobit approach provides fine channelization but low instantaneous dynamic range. The monobit receiver can process only two simultaneous signals, however, the receiver design is very simple and can be fabricated on a single chip. The future approach to build narrow bandwidth receivers will be through software processing. The function of the receiver can be changed by only using different software. Therefore, one receiver can be used as many different kinds of receiver applications.

C/D1-3 1540 ANALOG ADAPTIVE EQUALIZATION IN MOBILE COMMUNICATIONS

R.L. Ewing (Air Force Research Lab)

C/D1-4
1620

HIGH PERFORMANCE InP HBT TECHNOLOGY FOR ANALOG-TO-DIGITAL CONVERSION AND SIGNAL PROCESSING

Joseph F. Jensen* Gopal Raghavan Bob Walden Bill Stanchina
Hughes Research Laboratories
3011 Malibu Canyon Road
Malibu, CA 90265

The trend in modern communications and radar systems is to move the analog-to-digital interface as far forward in the signal path as possible toward the antenna or sensor. Moving the digital interface forward in the signal path eliminates stages of downconversion and analog filtering that are bulky, expensive, drift with temperature, and require calibration. Ultra-fast device technologies are required to perform direct analog-to-digital conversion on radio frequency (RF) or intermediate frequency (IF) signals that enables moving the digital interface forward in the signal path. This paper describes the performance limits of current analog-to-digital converters (ADCs) and shows how the ultra-fast performance of InP HBT technology is extending the performance of ADCs to higher levels to enable all digital approaches to communications receivers. Using InP HBT IC technology with an 80-GHz f_T and f_{max}, we have demonstrated an 8 GSPS 3-bit flash ADC, a low-pass second-order DS modulator sampling at 3.2 GHz producing 70 dB dynamic range for 50 MHz signal bandwidth, and 4 GSPS sample rate second-order bandpass DS modulator producing SNR values ranging from 89 dB over a 366 KHz bandwidth to 42 dB over a 62.6 MHz bandwidth centered at an IF of 60 MHz. In the area of digital signal processing we have demonstrated 12-bit pipelined accumulators operating at 7 GHz in the same technology. New results using our advanced InP HBT process have extended our transistor cutoff frequency to greater than 200 GHz. Using these high-speed transistors, we now have demonstrated flip-flop toggle rates of greater than 50 GHz. This new work will have a great impact on analog-to-digital conversion, all-digital receivers, and digital signal processing.

F2-1
1340

WALLOPS'98 PROPAGATION EXPERIMENT REFRACTIVITY DATA ANALYSIS

G. Daniel Dockery and Michael H. Newkirk
The Johns Hopkins University Applied Physics Laboratory
11100 Johns Hopkins Road
Laurel, MD 20723-6099

In March 1998, The Johns Hopkins University Applied Physics Laboratory performed environmental measurements to support the ONR-sponsored Wallops'98 Propagation Experiment. This experiment brought together investigators from several organizations to study multi-spectral propagation effects. In this presentation, the APL measurements are used to generate predictions of the propagation conditions that occurred during several of the test days. These predictions are used in the Georgia Tech (GIT) sea clutter model and compared to measured sea clutter levels provided by SPANDAR, the S-band radar located at NASA – Wallops Island. Surface wind and wave conditions and modeled evaporative duct profiles were provided by APL's SEAWASP-instrumented *Chessie* research vessel, which was present for all but one day of the main test event. *Chessie* also provided a platform for numerous rocketsonde launches. The propagation predictions are performed with APL's TEMPER model using input refractivity data from both helicopter and rocketsonde measurement systems where appropriate. A brief description of the evaporative duct models and refractivity processing programs will be included.

Helicopter measurements from this test show significant time and range dependence in the refractivity data. A variety of ducting, sub-refractive and nearly standard atmosphere conditions were observed during the month-long test event. Rocketsonde measurements provide altitude-dependent, single location refractivity data primarily when weather conditions prevented helicopter flights. Surface data from *Chessie* provides roughness information that is used in TEMPER. The output grazing angle and propagation factor from TEMPER is combined with the roughness information in the sea clutter model to obtain modeled sea clutter levels that are compared to measurements made with the SPANDAR radar.

F2-2
1400

REFRACTIVITY FROM CLUTTER: EXPERIMENTAL RESULTS FOR EVAPORATION DUCTING

L. Ted Rogers
Propagation Division
Space and Naval Warfare Systems Center
49170 Propagation Path
San Diego, CA 92152-7385
Email: trogers@spawar.navy.mil

The refractivity profile for an evaporation duct is normally generated by inputting in situ measurements of meteorological parameters into a Monin-Obukhov similarity theory based model, and is often fully described by a single parameter, the evaporation duct height. An alternative method for sensing evaporation ducts -- by inferring them from radar sea clutter returns -- is now investigated. This investigation was prompted by the results of *Pappert, Paulus and Tappert*, (Radio Science, 27(2), pp. 189-209, Mar.-Apr., 1992) which indicated the slope of the clutter power with respect to range (for the case of horizontally homogeneous environmental conditions) was very nearly a 1:1 function of the evaporation duct height. This implied to the author that the evaporation duct height could be inferred from measuring the slope of the clutter power with respect to range, provided the spatial variability of the sea clutter radar cross section (RCS) was not too great.

An experimental effort was undertaken using the Space Range Radar (SPANDAR), a high-powered S-Band radar located at Wallops Island, Virginia. Evaporation duct heights are inferred from the radar clutter using spatial filtering to mitigate the effects of some scales of the spatial variability of the sea clutter RCS. Inferred duct heights are compared to evaporation duct heights calculated from in-situ meteorological measurements. It is found that the inferred duct height values are strongly correlated but positively biased with respect to values obtained from in situ sensing.

F2-3
1420

SCALING NEAR-SURFACE INFLUENCES ON RADAR PROPAGATION

K. L. Davidson* P. A. Frederickson
Department of Meteorology
589 Dyer Road
Naval Postgraduate School
Monterey, CA 93943-5114

Persons and platforms from the Naval Postgraduate School participated in a one-month long observational experiment on processes affecting and prediction of radar propagation in the over water coastal region, Wallops'98. A defining feature of Wallops'98 is the coordinated atmospheric surface-layer and surface wave measurements made to establish near-surface gradients affecting radar field strength and backscatter inversion measurements. A second defining feature is that Wallops'98 occurred in a coastal region with a wide range of surface layer stability and wave conditions. The latter factors made the NPS measurements important in interpretations. The measurements were made from a buoy instrumented mean (5-minute averages) values of temperature, humidity and vector wind at the 5-meter level, and for sea surface temperature using both a buoy hull mounted thermistor and mast-mounted IR sensor. A 2nd buoy was instrumented for two-dimensional surface waves and a small vessel was instrumented for turbulent values of wind and temperature. The buoy measurements were made continuously over the one-month walops'98 period and the vessel measurements were made on most days when radar measurements were being made.

Interpretations of the multi-variable and multi-sensor in situ data set are being performed relative to the adequacy of existing bulk expressions in describing the near-surface gradients. It is expected that coastal circulation and lack of wave influences are not taken into account by existing expressions. Further, a wide range of the thermal stability conditions existed. The vessel obtained turbulence data enable evaluation of suitability of drag and exchange coefficients within the existing bulk expressions. The two-dimensional wave measurements enable relating differences to equilibrium or non-equilibrium wave forcing and wave-age values. Most important, application of the atmospheric surface- layer and surface wave conditions to observed radar field strength and backscatter will enable evaluations of the impact of the demonstrated deficiencies in the assumed scaling expression on predicting the latter.

Collaborative measurements of near-surface profiles from the vessel and turbulence measurements during a more recent experiments will also be introduced into the discussions. It is concluded that the overwater stable thermal conditions are those least well determined by existing bulk expressions for near-surface gradients affecting radar propagation and backscatter.

F2-4
1440

REMOTE SENSING OF TIDES AT WALLOPS ISLAND

Kenneth D. Anderson
Propagation Division
Space and Naval Warfare Systems Center
49170 Propagation Path
San Diego, CA 92152-7385
Email: kenn@spawar.navy.mil

The objective of this effort was to establish the height of a reference point on Wallops Island, VA, with respect to the surface of the Atlantic Ocean. For our particular problem, we needed to establish antenna heights above the sea for the month of March 1998, when the Naval Surface Warfare Center, Dahlgren Division, was conducting a series of propagation experiments. At first glance, this task seems straightforward; Wallops Island, a NASA test facility, is well documented with geodetic monuments that are referenced in the vertical to some secular mean of sea level, such as mean low-lower water, mean sea level, or mean high-higher water. However, these secular data are not applicable to "real-time" measurements. For example, the sea surface in San Diego, CA, was raised 10 cm above the secular by the 1998 El Nino.

Obviously, the only way to establish the height of a point above the sea surface in "real time" is to measure the height of the sea surface. For two months in 1969 NOAA's National Ocean Survey (NOS) established a tide gauge at Wallops Island, and they were able to make precise sea level measurements *relative to secular data*. Although the tide gauge was located up a "sea channel" and did not measure the Atlantic Ocean surface, NOS provided data relating measurements at a continuously operating tide gauge, (Wachapreague, VA, about 30 km to the SW) to the location of the Wallops Island tide gauge-- the best that one can do, yet questionable.

New techniques in remote sensing developed at the Space and Naval Warfare Systems Center San Diego (SSC-SD) are applied to this problem, and we can demonstrate an overall standard error of less than 8.2 cm in *remotely sensed* sea surface measurements.

F2-5
1500

A THREE DIMENSION MATCHING METHOD FOR TROPOSPHERIC FEATURES

Dr. Stephen A. Fast and Jason Nathaniel Bode
Applied Research Laboratory
The Pennsylvania State University
P.O. Box 30, State College, Pa 16801-0030
Dr. George S. Young
Department of Meteorology
The Pennsylvania State University
503 Walker Building, University Park, PA 16802

In order for high fidelity radio wave propagation models to make accurate predictions, a correct model of the refractivity is required. To this end, several methods have been developed to match refractivity profile structures between multiple range dependent profiles (G. D. Dockery and J. Goldhirsh, "Atmospheric Data Resolution Requirements for Propagation Assessment: Case Studies of Range-Dependent Coastal Environments," and J. Cook, G. Vogel, and G. Love, "Operational Support for a Range-Dependent Radio Propagation Model," both in AGARD Conference Proceedings 567 titled *Propagation Assessment in Coastal Environments*, 1995). There is broad agreement that using refractivity to match features dismisses relevant information that should be used. The method presented here takes a different approach. When the parabolic equation methods are used to calculated propagation loss, the refractivity is only required at each range step. Hence, any method which can correctly predict refractivity at the range step is appropriate. Previous methods match features for a given vertical cut of the atmosphere, thus introducing sampling errors and ignoring off planar effects. In this paper, we match features in three dimensions using the potential temperature, a conserved quantity derived from temperature and pressure. The variables used to compute refractivity are then interpolated in this matched coordinate system using splines. This results in a correct mapping of features over a region which resolves sampling issues thus replacing refractivity with a smooth function in three dimensions. Therefore as a parabolic equation steps in range, the refractivity is derived from the matched gridded data. This paradigm eliminates the burden of refractivity interpolation/extrapolation from the propagation prediction software. Examples of matched atmospheres are presented along with propagation predictions based upon the matched atmosphere.

F2-6
1540

THE LARGE-SCALE ATMOSPHERIC REFRACTIVITY RANGE INTERPOLATOR (LARRI)

G. C. Konstanzer
The Johns Hopkins University Applied Physics Laboratory
11100 Johns Hopkins Road
Laurel, MD 20723-6099

The Large-scale Atmospheric Refractivity Range Interpolator (LARRI) program was originally developed to process measurements from the JHU/APL helicopter system in support of in situ TEMPER RF propagation analyses for range inhomogeneous environments. It has been successfully applied to measured data for over ten years, for several hundred cases. The algorithm has also been applied to other measured data sets by other organizations as well. The objective of LARRI is to automatically deduce from the measurements a reasonable scheme for the range evolution of those refractivity structures that impact RF propagation so that those structures are realistically preserved in vertical refractivity interpolations for propagation models. To accomplish this, LARRI first filters out small-scale perturbations that do not persist over significant ranges, preserving large-scale structures, and then categorizes features in the resulting profiles. It next develops a scheme for merging similar structures in adjacent profiles, which may be at different altitudes, based on the categorizations and fades out structures that do not persist over range. Finally, vertical profiles are interpolated based on the structure evolution scheme onto a user-defined range grid. All resulting refractivity profiles have the same number of points, a key assumption of most PWE propagation models solved via Fourier Split-Step. Improvements being considered for LARRI include processing based on conserved quantities such as virtual temperature, better categorization and filtering techniques, and characterization of the small-scale perturbations for later inclusion in propagation analyses.

F2-7
1600

REFRACTIVITY ASSESSMENT/FORECAST TOOLS FOR ESTIMATE ENROUTE CONDITIONS

By

Jay Rosenthal, Roger Helvey, Matthew McGovern
and Paul Greiman
Geophysics Branch (521400E)
Naval Air Warfare Center Weapons Division
Point Mugu, California 93042-5001
Voice: (805) 989-7893
Fax: (805) 989-4817
e-mail: rosentj@mugu.navy.mil

Techniques are described for estimating elevated duct height along planned routes based on extraction of cloud top and sea surface information from infrared (IR) and corresponding visual satellite imagery. The approach which uses a radiosonde data base to convert cloud-top temperatures to height, has recently been updated to include superposition of derived duct heights on satellite data displayed on a TESS Remote Workstation (TRWS) and fused with operational geometry to highlight expected conditions in regions of interest. From the TRWS, the derived, fused product can be disseminated to other operational centers ashore or afloat via SIPRNET and web-site communications. The approach requires the presence of marine layer low cloud conditions over ocean or coastal regions. Another approach uses other data and weather-refractivity relationships, previously developed and validated, to develop an expert system (EXPERDUCT) which statistically integrates a number of synoptic, satellite and climatological factors or rules of thumb to statistically estimate duct occurrence, height and intensity. In this mode, estimates can be derived either for current conditions over some region, or predicted conditions, depending on the source of input. EXPERDUCT has been developed for the Eastern Pacific Ocean, and a prototype for the Arabian Gulf area. Both of the above techniques provide potentially independent means of estimating the horizontal variability of the RF propagation environment when sufficient direct measurements are unavailable, and where accurate high-resolution models for the specific area, time and parameters cannot be run with confidence. The indirect, computer-aided techniques described above can provide information useful for input into EM propagation assessment models to provide rough inferences of expected sensor performance.

F2-8
1620

DEVELOPMENT OF AN EXPERT SYSTEM FOR SHIPBOARD ENVIRONMENTAL ASSESSMENT

J. R. Rowland, M. Neves, J. H. Meyer
The Johns Hopkins University Applied Physics Laboratory
11100 Johns Hopkins Road
Laurel, MD 20723-6099

For the past several years, the JHU Applied Physics Laboratory has been investigating methods to effectively assess the electromagnetic propagation environment using a combination of shipboard sensors and meteorological physics. The most well-known product of these efforts is the Shipboard Environmental Assessment/Weapon System Performance (SEAWASP) system, which combines fixed shipboard instruments and expendable rocketsondes with various models and algorithms to estimate the refractive conditions. The challenge in developing such a shipboard assessment capability is to deduce as much about the propagation environment using as few simple measurements as possible. In this paper, the methodology for indirectly extracting information from SEAWASP measurements and other simple observations is referred to as the Environmental Expert System.

The expert system uses physical arguments to combine in situ measurements of air & sea temperature, humidity, visibility, cloud height & appearance, irradiance and other data in order to characterize aspects of the atmosphere that are not directly measured. This process involves a combination of simple algorithms and logic trees to get likelihoods of surface-based ducting or subrefraction, or to indicate that significant changes have occurred and other measurements are required. These methods are also used to determine when evaporation duct models are probably invalid and when conditions can be expected to be highly variable in range. This paper presents the various observations and describes the methodology for inferring various conditions from these observations in an automated manner. Examples from several propagation experiments and SEAWASP deployments are presented to demonstrate the operation of the expert system in its current form.

F2-9
1640

10.5 AND 35 GHZ PROPAGATION IN THE NORTH SEA

Herbert V. Hitney
Propagation Division
Space and Naval Warfare Systems Center
49170 Propagation Path
San Diego, CA 92152-7385
Email: herb@spawar.navy.mil

During 1988 the Netherlands Physics and Electronics Laboratory FEL/TNO conducted an over-the-horizon radio propagation experiment at 10.5, 35, and 94 GHz in the North Sea. The transmitters were on the sea based platform Noordwijk approximately 13 m above mean sea level (msl) and the receivers were on the coast approximately 10 m above msl. The path length was 34.6 km. Supporting measurements including tide height, significant wave height, sea temperature, air temperature, humidity, wind speed and wind direction were also made at the platform. At the time of the measurements these data were only analyzed using the FFACTR propagation model associated with the Engineer's Refractive Effects Prediction System (EREPS), which is an approximate model based on function fits to normal mode waveguide propagation model results which do not account for any rough surface effects. The purpose of this paper is to re-analyze the 10.5 and 35 GHz data using a modern model that includes rough surface effects. The 94 GHz data are not included since the measured data were very sparse.

The evaporation duct can substantially enhance signal levels for over-the-horizon over-sea paths at frequencies above approximately 3 GHz (H.V. Hitney and R. Vieth, *IEEE Trans. Antennas & Propagat.*, 38, 6, 794-799, June 1990; R.A. Paulus, NRaD TR 1644, March 1994). Waveguide and other propagation models and some limited experimental data indicate that wind-driven sea-surface roughness counteracts the effectiveness of the evaporation duct at higher frequencies when both the duct height and the wind speed are relatively high (K.D. Anderson, *IEEE Trans. Antennas & Propagat.*, 38, 5, 746-753, May 1990; H.V. Hitney, AGARD-LS-196, Paper 4B, September 1994). Several methods have been proposed to model the effects of surface roughness under these ducting conditions, but generally these models have not been experimentally validated. The MLAYER waveguide model is used for this study.

Results will be presented for subsets of the FEL/TNO measurements to illustrate the differences in modeled and measured results for both low and high significant wave heights.

G2-1
1420

DATA ASSIMILATION TECHNIQUES AND FORECASTING THE THERMOSPHERE IONOSPHERE SYSTEM

Tim Fuller-Rowell
CIRES, University of Colorado and NOAA, SEC
325 Broadway
Boulder, CO80303

To forecast the future structure of Earth's thermosphere and ionosphere requires a reliable estimate of the current state of the system. This can only be achieved by using data assimilation techniques. The two most widely used techniques are Kalman filters and adjoint models. Adjoint methods and Kalman filters are methods of optimally combining data and physical models to specify the state of the system. The attractive property of both methods is the ease with which direct measurements can be assimilated without the need for costly error-prone data inversions. Until now the sparse availability of data has made it impossible to accurately specify the global state of the system such that realistic forecasts have been impractical. A fundamental change in data availability will shortly arise from a new constellation observing system (COSMIC) and from measurements from instruments on the DMSP series of satellites. These multi-satellite systems will provide the first real-time, global ionospheric and thermospheric observations, which will enable accurate specification of the current state, and lead to the real possibility of forecasting the thermosphere and ionosphere into the future. Data assimilation techniques can also be used to explore the physics of the upper atmosphere, as well as provide the framework for real-time operational use. These techniques although widely used in other disciplines, such as weather forecasting, are only now beginning to be utilized by the upper atmosphere community. The fundamental difference in the upper atmosphere is that the system is strongly forced by the sun, the magnetosphere, and the lower atmosphere. In spite of the strong external forcing, the long internal time-scales of the thermosphere ionosphere system renders forecasts one or two days into the future a practical prospect.

G2-2
1440

THE DEVELOPMENT OF A PHYSICS BASED IONOSPHERIC DATA ASSIMILATION MODEL

G. A. Hajj,* X. Pi and L. J. Romans
Jet Propulsion Laboratory
4800 Oak Grove Dr.
Pasadena, CA 91109
C. Wang
University of Southern California
Department of Mathematics
Los Angeles, CA 90089

In the last decade, ionospheric tomography has been established as a technique to image electron density distribution and its response to magnetic storms. At the same time, the global positioning system (GPS) infrastructure has grown to a level where ionospheric imaging is becoming truly global and continuous. For instance, there are 200 continuously operating globally distributed ground GPS receivers, each providing 6-8 simultaneous measurements of Total Electron Content (TEC). In addition, in the the next three years, it is expected to have 6-12 receivers in LEO which, along with the ground measurements, will provide an unprecedented coverage of the ionosphere.

Although ionospheric tomography is a powerful technique for imaging electron density, it does not directly reveal the physical drivers behind the ionospheric state. It is also not suitable for the purpose of ionospheric weather forecasting. In order to overcome these limitations, we have embarked on developing a physics based model capable of assimilating TEC data collected from GPS in a manner similar to conventional numerical weather data assimilation models. Our model is based on solving the equations of continuity and conservation of momentum at middle and low latitudes. A magnetic dipole is used to model the Earth magnetic field. The ionosphere is divided into pixels bounded by constant magnetic field lines, constant magnetic geopotential lines, and local time. Our approach is to solve for the initial state as well as some of the driving forces (e.g. neutral wind and plasma drift) such that the ionospheric state best fits the TEC data obtained from GPS. We will present the concept of data assimilation, the sensitivity to the basic physical forces based on the adjoint modeling technique, and some preliminary results obtained from a global network of GPS ground receivers and the GPS/MET flight receiver.

G2-3
1500

IONOSPHERIC ASSIMILATION MODELS

R. W. Schunk and J. J. Sojka
Center for Atmospheric and Space Sciences
Utah State University
Logan, UT 84322-4405

As a result of nearly forty years of research, it is now well known that the ionosphere is strongly affected by magnetospheric, thermospheric, and mesospheric processes. It has also been clearly established that the external processes which operate on the ionosphere can be localized, spatially structured, and unsteady. As a consequence, the ionosphere can vary appreciably from hour-to-hour and from day-to-day at a given location and these variations can have a significant effect on both military and civilian systems. However, the adverse effects can be minimized or circumvented with the aid of a reliable ionospheric specification model. Currently, the most promising approach for the construction of such a model involves data assimilation techniques. With this approach, either a single data type or diverse sets of data types are used to reconstruct the ionospheric density distribution via tomographic techniques. Some of the data types that are available for assimulation include in situ density measurements from satellites, altitude profiles of density obtained from ground-based radars, line-of-sight TEC measurements from GPS satellites, occultation data, and line-of-sight optical emission data, which can be used to infer ionospheric parameters. However, the routine ingestion of different data types into an assimulation model can lead to erroneous ionospheric reconstructions if care is not exercised. For routine data ingestion, software has to be developed to detect and eliminate bad data, to fill data gaps, and to account for data outages. Procedures have to be developed to independently analyze data streams for long-term problems, such as changes in bias and thresholds. In addition, the tomographic technique adopted may inadvertently smooth ionospheric density gradients. These and other data assimilation issues will be discussed.

G2-4
1540

A KALMAN FILTER APPROACH TO TIME-DEPENDENT IONOSPHERIC DATA ASSIMILATION

B. M. Howe K. Runciman
Applied Physics Laboratory
University of Washington
1013 NE 40th St.
Seattle, WA 98105

J. A. Secan*
Northwest Research Associates. Inc.
14508 NE 20th St.
Bellevue, WA 98007

An approach to assimilating data in geophysical models developed in the disciplines of atmospheric and oceanographic physics, known generally as Kalman filtering, has been applied to the domain of ionospheric physics. Using a four-dimensional stochastic model of ionosphere perturbations, simulations are made of a tomography system based on data from the Global Positioning System and a low earth-orbiting satellite. The perturbations are departures from a simple time-independent reference state. The spatial structure is parameterized in terms of empirical orthogonal functions (EOFs) in the vertical and spherical harmonics in the horizontal. A sun-fixed coordinate system is used so that ionospheric features are more nearly steady in time. The horizontal covariance structure is specified by variance and correlation length scales as functions of latitude and longitude. Time dependence is modeled as a first-order Markov process with a 6-hour time scale and white-noise forcing ("modified persistence").

A Kalman filter is used to objectively assimilate the simulated data into the simple time-dependent model. In addition to solving for the three-dimensional electron density field at each time step, the procedure solves for instrumental biases. The simulations show that the fractions of resolved variance for vertical EOF modes 1, 2, and 3 are 0.99, 0.93, 0.73, respectively. The resolution of the vertically integrated total electron content is 0.99.

Future efforts with this technique will focus on modifications to replace the simple time dependence with a more realistic representation of the state-change operator. The first stage will be to develop an improved description of the state-change operator based on a model such as the Parameterized Ionosphere Model (PIM). Knowledge gained in this stage regarding the model- and observation-error covariance matrices and refinements made to the spatial representation of the ionosphere will lead to the second stage: integration with a formal time-dependent ionospheric model. Given the size of the state space represented by the more complete model, this second stage will require development of an approximate Kalman filter based on a reduced-state version of the full model.

G2-5
1600

A NEW DATA ASSIMILATION ALGORITHM FOR PRISM

R. E. Daniell*
Computational Physics, Inc.
240 Bear Hill Road, Suite 202A
Waltham, MA 02451

The Parameterized Real-time Ionospheric Specification Model (PRISM) is currently operational at the 55th Space Weather Squadron (55 SWXS) at Schriever AFB, CO, and is also undergoing extensive validation at the Air Force Research Laboratory (AFRL) at Hanscom AFB, MA. PRISM has two components: (1) a physics-based climatological model (the Parameterized Ionospheric Model, PIM) and (2) a data assimilation algorithm. The first component, PIM (R. E. Daniell et al., *Radio Science*, **30**, 1499-1510, 1995), was derived from a set of regional, physics based models by making a series of runs for a range of input parameters (solar activity, geomagnetic activity) for the two solstices and an equinox. The second component compares PIM with data from a variety of sources (e.g., ionosondes, dual frequency GPS receivers, satellites) to produce global correction fields for each of several electron density profile characteristics (E- and F-layer peak density and height, topside scale height, etc.). The global correction fields are applied to PIM to produce a global ionospheric specification that matches the ingested data.

We are embarking on a project to improve both components of PRISM, resulting in a new version, to be known as PRISM 2. The primary improvement to the physics-based climatology (PIM 2) will be the inclusion of longitude dependent parameters that describe the low latitude vertical drift and the thermospheric winds. Another improvement will be the move from seasonal to monthly coefficient sets. The PRISM 2 data assimilation algorithm will be a complete departure from the present algorithm. The new algorithm will take the form of an optimal estimation algorithm (a Kalman filter) that will adjust the input parameters of the model to provide the best fit to the data. The advantage of this approach is that it preserves the parameterized physics of the climatology model.

A Kalman filter for a given system requires a "state model" that describes the state of the system in terms of a set of parameters (the "state vector") and a "measurement model" that relates the system parameters to the measurement data ("measurement vector"). The parameterized, physics-based climatology of PIM 2 will provide the state model and its input parameters (solar activity, magnetic activity, low latitude drift, thermospheric winds) will be the components of the state vector. The Kalman filter provides a mechanism for estimating the state vector that reproduces the measurement vector with the least error, and it has the advantage over a straightforward least squares fit of taking into account the time history of the system.

G2-6
1620

CIR MULTIPLE-DATA SOURCE FOUR DIMENSIONAL TOMOGRAPHY ALGORITHMS

G. S. Bust* D. S. Coco T. L. Gaussiran C. Coker
Center for Ionospheric Research
Applied Research Laboratories, The University of Texas at Austin
P.O. BOX 8029
Austin, TX 78713

Over the last two years, the Center for Ionospheric Research (CIR) at the Applied Research laboratories, the University of Texas at Austin (ARL:UT) has developed two 4D tomography algorithms. Both algorithms provide regional three dimensional specification of the ionospheric electron density at user selectable sample times, and the algorithms accept input data from beacon transmitters, ground based GPS data, and ionosonde data. Typical sample times are every 30 minutes. The Tomography Reconstruction using Interpolation and Mapping 4D (TRIM4D) algorithm separately computes 2D tomography and 2D GPS TEC map solutions and then merges the two complementary results together. The Previous Reconstruction Inititialized Volume Iterative Tomography 4D (PRIVIT4D) algorithm is a true 3D reconstruction algorithm that treats both the GPS and beacon data as slant line integral data, and uses the previous time step reconstruction weighted with a climate model as the initialization field. In addition, both TRIM4D and PRIVIT4D take into account the plasmasphere effect on GPS TEC data, and PRIVIT4D provides an estimate of the plasmasphere along with the ionosphere electron density. Finally, as part of its inversion process, the PRIVIT4D algorithm provides a running average of improved GPS receiver station biases in addition to the ionosphere and plasmasphere electric density.

A discussion of algorithms will be presented, with particular focus on how the multiple data sources have been ingested, and how ionospheric models are used. In addition, a discussion of relative strengths and weaknesses in the algorithms will be presented, along with planned enhancements to the algorithms. Results will be presented from several tomographic experimental campaigns carried out by ARL:UT. The estimates from the 4D algorithms will be compared with independent measurements, along with a discussion of accuracy of the estimates. Finally, several interesting features that have been observed in the 4D electron density will be presented.

G/H3-1
1340

FURTHER EVIDENCE OF ELECTRICAL CURRENT IN SPRITES USING MEASUREMENTS OF ELF RADIO ATMOSPHERICS AND HIGH TIME-RESOLUTION MULTI-ANODE ARRAY PHOTOMETER OBSERVATIONS

S. C. Reising*
University of Massachusetts
Amherst, MA 01003
U. S. Inan T. F. Bell
Stanford University
Stanford, CA 94305
Y. Takahashi M. Sera
Tohoku University
Sendai, 980-77, Japan

The magnetic field signature of extremely low frequency (ELF, here defined as 15-1500 Hz) radio atmospherics ("sferics" for short), originating in positive cloud-to-ground (CG) discharges in a Kansas and Texas panhandle thunderstorm and measured ~500 km away at Yucca Ridge Field Station, Colorado, consists predominantly of a positive-going pulse of ~1 ms width. Of the ELF sferics which were launched by sprite-producing positive CG flashes, roughly 20% exhibit a second ELF pulse, which has been shown to be simultaneous with Sprite luminosity by comparison with high time resolution (~30 μs) photometer measurements (*Cummer et al., GRL*, **25**, 1281, 1998). The explanation of the second ELF pulse as radiation from electrical currents in sprites is consistent with recent results of theory and simulation (*Pasko et al., GRL*, in press, 1998). Related work has shown that in many cases the total Sprite luminosity, as measured using an intensified CCD video camera, is linearly related to the moment of charge transfer in the sprite (*Bell et al., EOS*, **78**, F70, 1997). In addition, measurements of ELF radio atmospherics show that for large values of charge transfer within the causative CG, the time delay between the CG and sprite onset is <3 ms, whereas for small CG charge transfers, the waiting time varies from 3 to many tens of ms.

We present new results of simultaneous ELF measurements of radio atmospherics and multi-anode array photometer (MAP) measurements which demonstrate that the second ELF pulse and sprite luminosity occur simultaneously and that the delay between the causative positive CG and the sprite varies between 1 and 70 ms. In addition, our data set indicates a clear distinction between "columnar" sprites, with a delay of <3 ms between CG and sprite, and "carrot" sprites, with a delay of >3 ms between CG and sprite. Elves are often clearly observed preceding the occurrence of column sprites. The MAP data measure vertical structure in sprites with ~10 km altitude resolution and provide time series of optical intensity with ~50 μs resolution. Comparison of MAP data with the second ELF pulse allows a preliminary assessment of the altitude distribution of electrical currents in sprites.

G/H3-2
1400

INITIAL FINDINGS FROM THE SPRITES'98 CAMPAIGN AT YUCCA RIDGE

Walter A. Lyons, Thomas E. Nelson
FMA Research, Inc.
46050 Weld County Road 13
Ft. Collins, CO 80524

SPRITES'98 was conducted at the Yucca Ridge Field Station near Fort Collins, CO from mid-May through August 1998. Scientists participating on site were from Los Alamos National Laboratory, Mission Research Corporation, Tohoku University, Utah State University, SRI International, and briefly, the University of Arizona. Using multiple remote sensing technologies, coordinated measurements of individual sprite and elve events were obtained. Both red and blue low-light imagers (LLTVs) and multi-color broad- and narrow-band photometers were used to monitor optical emissions. Evidence of ionization within sprites obtained in previous programs was confirmed from simultaneous 4278 and 4709 nm emissions. High speed (1000 fps) images of sprites reveal new details of the temporal sequence of events. In addition, numerous high speed videos of the entire CG lightning event for both positive and negative polarity strokes provide new insights on the continuing currents and horizontal dendritic discharges. These videos were coordinated with optical measurements made with a photodiode array plus VLF and ELF transients (Q-bursts) made at MIT's Rhode Island Schumann resonance observatory. Storms ingesting smoke from Mexican fires produced unprecedentedly high percentages of +CGs, which in turn had twice the normal peak currents. A record number of sprites (nearly 400 in 208 minutes) were imaged above one such smoke-influenced storm. Sprites again were typically associated with storms with radar echoes larger than 10,000 km2, but some exceptions were noted, especially bursts of sprites in the dying phases of some supercell class thunderstorms. An unusual interaction between a meteor and a sprite was recorded. Monitoring activities were also coordinated with scientific teams from New Mexico Tech, Stanford (STAR Lab), Massachusetts Institute of Technology and the University of Alaska.

G/H3-3
1420

HAIL MEASUREMENTS OF LOWER IONOSPHERIC CONDUCTIVITY CHANGES ASSOCIATED WITH THUNDERSTORMS, LIGHTNING DISCHARGES AND SPRITES

M. P. Johnson* S. J. Lev-Tov U. S. Inan T. F. Bell
STARLab
Stanford University
Stanford, CA 94305

Localized nighttime D-region ionospheric conductivity changes occurring in association with lightning discharges lead to transient changes in the amplitude and phase of VLF transmitter signals propagating in the Earth-ionosphere waveguide [e.g., *Inan et al., JGR, 101* 5219, 1996]. The Summer 97 campaign with the Holographic Array for Ionospheric Lightning Research (HAIL) provided evidence of strong forward scattering by these disturbances in agreement with existing models [e.g., *Chen et al., Radio Science, 31*, 335, 1996], although the data did suggest a more complicated than previously believed disturbance structure. In the Summer 98 campaign, four more amplitude and phase receivers were interspersed with the HAIL array, making a total of nine VLF receiving sites with approximately 65km (5λ) spacing. This improvement in the receiver density corresponds to an increased spatial resolution of the scattering pattern. We present the results of a comparison between the measured scattered field along the array and a three-dimensional numerical model of VLF propagation in the Earth-ionosphere waveguide. In general, lightning associated VLF events are observed at multiple receiver sites; however, in some cases events are observed at only one site, while VLF paths only 65km farther (on both sides) are not affected. In some cases, this comparison strongly suggests the existence of two superimposed disturbed regions, which decay at different rates. In addition, we will present a new Internet-based method of browsing data from this array and its impact on our educational outreach collaboration with high school students.

G/H3-4
1440

VIDEO AND PHOTOMETRIC OBSERVATIONS OF A POSSIBLE METEOR-TRIGGERED SPRITE/JET EVENT

R. J. Strabley*
Department of Physics
2500 California Plaza
Creighton University
Omaha, NE 68178
D. M. Suszcynsky R. Roussel-Dupre E. Symbalisty
Los Alamos National Laboratory
Space and Atmospheric Sciences Group, MS D466
Los Alamos, NM 87545
R. A. Armstrong
Mission Research Corp.
Suite 302, 1 Tara Blvd.
Nashua, NH 03062-2801
W. A. Lyons
FMA Research
46050 Weld County Rd. 13
Ft. Collins, CO 80524

This paper presents video and photometry data of a possible meteor-triggered sprite/jet event. The data was recorded with a white-light Xybion video camera with millisecond time-stamping, a gps time-tagged broadband red photometer with 50 micro-second time resolution, and a VLF receiver. The event was collected on August 1, 1998 over a 1.5 second time interval during the SPRITES '98 campaign at Yucca Ridge Field Station operated by FMA Research in Ft. Collins, CO. The event consisted of three stages, (1) the observation of a moderately bright meteor of about third magnitude, (2) the development of a sprite in the immediate vicinity of the meteor as the meteor reached the 60 to 70 kilometer altitude range, and (3) a slower forming "jet" of luminosity that appeared during the late stages of the sprite and propagated back up along the ionization trail of the meteor. The development of the sprite immediately after the transit of the meteor appears to have been coincidental. However, the jet stage of the eve nt is clearly related to the presence of the meteor and provides a unique opportunity to study the effect of injecting a volume of ionization into an active sprite environment. The amount of ionization associated with the meteor is estimated to be about 10^{16} electrons per meter. The photometer curve for the sprite shows a sharp risetime of less than one milli-second followed by a gradual falltime of about 15 to 20 milliseconds. No VLF signature was observed. The event is analyzed in terms of its geometry, its association with the meteor, and the implications to existing theories for sprite and jet formation.

G/H3-5
1500

TELESCOPIC IMAGING OF FINE STRUCTURE IN SPRITES

U. S. Inan* C. P. Barrington-Leigh E. A. Gerken T. F. Bell
Durand 324, STAR Laboratory
Stanford University
Stanford, CA 94305

Recent theoretical work has indicated that the sprite optical luminosity as observed in regular video may be constituted by a superposition of a large number of highly structured streamers having fine structure with scale sizes of few meters. To look for the presence of such fine structure, we use a 40-cm wide, 2-m tall Newtonian telescope with a field-of-view of 0.92 x 0.7 degrees (10-m video resolution at a range of 500-km), boresighted with a wide field-of-view (12 x 9 degrees) video camera. The rotatable and tiltable mounting base of the telescope provides easy elevation and azimuth control, while aiming of the telescope is facilitated by the known phenomenology of sprites, i.e., that they often tend to occur at approximately the same location for tens of minutes. Both the wide- and narrow-fields-of-view are recorded with image intensified CCD video cameras, with simultaneous recording of the broadband very low frequency sferic signal from causative lightning flashes. The first observations with the telescopic imaging system were conducted from the Langmuir Laboratory annex, located on the 11,000 ft high South Baldy peak, providing clear views of thunderstorms in Kansas, Colorado, Texas, and the north-west coast of Mexico. Preliminary data from the telescope show the presence of a fascinating complex of fine structures within the body of the sprite, clearly indicating the presence of columnar channels of luminosity with lateral extent ¡¡10-m. In one case, on July 13, 1998, observing a storm ata range of 580 km, many tens of multiply-oriented (but mostly vertical) streamer-like structures were simultaneously observed within the field of view, with lateral scales ranging from ¡¡10-m to up to 100-m. The telescopic measurements were conducted during July and August, 1998, durign which time many sprites were observed at ranges of up to 900 km. We report on the morphology of observed sprites, their association with storm activity and sferic waveforms, and the variety of fine structure observed in the telescopic imager.

G/H3-6
1540

IONIZATION IN THE MIDDLE ATMOSPHERE ASSOCIATED WITH SPRITES - MULTI-COLOR PHOTOMETRIC ANALYSIS AND ASSOCIATED CHEMICAL DYNAMICS MODELING

R. A. Armstrong (Mission Research Corp, Geophysics and Information Technologies Sector, 1 Tara Blvd., Nashua, NH 03062; 603-891-0070 (x203); e-mail:rarmstrong@mrcnh.com); D. M. Suszcynsky and R. Strabley (Los Alamos National Laboratory, Space & Atmospheric Sciences Group, Los Alamos, New Mexico 87545; 505 665-3119; e-mail: dsuszcynsky@lanl.gov); W. A. Lyons and T. Nelson (Both at: FMA, Fort Collins, CO 80524; 970-568-7664; e-mail: walyons@frii.com)

Although there have been many measurements of the signatures of electrodynamic events above thunderstorms, there remains significant controversy concerning the level and persistence of ionization in these events. The first indication of ionization in sprites was obtained by Dowden, et al (EOS Transactions (supplement), 76(46), F114, 1995) using VLF measurements. In 1995, Armstrong, et al (J. Atmos. Solar Terr. Physics, in press, 1998) obtained the first photometric evidence of 427.8 nm emission from the N_2^+ first negative radiative system. In 1996, Suszcynsky, et al (Ibid) and Armstrong, et al (Ibid) obtained a combination of blue imagery and blue photometry which again indicated significant ionization in sprites. However, the bandpass of the optical filters in these studies precluded the unique assignment of the signature to nitrogen first negative emission. In SPRITES'98, we obtained new multi-color photometry data simultaneously with blue, red and high-resolution broad-band video imagery of sprite events which confirms the assignment of the blue emissions to nitrogen first negative radiative system, confirming significant ionization in these events. These measurements coincide with the aircraft-based 427.8 imager data of Sentman et al (private communication, 1998). The new results indicate that more than one mechanism can cause sprites and that the ionization level is variable. The time-resolved emissions from the nitrogen first-positive, second positive and first negative systems suggest different time histories for different types of events. The relative time histories are not unique from event-to-event but generally fall into two (or perhaps three) categories. We find that the time histories can be interpreted to yield both the ionization level and the energy accommodation. The data indicates ionization in sprites varying from very strongly ionized to relatively weakly ionized. Self-consistent modeling of the chemical dynamics of these events yields strong indications of the mechanisms of the ionization and the energetic channels associated with them. We will present the systematic analysis of the time-histories of the photometric emission behavior of the sprite events, correlate them with the corresponding imagery and discuss implications for the chemical and electrodynamic modeling of the phenomena.

G/H3-7
1600

THERMAL RUNAWAY ELECTRONS IN SPRITES

V. P. Pasko* U. S. Inan T. F. Bell
Durand 324, STAR Laboratory
Stanford University
Stanford, CA 94305

Electrical breakdown of air associated with sprites starts in atmospheric regions above thunderstorms where the local electric field (E) exceeds the breakdown field (E_k) following intense lightning discharges [e.g., Pasko et al., *J. Geophys. Res.*, **102**, 4529, 1997]. It has been proposed [Pasko et al., *Geophys. Res. Lett.*, **25**, 2123, 1998; hereafter denoted I] that in certain altitude ranges above thunderstorms the breakdown may take the form of very narrow ionization channels (streamers) having transverse extents <10 m. The presense of a fascinating complex of fine columnar structures within the body of the sprite with lateral extent <10 m has recently been experimentally documented using a new high spatial resolution telescoping imager [Inan et al., *EOS Trans. AGU*, **79**, Fall Meet. Suppl., 1998].

The previous analysis of the dynamics and optical properties of streamer breakdown [I] is generally valid for low applied electric fields E_o ($E_o<\sim 2E_k$) for which streamer velocity does not exceed ~2 km/ms. There are experimental indications, however, that the vertical velocities of sprite development may sometimes be up to 10% of the speed of light (30 km/ms) or even higher [Fukunishi et al., *EOS Trans. AGU*, **77**, Fall Meet. Suppl., F60, 1996]. It is known that for $E_o>\sim 3E_k$ the streamer is able to generate thermal runaway electrons in its tip, with the runaway electrons moving in phase with the streamer tip and continuously gaining energy, leading to further acceleration (self-acceleration) of the streamer [e.g., Babich, *Sov. Phys. Dokl.*, **27**, 215, 1982; and references therein]. In laboratory experiments, the self-acceleration manifests itself as measured X-ray radiation believed to be produced from fast electrons with energies greater than the applied voltage (up to hundreds of keV) [e.g., Tarasova et al., *Sov. Phys. Tech. Phys.*, **19**, 351, 1974].

The investigation of the effects of thermal runaway electrons on the dynamics and optical properties of the electrical breakdown in different altitude ranges above thunderstorms thus currently consitutes an important component for our understanding of the energetics and phenomenology of sprites. In our talk we report the results of simulations of electron energy distributions and optical excitation rates associated with electrical breakdown in air obtained using a Monte Carlo approach. The Monte Carlo approch is superior to the kinetic modeling used in previous work [e.g., I] which uses two-term spherical harmonic expansion of the electron distribution function for the solution of the Boltzman transport equation [e.g., Taranenko et al., *Geophys. Res. Lett.*, **20**, 1539, 1993], not suited for the treatment of electron distributions at very large electric fields ($>\sim 10E_k$) leading to the phenomena of runaway electrons in tips of streamers.

G/H3-8
1620

NONUNIFORM RUNAWAY IN THE PRESENCE OF A MAGNETIC FIELD

N. G. Lehtinen* U. S. Inan T. F. Bell
STARLab
Stanford University
Stanford, CA 94305

A three-dimensional Monte Carlo model of relativistic runaway electron breakdown in air in the presence of static electric and magnetic fields is used to study the properties of non-uniform breakdown. The uniform model developed earlier could predict accurately only the temporal growth of avalanche. In addition to this result, using the non-uniform model we now calculate the e-folding distances, which characterize the spatial growth, and the velocity of the breakdown propagation in space from the starting point. We calculate the widening of the electron beam due to diffusion and compare the results to analitical predictions in the absence of a magnetic field by *A. V. Gurevich, G. M. Milikh and R. A. Roussel-Dupré* [*Phys. Lett. A, 187*, 197, 1994]. We study what happens to the energetic electron beam created as a result of breakdown when the perpendicular magnetic field prevents further breakdown development. This situation describes the runaway breakdown due to thunderstorm quasi-electrostatic fields at the geomagnetic equator, and is essential to the understanding of the gamma rays of terrestrial origin observed by the BATSE instrument on CGRO, which is a low-inclination satellite. We investigate the optical and gamma ray signatures of runaways, which can be related to the obseved phenomena of red sprites and terrestrial gamma ray flashes in the Earth's atmosphere.

G/H3-9
1640

MIDDLE ATMOSPHERE ELECTRODYNAMICS: RELEVANCE OF PENN STATE MEASUREMENTS

Leslie C. Hale
Communications and Space Sciences Laboratory
Department of Electrical Engineering
Penn State University, 332 EE East, University Park, PA 16802

The explanation of "undisturbed" daytime D-region ionization as due to ionization of NO by solar Lyman-α (M. Nicolet and A.C. Aikin, JGR 65, 1469, 1960) was essentially correct, even though the assumed NO densities and recombination coefficient were in error by several orders of magnitude, with cancelling effects. The discovery of dissociative recombination required a much higher NO density in the middle atmosphere, which was verified by rocket measurements (B.A. Pontano and L.C. Hale, Space Res. 10, 208, 1970) and others. The extremely low electron density below 80 km at night was discovered by early "blunt probe" measurements (L.C. Hale, D.P. Hoult and D.C. Baker, Space Res. 8, 320, 1968), which also indicated much lower than expected nighttime ionic conductivities. A solar eclipse (D.C. Baker and L.C. Hale, Space Res. 10, 712, 1970) showed a much more rapid electron loss rate than expected (a result confirmed in subsequent eclipses - L.C. Hale, et al., JATP 45, 515, 1983), and the temperature dependence of ionic conductivity was found to be much greater than expected from gas phase theories (J. Cipriano, et al., JGR 79, 2260, 1974). It was postulated (E.T. Chesworth and L.C. Hale, GRL 1, 347, 1974) that the body of data was best explained by the existence of substantial numbers of "invisible" ice or ice-coated aerosol particles in the mesosphere, even at mid- and low-latitudes.

The coordinated measurements of lightning-related transients in the middle atmosphere by Penn State and higher ionosphere by Cornell (M.C. Kelley, et al., JGR 90, 9815, 1985) showed much larger than expected pulses of current in the ULF and ELF (millisecond) range. The ULF data were well explained by a theory (C. and P. Greifinger, JGR 81, 2237, 1976), and a computer model (L.C. Hale and M.E. Baginksi, Nature 329, 817, 1987) indicated that the large millisecond ELF pulses are generated by a transition between "electrostatic" solutions without and later (after propagation delay) with the presence of the ionosphere, without the need for "continuing currents."

It has recently been observed (L.H. Marshall, et al., JASTP - in press, 1998) that millisecond ELF pulses are associated with "red sprites" and that these are accompanied by strong VHF emissions. This generates a requirement for pre-existing free electrons in much larger quantities that can be explained with gas phase processes. It was suggested that these may be from lightning-induced photo-detachment from the ice crystals (L.H. Marshall, Ph.D. Thesis, Penn State, 1998). These crystals may grow at night above thunderstorms in the lee of mountains, explaining the "cooking time" that has been observed.

G/H3-10
1700

THE 1999 SPRITES BALLOON CAMPAIGN

E. A. Bering, III* J. R. Benbrook
Physics Department
University of Houston
4800 Calhoun
Houston, TX 77204-5506
E. M. Wescott D. D. Sentman H. C. Stenbaek-Nielsen
Geophysical Institute
University of Alaska
Fairbanks, Alaska
W. A. Lyons
FMA Research, Inc.
Yucca Ridge Field Station
46050 Weld County Road 13
Ft. Collins CO 80524

There are several competing models for the production of sprites, jets and elves. It has become clear it is not possible to select between these models using only ground-based data, owing to the fact that the ground shorts out the field signatures of interest. Consequently, a balloon campaign was proposed and funded. The campaign, which was originally scheduled for July, 1998, has been rescheduled for July and August of 1999. The 1999 Sprite Balloon Campaign will attempt to conduct six high altitude balloon flights from Ottumwa, Iowa, during the dark of the moon in the summer of 1999. Nominal campaign dates include July 6-21, and August 4-19, with lower priority fall-backs of June 7-21 and Sept. 3-17. The balloons will be launched at sunset, float at a nominally constant altitude of 32 km and drift westward at a predicted speed of 40 knots. Cutdown will occur after sunrise in central Colorado. Balloon tracking will be made available in real-time on redundant Web sites. The balloon payloads will be instrumented with dual three axis electric field detectors, three axis fluxgate and induction magnetometers, X-ray scintillation counter, Geiger-Mueller tube, upward looking high-speed photometer, vertical current density ammeter, conductivity measurements, and an ambient temperature thermometer. A multiply redundant telemetry scheme will give us five orders of magnitude of dynamic range in field amplitude sensitivity. The use of event triggered on-board memory will allow us to sample 8 quantities at a digitization rate of at least 50 kHz per channel during sprite events. The efficiency of the on-board event trigger will be checked by using 4 broad-band analog waveform channels. Ground observations will include low light level TV observations from three possible sites, WIRO, on Jelm Mtn., Wyoming, Mt Evans, Colorado, and Yucca Ridge, Colorado. At least one of these sites will also have a fast photometer. Other topics that will be covered include: why the program was postponed and the trigger criteria for the on-board fast memory.

G/H3-11
1720

MONTE CARLO SIMULATION OF RUNAWAY MEV ELECTRON BREAKDOWN IN THE PRESENCE OF A STATIC MAGNETIC FIELD WITH APPLICATION TO THE PHENOMENA OF RED SPRITES AND TERRESTRIAL GAMMA RAY FLASHES

N. G. Lehtinen*
STARLab
Stanford University
Stanford, CA 94305

A three-dimensional Monte Carlo model of the uniform relativistic runaway electron breakdown in air in the presence of static electric and magnetic fields is developed. The model is used to calculate electron distribution functions, avalanche rates and the direction and velocity of avalanche propagation for different field configurations. We also study the conditions required for an electron with given momentum to start an avalanche (in the absence of a magnetic field). The results are compared to previously developed kinetic and analytical models, and it is concluded that the rates used in previous models are overestimated by a factor ~ 4.

Next, we investigate the role of avalanching runaway electrons in the production of red sprites and terrestrial gamma ray flashes. The Monte Carlo simulation results are applied to a fluid model of runaway electron beams in the middle atmosphere accelerated by quasi-electrostatic fields following a positive lightning stroke. In particular, we consider the case of lightning draining positive charge from remote regions of a laterally extensive (> 100 km) thundercloud, using a cartesian 2D model. The obtained optical emissions in red sprites associated with the runaways are negligible compared to the emission from thermal electrons in the conventional type of breakdown. The calculated gamma ray flux is of the same order as the terrestrial gamma ray flashes observed by the BATSE detector on the Compton Gamma Ray Observatory.

J3-1
1340

K-12 TEACHER INSTITUTE AT NRAO/GREEN BANK

S. A. Heatherly J. R. Fisher*
NRAO
P. O. Box 2
Green Bank, WV 24944

In 1987, the National Radio Astronomy Observatory at Green Bank and the West Virginia University began a teacher education program whose mission is to make the teaching of science more like science research itself. Funded through grants from the National Science Foundation, we have established residential institute programs that immerse elementary and secondary teachers in a research environment. The first Institutes included mainly experienced secondary school teachers, but the program has evolved to include middle and elementary school teachers with a broader range of professional experience.

At the NRAO/WVU Institutes teachers work in small teams to conduct open-ended investigations using a working 40-foot radio telescope. Each team must design its own experiments, collect and analyze data, and interpret that data. After participating in our program, teachers adapt their experience to the classroom, guiding their students through investigations of unfamiliar, open-ended questions. The program has significantly increased participants' understanding of the nature of science and has resulted in greater use of cooperative learning and new strategies for evaluating a student's understanding of science concepts.

The participants' one or two weeks at the Observatory is quite different from nearly all of their previous experiences with science. The Institutes emphasize close interaction with Observatory staff scientists and engineers. The program includes a short course on astronomy, featured speakers on current research topics, and full access to Observatory facilities such as the library, lab, staff cafeteria, and telescope control rooms. The teachers live on site, so their 40-foot telescope projects go on day and night. Most participants find the Institute an intense, sometimes frustrating, but usually rewarding experience.

In 1993, the NRAO expanded its program to include university students who are in training to be future science teachers. Students attending two West Virginia colleges participate in an NRAO institute which is integrated into their "methods-of-teaching-science" course. Over 160 preservice elementary and secondary teachers have participated so far. This program continues past the NSF grant period with funds from the participating college.

In 1998 the Observatory was awarded a new grant from the NSF, which will run until 2002. Elementary and secondary teachers from West Virginia and surrounding states participate. Targeted are those rural school districts which have been underserved by recent science reform initiatives. Participants receive 9 hours of graduate credit from West Virginia University.

J3-2
1400

THE GOLDSTONE-APPLE VALLEY RADIO TELESCOPE EDUCATION PROJECT

Michael J. Klein
Jet Propulsion Laboratory / Caltech
Pasadena CA 91109

James P. Roller
Lewis Center for Educational Research
Apple Valley, CA 92307

The Goldstone-Apple Valley Radio Telescope project (GAVRT) is bringing "hands-on" scientific discovery to life in America's classrooms. Middle and high school students at participating schools remotely control a dedicated 34-m radio telescope at NASA's Deep Space Network Goldstone Complex. Connected via the Internet from their classrooms, they point the massive dish at natural radio sources, analyze the data and report their findings to Mission Control located at the Lewis Center for Educational Research in Apple Valley, CA.

A primary objective of the GAVRT project is to address the need to improve scientific literacy among America's youth. With the support and participation of NASA/JPL scientists and engineers in partnership with the staff and volunteers at the Lewis Center, GAVRT students and teacher are able to experience the real world of scientific research and discovery. Participating teachers are provided with comprehensive scientific curriculum, in-depth training opportunities and a growing library of teaching tools and technological resources.

Participating students study basic principles of radio astronomy, learn antenna operations and create detailed mission plans. With the first mission, Jupiter Quest, students plan a hypothetical space mission to the Jovian system. Built into the curriculum are experiments using the radio telescope to measure the temperature of Jupiter's atmosphere and observe the variations in the synchrotron emission from the radiation belts. In addition to Jupiter Quest, new curricula are being developed to map the microwave brightness of the sun and radio emissions near the galactic plane.

The GAVRT project is operated as a partnership involving NASA, the Jet Propulsion Laboratory (JPL), and the Lewis Center for Educational Research (Apple Valley, CA). The JPL portion of the research reported in this paper was performed by the Jet Propulsion Laboratory, California Institute of Technology, under contract with the National Aeronautics and Space Administration

J3-3
1420

THE MIT HAYSTACK OBSERVATORY RESEARCH EDUCATIONAL INITIATIVE

Preethi Pratap Joseph E. Salah*
MIT Haystack Observatory
Route 40
Westford, MA 01886

The MIT Haystack Observatory Undergraduate Research Initiative is an NSF- funded program aimed at involving undergraduate students in active radio astronomical research. The project has two major thrusts - students get hands-on experience using a small radio telescope that is being designed and built at Haystack and which will be provided as a low cost kit. The second component is a research experience with the Haystack 37-m telescope. These projects range from one-time short projects to long-term research projects that use the full capabilities of the antenna.

The Small Radio Telescope (SRT) project consists of a 3m dish with a 1420 MHz receiver. The antenna has a two axis mount that provides full sky coverage. The current prototype version can observe the HI line in a frequency scanning mode. Continuum observations of the Sun, the Moon, Cas A and Cyg A can also be done, providing a source of calibration. Future plans for this telescope include adding a spectrometer capability and extending the receiver range to provide access to the OH maser lines (1665 and 1667 MHz).

The 37-m telescope program has, so far, involved students from colleges in the Northeast region in pilot research projects at the 20 and 40 GHz frequency bands. Students travel out to Haystack and perform projects with the telescope, as part of observational astronomy courses. However, several students have also performed more detailed projects such as the correlation of ammonia temperatures in star forming clouds with the star formation properties, mapping the sun, monitoring water masers in NGC 4258 etc. We have also provided training to faculty who are not familiar with radio astronomical techniques. A collaboration has been developed with Univ. of Massachusetts at Lowell which does not have an active astronomy research program. Remote access to the 37-m is being developed to allow national access to the telescope in the future. This will enable students who are unable to travel to Haystack to use the telescope in meaningful research. This setup will also enable long term projects to be performed. We are also developing materials on the WWW which include a radio astronomy tutorial as well as project books for the SRT and the 37-m.

Other educational programs at Haystack including the Research Experience for Undergraduates program will also be reviewed.

J3-4
1440

THE RADIO ASTRONOMY STUDENT LAB AT FLORIDA TECH.

Michael H. Thursby
Antenna Systems Lab
Florida Institute of Technology
150 W. University Blvd.
Melbourne, FL 32901

In 1995 at the request of a group of undergraduate students in Physics and Space Science and Electrical and Computer Engineering an undergraduate student project investigating techniques used in radio astronomy was begun. During the first year an existing Dicke radiometer was installed at the Applied Research Lab. of Florida Institute of Technology (Florida Tech.) and the temperature of the sun in the 4-5 GHz Band was measured. Drift measurements were made so that the antenna pattern could be estimated. During the first year many valuable lessons were learned by the students especially lessons on determining whether signals and system responses are real or artifact, the effects of external interference on the system, and the meaning of reliability on the operation of such a system.

This humble beginning led to a continuing effort that has financially supported three visiting undergraduate students over three summers through an on campus NSF Summer REU program in astronomy. Two U.S. Air Force Grants through the Air Force Office of Scientific Research(AFOSR)(F49620-96-1-429 and F49620-97-0422) currently provide funds for antenna research at the Antenna System Laboratory of Florida Tech. have provided specific undergraduate teaching funds for students to work on this project during the academic year. Two other students received funding through a seed grant from the Florida Solar Energy Center Grant Nr 820009) (FSEC), With this funding several students have been able to continue in the lab with emphasis on the radio astronomy measurements thus providing continuity in the program.

Most of the RF equipment used in this project has been obtained through generous donations from the Harris Corporation, and Mini-Circuits. A number of Parabolic reflectors have also been donated by various people and companies. The computers used were purchased on the FSEC grant. National Instruments has donated most of the data acquisition hardware and software. During the second year an equatorial mount for the 4 GHz antenna was added and a Right ascension (RA) drive motor has made the study of details of the antenna pattern easier. Three dimensional plot of the antenna beam has been constructed. Measurements are being routinely made in the 4GHz frequency range (driven by the availability of donated equipment.) The results of these measurement are being analyzed to determine the noise level of the receiver. At present the measurements are being made on the Sun's emissions in this band. A second system is nearing completion. This telescope will observe the OH emissions at 1.667 GHz.

Work on the project includes Hardware design and maintenance, Software design and maintenance, and Data Collection. Day to day telescope operation and maintenance, are under student control.

The radio telescope provides a framework on which to teach a number of different disciplines. Obviously, Electrical Engineering Principles are intimately involved, as are Computer and Software Engineering. Although the size and sophistication of the receiver limits the type of radio source that can be measured, there are a number of measurement issues concerning the sun's emission especially as we move into more active times that a long term baseline type measurement may be able to detect. The fact that we can dedicate a telescope to solar measurement over a long period of time can provide valuable long term measurements. Currently we are implementing all of the antenna control and signal processing algorithms using the graphical language, G, part of the National Instruments LabView system. This allows us to prototype the software off line and to easily design user interface for a window's environment.

J3-5
1500

THE MOREHEAD RADIO TELESCOPE: AN INSTRUMENT FOR UNDERGRADUATE RESEARCH

Benjamin K. Malphrus
Astrophysical Laboratory
Morehead State University
Morehead, KY 40351

The Morehead Radio Telescope (MRT) is a research instrument for undergraduate astronomy and physics students and an active laboratory for physics, engineering, and computer science undergraduates and faculty. The telescope incorporates a modular design in which components may be easily removed for use in laboratory investigations and for student research and design projects. The instrument is currently capable of operating in total power mode with a 6 MHz bandwidth, centered at 1420 MHz (21 cm)- the rest frequency of the hyperfine transition of atomic hydrogen. The primary function of the instrument is the observation and mapping of the distribution of atomic hydrogen associated with galactic and extragalactic radio sources. The basic design of the MRT includes a wire-mesh parabolic reflecting antenna, alt-azimuth tracking positioner control and drive systems, receiver and signal processing system, a controlling computer with an interface device, and supporting electronics and hardware. The MRT employs a high gain forty-foot high antenna designed for L-Band operation. A surplused Army NIKE-Hercules ANS-17 Radar antenna and its associated superstructure are utilized as the antenna system. The overall receiver system design utilizes a low noise, sensitive, stable receiver to convert the 1420 MHz Hydrogen line to a frequency regime suitable for processing by standard laboratory equipment. A DC voltage derived from an envelope detector is incorporated in the final stage. Advances in GaAs FET technology allowed the fabrication of amplifiers with 35 degree noise temperatures with the device junctions at room temperature. The sensitivity and versatility of the telescope design facilitate the investigation of a wide variety of astrophysically interesting phenomena. The overall design of the instrument as well as a brief discussion of data collected to date is provided.

J3-6
1540

GALACTIC ROTATION FROM HI & OH RADIO SPECTROSCOPY WITH A 5-meter ANTENNA

D. L. Kaplan* J. M. Cordes
Department of Astronomy
515 Space Sciences Building
Cornell University
Ithaca, NY 14853

Since 1989 we have used a 5 meter antenna outfitted with an L-band receiver for use in a junior-senior level laboratory course at Cornell University. The prime focus helical feed's signal is filtered with a 1400-1700 MHz bandpass filter prior to amplification with an uncooled low-noise amplifier. This is necessary to avoid amplifier saturation in the harsh interference environment on campus. A patch-panel setup allows various narrower filters and amplifiers to be inserted into the signal path. The system temperature is about 60K and the gain is about 3 mK Jy^{-1}. Backend systems include a total power signal path and a baseband FFT spectrometer. The telescope drive system and data acquisition systems are controlled by a PC.

In the main lab exercise, students obtain long ($>$ 24 hr) drift scans using the FFT spectrometer to acquire spectra that show the 21 cm HI line of hydrogen. Over the course of the drift scan, the strength and Doppler shift of the line change, so that students may determine the rotational velocity and size of the Galactic disk. Data consist of 256-point spectra across 2.5 MHz dumped every 1 to 10 sec. These fast dumps allow excision of radio-frequency interference in the post processing.

We will show examples of spectra obtained with the antenna and some of the quantitative analyses that can be done to study Galactic structure.

The frequency agility of the superheterodyne receiver also allows us to search for maser emission from interstellar and stellar OH masers in the 1612, 1665 and 1667 MHz transitions.

J3-7
1600

STUDENT SCIENCE AND ENGINEERING WITH A SMALL RADIO TELESCOPE

S. R. Spangler* R. L. Mutel
Department of Physics and Astronomy
University of Iowa
Iowa City, IA 52242

The radio astronomy group in the Department of Physics and Astronomy at the University of Iowa has operated a small radio telescope since 1993. The instrument is a 4.5 meter paraboloid located on the roof of Van Allen Hall on the campus. At present, the antenna is steerable in elevation angle, operating as a transit instrument. The telescope has been operated at 1.4 GHz and 5.0 GHz. At the lower frequency, observations have been made of the galactic 21cm emission. This capability has recently been expanded through development of a Fourier spectrometer which utilizes a DMA board in a small computer. Observations at 5 GHz have been continuum only. Flux density measurements at 5 GHz have been made of the Sun, Moon, the Crab Nebula, and Cygnus A. In addition, a feed has recently been fabricated at 610 MHz for use in a 50 cm system. This decimetric system will be used for continuum measurements, radio frequency interference (RFI) monitoring, and possibly pulsar observations. The construction of instrumentation and calibration and operation of this instrument has heavily involved undergraduate and graduate students. This paper will discuss a number of advanced student projects which can be undertaken with an instrument of this sort. The projects can be described as being on the boundary between radio astronomy and radio engineering. One of the most important is the monitoring of the RFI impact of communication satellites on radioastronomical observations. Such observations will be increasingly important as the number of Low Earth Orbit communications satellites expands dramatically in the next decade. An antenna such as the one described above is capable of detecting a number of radio sources of known flux density. The radiometer can therefore be calibrated in Janskys, and the interference level of satellites reported in units which are immediately usable by radio astronomers. A program of this sort is presently in development at Iowa, with observations planned in the 1612 MHz OH band.

J3-8
1620

THE STEWARD OBSERVATORY STUDENT RADIO TELESCOPE

C. K. Walker[1], *J. Clarke*[2], *B. D. Jones*[1], *C. E. Walker*[1], *and D. W. McCarthy*[1]

Steward Observatory has constructed a 3.7 m radio telescope for use in undergraduate education and public outreach. The observatory can be used to perform spectroscopic investigations of galactic HI emission, L-band continuum observations, SETI, and monitoring of artificial satellites. The primary reflector is a surplused satellite dish with a wire mesh surface. The telescope has a custom designed prime focus feed system (constructed in a collaborative effort with NRAO, Tucson) and a computer controlled Azimuth-Elevation mount. The feed is a simple corrugated design consisting of a central circular waveguide surrounded by a ring-type waveguide. The dimensions of the feed are chosen to excite the proper modes in an effort to generate a symmetric radiation pattern and reduce cross-polarization. The desire to measure circularly transmitted power from satellites drove the design. This type of feed is suitable for a range of low f/D ratios. The rf signal is picked-off by two $\sim 0.25\lambda_o$ probes soldered to the central pin of SMA connectors. These probes are set orthogonally in the guide. A hybrid coupler follows the feed and allows the selection of polarizations. The signal then enters a bandpass filter centered on the HI line (1420 MHz) and is amplified $\sim$ 60 dB using an NRAO low noise amplifier followed by a Miteq amplifier. After amplification, the signal travels along RG-214 coax to a commercial ICOM R7100 receiver located in the control room. The receiver downconverts the amplified L-band signal to an externally accessible IF band (10.7 MHz) and to baseband. The IF output feeds external circuitry which further amplifies, filters and detects the IF signal. Both the externally detected IF signal and the receiver's own baseband signal are then sampled by a computer. The externally detected IF signal is used for broad-band observations. The receiver's internally conditioned baseband signal is used for spectroscopic observations. By switching observing modes through the receiver's RS-232 port, the observer can vary the effective frequency/velocity resolution of the baseband signal. Spectral line observations are made by scanning through the line and recording the power in the baseband signal at each frequency setting. The Az-El mount was designed and built in-house and uses a combination of stepper motors and absolute encoders to provide full computer control. The observatory has been used in both freshmen and junior level astronomy courses. The control system is currently being upgraded to provide an exportable graphical interface for both on and off campus users. Over the next year, the commercial receiver will be replaced by a correlator system originally used at the Algonquin Radio Observatory.

[1]*Steward Observatory, University of Arizona*
[2]*National Radio Astronomy Observatory, Tucson*

J3-9
1640

BERKELEY'S ADVANCED UNDERGRADUATE LAB: A 21-CM HORN AND 12-GHZ INTERFEROMETER

D. D. Cudaback Carl Heiles*
Astronomy Department
University of California
Berkeley, CA 94720-3411

Our course emphasizes basic microwave electronics and techniques in both the single-dish and interferometer environments. We begin with four laboratory exercises to introduce the students to the fundamentals of microwaves electronics and radio astronomy techniques. The titles are self explanatory and are as follows: **(1)** Transmission Lines, Waveguides, Impedance Matching; **(2)** Mixers, Single-Sideband Mixers, Phase Measurements; **(3)** Noise Power per Unit Bandwidth as Described by Temperature; **(4)** Spectral Analysis with Fourier Techniques. All of these labs emphasize hands-on use of laboratory instruments and computer-controlled data taking. Students write their own software, using the IDL language, to reduce data and prepare them for the lab reports. Quality reports are an important part of the course, and we strongly urge (successfully!) the students to use LATEX.

The second part of the course emphasizes astronomy. We begin by using a horn with $\sim$ 1 m^2 aperture—very similar to Ewen and Purcell's horn—to map the HI in the Galaxy. This horn, with its 15° beam, requires no tracking; rather, the students move it by "brute force" (and, as part of this, must make the transformation from Galactic to Az/El coordinates themselves). With this horn they can map the Galactic rotation and get a good idea of the global distribution of HI. We finish with a 12-GHz two-element interferometer composed of $\sim$ 1 m diameter dishes on a $\sim$ 10 m baseline; the telescopes are computer-controlled and the students can write scripts for automatic observing—it's just like a "real observatory". The fringe spacing of $\sim 9'$ is ideal for accurately measuring the fringe pattern and diameter of the Sun and Moon by tracking them from rise to set and forcing the students to use Fourier analysis in a real-world experiment. The instrument is sensitive enough to see the major continuum sources such as Tau A and Ori A, and by using fringe-fitting the students measure declinations to within a few tens of arcsec.

J3-10
1700

THE NRAO SUMMER SCHOOL ON SYNTHESIS IMAGING

R. A. Perley* G. B. Taylor
National Radio Astronomy Observatory
P.O. Box O
Socorro, NM 87801

Since 1982, and every 3 years on average, the NRAO holds a summer school on synthesis imaging in radio astronomy. The primary goal of this school is to teach the fundamental techniques of aperture synthesis to potential users of NRAO instruments. Most of these come from the astronomical community, although people have come with backgrounds in medical imaging, mathematics, engineering, high-school teaching, and physics. Graduate students in astronomy make up by far the largest fraction of attendees. Participation is generally very international, with roughly one third of the participants coming from outside the US. The average size of the school is ~100 participants, and ~20 lecturers. The latest school was held on June 17-23, 1998 and had the largest turnout so far with 139 participants from 13 countries.

Lectures are given by the NRAO staff, faculty from New Mexico Tech, Harvard, Univ. of Maryland, and Caltech, and by staff members of other observatories around the world. The range of subjects can be reviewed by consulting "Synthesis Imaging in Radio Astronomy", the published collection of lectures from the 3rd NRAO Synthesis Imaging Summer School (ASP Conference Series, Volume 6, 1989) edited by R. A. Perley, F. R. Schwab, & A. H. Bridle. The proceedings from the latest School will also be published by ASP.

The school lasts 1 week and is generally scheduled to encompass a weekend. The first 3 days are usually spent on lectures covering the fundamentals. The following day (usually on the weekend) is devoted to data reduction tutorials at the Array Operations Center (AOC) allowing attendees to get "hands-on" experience with data calibration and imaging for both VLA and VLBA data. NRAO scientific staff are available at the AOC to aid and advise participants. Then on Sunday an in depth tour of the VLA site is given. The tutorial and the tour are generally the most popular events. The last two days of the school are usually devoted to more advanced lectures.

The next school is tentatively scheduled for June 2001.

Session B2, 0815-Wed., ECCR151
ROUGH SURFACE SCATTERING AND RELATED PROBLEMS (I)
Chairperson: A.A. Maradudin (Univ. of California, Irvine)

B2-1
0820

PHASE FACTORS REPRESENTATION FOR EM SCATTERING BY ROUGH SURFACE

Valerian I. Tatarskii
University of Colorado/CIRES
and NOAA/ERL/ETL
325 Broadway
Boulder, CO 80303

The problem of EM scattering from the random surface $z = \zeta(x, y) = \zeta(\mathbf{r})$ is considered in this paper. In a previous paper, (Tatarskii V.I., *Waves in Random Media*, vol. 7, pp 557-578, 1997), scattering from the acoustic interface described by either the Dirichlet or by the Neumann boundary conditions (BC) was considered. It was shown that for both problems it is possible to present the bistatic scattering amplitude S and scattering cross-section as a functional depending not on the function $\zeta(\mathbf{r})$, but as a functional, depending on the function of three variables of the form $\mathcal{L}(\nu, \mathbf{r}) = \exp[i\nu\zeta(\mathbf{r})]$ (here, ν is some vertical wave-number). The general form of the solution is $S = \Phi[\mathcal{L}(\cdot, \cdot)]$. The functional Φ depends on the BC. In the above mentioned paper the expansion of S was obtained that starts with the Kirchhoff approximation and corresponds to a multiplicity of the "optical" scattering. The first two terms of this expansion include as particular cases Bragg scattering, Kirchhoff approximation, small-slope approximation (see, e.g., Voronovich A. G. *Wave Scattering from rough surfaces* Berlin: Springer, 1994), tilt-invariant approximation (Charnotskii M.I. and Tatarskii V.I. *Waves in Random Media* **5** 361-80, 1995), and double Kirchhoff approximation (Ishimaru, A. and Chen, J. S. *J. Acoust. Soc. Am.* **88**(4) 1877-83, 1990).

In this paper a similar consideration is presented for EM scattering from the random interface between the vacuum and the medium characterized by the complex dielectric permittivity ε and the magnetic permeability μ. All the components of the scattering amplitude matrix S_{HH}, S_{HV}, S_{VH}, and S_{VV} (indexes H and V correspond to the horizontal and vertical polarizations) can be presented as the functionals depending on the function $\mathcal{L}(\nu, \mathbf{r})$. The expansion based on the multiplicity of the scattering can also be obtained by iteration of the corresponding system of integral equations.

All necessary statistical moments can be directly presented in terms of mean values $\langle \mathcal{L}(\nu_1, \mathbf{r}_1)\, \mathcal{L}(\nu_2, \mathbf{r}_2) \cdots \mathcal{L}(\nu_n, \mathbf{r}_n) \rangle$ that are equal to the characteristic functions of the joint PDF of the surface elevations. Because of this the representation of the scattering problem described here matches the statistical non-Gaussian anisotropic model of the sea surface (Tatarskii V.I. and Tatarskii V.V., NOAA Technical Memorandum ERL ETL-289, Boulder, Colorado, May 1998). The version of the scattering theory considered here makes it possible to perform calculations of scattering cross-sections for EM waves scattered by the sea surface on the base of this model.

B2-2
0840

NEAR FIELDS AND FAR-FIELDS EXCITED BY SMALL AND LARGE SCALE FLUCTUATIONS IN THE MEDIUM PARAMETERS

Ezekiel Bahar
Electrical Engineering Department
University of Nebraska-Lincoln
Lincoln, NE 68588-0511

It is well established that the perturbation theory can be used to correctly predict the co-polarized and cross-polarized electromagnetic fields scattered by slightly rough two dimensionally random rough surfaces, that separate two semi-infinite media characterized by distinct electrical and magnetic properties. Perturbation theory is valid provided that the mean square heights and slopes of the rough surfaces are of the same order of smallness. These analytical results, which have been extended to "tilted" slightly rough surfaces, have been validated experimentally and numerically for both vertically and horizontally polarized excitations for arbitrary angles of incidence and scatter.

It is also generally assumed that the physical optics approach (which is based on the Kirchhoff approximations of the surface electromagnetic fields) can be used to correctly predict the scattered electromagnetic fields from two dimensionally random rough surfaces provided that the radii of curvature of the rough surface are very large compared to wavelength. However, implicit in the physical optics approach is the requirement that the major contributions to the scattered fields come from regions of the rough surface that are in the vicinity of the specular points on the rough surface.

The full wave solutions are not restricted to electromagnetic scattered by layered media with irregular interfaces. Scattering due to inhomogeneities in the complex electrical permittivities and magnetic permeabilities in each layer can also be accounted for in the analysis.

The full wave solutions can also be used to determine the coupling between the radiation fields, the lateral waves and the guided (surface) waves of the layered structures. They can be used to determine the scattered near fields as well as far fields. Thus both large scale and small scale (including subwavelength) fluctuations of the rough surface and medium parameters are accounted for in the analysis.

B2-3
0900

SCATTERING FROM WALL ROUGHNESS IN A PLANAR WAVE GUIDE

J. Merle Elson
Research and Technology Group
Code 4B4400D
Naval Air Warfare Center Weapons Division
China Lake, California 93555

Referring to the figure, we calculate the effects of wall roughness for the case where a Gaussian beam, which can excite guided wave modes, is incident on the planar wave guide structure. The guided wave modes can

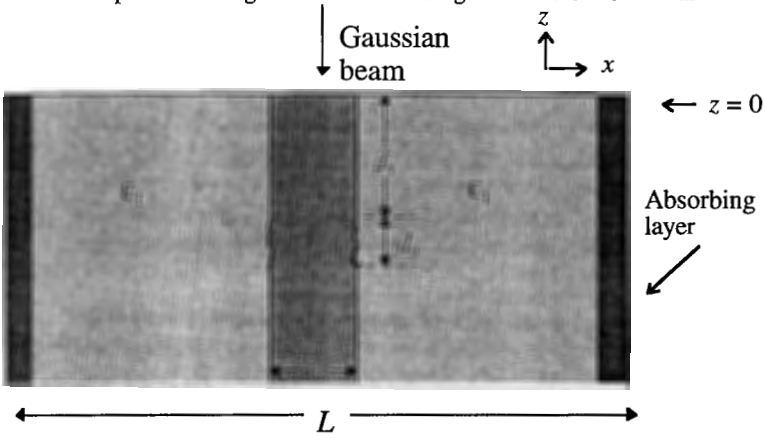

propagate downward and encounter the wall roughness. The roughness, which covers length d_2, begins at depth d_1 below the $z = 0$.

We solve Maxwell's equations for $z < 0$ by discretizing the x-coordinate and obtaining the z-dependence of the solutions as modal expansions. For the solutions in region $0 > z > d_1 + d_2$, we use the R-matrix propagator. The regions $z > 0$ and $d_1 + d_2, > z$ are assumed to be semi-infinite half spaces. Since the calculation domain in the x-direction is of length L, we utilize impedance matched absorbing layers denoted by the dark left and right borders. The surface roughness of the wave guide is numerically generated. Numerical results are given which show the effects of wave guide wall roughness on propagation and losses of guided wave.

B2-4
0920

GRAZING ANGLE SCATTERING BY ONE-DIMENSIONAL RANDOMLY ROUGH SURFACES

Rafael Hernández-Walls Eugenio R. Méndez*
CICESE
Ensenada, Baja California, México
Víctor Ruiz-Cortés
Imperial College
London, UK

The backscattering of light at grazing angles of incidence has historically been a topic of great interest in remote sensing. Many radar systems operate in this kind of geometry. Grazing incidence problems might also become relevant in more modern applications such as advanced technologies in ground transportation, and multiple-satellite communication systems.

In recent years, numerical techniques have been developed, and used in rigorous analysis of the problem of scattering by randomly rough one-dimensional surfaces. These methods have been used to test the validity of the classical approximate approaches to the scattering problem. Unfortunately, in their usual formulation, these methods have proved to be inaccurate for large angles of incidence and scattering.

In this paper we will present grazing angle of incidence calculations with one-dimensional randomly rough surfaces with Gaussian statistics and compare them with experimental results. The main motivation for this work is provided by the need to model the signals obtained by oceanographic radars in near grazing geometries. In order to avoid the problems associated with the numerical treatment of a finite-length surface at large angles of incidence, we study the related problem of scattering from a periodic random surface. The scattering problem is then reduced to that of solving a matrix equation for the Bragg waves diffracted by each realization of the grating.

B2-5
0940

THE SCATTERING OF LIGHT FROM AN AMPLIFYING MEDIUM BOUNDED BY A RANDOMLY ROUGH SURFACE

Andriy V. Tutov Alexei A. Maradudin*
Department of Physics and Astronomy
and Institute for Surface and Interface Science
University of California
Irvine, California 92697
Tamara A. Leskova
Institute of Spectroscopy
Troitsk, 142092, Russia
Jose A. Sánchez-Gil
Institute de Estructura de la Materia, C.S.I.C.
Serrano 121, 28006 Madrid, Spain

We study theoretically the scattering of s-polarized light from a system consisting of a vacuum in the region $x_3 > \zeta(x_1)$, a dielectric medium in the region $-d < x_3 < \zeta(x_1)$, and a perfect conductor in the region $x_3 < -d$. The plane of incidence is the x_1x_3-plane. The surface profile function $\zeta(x_1)$ is assumed to be a single-valued function of x_1 that is differentiable as many times as is necessary, and constitutes a zero-mean, stationary, Gaussian random process, characterized by a surface height autocorrelation function of Gaussian form, $\langle\zeta(x_1)\zeta(x_1')\rangle = \delta^2\exp[-(x_1 - x_1')^2/a^2]$. The angle brackets here denote an average over the ensemble of realizations of the surface profile function, $\delta = \langle(\zeta(x_1))^2\rangle^{\frac{1}{2}}$ is the rms height of the surface, and a is the transverse correlation length of the surface roughness. The dielectric constant of the dielectric film is assumed to be complex $\epsilon = \epsilon_1 + \epsilon_2$, where the real part ϵ_1 is taken to be positive. The imaginary part of ϵ, ϵ_2, is varied systematically from small positive values (passive medium) to small negative values (active medium). For each value of ϵ_2 the angular dependence of the intensity of the light scattered incoherently is calculated as a function of the scattering angle in the weak roughness limit by a numerial solution of the Bethe-Salpeter equation it satisfies. It is found that the overall intensity of the incoherent component of the scattered light increases significantly when ϵ_2 becomes negative, so that the medium is amplifiying rather than absorbing, and the widths of the enhanced backscattering and satellite peaks decrease from their values for positive values of ϵ_2.

B2-6
1000

SYMMETRY OF SPECKLE CORRELATION AROUND THE SPECULAR AND BACKSCATTERING DIRECTIONS

Zu-Han Gu
Surface Optics Corporation, 11555 Rancho Bernardo Road,
San Diego, CA, 92127, USA
TEL: (619) 675-7404 • FAX: (619) 675-2028
E-mail: zgu@surfaceoptics.com

ABSTRACT

Theoretical studies of volume scattering have shown that there are novel correlations among the speckle patterns in the multiple-scattering regime and that they can be divided into three types: the short-range $C^{(1)}$ correlation, long-range correlation $C^{(2)}$, and the infinite-range $C^{(3)}$ correlation. These three types of correlations play different roles in different scattering system geometries. The short-range correlation, which includes the memory effect and the time-reversed memory effect, is the dominant type in a system where the dimension in the direction of the light propagation is much smaller than that in the directions perpendicular to it. The long-range and infinite-range correlations will be the dominant types in a system where the dimension in the direction of the light propagation is larger than those in the directions perpendicular to it (S. Feng, C. Kane, P.A. Lee, and A.D. Stone, *Phys. Rev. Lett.*, 834 (1988); Jun Q. Lu and Z.H. Gu, *Appl. Opt.* Vol. 36, 4562-4570 (1997)).

Recently, McGurn and Maradudin have predicted an additional short-range correlation, $C^{(10)}$, which shows the symmetry of the speckles pattern around the specular direction in the far-field scattering from a rough surface (A.R. McGurn and A.A. Maradudin, SPIE Vol. 3141, 255-268 (1997)). We have measured this peak in the scattering of light from a one-dimensional rough dielectric film on a glass substrate. We have also measured $C^{(10)}$ in the double passage of waves through a one-dimensional random phase screen. The experimental results are presented to verify the validity of the theoretical analysis. The angular correlation function of far-field speckle patterns scattered from a one-dimensional random rough surface of a thin dielectric film on a glass substrate is measured when a polarized beam of light is incident on the rough surface from vacuum. It is found that the intensity correlation function exhibits two distinct maxima: one arises from the autocorrelation $C^{(1)}$ and the other from cross-correlation $C^{(10)}$. They are located symmetrically around the specular and backscattering directions.

B2-7
1040

COMPUTER SIMULATION STUDIES OF THE SPECKLE CORRELATIONS OF LIGHT SCATTERED FROM A RANDOM ARRAY OF DIELECTRIC SPHERES

A. R. McGurn*
Department of Physics
Western Michigan University
Kalamazoo, MI 49009
A. A. Maradudin
Department of Physics and Astronomy
University of California
Irvine, CA 92697

The speckle correlations in the light scattered from a volume disordered dielectric medium consisting of a random array of dielectric spheres are studied using computer simulation techniques. The random medium is formed by placing dielectric spheres of radius R and dielectric constant ϵ randomly on the vertices of a simple cubic lattice, so that a fixed fraction ρ of the vertices is occupied by the spheres. The region outside the spheres is vacuum, and the radius of the spheres is assumed to be much smaller than the lattice constant of the cubic lattice. For simplicity the elecromagnetic fields are treated in a scalar wave approximation. The scalar wave field equations of this system are integrated numerically to determine the scattered fields, and these fields are used to calculate the angular speckle correlation function, $C(\vec{q},\vec{k}|\vec{q'},\vec{k'})$, of the scattered radiation. The angular speckle correlation function is defined by $C(\vec{q},\vec{k}|\vec{q'},\vec{k'}) =< [I(\vec{q}|\vec{k})- < I(\vec{q}|\vec{k}) >][I(\vec{q'}|\vec{k'})- < I(\vec{q'}|\vec{k'}) >] >$, where $I(\vec{q}|\vec{k})$ is proportional to the differential scattering coefficient for the elastic scattering of light of wavevector $\vec{k}$ into light of wavevector $\vec{q}$, and <> indicates an average over random configurations of the spheres. Results are presented for $C(\vec{q},\vec{k}|\vec{q'},\vec{k'})$ in the approximation that $C = C^{(1)} + C^{(10)} + C^{(1.5)}$, where $C^{(1)}$, $C^{(10)}$ and $C^{(1.5)}$ are terms arising from three distinct scattering processes. The contribution $C^{(1)}$, which contains the memory and time-reverse memory effect terms, has been studied before, and is proportional to $\delta(\vec{q}-\vec{k}-\vec{q'}+\vec{k'})$. $C^{(10)}$ is a new term in the scattering of light from volume disorder that is found to be proportional to $\delta(\vec{q}-\vec{k}+\vec{q'}-\vec{k'})$. $C^{(1.5)}$ is a new term in the scattering of light from volume disorder that exhibits an unrestricted dependence on $\vec{q},\vec{k},\vec{q'},\vec{k'}$ and a series of interesting intensity peaks related to the resonant scattering of light by the volume disorder. The contributions $C^{(10)}$ and $C^{(1.5)}$ were considered in the earlier study of the speckle correlation function for the scattering of light from randomly rough surfaces, but have only recently been considered in the scattering of light from volume disorder.

B2-8
1100

ROUGH SURFACE CHARACTERIZATION FROM BACKSCATTERING DATA

P. Tran and J. Merle Elson
Research and Technology Group
Code 4.0T4000D
Naval Air Warfare Center Weapons Division
China Lake, Caifornia 93555

Characterization of surface roughness from scattering data is a difficult problem. For weakly rough surfaces, a procedure for retrieving the rms height and correlation length of the surface from the specular intensity was proposed by Garcia and Nieto-Vesperinas (N. Garcia and M. Nieto-Vesperinas, Phys. Rev. Lett. **71**, 3645-3648,1993). For surfaces with roughness on the order of the radiation wavelength or larger, the specular intensity disappears or is too small to be useful. Even if there is measurable specular intensity, this type of surface is beyond the validity of their theory. Although the specular intensity is negligible, there is significant enhanced backscattering from these surfaces. We will examine the possibility of retrieving the rms height and correlation length of a rough surface from the backscattering data. In particular, we will look at the strength of the backscattering peak relative to the diffuse background and the width of the backscattering peak to determine if these data can provide us with a unique inversion. The backscattering data for our study will be obtained numerically. The rough surface is assumed to be perfectly conducting and to have normal statistics and a Gaussian correlation. The integral equation for the surface current is solved by the Method of Ordered Multiple Interaction (D. A. Kapp and G. S. Brown, IEEE Trans. Antennas Propagat 44, 711-721, 1996). Because of the complexity of the numerical solution, we restrict ourselves to the case of a one-dimensional surface. After the surface current distribution is obtained, the scattered field is computed. The backscattering strength and width as a function of the surface rms height and correlation length will be studied.

B2-9
1120

THEORETICAL STUDIE OF A MODEL SCATTERING-PROBE NEAR-FIELD OPTICAL MICROSCOPE

Tamara A. Leskova
Institute of Spectroscopy
Troitsk, Russia
Eugenio R. Méndez*
CICESE
Ensenada, Baja California, México
Alexei A. Maradudin
University of California
Irvine, CA 92697

We study theoretically the scattering of $s-$polarized light from a model scatter–probe near–field microscope consisting of an infinitely thin half-plane of a perfect conductor defined by $x_1 \geq x_0$, $x_3 = d$ above a rough perfectly conducting surface defined by $x_3 = \zeta(x_1)$ for $-\infty < x_1 < \infty$. This structure is invariant along the x_2-axis. It is assumed that $\zeta(x_1)_{max} < d < \lambda$, where λ is the wavelength of the incident light. The presence of the half-plane within a wavelength of the surface creates a scattered evanescent field that interacts with the rough surface to generate a propagating field that can be detected in the far field. In this way structure on the surface with sub–wavelength dimensions contributes to the scattered intensity in the far field. To extract this information from the far field signal the scattering amplitude is calculated in zero- and first–order in the surface profile function $\zeta(x_1)$ by the analytic solution of an integral equation of Wiener–Hopf type in each order. The intensity of the scattered light, $|E_2(x_1, x_3|\omega)_{sc}|^2$ is then calculated at the point of observation $\{x_1, x_3\}$ in the far field as a function of the position of the half–plane x_0 to first order in $\zeta(x_1)$. From this result $\zeta(x_1)$ can be obtained by Fourier analysis from experimental data for $|E_2(x_1, x_3|\omega)_{sc}|^2$. For the experimental values of $|E_2(x_1, x_3|\omega)_{sc}|^2$ we use the results of an exact numerical solution of the scattering equations based on Green's second integral identity in the plane. From these calculations it is found that $\zeta(x_1)$ can indeed be reconstructed from far–field scattering data with su b–wavelength resolution.

B2-10
1140

NONLINEAR EFFECTS IN SCATTER-PROBE NEAR-FIELD OPTICAL MICROSCOPY

Eugenio R. Méndez* Saúl A. Zavala
CICESE
Ensenada, Baja California, México
Tamara A. Leskova
Institute of Spectroscopy
Troitsk, Russia
Alexei A. Maradudin
University of California
Irvine, CA 92697

Recent progress in Scanning Near-field Optical Microscopy (SNOM) has demonstrated the possibility of beating the diffraction limit of conventional optical systems. In near-field microscopy the resolution is primarily determined by the size of the probe, and not by the wavelength of the illuminating radiation as in classical image forming instruments. Although in principle there is no limit to the resolution achievable by near-field techniques, a common figure for the resolution of current instruments is about $50\,nm$. Rather than a fundamental limitation, this is a manifestation of the difficulties involved in fabricating sharp and efficient fiber optic tips. An alternative technique that circumvents these difficulties consists of using scatterers instead of tapered optical waveguides as probes. The production of metallic probes of near atomic dimensions, such as those employed in Scanning Tunneling Microscopy (STM), is a practical proposition, making scatter-probe scanning near-field optical microscopy an attractive technique.

One way of visualizing the principle of scatter-probe microscopy is the following. The probe, whose critical dimensions are small in comparison with the wavelength, scatters the incident light. The scattered light illuminates the sample and the reflected field is detected in the far-field region. In this picture, that neglects the interaction between the source and the sample, the probe acts as a small source in the proximity of the sample. Although this naive picture is not entirely correct, it provides some insight into the nature of the technique and an indication of the achievable resolution. It has now been realized that not only the size of the probe, but also its shape, are important in the technique. The strength of the secondary source depends on the geometry of the probe and on the conditions of illumination.

In this work we present a numerical study of a scanning scatter-probe near-field optical microscope working in reflection. Our efforts are concentrated on the design of efficient probes (small and intense secondary sources), in the form of metallic tips. The creation of intense fields in the tip of the probe may lead to nonlinear optical effects and the possibility of forming second harmonic images is also considered.

D1-1
0820

OPPORTUNITIES FOR QUASI-OPTICAL TECHNOLOGY IN RF SYSTEMS

E. R. Brown*
University of California, Los Angeles
Electrical Engineering Department
Los Angeles, CA 90095
J. F. Harvey
U.S. Army Research Office
Research Triangle Park, NC 27709

Quasi-optical technology has advanced significantly in the past year with the first demonstration of a spatially-combined RF (X-band) power amplifier having high output power (> 40 W), high instantaneous bandwidth (> 33%), and good power-added efficiency (> 25%) (N. S. Chang, A. Alexanian, M. G. Case, and R. A. York, "20-W Spatial Power Combiner in Waveguide," *IEEE MTT-S International Symposium Digest,* 1457, 1998). These performance characteristics are making quasi-optical technology competitive with the state of the art in power amplifiers, currently defined by the microwave power module (MPM), a hybrid device having a solid-state exciter and a vacuum traveling-wave booster. Several niche applications may avail, such as > 100-W class satellite transponders and airborne coherent sensor illuminators.

While these results are remarkable, they may be just a milestone on the road to more pervasive system applications in which a higher degree of RF functionality is required than is possible from traditional MMIC or vacuum-tube technology. For example, quasi-optical approaches will afford a natural extension of spatial power combining to beam steering and forming, and reciprocal transmit/receive control. Hence, it should be possible to use quasi-optics to carry out the entire RF front-end function of millimeter-wave (e.g. missile) seekers, a task that has traditionally required a high-power vacuum-tube transmitter coupled to a mechanically steerable dish or lens assembly. On the commercial side, quasi-optical transceivers should be attractive in base stations or mobile communications terminals operating at high frequencies (e.g. Ka band) and requiring both high directivity (for good link margin) and broad area coverage. In all cases, we believe that the pervasive system insertions will be those in which most if not all of the analog RF function is carried out quasi-optically. Mixed electronic/quasi-optical approaches, while essential during the development of new components, may not persist because of their limited functionality.

D1-2
0900

PLANAR-CIRCUIT ORIENTED SPATIAL POWER COMBINING

W. R. Deal* V. Radisic Y. Qian T. Itoh
University of California, Los Angeles
Electrical Engineering Department
School of Engineering and Applied Science
405 Hilgard Avenue
Los Angeles, CA 90024

Most quasi-optical systems utilize a three-dimensional approach for spatial power combining. In this scheme, a two-dimensional oscillator or amplifier array is placed perpendicular to broadside-directed antennas. Lenses may also be introduced into the system. The overall system is complicated, and heat sinking may be a problem for densely active arrays. An alternative technique is to use a two-dimensional system and use a dielectric slab for the propagation medium. Both TE- and TM-type active lens combiners have been realized at X-band using planar antennas for surface wave launching (A. R. Perkons, Y. Qian, T. Itoh, *Proc. 1997 IEEE MTT-S,* pp. 691-694 and *1998 MTT Trans.,* vol. 46 No. 6, June 98, pp. 778-783). This type of quasi-optical system is completely planar and reduces heat-sinking and alignment problems. The TE-surface wave amplifier demonstrates system gain greater than 7 dB over a 56% bandwidth. The TM-surface wave amplifier demonstrates 11 dB of gain for a 4% bandwidth. A two-dimensional quasi-optical oscillator has also been demonstrated (A. R. Perkons, Y. Qian, T. Itoh, *Proc. 1996 IEEE MTT-S,* pp. 1907-1910). An output power of 15.4 dBm is measured at the oscillator output connector at a frequency of 8.16 GHz. Two-dimension quasi-optical systems are expected to be highly useful at millimeter frequencies. Because they are completely planar, the entire system can be realized on a single MMIC.

The active antenna has also been demonstrated to be effective in three-dimensional quasi-optical systems. Because quasi-optical systems require a large number of active devices to be integrated into a relatively small area, active antennas using multi-port planar antennas have been developed. In this case, a planar antenna is excited from multiple feeds to increase device integration. If the outputs of multiple amplifiers excite these ports with proper amplitudes, the antenna can be operated with the desired mode. This concept has been used in a three-dimensional power combiner (S. T. Chew and T. Itoh, *Proc. 26th European Microwaves Conference,* pp. 208–210). More recently, this concept has been extended to an active antenna version of the Push-Pull power amplifier (W. R. Deal, V. Radisic, Y. Qian, T. Itoh, to appear in *1998 APMC Proc.*). The multi-feed structure allows for low-loss power combining and has been demonstrated in a system with excellent power-added efficiency and linearity.

D1-3
0940

WAVEGUIDE-BASED SPATIAL POWER COMBINING

Nai-Shuo Cheng Lee-Yin Chen Robert A. York*
Department of Electrical and Computer Engineering
Engineering I
University of California
Santa Barbara, CA 93106

Spatial power combiners are attractive for efficient combining of large numbers of solid-state devices. Spatially-fed/Spatially-combined arrays have been the focus of much research activity during the past decade. Most of the work has centered on planar arrays with normally incident or outgoing beams. Such arrays have (generally) limited bandwidths and also present difficult challenges in thermal management (edge cooling) and efficient power collection (coupling to Gaussian beams). We have developed a broadband waveguide-based spatial combining approach which addresses these issues.

The waveguide-based system uses stacked trays of broadband travelling-wave antenna structures such as tapered-slot antennas, housed in a metal waveguiding enclosure that is operated in the dominant TE mode. Each antenna is then essentially a waveguide-to-transmission line transformer that couples energy from the waveguide mode to a set of power amplifier circuits. We have found that the antennas can be placed electrically close for high power density. Thermal management is simplified by virtue of the "tray" architecture and the surrounding metallic walls which provide a convenient heat sink. Power enters and leaves the system in a single well-defined mode, and therefore power distribution and collection is simplified. Such arrays also pose a well-defined electromagnetic problem, and consequently significant progress has been made towards optimization of the structures for bandwidth and combining efficiency.

We will report on recent results in the development of X-band and K-band waveguide-based systems. Current state of the art at X-band is a 40 Watt system with 70% combining efficiency from 8–11 GHz which uses GaAs-based MMIC amplifiers and optimized finline transitions. Modelling and optimization techniques will be discussed, as well as other potential enhancements for bandwidth and power handling. A multi-octave 64-way passive combiner system using oversized coaxial waveguide will also be presented.

D1-4
1040

RECENT RESULTS IN QUASI-OPTICAL ACTIVE ANTENNA ARRAYS

Z. Popović*
Department of Electrical and Computer Engineering
Campus Box 425
University of Colorado
Boulder, CO 80309

A number of active quasi-optical components, such as oscillators, amplifiers, multipliers, mixers and beam-control grids, have been presented in the past decade, with the main goal of providing high power levels at millimeter-wave frequencies (*Quasi-Optical and Active Arrays for Solid-State Power Combining, eds. R. York and Z. Popović, Wiley, 1997*). This talk will present an overview of results obtained in this field since 1997. In particular, it will discuss in more detail some new results from the University of Colorado: several Ka-band power amplifier arrays, an X-band high-efficiency switched-mode power amplifier array, and two T/R amplifier arrays.

The goal of the Ka-band amplifier arrays is to obtain 2 W of CW power without liquid cooling using commercial MMIC amplifiers. The chips are connected to second resonance slot antennas arranged in triangular arrays, and fabricated on aluminum nitride substrates. Small-signal measurements show good stability, electrical as well as thermal, with gains around 30GHz as predicted from the data sheets. Large signal measurements are in progress. The X-band high-efficiency array uses patch antennas with class F amplifiers and commercial single packaged MESFET devices. Based on far-field measurements, we estimated about 50% PAE with about 10 W of output power at about $60 per watt. This array was designed as a planar amplifier lens fed from the near field, and predictable pattern changes due to nonuniform saturation across the array are measured. To demonstrate functionality of the quasi-optical approach, an X-band and Ka-band T/R lens amplifier arrays were designed and characterized. The X-band array uses hybrid switches, LNAs and PAs, along with broadband slot antennas. The Ka-band lens is designed with a folded feed, in which the center element is sacrificed for the primary feed with negligible pattern degradation. It is implemented with MMIC SPDT switches, LNAs and PAs.

D1-5
1120

A FRESH LOOK AT COUPLED-OSCILLATOR SPATIAL POWER COMBINING

L. W. Pearson*
Holcombe Dept. Elec. & Comp. Eng., Clemson University
Clemson, SC 29634-0915 pearson@ces.clemson.edu
R. J. Pogorzelski
Jet Propulsion Laboratory, 4800 Oak Grove Drive
Pasadena, CA 91109 pogo@jpl.nasa.gov

Quasi-optical oscillators were proposed a little more than ten years ago as a means of developing the power levels needed for applications at millimeter frequencies using large numbers of individual semiconductor devices, each of which produces only a modest amount of power (J. W. Mink, *IEEE Trans. MTT* **34**, 273, 1986). An operating system was demonstrated soon after (Z. B. Popović et al., *Int. J. Infrared and Millimeter Waves* **9**, 647, 1988) in the form of a so-called grid oscillator. This device constituted a rectangular array of oscillating devices that are mutually coupled so that they oscillate coherently. The interconnecting lines in one direction serve as radiators so that the oscillators radiate directly, and the radiated fields add. Subsequently, coupled oscillators using resonant transmission line lengths was demonstrated by Mortazawi and Itoh (A. Mortazawi and T. Itoh, *IEEE Trans. MTT* **38**, 86, 1990). In recent work, coupled-oscillator power combiners have received less attention, with amplifier/combiners receiving more attention. Specific weaknesses of spatial-combining oscillators have motivated this transition. Namely, the oscillators employ low-Q resonators (resulting in low signal quality), and no clear means of modulation has been identified until recently.

In this presentation, we review coupled-oscillator combiners in broad terms, indicating the features that make particular systems viable. We indicate how these features can be reconciled to functional requirements for system applications. Comparisons are drawn between two approaches to obtain mutual coupling. One employs low-Q oscillator circuits at each site, with concomitantly high propensity for the oscillators to couple. The other approach employs moderate-Q oscillators at each site with the concomitant requirement to tune the oscillators so that they share a range of frequencies over which they can couple and lock. In either case, precise frequency control and modulation can be achieved through locking to an external frequency source that ensures high-quality signals.

A recent development in coupled-oscillator arrays provides a means for beam-steering the radiation field of coupled oscillators through detuning of the edge elements in the array. This detuning introduces a progressive phase shift across the oscillator array. This suggests architectures that can replace the functionality of a phased array without the cost incurred by phase shifters. A comprehensive theory of the phase interactions among devices in such arrays is under development (e.g. R. J. Pogorzelski, R. A. York, and Maccarini, *Proc. 1998 AP-S International Symposium,* Atlanta, GA, June 1998).

Session G3, 0935-Wed., ECCR245
IONOSPHERIC PROPAGATION AND SYSTEM EFFECTS
Chairperson: James LaBelle (Dartmouth College)

G3-1
0940

OBSERVATIONS OF LF/MF/HF PROPAGATION PHENOMENA AT HIGH LATITUDES

J. LaBelle*
Department of Physics and Astronomy
Wilder Laboratory 6127
Dartmouth College
Hanover, NH 03755

For several years, Dartmouth College has operated programmable radio receivers from multiple high latitude sites in order to study radio emissions of auroral origin. In addition to detecting auroral radio emissions, these receivers record characteristics of the propagation of natural and man-made signals at 0.1–5.0 MHz. These records document well known effects such as polar cap absorption events and diurnal variations in the propagation characteristics of short and long waves. Auroral substorm onsets are accompanied by prompt fading of distantly propagating transmissions over a wide range of frequencies. The radio data also reveal more subtle effects for which little evidence has appeared in the literature. For example, at auroral zone sites near equinox, the amplitudes of distant MF/HF transmissions are often enhanced by a few dB just before they fade away at dawn. On other occasions, nighttime reception of MF/HF signals is strongly modulated with periods of a few minutes, sometimes in concert with geomagnetic pulsations. Geomagnetic storms produce particularly striking signatures in the latitude and time dependence of distantly propagating radio signals received at high latitudes. During the sun-earth connections event on November 4, 1997, prompt attenuation of distantly propagating signals was recorded at the highest latitudes ($\sim 80°$) immediately following the initial CME occurrence at 0530 UT; a few days later, attenuation of signals was observed at lower latitudes (down to 65°) coinciding with the arrival of the shock front. Wave receivers with broadband sensitivity placed at a range of latitudes provide a detailed picture of these effects.

G3-2
1000

IONOSPHERIC EFFECTS ON P-BAND SAR IMAGING

Jun Liu, Akira Ishimaru and Yasuo Kuga
Department of Electrical Engineering, Box 352500
University of Washington, Seattle, WA 98195-2500
Email: kuga@ee.washington.edu

ABSTRACT

Recently, there has been an increasing interest in the use of space-borne SAR for measuring forest biomass. However, it is noted that conventional SAR using C-band or higher frequencies cannot penetrate into foliage, and therefore, the biomass measurements require longer wavelengths, typically P-band (500 MHz). It is also known that the ionosphere is highly dispersive causing group delay and broadening of pulses. The variance of the refractive index fluctuations due to turbulence is approximately proportional to f^{-4}. In addition, the Faraday rotation due to the geomagnetic field in the ionosphere becomes significant. This paper presents an analysis with numerical examples of the following effects in the frequency range from 100 MHz to 2 GHz in order to show the frequency dependence and the effects of TEC (Total Electron Content) of the ionosphere. First, the ionospheric turbulence can reduce the coherent length below the equivalent aperture size, and the azimuthal resolution becomes greater than $D/2$, where D is the antenna aperture size. Second, the ionospheric dispersion causes a shift of the imagery due to the group velocity. Third, the dispersion also creates broadening of the pulse. In addition, multiple scattering due to ionospheric turbulence gives rise to pulse broadening. Fourth, we consider the Faraday rotation effect and show that the ellipticity change is negligible, but that the orientation angle changes significantly at P-band. Numerical examples are shown using typical ionospheric parameters, turbulence spectrum, and TEC values. In order to show the effects on the SAR imaging caused by the ionosphere, a 2-D SAR imaging of a point source on the ground is performed with the presence of a horizontally inhomogeneous ionosphere.

The TEC measurement is important in studying the ionospheric effects on SAR imaging. The straight-ray assumption is usually applied to the tomography of the structure of the ionosphere. The ray-bending of radio waves in the ionosphere is studied. The simulation results indicate that the straight-ray assumption could be invalid particularly at low frequencies. Although the ray-bending may not be severe at P-band, the phase error caused by ray-bending could still present a problem in SAR imaging and tomography of the ionosphere.

G3-3
1040

MEASURING THE ANGLE-OF-ARRIVAL AND THE CHARACTERISTIC POLARIZATIONS OF RADIO WAVES IN GEOSPACE

Bodo W. Reinisch and Gary S. Sales
University of Massachusetts
Center for Atmospheric Research
Lowell, MA 01854

Satellites with three orthogonal antennas are able to measure the angle-of-arrival of radio waves and their polarization ellipse. The technique is applicable to the ionosphere, magnetosphere and interplanetary space. It will be applied for the first time by the Radio Plasma Imager (RPI) instrument on the IMAGE mission scheduled for launch in January 2000 with an elliptical orbit varying in altitude from 1,000 km to 45,000 km. RPI simultaneously samples all three antennas twice within an RF (or IF) cycle. The two sampling times are spaced by one quarter of a wave period. This quadrature sampling method is identical to the one used by the groundbased Digisondes where the samples are taken on spaced receive antennas. Each three-antenna sample represents the instantaneous spatial **E** field vector of the arriving wave. In a magnetoionic medium the waves are generally elliptically polarized and the **E** vector has a component in the direction of the wave normal. As long as the radio frequency is significantly larger than the plasma frequency at the location of the satellite, this component is small and the plane of polarization defines the wave normal.

The quadrature samples provide two orthogonal **E** vectors within the polarization plane and the vector product defines the wave normal. Once the plane of polarization is determined, the major and minor axes of the polarization ellipse and its tilt angle can be calculated from the six voltage measurements at the three antennas. In the case of radio plasma sounding used by RPI, the orientation of the transmitted wave is known and can be compared with the polarization of the received signal to determine the Faraday effect. The paper also shows how to determine the amplitudes of the two characteristic waves, i. e. the ordinary and extraordinary waves, from the measurements.

G3-4
1100

ANALYSIS AND VALIDATION OF GPS/MET RADIO OCCULTATION DATA IN THE IONOSPHERE

C. Rocken W. Schreiner* S. Sokolovskiy
University Corporation for Atmospheric Research
GPS Science and Technology Program
Boulder, CO 80301

Ground and space-based dual frequency amplitude and phase measurements from the Global Positioning System (GPS) are useful for monitoring the distribution and variability of the Earth's ionospheric electron density. A GPS receiver in low Earth orbit (LEO) can precisely measure the total electron content (TEC) along the signal paths to all visible GPS satellites, even those at negative elevation angles which profile the ionospheric electron density from orbit altitude downwards. We examine two different profiling algorithms and compare the GPS occultation results from the GPS/MET experiment with correlative data. First, we find that profiles computed from single frequency signal bending observations are equivalent to inversions computed from dual frequency TEC observations for a wide range of ionospheric conditions. This finding implies that real-time on-orbit profiling of electron density is feasible without significant loss in accuracy. The two profiling algorithms that are discussed in detail include: 1) the Abel inversion which assumes spherical symmetry; and 2) a 3D inversion that is constrained with the horizontal structure of an a priori 3D electron density field. The retrieved profiles are validated by statistically comparing four days of profile inversions to foF2 data from a network of 45 ionosonde stations, and to vertical TEC data from the global network of GPS ground receivers. Globally the Abel inversion approach agrees with the foF2 correlative data at the 0.5 MHz root mean square (rms) level with a negligible mean difference. All tested 3D constrained inversion approaches, compare slightly worse than the Abel approach in terms of rms difference, and mean bias. The vertical TEC correlative comparisons for both the Abel and constrained inversions generally agree at the 3 TECU rms level, with a significant portion of 2-3 TECU from electrons above the 735 km LEO orbit altitude. Currently, UCAR and the government of Taiwan are collaborating on a project called the Constellation Observing System for Meteorology Ionosphere and Climate (COSMIC). The goal of COSMIC is to launch 8 micro-satellites into orbit by June 2001 which will each carry three scientific payloads: 1) a GPS receiver for TEC and scintillation monitoring; 2) a Tri-band beacon that will measure TEC to ground receivers and 3) a Tiny Ionospheric Photometer (TIP) that will measure sub-satellite TEC. These highly-orthogonal data will enable high-resolution tomographic reconstruction of the Earth's ionosphere and data assimilation into dynamic ionospheric models in near real time.

G3-5
1120

ON THE HEIGHT OF THE EQUIVALENT SHELL FOR THE DETERMINATION OF IONOSPHERIC TOTAL ELECTRON CONTENT USING THE GLOBAL POSITIONING SYSTEM

K. Davies*
Space Environment Center, NOAA
325 Broadway
Boulder, CO 80303

To obtain the vertical total electron content from oblique dual frequency time delay measurements using GPS radio signals it is customary to use an equivalent thin shell model. This shell is usually set at a height of 350 km, or 400 km. To determine a more appropriate average shell height, electron density profiles have been obtained from the International Reference Ionosphere at 25 locations. These locations are distributed around the world over a wide range of geodetic latitudes and longitudes. Electron density profiles have been computed for conditions of low, medium, and high sunspot numbers of 20, 100, and 150, for summer and winter, noon and midnight, and with satellite elevations of 10, 20, 30, 45, and 60 degrees above the horizon . These calculations show that, at 45°,an average shell height of about 620 km is appropriate. This higher height of the equivalent shell may be expected from the following considerations: (1) At a number of locations, especially those near the magnetic dip equator, the height of maximum electron density is often near and above 350 km, and (2) Most of the electron content lies in the topside. Both considerations increases the shell height.

The IRI profiles terminate at 2000 km and, therefore, exclude a protonospheric content between 2000 km and 20,000 km. This protonospheric content will raise the shell height even more. Based on Faraday rotation and time delay radio data from the ATS-6 Radio Beacon Experiment between 1974 and 1978, over a wide range of latitudes and longitudes, it was found that the total columnar electron content of the protonosphere above a height of 2000 km is about 3 TEC units. To a first approximation, this protonospheric content is independent of geographical location, local time, season, and sunspot number. An exponential protonosphere, with a vertical total electron content of 3 TEC units, has been added to the IRI profiles. The electron densities of the ionosphere and the protonosphere are matched at the 2000 km level. The addition of such a protonosphere raises the height of the equivalent shell. For example, at an angle of elevation of 45°, to around 850 km.

H1-1
0800

CHARGED DUST PARTICLES IN THE EARTH'S MESOSPHERE

O. Havnes
Faculty of Science
Department of Physics
University of Tromsø
N–9037 Tromsø
Norway

The Earth's mesosphere is the site of several strange phenomena such as noctilucent clouds and anomalous radar backscattering layers. These are mainly polar phenomena above $\sim$ 50-60° latitude occurring at heights between 80 and 90 km during the summer season when the mesosphere temperature drops dramatically relative to its winter temperature. In situ measurements by rockets have shown that charged dust particles can be present in large numbers and that they can totally dominate the local charge balance. The dust may have positive or negative charges at different occasions. We will discuss the nature of the mesospheric dust, its charges and charging mechanisms, size distribution, number density and influence on other mesospheric phenomena.

We have no direct knowledge of the material and structure of the dust particles. Although ice probably is a major constituent other elements with much lower workfunctions for photoionization must be present in the dust to explain the positively charged dust. The dust radius, during the few events from which we have in situ observations, is probably not more than several times 10 nm. Densities can be large with values sometimes probably exceeding 5000 cm^{-3}. Observations may indicate a very narrow size distribution.

The dust clouds have similar structure as the radar backscattering layers, which they seem to be closely associated with. The overall cloud thicknesses are of the order of a few km with much internal structure down to thin layers and "holes" of only a few meter thickness. We will discuss the structure of the dust clouds and the effects and forces which influence the structure of them.

H1-2
0820

OBSERVATION OF CHARGED DUST IN THE TROPICAL MESOSPHERE

L. J. Gelinas* K. A. Lynch
Space Science Center
University of New Hampshire, Durham, NH 03824
M. C. Kelley, S. Collins
Dept. of Electrical Engineering,
Cornell University, Ithaca, NY 14853
Q. Zhou, J. S. Friedman
Arecibo Observatory, Arecibo, PR 00613

A recent sounding rocket experiment found evidence of nanometer-sized, positively charged dust in the Earth's tropical mesosphere. The Sporadic Atom Layers (SAL) sounding rocket, launched from Puerto Rico on 19 Feb 1998 at 0805 LT, was instrumented to characterize the electrodynamics and chemistry of sporadic sodium layers (Na_s). The SAL payload also included a charged dust detector to test for the existence of mesospheric dust, as dust may play a role in the formation of Na_s layers (von Zahn et al., *GRL, 14*, 76-79, 1987).

The SAL mission flew through a background neutral sodium layer stretching from 80 km to over 105 km altitude, containing two Na_s layers at 94 km and 97 km, as detected by the Arecibo lidar. The Arecibo radar observed an accompanying sporadic E (E_s) layer at 93 km. The charged dust detector observed a low density layer of positively and negatively charged dust stretching from $\approx$89 km to $\approx$ 94km, in the vicinity of both the E_s and the lower Na_s layers. The bottom edge of the dust layer appeared to be negatively charged, but the bulk of the layer was positive.

The SAL dust detector used a synchronous detection method to measure the charged dust flux to the detector. The detector output should have been insensitive to the charge sign of the dust; dust charge was to be inferred from a stepped-voltage veto screen at the entrance aperture which would reject specific mass sizes of negatively charged dust particles. Surprisingly, the in situ operation of the detector showed a distinct sensitivity to the charge sign of the incident dust particle. This effect is likely related to how the dust impact affects charge collection at the anode, and suggests some interesting physical and charging characteristics of the mesospheric dust. Possibilities include a low dust tensile strength resulting in impact fragmentation of the dust particle, and an insulating dust surface or irregular shape which allows collected plasma particles to attach to the surface rather than recombining.

We will discuss the dust detector operation, including the physical and charging characteristics of dust which may influence detector operation, and present the charged dust data.

H1-3
0840

DUSTY PLASMAS IN THE MESOSPHERE

M. Horanyi*
Laboratory for Atmospheric and Space Physics
University of Colorado
Boulder, CO 80309-0392

Small grains immersed in low density plasmas and UV radiation can significantly alter the density, energy distribution and the composition of their plasma environments by continuously collecting and releasing electrons and ions. For example, Noctilucent clouds (NLCs) and polar mesospheric summer echoes (PMSEs) are good candidates, where plasma depletion due to the presence of small aerosol particles is thought to explain unusually large radar echoes.

I will discuss the most important charging processes that apply in the mesosphere, and show possible extensions of the traditional orbit limited charging calculations to account for electron-neutral and ion-neutral collisions in this partially ionized plasma environment. I will show how charging can influence the condensation and coagulation processes that control the growth rates of the aerosols. The difficulites of rocket-born dust and charge measurements will also be discussed.

In addition, I will aslo discuss the continuous meteoritic dust input into the atmosphere that is likely to play important roles in a number of issues. For example, meteoritic dust is suspected to provide the sites where heterogeneous nucleation and, in general, surface chemistry can take place at highly elevated rates.

Most of the extraterrestrial material accreted by the Earth are submillimeter sized particles. The flux of meteoroids in the mass range 10^{-9} to 10^{-4} grams has been recently determined directly from the hypervelocity impact craters on the Long Duration Exposure Facility (LDEF) satellite (Love and Brownlee, *Science 262*, 550, 1993). The measured meteoroid mass distribution peaks near 1.5×10^{-5} grams (≈ 100 μm radius particles) and the total mass accretion rate is $(40 \pm 20) \times 10^9$ grams per year. This rate is a factor of 2 to 3 higher than earlier estimates (Grün *et al.*, *Icarus 62*, 244, 1985). However, the cratering record as well as any other techniques to date, doe not provide information on the smaller end of the size spectrum (submicron sized particles) and does not yield information on the temporal variability of the bombardment rates.

H1-4
0900

LABORATORY EXPERIMENTS RELATING TO NOCTILUCENT CLOUDS

Scott Robertson and Mihály Horányi
Laboratory for Atmospheric and Space Physics
Campus Box 392
University of Colorado
Boulder, CO, USA 80309-0392

Laboratory experiments are in progress to determine the mechanisms leading to charging of noctilucent cloud particles. This is done by creating a beam of molecular clusters of ice and determining the charge state of the clusters after passage through plasma or through a beam of ultraviolet light. A vacuum chamber (0.9 m diameter x 1 m) has been fitted with emissive filaments for generation of plasma in argon gas. Initial data indicate an electron density of 10^8 cm^{-3} and a temperature of 3 eV. Above the chamber is a supersonic nozzle (a 50 micron diameter pinhole) containing a mixture of 600 Torr argon and 20-200 Torr water vapor. Adiabatic expansion results in cooling of the argon and the nucleation of molecular clusters of ice. The cluster beam is diagnosed by a Faraday cup, a velocity filter and a magnetic mass spectrograph. In addition, a 1,000 watt Hg(Xe) arc lamp is used to study photoionization and photodetachment. Initial data are expected in the Fall of 1998.

A rocket-borne instrument for the detection of charged atmospheric aerosols (including noctilucent cloud particles) has been constructed, tested in the laboratory and mounted in a rocket to be launched in November 1998. The detector is a charge-collecting surface, shielded from ambient electrons and ions by a magnetic field. The concept has been tested in a laboratory plasma by verifying that electron collection is suppressed by the magnetic field. The test flight will be from White Sands, New Mexico, which is outside the range of noctilucent clouds. This will test the instrument under rocket conditions and search for the meteoric smoke particles which may cause nucleation of cloud particles in the polar mesosphere.

H1-5
0920

PLASMA CRYSTALS IN THE LABORATORY AND IN SPACE

H. M. Thomas* G. E. Morfill U. Konopka H. Rothermel
M. Zuzic
Max-Planck-Institut für extraterrestrische Physik
Giessenbachstrasse
85740 Garching
Germany

Plasma crystals are a special form of a dusty plasma - the ordered phase of charged micro particles in a neutralizing electron/ion plasma. Dusty plasmas constitute one of the most interesting forms of matter for research into strong coupling phenomena, including spontaneous self organization. There are two main reasons for this: The microspheres are a constituent of the system (not a tracer) - their visualisation therefore allows experimental studies of classical plasma, crystal and fluid phenomena at the equivalent of the "atomic" level - at least in principle - and, compared to liquid colloid suspensions, the plasma systems react typically a million times faster - opening up the possibility to investigate fundamental processes on time scales not accessible before.

In the laboratory we investigated monolayer plasma crystals and crystals composed of a few lattices in the vertical direction as well as their liquid phases. Some interesting phenomena could be studied, like the intermediate states between solid and liquid, wave propagation through plasma crystals as well as the forming of finite systems in 2-D.

However, there exists a major constraint - gravity. The electrostatic forces between the microspheres are long range, and the external gravitational pressure therefore restrics the laboratory investigations to a limited range of state variables. Consequently it was recognized long ago that microgravity measurements were needed to complement laboratory research. Experiments in space have been performed and the results are presented. Here we concentrate on the fluid properties of the strongly coupled colloidal systems - "liquid plasmas", and compare these with other fluids.

H1-6
0940

INTERACTION OF MOVING AND STATIONARY OBJECTS WITH DUSTY PLASMAS

C. Thompson R. L. Merlino* N. D'Angelo
Department of Physics and Astronomy
The University of Iowa
Iowa City, IA 52242 USA

In typical laboratory dusty plasmas dynamical processes involving dust grains occur on a timescale which is much slower than the usual plasma time scales, i.e., $\omega_{pd}^{-1} \gg \omega_{pi}^{-1} \gg \omega_{pe}^{-1}$, where $\omega_{p\alpha}(\alpha = d, i, e)$ is the dust, ion, and electron plasma frequency, respectively. In such a system it is possible to study the interaction of dust grains with objects moving on timescales short compared to the response time of the grains.

We have performed experiments in which negatively charged dust grains were trapped in a nitrogen glow discharge plasma. The plasma was produced using a spiral filament thermionic electron emitter and a positively biased ($\sim$ 300 V) anode disk (5 cm diameter). Dust grains (micron-sized aluminum oxide) were embedded in steel wool which covered the surface of the anode. These grains were attracted into the plasma and formed a trapped dust cloud of several centimeter diameter that extended about 20 cm from the anode.

Video recordings were made of the interaction of this levitated dust cloud with an electrically floating (negative) rod that was passed through the cloud at varying speeds. Experiments were performed in which the motion of the rod took place on a timescale either slow or fast compared to the response time of the charged dust grains, depending on the speed of the rod. The effect of a stationary rod placed inside the dust cloud was also studied. Analysis of the video images obtained may provide some insight into the nature of Debye shielding in a dusty plasma.

This work was supported by The National Science Foundation.

H1-7
1000

ION DRAG INSTABILITY AND DUST ACOUSTIC WAVES IN A DUSTY PLASMA

John Goree* Dmitry Samsonov
Department of Physics and Astronomy
The University of Iowa
Iowa City, IA 52242

Laboratory experiments have been carried out to characterize a new kind of instability in plasmas as well as a compressional wave called the dust acoustic wave.

The ion drag instability arises from Coulomb collisions between ions and dust particles. The instability requires a high particle charge, which is easily attained in a dusty plasma. The instability is driven by Coulomb collisional drag by ions flowing past the highly charged dust particles. The ion flow exerts a drag force on the dust particles. When electron-impact ionization is present, as it is in our laboratory experiments, it creates 'voids', or dust-free regions within the dust cloud. Inside a void, the electron density is enhanced, producing an enhanced ionization and therefore an enhanced outward flow of ions which drives dust particles out of the void. In the laboratory experiments, with dust particles that grew in time to a diameter d of 350 nm, we observed the unstable onset of this instability at a critical particle size. The reason that the particle size determines the onset is that $Q \propto d$. The destabilizing ion drag force is $\propto Q^2$, whereas the opposing Coulomb force QE is $\propto Q$. When the charge exceeds a critical level, the ion drag force exceeds the Coulomb force, and a void abruptly appears.

Experiments with the 'dust acoustic wave' in a strongly-coupled dusty plasma were also carried out. The DAW is analogous to the ion-acoustic wave, with a lower frequency. The term 'strongly coupled' means that the dusty plasma is in a liquid or crystalline state, due to the strong inter-particle Coulomb repulsion between particles. Using microspheres levitated above an electrode, and exciting the wave by applying a sinusoidal voltage of a few Hz to a wire in the dust cloud, we excite the DAW. We measure the k_r and k_i components of the wavenumber, and produce an experimental dispersion relation to compare to theory.

Work was supported in the U.S. by NASA and the NSF. The authors thank Prof. G. Morfill for support in 1998 at the Max-Planck-Institut fuer extraterrestrische Physik. Further information can be found at http://dusty.physics.uiowa.edu

H1-8
1040

DIPOLE EFFECTS IN DUSTY PLASMAS

M. S. Murillo*
Plasma Physics Applications Group
XPA MS B259
Los Alamos National Laboratory
Los Alamos, NM 87545

Dusty plasmas are commonly modeled by treating the interparticle interactions as spherically symmetric screened Coulomb potentials. However, for some examples of dusty plasmas, a more accurate model includes additional multipole moments. Deviations from the simple screened Coulomb potential may arise as a result of an intrinsic dipole moment, as has been speculated for grains composed of ice crystals, or by an induced mechanism, as occurs in the presence of an external electric field. An external electric field will also affect the background plasma and leads to a distortion of the screening cloud as well as nonuniform grain charging. In laboratory dusty plasma experiments grains are typically trapped using electric fields and novel crystal structures consistent with nonspherical potentials have been observed.

To study the effects of multipole moments on dusty plasma dynamics we are employing theoretical, experimental, and computational methods. In our effort we have focussed primarily on wave phenomena and phase behavior assuming that the first two multipoles (monopole and dipole) dominate the dynamics. We have developed models for crystal structure and wave behavior and have incorporated our analytic models into three dimensional molecular dynamics simulations. Experiments have also been performed in a radio-frequency discharge plasma and our models are in qualitative agreement with experimental observations.

H1-9
1100

INVESTIGATION OF DUST CHARGE FLUCTUATIONS IN EXPANDING DUST CLOUDS IN A PLASMA

W. A. Scales
Bradley Department of Electrical and Computer Engineering
Virginia Polytechnic Institute and State University
Blacksburg, VA 24061-0111

Dust charge fluctuations are an important fundamental collective effect in dusty plasmas that have not been studied extensively. Past theoretical investigations have shown that these fluctuations may result from the unique interdependence of dust grain charging and plasma irregularity development. Fundamental physical changes may be made to the evolution and characteristics of plasma irregularites upon including dust charge fluctuation effects. The special case of dust charge fluctuations generated in a localized dust cloud expanding into a background plasma across a magnetic field is considered in this investigation. This configuration has important applications for dusty plasmas in space and in the laboratory. Under these circumstances, the charging time of the dust grains may be comparable to the timescales for development of fluctuations due to plasma instabilities. Therefore, dust charge fluctuations are expected to play an important role in plasma collective effects in this case. First, a theoretical model is discussed that describes the generation of plasma irregularities in the boundary of the expanding dust cloud. Irregularity development in this case is primarily due to the inhomogeneities in the electron depletion boundary layer produced by the initial dust charging. Important characteristics of these irregularities with and without dust charge fluctuation effects will be compared and discussed. To study the nonlinear temporal evolution of the unique plasma collective response under such conditions, a new two-dimensional numerical simulation model has been developed. A fluid model is used for the background plasma ions and electrons. The dust is treated with a Particle-In-Cell (PIC) model. The standard dust charging model is used. Comparisons between predictions of the theoretical model and the numerical model results are made and discussed. The consequences of the results of this investigation on understanding dust charge fluctuation effects in general are also discussed.

H1-10
1120

THE EFFECT OF SIZE ON DUST GRAIN CHARGING

V. W. Chow* D. A. Mendis M. Rosenberg
Department of Electrical and Computer Engineering
University of California, San Diego
La Jolla, CA 92093

Central to the study of dusty plasmas is the charge acquired by a dust grain. A grain's equilibrium surface potential, which is related to the charge by the capacitance, is determined by the condition that the net current to the grain be zero. Depending on the plasma environment, several charging currents can be important. Some of these charging processes include: plasma collection, photoemission, electric field emission, secondary electron emission, and thermionic emission. In the Jovian magnetosphere, for example, where the plasma electrons are energetic, secondary electron emission is important, whereas in the circumsolar dust rings, photoemission and thermionic emission are important due to the UV flux from the sun.

Many of the above mentioned charging processes depend not only on the plasma environment, but also on the grain size. When these size dependent currents dominate, the dust grain charge can vary significantly possibly even leading to oppositely charged grains. Also when the grain is very small (on the order of a few nanometers) stochasticity of the charging process needs to be considered. The difference in the polarity of the charge for grains of different size can have important implications on grain coagulation, as well as grain dynamics.

In this talk, we point out the effect of grain size on the secondary electron emission, thermionic emission, and photoemission. We also discuss several terrestrial as well as space environments in which these effects might be important.

H1-11
1140

INSTABILITIES IN COLLISIONAL DUSTY PLASMAS

M. Rosenberg
Department of Electrical and Computer Engineering
University of California, San Diego
La Jolla, CA 92093

Ionized gases laden with fine (micron to sub-micron sized) charged dust, loosely referred to as dusty plasmas, occur in many space environments including planetary rings, comets, and dusty regions of the Earth's mesosphere, as well as in various laboratory plasma devices. The dust grains can be multiply charged, and are orders of magnitude more massive than the ions. The presence of a charged dust species in a plasma can modify standard ion wave instabilities, and lead to the appearance of very low frequency dust wave instabilities when the plasma ions/electrons stream relative to the dust. Certain dusty plasmas both in space and in the laboratory are weakly ionized so that charged particle -neutral collisions affect the properties of waves and instabilities. In this paper, several electrostatic instabilities in collisional dusty plasmas are discussed with attention given to parameter regimes representative of dusty regions in the ionosphere. Instabilities driven by particle drifts across an external magnetic field are primarily considered. Recent work on the effect of dust on the Farley-Buneman instability (M. Rosenberg and V.W. Chow, *Planet. Space Sci.*, **46**, 103-108, 1998) is reviewed, and applications to dusty plasma environments in the upper D/lower E region are discussed. Studies of the effect of collisions on drift instabilities and dust acoustic instabilities are presented, and applications to natural and artificial dusty plasmas in near-Earth space and to laboratory dusty plasmas are considered.

Session J4, 0815-Wed., ECCR200
ATMOSPHERIC TRANSMISSION AT MM/SUBMM WAVELENGTHS (I)
Chairperson: Simon Radford (NRAO)

J4-1
0820

OBSERVATIONAL CONSEQUENCES OF MILLIMETER AND SUBMILLIMETER OPACITY

M.A. Holdaway
National Radio Astronomy Observatory
949 N. Cherry Ave.
Tucson, AZ 85721-0655
email: mholdawa@nrao.edu

We are most interested in the question of atmospheric opacity because we would like to know just how much cosmic radiation gets through to our site as a function of wavelength. However, understanding the optical depth of the atmosphere helps us to address more subtle issues which a millimeter or submillimeter astronomical telescope faces:

- What is the sensitivity of the instrument at the various observational bands?
- How does the sensitivity vary with zenith angle? How does this impact the way the telescope will be used, and how should it impact the design of the telescope?
- How severe are the continuum atmospheric total power fluctuations, and how can we make total power continuum observations which are not limited by these fluctuations?
- Inhomogeneously distributed water vapor causes both phase errors and short time scale refractive pointing errors. In the millimeter, the water vapor is nondispersive, so the rms phase errors increase linearly with frequency and the refractive pointing errors do not vary with frequency. However, the water vapor becomes dispersive in the submillimeter, and the phase errors and refractive pointing do not follow their simple scaling. The degree of dispersion seen in the water vapor can be estimated by the same transmission models which predict the opacity. If these models can reproduce the measured submillimeter opacity, that will give us more confidence that their dispersion predictions are accurate.
- High frequency observations will be very demanding of the MMA and the conditions on the site, requiring excellent pointing (ie, low winds and small thermal gradients), low atmospheric opacity, and good phase stability. What fraction of the time will all of these quantities be good enough to permit submillimeter observations?

The new data on submillimeter opacity from the current generation of site testing equipment is helping to answer these questions.

J4-2
0840

UNDERSTANDING THE LIMITATIONS OF SUBMILLIMETRE CALIBRATION WITH SCUBA ON THE JCMT

Wayne S. Holland* T. Jenness E. I. Robson
Joint Astronomy Centre
660 N. A'ohoku Place
University Park
Hilo, HI 96720, U.S.A.
W. D. Duncan J. F. Lightfoot
U.K. Astronomical Technology Centre
Royal Observatory
Blackford Hill, Edinburgh EH9 3HJ, U.K.

The new generation of broadband submillimetre cameras are often cooled to less than 0.3 K to achieve sensitivities limited by the photon noise from the sky background. The Submillimetre Common-User Bolometer Array (SCUBA) has been in routine operation on the JCMT on Mauna Kea since May 1997. SCUBA operates in all the atmospheric transmission windows from 350 μm to 2 mm, selecting the wavelength of operation via broadband filters (with $\lambda/\Delta\lambda \approx 12$).

The problems of ground-based research in the submillimetre region have been well-known for a number of years. The atmosphere not only attenuates the signal from an astronomical source, but also undergoes spatial and temporal fluctuations (producing "sky-noise"). In addition, variations in the atmospheric refractive index across the beam can affect the accuracy of telescope pointing, and also reduce the signal-to-noise of an observation.

The determination of the atmospheric attentuation of a source signal is critical for the calibration of data in the submillimetre waveband. SCUBA uses the technique of skydipping to measure atmospheric transmission. A large database of skydip measurements now exist, and correlations have been performed between dips at SCUBA wavelengths and the nearby CSO radiometer (at 225 GHz/1.3 mm). In the near future a three-load calibration scheme, similar to that used by heterodyne systems, is likely to be implemented, to provide quick and accurate estimates of the sky opacity close to the object being observed. A 183 GHz line-of-sight water-vapour meter may also come on line before the end of 1998.

Sky-noise often sets the fundamental limit to sensitivity, particularly at the shorter submillimetre wavelengths (350 and 450 μm), and occurs in atmospheric cells that are larger than the projected array diameter on the sky. We show that the resultant noise is well-correlated across the array and that the effective point-source NEFD can be improved by up to an order of magnitude by the removal of such noise. With SCUBA operating in two wavebands simultaneously, most often 450 and 850 μm, there is also a clear correlation of sky-noise as a function of wavelength.

J4-3
0900

COMPARATIVE MEASUREMENTS OF ATMOSPHERIC TRANSPARENCY AT 350 μm WAVELENGTH

Simon J. E. Radford*
National Radio Astronomy Observatory
949 N. Cherry Ave.
Tucson, AZ 85721-0655
email: sradford@nrao.edu

Comparative measurements of atmospheric transparency are underway at three current or proposed sites for submillimeter wavelength astronomy: the South Pole (2835 m), Mauna Kea (CSO, 4070 m), and Chajnantor, Chile (5000 m). Identical broadband tipping photometers determine the atmospheric transparency at each site about four times per hour by measuring the increase in sky brightness with zenith angle. The instruments, based on ambient temperature pyroelectric detectors, have resonant metal mesh filters defining a 105 GHz passband (FWHM) matched to the 350 μm atmospheric window. Two internal loads at different temperatures are used to calibrate the detector response. Data from Mauna Kea are being cross calibrated against data from a 225 GHz tipping radiometer, from 808–846 GHz heterodyne measurements (CSO), from 350 μm broadband (SCUBA on JCMT) measurements, and from broadband spectroscopy (FTS on CSO). Data from Chajnantor are being cross calibrated against data from a 225 GHz tipping radiometer and from a broadband spectrometer (FTS). Data from both Chajnantor and the South Pole will be compared to radiosonde data.

Measurement of the atmospheric transparency in the 350 μm window directly assesses site quality for broadband astronomy. The relative shapes of the filter bandpass and the atmospheric window might, however, vary with site conditions, as might the relationship between the measured broadband transparency and the narrowband transparency at any particular frequency in the window. These effects were gauged with atmospheric models. Both effects show little or no dependence on site conditions or on model details. Hence broadband transparency measurements are good indicators of narrowband transparency. Sites may be compared on the basis of the measured broadband transparency without recourse to models of how the transparency depends on atmospheric water vapor, temperature, and pressure.

Cumulative distributions of the measured zenith transparency at the three sites will be discussed as well as seasonal and diurnal variations.

The NRAO is a facility of the National Science Foundation operated under cooperative agreement by Associated Universities, Inc.

J4-4
0920

SOUTH POLE SUBMILLIMETER SITE CHARACTERISTICS FROM HETERODYNE MEASUREMENTS

Richard A. Chamberlin*
Caltech Submillimeter Observatory
111 Nowelo Street
Hilo, HI, 96720
Antony A. Stark
Smithsonian Astrophysical Observatory
60 Garden Street, MS 78
Cambridge, MA 02138

Here we present measurements of the 225 GHz, 460 GHz, and 492 GHz opacity of the South Pole sky. We have comprehensive measurements of the opacity for the years 1992 at 225 GHz, and for 1995 at 492 GHz. (R. A. Chamberlin, J. Bally, *App. Optics* , **33** (6), 1095-1099, 1994) (R. A. Chamberlin, A. P. Lane, A. A. Stark, *Astrophy. J.* , **476** , 428-433, 1997)

Opacity measurements were compared with concurrent water vapor measurements made by radiosonde and significant correlations were found. Radiosonde measurements of the South Pole atmospheric temperature profile are available going back to 1961 and these measurements can be used used to infer that the average characteristics of the South Pole atmosphere are about the same for every winter on record. The observed year to year consistency at the South Pole is in contrast to middle latitude, high mountain sites such as Mauna Kea which can show great variation from year to year.

In general, we found that the South Pole sky is extremely stable, with low opacity values likely to persist for days on end. In contrast, a high mountain top site, such as Mauna Kea, may momentarily have lower opacity values, but the time that such low opacity values persist can usually expected to be relatively short.

¿From comparisons with radiosonde data, we determined that the dry air opacity at 225 GHz (and 492 GHz) was significantly higher than expected from an orginal version of the Grossman AT atmospheric model which neglected the continuum contribution to the dry opacity from pressure induced nitrogen absorption, and non-resonant oxygen absorption. (R. A. Chamberlin, J. Bally *Int. J. of of IR and MM Waves*, **16** (5), 907-920, 1995)

J4-5
0940

CALIBRATION OF SUBMILLIMETER ATMOSPHERIC TRANSMISSION DATA

E. Serabyn* J.R. Pardo
Caltech 320-47
Pasadena, CA 91125

Atmospheric transmission data at millimeter and submillimeter wavelengths has in the past been limited both by the narrowband nature of the available long-wave detectors, and by calibration issues. The former limitation can be overcome at the shorter wavelengths by means of a Fourier transform spectrometer, which provides very broadband data. Likewise, accurate calibration can be attained with sufficient attention to the details of the experiment. Here we discuss our use of a Fourier transform spectrometer to measure atmospheric transmission spectra above the summit of Mauna Kea. At this high, dry site, the water vapor content is typically low enough for foreign gas broadening to dominate, leading to simplifications in the lineshape analysis. The site is also high enough that the assumption of a constant vertical temperature gradient in the atmosphere is reliable.

Several observing sessions have been used to acquire data covering various atmospheric water vapor contents, and to address the calibration issues involved. These include measuring and modifying the coupling efficiency of the detector beam to the sky, accounting for operation beyond the Rayleigh-Jeans regime, and accounting both for the sky's vertical temperature gradient and for the possible differences in ambient surface and ground-level air temperatures. As will be detailed, the first of these can be calibrated with a skydip. Operation beyond the Rayleigh-Jeans regime leads to slightly more complicated, but nevertheless tractable equations. It is also possible to correct the transmission data for the sky's vertical temperature gradient and for ground level temperature offsets. The latter in particular are directly revealed by zero offsets at the centers of very opaque lines. Correction for the vertical lapse rate requires a measure of its magnitude (typically 5.6 K/km above Mauna Kea), which, together with the water vapor scale height, allows inclusion of a second order correction term to the transmission data.

J4-6
1000

ANALYSIS OF FTS ATMOSPHERIC MEASUREMENTS AT MAUNA KEA AND IMPLICATIONS ON ATMOSPHERIC RADIATIVE TRANSFER MODELING

J. R. Pardo *
NASA-Goddard Institute for Space Studies
2880 Broadway
New York, NY 10025
E. Serabyn
California Institute of Technology
MS 320-47
Pasadena, CA 91125

Atmospheric transmission spectra have been obtained during the last 3 years with a Fourier-transform spectrometer at the Caltech Submillimeter Observatory on Mauna Kea, Hawaii. This instrument can reach a best frequency resolution of ~200 MHz and in its actual configuration can cover the frequency range ~250-1200 GHz. A wide range of atmospheric conditions has been covered (water vapor columns from ~ 0.2 mm to 2 mm). The compiled data base, completed with simultaneous radiosoundings from Hilo airport when available, has been analyzed with the aim of defining the atmospheric transmission curve for applications to ground-based submillimeter astronomy. From the modeling point of view one of the main interests of this analysis is whether or not the true H2O and dry continuum opacities (both included as empirical terms in current models) can be quantified and separated from the far wing opacity associated to far infrared H2O lines. If they can be accurately determined then we may have some progress in identifying their nature.

In one of our recent observing runs at Mauna Kea a supra-THz atmospheric window has been reported under excellent atmospheric conditions (~200 microns of precipitable water vapor). The access to a partially transparent atmosphere at such high frequencies, where the relative importance of the continuum opacity is much larger than at millimeter waves, has provided us with precious data to make a step forward in the problem of characterizing the water vapor continuum.

The data have been fitted using a multilayer atmospheric radiative transfer model with different line shapes and continuum descriptions. The results and implications of these fits will be discussed at the conference.

J4-7
1040

FTS MEASUREMENTS OF SUBMILLIMETER-WAVE ATMOSPHERIC OPACITY AT PAMPA LA BOLA

H. Matsuo* S. Matsushita
Nobeyama Radio Observatory
Minamimaki, Minamisaku, Nagano 384-1305
Japan

Fourier transform spectrometer (FTS) measurements of submillimeter-wave atmospheric opacity spectra have been performed in two winter seasons at the Pampa la Bola site (Northern Chile, Atacama 4800 m altitude). Atmospheric emission spectra, as a function of airmass, were measured under various weather conditions. In 1997 measurement, atmospheric opacity was rather high during all the observing period. In 1998 measurement, we could make opacity measurement under better weather condition during the observing period.

Atmospheric opacity was evaluated from sky temperature at the zenith as well as from tipping measurements, which are independent measures but give consistent results. The measurement also shows good match with radiometer measurements at 220 GHz, which is a good cross check between each method. Correlation diagrams between 220 GHz and 345 GHz, 410 GHz, 492 GHz, 675 GHz, 691 GHz, 809 GHz, 875 GHz are shown. In 1998 measuremnt we also measured correlation between 220 GHz opacity and opacities of three higher atmospheric windows at 1030 GHz, 1300 GHz and 1500 GHz. By comparing with the radiometer measument at Chajnantor site (S. Radford and M. Holdawa., SPIE **3357**, 486-494, 1998), it is indicated that submillimeter-wave opacities are less than 1.0 about 40-60% of total period and the opacity is less than 0.5 about 10-20% of the period, when opacities at three higher atmospheric windows is less than 3.

Correlations between millimeter-wave and submillimeter-wave opacities get worse when 220 GHz opacity is larger than 0.1. Deviations from the opacity correlation at each frequency show good correlations themselves, but have different relative variations at each frequency. This indicates that atmospheric transparency cannot be characterized only by millimeter-wave opacity, but requires simultaneous opacity measurements at millimeter and submillimeter-wavelengths.

J4-8
1100

FTS MEASUREMENTS OF SUBMILLIMETER ATMOSPHERIC TRANSMISSION AT CHAJNANTOR, CHILE

Scott Paine, Raymond Blundell
Smithsonian Astrophysical Observatory
60 Garden Street, MS 78
Cambridge, MA 02138
USA

Theoretical models of atmospheric opacity at submillimeter wavelengths are unreliable predictors of the opacity at a particular site, because they depend upon semi-empirical terms that may not be correct for the site in question. Few measurements have been made covering a broad frequency range, and above 1 THz, present atmospheric models are essentially unconstrained by experimental data. This is an important problem in the frequency range from 1 THz to 2 THz, where several windows exist that may be usable for ground-based astronomy from a sufficiently high, dry site.

We have deployed a Fourier Transform Spectrometer (FTS) at 5000 metres altitude at a site near Cerro Chajnantor in northern Chile, located within the unusually dry climate of the Atacama. The FTS measures the sky brightness in order to determine the zenith atmospheric opacity over the frequency range 350 GHz to 3 THz, with 3 GHz resolution. It operates autonomously, recording spectra at 10-minute intervals. The primary goal of this project is to measure the opacity in the transmission windows above 1 THz, and to assess the prospects for using these windows for ground-based astronomical observations.

The FTS has recorded a nearly continuous record of opacity covering two months of the 1998 austral winter. We find that significant transmission is frequently observed from the Chajnantor site in windows at 1.03 THz, 1.3 THz, and 1.5 THz. Our intention is to continue operation of FTS to continue gathering statistics on the opacity. Here we present our measurements and data reduction procedures, and discuss implications for astronomy and atmospheric modeling.

J4-9
1120

FIRST TESTS OF 183 GHZ WATER VAPOR MONITORS

M. C. Wiedner*
Harvard-Smithonian Center for Astrophysics
60 Garden Street, Cambridge, MA 02138, USA
R. E. Hills
MRAO, Cavendish Laboratory
Madingley Road, Cambridge, CB3 0HE, UK

At millimeter and submillimeter wavelengths the transmission and refraction of the atmosphere are mainly determined by water vapor and oxygen. In contrast to most other atmospheric gases the amount of water vapor can change by up to an order of magnitude within a few hours. In order to determine the changing atmospheric properties we built two radiometers which monitor the strong emission line of water vapor at 183 GHz. The main purpose of the radiometers is to allow phase correction of interferometric observations with the James Clark Maxwell Telescope (JCMT) and the Caltech Submillimeter Observatory (CSO). However, the radiometers are also important for single dish observations: ¿From the instruments' measurements the atmospheric transmission can be calculated. First, knowing the transmission allows the astronomer to find the appropriate observing frequency, since successful observations above 450 GHz require a dry atmosphere with less than 2 mm of precipitable water vapor, whereas lower frequency observations are possible in moister weather. Second, the flux of the astronomical source can be determined knowing the atmospheric transmission. Since the amount of water vapor and therefore the transmission varies with space and time, it is necessary to monitor the atmosphere along the line of sight of the astronomical beam and to update the measurement every few minutes. Third, the amplitude and frequency in the variation of water vapor give an indication of the submillimeter seeing.

Our radiometers (M. C. Wiedner, PhD thesis, Cambridge University, 1998) measure the intensity 1.2, 4.2 and 7.8 GHz away from the line center at 183.3 GHz, giving an indication of the line shape. To keep maintenance simple the instruments are uncooled resulting in system temperature of 2000 to 3000 K depending on the channel. However, a one second integration over 1 GHz bandwidth has thermal noise of only 0.1 K, which results in an error in opacity of less than 0.002. The instruments are mounted on the JCMT and the CSO. A system of four mirrors directs the beam from the secondary mirror of the telescope to the radiometers. A small flat mirror switches in a one second cycle between the sky position, a hot load (370 K) and a warm load (300 K). Due to the frequent calibrations any gain variations of the instrument are removed. With the radiometers we have so far successfully corrected the phase of interferometric observations of test objects. In the near future we hope to also use the instruments during single dish observations.

J4-10
1140

183 GHZ WATER VAPOUR MEASUREMENTS AT LLANO DE CHAJNANTOR

G. Delgado* A. Otárola
European Southern Observatory
Casilla 19001
Santiago 19, Chile
D. Urbain
Department of Radio and Space Science with Onsala Space Observatory
Chalmers University of Technology
S-412 96 Gothenburg, Sweden

The European Southern Observatory is conducting, in collaboration with NRAO, a site survey at Llano de Chajnantor in the frame of the Large Southern Array Project (LSA). The Onsala Space Observatory, representing Sweden in a consortium of European countries interested in the development of this sub-millimetre array in the Southern Hemisphere has designed and built, through the Advanced Receiver Group at Chalmers University of Technology, in collaboration with MRAO, Cavendish Laboratory, two radiometers for the water vapour line at 183.3 GHz. The radiometers are similar to the one described by M. Wiedner in this session. The two radiometers have been installed at Llano de Chajnantor in Northern Chile at an altitude of 5.000 m; they are situated at the ends of a 300-m baseline of a 12 GHz interferometer, the idea is to correlate the atmospheric phase fluctuations as determined from both systems.

The radiometer has three IF channels at different frequencies from the line centre to obtain the line intensity and shape. From this data it is possible to infer the water vapour content and opacity. The instruments are flexible enough to allow, under computer control, a complete movement of the beam across the sky. The radiometer run autonomously and is controlled by a PC running a LabView program that takes the data and stores it. The data is recovered on a monthly basis during regular visits to the site 2E

Here we present the results of the first four months of data gathering, and its correlation with weather data. Also some results for the opacity are presented.

Session B3, 1415-Wed., ECCR151
ROUGH SURFACE SCATTERING AND RELATED PROBLEMS (II)
Chairperson: G.S. Brown (Virginia Tech)

B3-1
1420

DESIGN OF TWO-DIMENSIONAL BAND-LIMITED UNIFORM DIFFUSERS OF LIGHT

Alexei A. Maradudin*
Department of Physics and Astronomy and Institute for Surface and Interface Science University of California, Irvine, CA 92697, U.S.A.

Andrei V. Shchegrov
Rochester Theory Center for Optical Science and Engineering, University of Rochester, Rochester, NY 14627-0171, U.S.A.

Tamara A. Leskova
Institute of Spectroscopy, Troitsk, 142092, Russia

Eugenio R. Méndez
División de Física Aplicada, Centro de Investigación Científica y de Educación, Superior de Ensenada, Apartado Postal 2732, Ensenada, Baja California, 22800 México

In our recent paper [Appl. Phys. Lett., **73**,1998] we presented two algorithms for designing a one-dimensional band-limited uniform diffuser of light — a non-absorbing optical element that scatters light uniformly within a range of angles and produces no scattering outside this range. In the present work we design two-dimensional band-limited uniform diffusers. Investigating the scattering of a normally incident scalar plane wave from a Dirichlet surface with the aid of phase perturbation theory, we show that such diffusers can be obtained by constructing a two-dimensional randomly rough surface $x_3 = \zeta(x_1, x_2)$ with a prescribed joint probability density function of slopes, $p(s_1, s_2) = \langle \delta(s_1 - \partial\zeta/\partial x_1)\delta(s_2 - \partial\zeta/\partial x_2)\rangle$, where the angle brackets denote an average over the ensemble of realizations of the surface profile $\zeta(x_1, x_2)$.

We focus our attention on two cases. The first case, where $p(s_1, s_2) = \theta(a_1 - |s_1|)\theta(a_2 - |s_2|)/(4a_1a_2)$, with $\theta(s)$ the Heaviside unit step function, describes a surface that scatters light uniformly within a rectangular region of the scattering angles. This surface can be obtained by a simple superposition of one-dimensional random processes: $\zeta(x_1, x_2) = \xi_1(x_1) + \xi_2(x_2)$, each of which defines a one-dimensional band-limited uniformly diffusing surface. This conjecture, first obtained by the phase perturbation theory, is proved rigorously by formally exact scattering simulations. These simulations show that the surfaces obtained by this method are indeed band-limited diffusers with the desired properties.

The second case, where $p(s_1, s_2) = \theta(a - \sqrt{s_1^2 + s_2^2})/(\pi a^2)$, describes a surface which scatters light uniformly within a circle. We describe a method for generating such surfaces by the deposition of two-dimensional defects on a flat surface.

B3-2
1440

ANGULAR CORRELATION FUNCTION (ACF) FOR MODEL-BASED CLUTTER ESTIMATION TO BE USED FOR ADAPTIVE ARRAY SAR IMAGING

J. D. Rockway, M. Curry, K. Ono, Y. Kuga, and A. Ishimaru
Department of Electrical Engineering, Box 352500
University of Washington, Seattle, Washington 98195-2500

Abstract

The difficulty in imaging target-to-clutter problems lies in the influence of the clutter. Depending on the strength of the clutter response, its presence can totally erase or obstruct a natural view of the target's response. Therefore, the desire exists to remove the presence of clutter without degrading the response of the target. Lately, in the work at the University of Washington, we have extended our concepts of modeling clutter to remove its contribution in detection and imaging problems. To achieve this, higher-order moments, or space-time correlation techniques must be analyzed to understand qualitative results from the random media. Specifically, the concept of ACF (angular correlation function), which is a correlation of scattered fields in angular separation, has been used as a means of modeling clutter return.

An imaging technique must now be realized in which clutter models like ACF maybe used to suppress clutter in images. The best imaging technique imaginable would be in a type of adaptive array imaging where the clutter may be adaptively suppressed by nulling its response, while remaining focused on the major return from the target. The process by which the clutter is adaptively suppressed depends upon the clutter model used to estimate it. To this end, we have proposed two new imaging techniques: the Adaptive Array SAR imaging technique and the ACF clutter estimation model used in conjunction with the Adaptive Array SAR imaging. For these two imaging techniques, a clutter correlation matrix is constructed in which the scattered fields from clutter are correlated in space-time. This clutter correlation matrix can then be used to adaptively weigh the synthetic aperture, in such a way that its beam pattern nulls high angular return from clutter. Thus the synthetic aperture remains focused on the target while nulling return from clutter. The first imaging technique constructs the clutter correlation matrix from the scattered fields. The second technique relies on the concept of ACF, which constructs a parameterized model of the clutter correlation matrix. This shows how knowledge of the statistical nature of clutter can be used to enhance the target-to-clutter response.

B3-3
1500

RESULTS FROM SCATTERING BY AN ELLIPTICAL CYLINDER ABOVE A ROUGH SURFACE

B. A. Davis* G. S. Brown
Electromagnetic Interactions Laboratory
Bradley Department of Electrical and Computer Engineering
340 Whittemore Hall, Virginia Tech
Blacksburg, VA 24061

In simulating the scattering from an object over a (rough) surface, questions arise concerning the significance of the interaction between the body and the surface. For example, in the computation of the radar return from vegetation above a rough surface, is the return from the foliage volume independent of the surface return and is the return from the surface independent of the volume return (with the exception of the path loss factor)? Recently, the Method of Ordered Multiple Interactions (MOMI) was extended to include scattering by closed bodies (Adams et. al, *IEEE APS/USNC-URSI Symposium Digest*, Atlanta, GA, 1998) using the combined field integral equation. We have taken this technique and have numerically examined the scattered power due to an object over a rough surface.

In this examination, we begin with the fully interactive solution between an elliptical cylinder and a rough surface; this result serves as a reference for subsequent approximations. The problem is formulated using the method of moments (MOM) technique and its solution is via the MOMI decomposition and iteration. Once this "exact solution" is found, approximate methods are examined. First, the incoherent addition of the power returned from the surface is added to that of the object. This yields adequate results for large separation distance-to-object size ratios. Next, we examine the single scatter result in which the fields on the elliptical cylinder (in isolation) are permitted to re-radiate in the presence of the surface. Hence, in addition to the currents that are produced for the surface in isolation, the cylinder acts as a secondary source for the surface currents. The surface result is then improved by including geometrical shadowing of the free space incident field due to the cylinder. As the final correction, this composite response from the surface radiates to produce a second iteration of the cylinder currents. The dependence on the relative separation to cylinder size is examined in each case.

In addition to these results, we have found that the iterations required in the MOMI solution increase as the level of interaction between the cylinder and the surface increases. Hence using the MOMI decomposition as a preconditioner, a separate solution to the MOM equations described previously has been attempted using the Biconjugate Gradient Stabilized method. The results of this effort will be discussed.

B3-4
1540

MULTIPLE SCATTERING AND DIFFRACTION BY A CONCAVE STATISTICALLY ROUGH SURFACE

Iosif M. Fuks
CIRES/University of Colorado/NOAA/ETL
Boulder, CO 80303

An approximate solution of the problem of electromagnetic wave diffraction by the impedance statistically rough surface that is concave in average rather than the plane one is studied. It is assumed that the radius of curvature of concave cylinder significantly exceeds the radiation wave length so that the parabolic approximation for undisturbed (smooth) concave surface can be used in Fock representation - as a superposition of grazing "normal" modes. For simplicity our consideration is restricted only by the two-dimension (i.e. cylindrical) surface roughness. There are no depolarization effects in this case, and the diffraction problem can be formulate for the scalar potential, that satisfies the Helmholtz equation and the impedance boundary condition. The diffraction problems for vertically (TM) and horizontally (TE) polarized waves differ only by different values of the effective impedance that depends not only on electrodynamic surface parameters (dielectric permittivity and conductivity) but on ratio of surface curvature to the radiation wavelength as well.

The grazing angles of "normal" modes (that can be considered also as a result of multiple scattering of glancing rays - in geometrical optics approximation) may be comparable with the Brewster angle that is assumed small enough. It is shown that for small enough "normal" mode grazing angles (smaller that the Brewster angle) the TM modes attenuate faster than the TE ones. Due to the difference in attenuation decrements, backscattered signal for the TE incident wave can be comparable or even bigger than for the TM one. This phenomenon can be used for interpretation of anomalous behavior of polarization ratio for back scattered electromagnetic waves of centimeter range from rough sea surface at low grazing angles.

B3-5
1600

A ROLE OF STEEP WAVES FOR LOW-GRAZING-ANGLE OCEAN MICROWAVE BACKSCATTER

A. G. Voronovich*
NOAA/ETL
325 Broadway, Boulder, CO 80303
V. U. Zavorotny
CIRES/University of Colorado/NOAA/ETL
325 Broadway, Boulder, CO 80303

Numerous experimental data show that an average microwave backscattering cross- section ratio of horizontal (HH) and vertical (VV) polarizations (polarization ratio) is very often of the order of a few negative dB at low grazing angles. On the other hand, calculations based on known empirical sea-surface roughness spectra produce a value of the order of -20÷-30 dB, thus underestimating the average experimental polarization ratio severely.

Another attempt to reproduce the experimental results through numerical simulations has been undertaken in this work. Monte-Carlo simulations have been performed with realizations of the 1-D sea-surface profile of 100 m length generated according to the Pierson-Moskowitz spectrum and Gaussian statistics. The scattering model used was based on a two-scale representation of surface roughness. The solution of a corresponding boundary integral equation for the large-scale (undulating) component of a surface roughness was calculated in the forward scattering approximation. Then backscattering which was due to the small-scale roughness was calculated in a perturbation manner. Thus, all possible multi-bounce and shadowing processes with respect to both incident and back scattered waves were taken into account. The polarization ratio thus calculated appeared to be very close to te value given by a standard two-scale model. Then a few relatively steep waves (bump-like features) with maximum slope of the front face equal to 0.5 were added to the roughness. It was also assumed that small-scale roughness enhances on the front face. Those "bumps" occupying only 2 % of the surface do not change significantly the roughness spectrum; only wings of the slope distribution are affected. However, now the average polarization ratio increases dramatically reaching experimentally observed values of a few negative dB. In particular, diffraction effects occurring for the HH-polarization on the front face of the "bumps" accounts for 10 dB of this increase.

Thus, experimentally observed values of the average polarization ratio could be explained by the appearance of steep features on the sea surface. The HH-polarization might be sensitive to sub-surface non-linear hydrodynamic processes which could presumably generate such steep waves on the sea surface. This corresponds to the scenario suggested in (A.V. Smirnov and V. U. Zavorotny, *J. Phys. Oceanogr.*, **25**, 2215-2228, 1995) for the explanation of polarization differences in low-grazing-angle radar images of an ocean surface.

D2-1
1400

PHOTONICALLY CONTROLLED SLOT ANTENNAS

Zoya Popović Shawn Stone*
Department of Electrical and Computer Engineering
Campus Box 425
University of Colorado
Boulder, CO 80309

By using photodiodes in active antenna elements, one can allow for optical control of an antenna. This optical control is benefitial in that it allows for remoting via fiber optic cable and, for unbiased photodiodes, removes at least one set of electrical control wires which might interfere with antenna transmission. This paper describes efforts to model the microwave characteristics of the photodiode and shows successful slot antenna configurations where the photodiode was used as an optically controlled load.

Various attempts were made to characterize the RF behavior of the photodiode response. Experimentally it was shown that by not allowing DC current flow through the photodiode, the photodiode exhibited change in RF impedance with incident light. This response could be thought of as a change in the capacitance of a photodiode (effectively, the photodiode behaves as an optically tunable varactor).

A second resonance slot fed by a microstrip is inherently broadband and can be relatively easily tuned (20% around 8 GHz) by varying a varactor attached to the feeding microstrip (M. Forman, Z. Popović, *IEEE Antennas and Propagation Society International Symposium 1997*, **1**, 18-21, 1997). This was done using a photodiode instead of the varactor with the photodiode connected in shunt at the end of the tuning microstrip feed line. Preliminary results show approximately 500 MHz optically tunable bandwidth centered at 11.25 GHz.

The antenna was measured using an HP 8510 network analyzer with the antenna connected to port 1. The match is described by the S_{11} parameter, which was seen to shift with incident light. In order to characterize the other parameter of interest (i.e. the radiation), we used both ports of the network analyzer with a receiving antenna connected to port 2. The S_{21} parameter therefore shows the radiated power as a function of the frequency and polarization. The measured S_{21} showed relatively good radiation over the entire range of tuning.

D2-2
1420

VOLTAGE TUNABLE DIELECTRICS FOR RADIO FREQUENCY AND MICROWAVE DEVICES

R. Benton, F. Barnes, and H-D Wu
Department of Electrical Engineering, University of Colorado-Boulder, Boulder, CO, 80309, USA

$Barium_{0.6}Strontium_{0.4}Titanate$ (BST) provides a voltage tunable dielectric constant which can be used to make variable capacitors and voltage-tunable delay lines (Wu, H-D, *et al*, *Integrated Ferroelectrics*, *v. 8, n. 1-2*, 171-184, 1994). Applications include phased array antennas, parametric amplifiers, and voltage-tunable oscillators. An important problem is obtaining low-loss materials. In this paper, we report the effects of doping of BST with Calcium Carbonate, Calcium Oxide, Ytterbium Oxide, and additional materials.

Samples of BST were doped with various concentrations of Calcium Carbonate and Calcium Oxide ranging up to 2.5% by weight. Curie temperatures of ~270°-280° were observed. The $CaCO_3$ samples had very little tunability, and minimum tangent losses of 0.1-.02 at or below T_c. Losses increased with an applied bias. The CaO samples had good tunability with losses of ~0.005 in the region of interest, just above the Curie temperature.

Ytterbium Oxide was used as a dopant in concentrations up to 5%. Good tunability was observed, with a sharp peak in the dielectric constant curve at the T_c of 275°-280°. Losses in the region of interest ranged from .05-.001.

Our results show Calcium Oxide doping reduces tangent loss in the region of interest by a factor of two over the undoped samples. Calcium Carbonate doping changes the shape of the loss curve and reduces tunability. Ytterbium Oxide doping gives good tunability and fair to excellent losses.

D2-3
1440

INVESTIGATION OF SURFACE WAVE MITIGATION USING PHOTONIC BANDGAP SUBSTRATES

P. Keith Kelly* Todd Lammers, Melinda Piket-May
Department of Electrical and Computer Engineering
Campus Box 425
University of Colorado
Boulder, CO 80309

Many propagation and radiation structures suffer performance degradation due to surface wave excitation. A well known example is the microstrip patch antenna efficiency on thick substrates. Other examples include scan blindness in phased arrays and parallel plate mode coupling around vias in stripline. Although the parallel plate mode coupling is not a surface wave, the prevention of this coupling may be accomplished using the same proposed technique. The results of a study on the effectiveness of using finite height photonic bandgap structures will be presented.

Photonic bandgap structures are 1D, 2D, or 3D infinite periodic lattices commonly made up of two dissimilar dielectric materials. Since the objective of this work is to operate on planar structures, only two dimensional periodicities are considered. The unique property of a structure of this type is the prevention of propagation in any direction over a band of frequencies for infinite height and extent. However, very little is known about the propagation characteristics when the lattice has a finite height, finite extent, and is placed on top of a ground plane. A finite difference time domain model has been constructed to aid in the understanding of these parameters on the surface wave propagation for such a structure. The conditions for establishing a bandgap will be discussed by presenting parametric plots for the substrate height, dielectric contrast, and volume fraction of the two dielectric materials for several lattice types. Also included are some results on the shape of the "atoms" making up the crystal structure where symmetric and asymmetric shapes have been selected.

D2-4
1500

CHARACTERISTICS OF AIR-BRIDGED TRANSISTORS

Samir M. Hammadi and Samir M. El-Ghazaly
Department of Electrical Engineering
Arizona State University
Tempe, AZ 85281-5706

The gain and output power of microwave transistors are limited by two factors. Namely, the width of the device and its gate length. The gate length controls the metallic gate resistance. Shorter gate length results in higher gate metallic resistance. This increased resistance can results excess signal attenuation along the device electrodes. While this factor is dominant at lower frequency applications, the other factor, namely the device width, is more pertinent to higher frequency applications. As the frequency increases, the device width becomes comparable to the wavelength, and the device starts to act like a transmission line. Because of the non-symmetric structure of the device and the different bias conditions on the electrodes, the gate and drain electrodes will manifest different input impedances. Therefore, the signals along each electrode will propagate with different phase velocities. Due to electronic and electromagnetic coupling between the two electrodes, the difference in phase velocities results in phase cancellation.

In this paper the air-bridged MESFET will be analyzed. In contrast to conventional MESFET, where the signal is fed at one end of the device, the air-bridged MESFET is excited uniformly along its width. The gate resistance can then be reduced by increasing its width. Traveling wave effects become negligible because of the fact that the wave travels along the device length, which is usually very short. The dc characteristics and the small signal parameters of the air-bridged gate MESFET are computed. These parameters are to be compared with those of conventional MESFET's.

D2-5
1540

10 GHZ HIGH-EFFICIENCY CLASS-E AMPLIFIER INTEGRATED WITH A SLOT ANTENNA

Zoya Popovic Manoja D. Weiss*
Department of Electrical and Computer Engineering
Campus Box 425
University of Colorado
Boulder, CO 80309

As RF circuits increase in complexity, the size and inter-element coupling due to radiating transmission lines also increase. To decrease circuit area and coupling, it is desirable to minimize matching and tuning circuits in the design. Consequently, in transmitter or receiver circuits, it is of interest to design the antennas to perform matching and tuning functions in addition to being a radiating element.

For example, in class-E high-efficiency power amplifiers, the transistor output load at the fundamental frequency is given by:

$$Z_{net} = \frac{0.28015}{\omega_s C_s} e^{j49.0524^\circ},$$

where $\frac{\omega_s}{2\pi}$ is the fundamental frequency, and C_s is the transistor switch output capacitance. At the second harmonic, the impedance presented to the transistor output is an open circuit (T. B. Mader, Z. B. Popovic, *MGWL*, **5**, 290-292, 1995). In conventional microstrip class-E amplifiers, tuned microstrip matching circuits at the output of the transistor provide the class-E operating conditions. It is possible to design an antenna with input impedance given by the conditions above, which removes the need to have a matching circuit and couples the amplifier to free space directly. Previous work has demonstrated a class-F high-efficiency power amplifier at 2.55 GHz with a circular patch antenna providing the load to the transistor amplifier (V. Radisic, Y. Qian, T. Itoh, *IEEE MTT-S Digest*, 687-690, 1997). We present a slot antenna integrated with a class-E power amplifier at 10 GHz.

The slot antenna is microstrip-fed and is designed to have an input impedance at the fundamental frequency given by the class-E requirement. Therefore it has both a real and imaginary part and is not a resonant antenna. Also in accordance with class E requirements, the antenna provides an open circuit load to the transistor at the second harmonic, due to the microstrip feed configuration. This antenna is connected to the output of the transistor amplifier with no conventional matching circuit, but only a length of microstrip line to provide the correct phase at the transistor. The radiation patterns of the slot antenna indicate a 15 dB cross-polarization ratio and 2 dB gain. The performance of the final integrated antenna is measured using the Friis transmission formula since the output of the circuit couples directly to free space. Preliminary measurements indicate the power-added efficiency of the class E circuit to be approximately 40%.

D2-6
1600

INTERNATIONAL DEVELOPMENTS IN LASER COMMUNICATIONS

K. E. Wilson
Jet Propulsion Laboratory

The advantage of laser communications in high rate free space links has been well recognized for decades. The terrahertz optical carrier frequencies allow data transmission rates far in excess of those achievable with radio frequencies. The diffraction-limited divergence of an infrared optical beam is four orders of magnitude less than that of an X-band radio frequency beam. This high directionality reduces the effects of cross talk and interference and makes the frequency spectrum allocations that are so common in the radio frequency spectrum, unnecessary.

The Japanese and the Europeans have been aggressively developing optical communications technology. The Communications Research Laboratory of Japan (CRL) and the National Aeronautics and Space Development Agency of Japan (NASDA) launched the laser communications experiment (LCE) terminal on board the ETS-VI satellite on August 28, 1994. The plan was to demonstrate a series of space-to-ground and space-to-space optical communications experiments (M. Shikatani et. al., Proc. SPIE, 1866, 21 - 29, 1993). Because of a failure I the apogee-kick motor, the ETS-VI satellite did not make geostationary orbit, and CRL asked NASA to participate in the optical communications experiments with the satellite when its transfer-orbit trajectory made it visible from the US. JPL, CRL, and NASDA performed a series of joint experiments over a six month period in 1995 and 1996, and demonstrated 1 Mbps bi-directional optical communications and the retrieval of satellite engineering data at ranges up to 40,000 km (K. Wilson et al., Proc. SPIE,, 2990, 23 - 30, 1997). Currently, NASDA is developing a second terminal, the laser utilizing communications equipment (LUCE), that will be launched on board the Optical Inter-Orbit Communications Engineering Test Satellite (OICETS) in the summer of 2000. LUCE will demonstrate a 50 Mbps link with the European Space Agency's (ESA) Advanced Relay and Technology Mission Satellite (ARTEMIS) scheduled to be launched into a geostationary orbit in the first quarter of 2000. The CRL is currently at the start point of developing an optical experimental terminal for Japanese Experimental Module (JEM) on the International Space Station (ISS). The terminal is scheduled for a year 2003 launch, and will demonstrate bi-directional optical communications with the ground station at 2.5 Gbps downlink, and 50 Mbps uplink.

ESA has developed several optical terminals for inter-satellite links. Among these are the Semiconductor-laser Inter-satellite Link Experiment (SILEX) terminals for a 50 Mbps cross-link demonstration between ARTEMIS and the Earth-observing SPOT-4 satellite (A. F. Popescu and B. Furch, Proc. SPIE, 1866, 10 - 20, 1993), and the small optical telecommunications terminal. (SOTT) for a 1 Gbps cross-link demonstration across the geostationary arc. SPOT-4 was launched in March '1998. Commercially, ESA has contracted with Oerlikon-Contraves Space to design, build, and test a compact lightweight optical terminal for short-range inter-satellite links (SROIL). ESA has also developed an Optical Ground Station on the Teide Observatory site of the Astrophysics Institute of the Canary Islands (IAC) to support future space-to-ground optical communications demonstrations.

D2-7
1620

THE NASA OPTICAL COMMUNICATIONS PROGRAM, AND OTHER NATIONAL PROGRAMS

Dr. James R. Lesh
Jet Propulsion Laboratory
California Institute of Technology
4800 Oak Grove Dr. 161-135
Pasadena, CA 91009
(818) 354-2766
james.r.lesh@jpl.nasa.gov

NASA has been developing optical communications technology for use on its future missions since the early 1970's. Since the early 1990's, that work has been concentrated at the Jet Propulsion Laboratory. This paper will describe the state of optical communications technology development within the NASA program. It will describe the development of a flight engineering model transceiver developed to functionally demonstrate a minimal complexity design for spatial beam steering, and how space-qualified versions of that transceiver are being developed for flight on the International Space Station and possibly the Space Transportation System. Included in that section will be a discussion of the Laser communications Test and Evaluation Station (LTES), a generic testing facility for measuring the performance of optical communications terminals. Next, developments underway for the supporting ground network, including the installation of a new 1-m diameter ground R+D station and the operation of a network of atmospheric visibility monitoring stations will be covered. The 1-m facility is beginning construction and will be ready for operation in late 2000. The visibility monitoring observatories are spread around the southwestern US and have been collecting data for the past several years. A set of system-level demonstrations that demonstrated mitigation techniques for atmospheric scintillation and which reached out to link distances as far as 6,000,000 km will also be covered. Finally, a brief discussion of other optical communications programs recently completed or under development within the United States will be described. These programs include the Air Force's LCS system and the BMDO-funded flight terminal for the STRV II mission.

F3-1
1340

FOUR YEARS OF ACTS PROPAGATION MEASUREMENTS - COMPARISON WITH MODELS

Robert K. Crane
School of Meteorology
University of Oklahoma
Norman, OK 73019

The NASA Advanced Communications Technology Satellite (ACTS) has been in orbit for more than four years. Continuous path attenuation measurements have been made at 20.2 and 27.5 GHz to seven different sites as a part of the ACTS propagation experiment (see *Proc IEEE* Special Issue on Ka-Band Propagation, 85(6), June 1997). The empirical distribution functions (edfs) for the first full four years of observations are now available for analysis. The sites are situated in different rain climate zones to provide a range of conditions to test attenuation prediction models.

A problem with the ACTS propagation terminal was caused by the antenna design. When the antenna is wet, water on the feed plus a water layer on the reflector can produce as much as 3 to 5 dB additional attenuation depending upon frequency and rain rate. The attenuation observations must be corrected for antenna wetting before any comparisons can be made between measurements and predictions. A wetting model was developed that provided the required correction. With correction, the attenuation observations at four of the seven sites compare favorably with popular attenuation prediction models and, where available, with earlier observations.

The circumstances at three of the sites are different. At one of the sites, the seasonal variation in rain occurrence does not match the assumptions behind the prediction models. The result is a large difference between model predictions and measurements. At two of the sites, the station heights are significantly higher than were employed for other observations. At these sites, large differences also occur between measurements and predictions. The ACTS observations confirm the use of the models where the climate and terrain are similar to other locations where measurements have been made. For the locations where the models do not perform adequately, the ACTS data will provide the additional information needed for model improvement.

Recent modeling efforts have been directed toward predicting the year-to-year variation of attenuation at specified probability levels. The ACTS observations provide a doubling of the amount of data collected worldwide that are useful for developing variability models. The observations show that the simple model that has been used in the past is not adequate to describe the large differences in the year-to-year variations that have been detected between the ACTS propagation experiment sites.

F3-2
1400

ACTS Ka-BAND DIVERSITY MEASUREMENTS IN FLORIDA

Henry Helmken* , Joey Duvall** and Rudolf Henning**
*Florida Atlantic University
777 West Glades Road
Boca Raton, Florida 33431
**University of South Florida
4202 East Fowler Avenue
Tampa, Florida 33620

The NASA Advanced Communications Technology Satellite (ACTS) Propagation Measurements program has accumulated five years of continuous propagation data at 20.185 GHz and 27.505 GHz at seven selected sites spanning the North American continent from Alaska to Florida. Since path loss at these frequencies is strongly affected by intense weather phenomena, reliable signal transmission system designs must rely heavily on both measurement data and validated models of channel characterization. The most stressed area in North America, weather-impact-wise, is Florida with its sub-tropical climactic region. In order to mitigate the effects of severe rain attenuation, the Florida ACTS propagation team has been conducting a series of experiments to study diversity gain. The study has concentrated on short base line (2-4 km) diversity gain which may be of most relevance to commercial systems.

NASA's ACTS program was developed to foster the creation and validation of communication technology expansion into the millimeter region. At Ka-band frequencies, reliable signal transmission system design depends heavily on validated channel models and accurate propagation statistics. The Space Communications Technology Center (SCTC) headquartered at Florida Atlantic University (FAU) is a NASA sponsored Center for the Commercial Development of Space and is developing systems for digital satellite communication of voice, data and video via Ka-band and thus is very dependent on accurate propagation information.

The diversity study was conducted with both the ACTS Propagation terminal (APT) and second transportable terminal expressly built for these experiments. The 1.2 m antenna is identical to that of the APT and the 20.185 GHz beacon signal is down converted to 70 MHz and measured with a digital receiver identical to that used in the APT terminal. The data is collected at the same rate and format which allows direct and easy comparison with the APT data. Rain events in either terminal are delineated and the APT calibrated baseline before and after each event is used to calibrate the baseline in the transportable unit. This procedure was validated by taking and comparing data with both terminals side by side.

This paper will focus on the results of a 1 year comparison of simultaneous rain event data collected by the APT terminal and by the transportable terminal located 2.4 km distance. Diversity gain will be examined for both the relatively dry winter months and the sub-tropical summer season. Data will be further sub-divided to examine possible diurnal variations of diversity gain.

F3-3
1420

WET ANTENNA EFFECT ON Ka-BAND SYSTEMS

Roberto J. Acosta
NASA Lewis Research Center
Cleveland, Ohio 44070
USA
Phone: 0-001-216-433-8016
e-mail : Roberto.J.Acosta@lerc.nasa.gov

Abstract

This paper describes an experimental and theoretical treatment of the contribution of wet reflector antennas to the signal path losses in a Ka-band low margin satellite communications system. The Very Small Aperture Terminals (VSAT) of the current commercial satellite systems operating in either C-band or Ku-band generally have their remote antenna reflectors and feed horn radomes coated with hydrophobic materials. The aim is to prevent the antenna and radome surfaces from becoming wet during a rainfall. This precaution relieves the burden of added rain margin necessary in link budgets. In the Ka-band, a greater sensitivity to wet antenna surfaces as been observed, with or without the application of hydrophobic material. Measured attenuation due to wet antennas is in the order of several dB.

The amount of water on ground reflector antennas (reflector and feed radomes) can cause additional signal loss (up 4-5 dB) from the expected propagation attenuation due to rain at Ka-band. This is one reason why the standard techniques for predicting rain fade statistics (propagation models) are not aligned with the ACTS Ka-band RF beacon measurements. In a Ka-band satellite communications system, an additional margin should be included to account for wetness of the antenna system.

The problem of wet antenna can be described as the additional signal loss caused by wetting of the antenna surfaces. Wetting consists of thin water layer or beads of water on the VSAT's antenna reflector surface and/or the antenna feed horn window. The amount of water layer on a surface depends upon the material, surface roughness, elevation angle and exposure of the surface to aging. A water layer in the feed horn window radome creates a high perturbation on the feed standing wave ratio. Water on the reflector creates an additional scattering and absorption loss due to raindrops' size at the surface of the reflector.

The analysis of wet reflector antenna and radome surfaces has been studied by Blevis, Ruze, Cheah, Othshi, Crane and Ramachadran. In this paper, extensive measurements and a simple transmission line model are provided as a guideline on designing antennas considering the effects of antenna wetting.

F3-4
1440 COMPARISON OF RADAR POLARIMETRIC MEASUREMENTS OF RAINFALL WITH 2D-VIDEO DISDROMETER OBSERVATIONS

A. Ryzhkov[1], T. Schuur[1], D. Zrnic[2], M. Schonhuber[3]

(1) Cooperative Institute for Mesoscale Meteorological Studies / University of Oklahoma, USA
(2) National Severe Storms Laboratory, USA
(3) Joanneum Research, Austria

Natural drop size distribution (DSD) variations substantially limit the accuracy of the conventional radar rainfall estimation algorithm based on radar reflectivity factor Z. Polarimetric rainfall estimators that use specific differential phase K_{DP} and differential reflectivity Z_{DR} are also affected by DSD uncertainty but to a much lesser extent (A. Ryzhkov and D. Zrnic, J. Atmos. Oceanic Technol.,12, 249-256, 1995). On the other hand, polarimetric methods imply certain assumptions about the shape of raindrops as a function of their size which are still being debated. 2D-video disdrometer provides unique capability to accurately measure drop size spectrum as well as the shape of individual drops in a very wide range of their sizes (M. Schonhuber et al. In Weather Radar Technology for Water Resources Management, UNESCO Press, 159-171, 1997).

This paper describes results of combined rain measurements with the NSSL's S-band polarimetric radar and 2D-video disdrometer for 11 rain events observed in the Spring of the 1998 in Central Oklahoma. Analysis of the disdrometer data indicates presence of big drops with diameters larger than 5 - 6 mm for most convective rain events. These big drops most likely originate from melting hail aloft and produce plateau-like tail in the drop spectrum that cannot be described in terms of conventional Marshall-Palmer or Gamma DSD.

The disdrometer data are used to compute actual rain rate R as well as radar variables Z, Z_{DR}, and K_{DP}, which are subsequently converted into "radar" rain rate estimates R(Z), R(Z, Z_{DR}), R(K_{DP}), and R(K_{DP}, Z_{DR}). These disdrometer-derived "radar" rainfall estimates are compared with those obtained from the radar polarimetric variables actually measured by the dual-polarization radar. It is shown that the estimator R(K_{DP}, Z_{DR}) is least sensitive to DSD variations in the absence of drops larger than 4 - 5 mm. If hail or large drops originating from hail are present, the R(K_{DP}) algorithm is the best option, although it is not totally immune to hail contamination.

Examination of raindrops' shape shows good agreement with the Pruppacher -Pitter equilibrium relation for stratiform events. For most convective events accompanied by gusty winds estimated shapes seem to be corrupted by local wind disturbances caused by the disdrometer itself.

F3-5
1500

POLARIMETRIC UPGRADE CONSIDERATIONS FOR NEXRAD

R. Doviak,[a] V. Bringi,[b] A. Ryzhkov,[c] A. Zahrai,[a] D. Zrnic[a]
[a] National Severe Storms Laboratory
[b] Colorado State University
[c] University of Oklahoma's CIMMS

Currently, the National Weather Service (NWS) and the National Severe Storms Laboratory (NSSL), are engaged in a project to upgrade NEXRAD (WSR-88D) to meet new requirements and to respond, in a cost effective manner, to advances in meteorological science and technology. The NWS provided radar components that made possible the assembly of a WSR-88D for research and enhancement of the weather service. This R&D radar, located on the grounds of the NSSL, is accessible to researchers to test and evaluate new ideas in hardware and software which have potential for implementation on the network of operational radars.

This paper reports on the steps taken by the NSSL to (1) develop open system hardware to facilitate upgrades, and (2) improve identification of the type of precipitation and its quantitative measure. An engineering evaluation is made to determine if the WSR-88D antenna with minimum modification could be used in a polarimetric mode. The secondary radiation patterns with a new dual port feed have low sidelobe levels and are well matched in the main and side lobes. The contours of the horizontal (H) and vertical (V) gain, where the antenna gain relative to the on-axis gain is larger than -20 dB, agree to within ±1 dB.

Considerations for the choice of polarimetric basis and design options are described. Although the circular basis can provide estimates of specific differential phase (K_{DP}) without switching the transmitted polarization, these estimates are corrupted in light rain. A polarimetric scheme employing simultaneous transmission of H and V polarized waves is suggested for the WSR-88D; this approach requires one transmitter and two receivers, and eliminates an expensive high power microwave switch. Theoretical considerations of feed alignment, canting, and backscatter depolarization suggest that simultaneous transmission of H and V signals would not be detrimental to measurements of K_{DP}, the principal polarimetric parameter which should lead to improved rainfall measurements. Overall, differential reflectivity Z_{DR} is much more affected by simultaneous transmission than the other polarimetric parameters. Experiments with the CSU-CHILL radar are performed to compare polarimetric variables obtained with alternate and simultaneous transmissions of H, V waves.

F3-6
1540

SIGNAL FADING ON A POINT-TO-POINT MICROWAVE LINK

A.R. Webster and H Yin,
The University of Western Ontario,
London, Ontario. N6A 5B9.

Experimental measurements have been made for a number of years on a 51 km line-of-sight microwave link. The main thrust of the observations has been to separate individual components in a multipath propagation scenario using a vertical wide aperture array at the receiving end of the link. From this, manipulation of the complex amplitude measured at each of the 16 equally spaced elements allows resolution ~ 0.1^0 in angle-of-arrival to be attained. Additionally, the amplitude of the signal arriving at the receiver is monitored on a separate reference channel. All of the receiving elements are sampled within an interval of about 50ms repeated continuously at I second. intervals. The system operates at a frequency of 16.65 GHz.

These angle-of arrival measurements have allowed considerable insight into the mechanisms involved in signal fading on such a link (see A.R. Webster, *Radio Science*, 32, 231-238, 1997). Significant fading persists over the months June to September inclusive but rapidly decreases on either side of this period. Here, emphasis is placed on the characteristics of this signal fading, including diurnal and seasonal variation of cumulative distributions of fade depth, fade duration and fade slope. It is clear that there are significant variations in all of these quantities, and in the diurnal behaviour, as the fading season progresses and these changes relate to the underlying physical processes involved. For example, the time of day of maximum fading shifts as the season advances which appears to be related to the changes in the refractive properties of the atmosphere.

F3-7
1600

EXTERNAL CALIBRATION OF MILLIMETER-WAVE CLOUD RADAR SYSTEMS

Stephen M. Sekelsky* Lihua Li Gregory A. Sadowy
Microwave Remote Sensing Laboratory,
Knowles 209C University of Massachusetts at Amherst, Amherst, MA 01002
Kenneth Sassen
Department of Meteorology,
University of Utah, Salt Lake City, UT 84112

Millimeter-wave (MMW) meteorological radars are becoming popular atmospheric research tools because they are both highly sensitive to cloud particles and extremely portable. However, because millimeter-wave components are delicate, questions arise about system calibrations. This is becoming an increasingly important issue as more and more research focuses on quantitative analysis of MMW radar data. This abstract discusses absolute calibration of millimeter-wave radar systems using a trihedral (corner) reflector, and illustrates a novel method for deriving polarimetric calibration constants using only high resolution melting layer or hail and precipitation measurements. Data collected with the University of Massachusetts 33 GHz/94 GHz Cloud Profiling Radar System (CPRS) and the University of Utah 95 GHz cloud radar are presented from the Remote Cloud Sensing Intensive Operations Period (RCS-IOP), which was held during April 1994 at the Department of Energy Atmospheric Radiation Measurement (ARM) Program Cloud and Radiation Testbed (CART) site near Lamont, OK. The CPRS system is mounted atop a precision computer controlled azimuth-over-elevation positioner. This allows repeated external calibrations using a trihedral reflector mounted on a forty foot high tower. The simple tower is designed to have a low radar cross section. The trihedral reflector has a known radar cross-section that does not require precise alignment with respect to the radar. The reflection from the trihedral reflector is large and overwhelms the residual reflection from the tower. We also show have reflections from insects near the surface affect calibration data.

Thunderstorms producing small hail and graupel were common during the RCS-IOP. Both CPRS and the Utah radar observed one hail event in which the 33 GHz radar observed localized circulation and a depolarization trail that connected the circulation to the surface where cigar shaped centimeter-long hail particles were observed. The 95 GHz radars experienced high extinction rates in the hail shaft and were unable to detect the circulation because of low signal-to-noise levels. However, the hail and preceding precipitation data were used to calibrate the polarimetric response of the Utah system, which was operating in a fully polarimetric mode alternately transmitting V and H polarized signals.

F3-8
1620

AN FM PULSE COMPRESSION 35 GHZ SCANNING CLOUD RADAR

Stephen M. Sekelsky*
Microwave Remote Sensing Laboratory,
Knowles 209C
University of Massachusetts at Amherst,
Amherst, MA 01002
James B. Mead
Quadrant Engineering Inc.
107 Sunderland Road
Amherst, MA 01002
Timothy Hiett
Air Force Research Laboratory
Hanscom AFB MA 01731

A new 35 GHz cloud radar design has been built by Quadrant Engineering for the The Weather Impact Decision Aid (WIDA) laboratory at Hanscom Air Force Base in Lexington, MA. Key features of this system include a liquid cooled 2 kW peak power 5% duty cycle Extended Interaction Klystron Amplifier, analog FM pulse compression, and a six foot diameter light-weight carbon fiber dual-polarized antenna and integral radome. A 3/4 height remote equipment rack houses a VXI-bus based data acquisition system and heat exchanger. All RF components are packaged in a liquid cooled, weather-tight enclosure. This and the antenna radome permit the radar to operate unattended in all weather conditions. The front-end is also compact and the radar can easily be attached to a pedestal for scanning.

The USAF system interlaces linear FM modulated 12.8 μsec long pulses and unmodulted 0.5 μsec pulses. Echoes from the 12.8 μsec pulse are routed through a surface acoustic wave (SAW) compression filter in the receiver, which results in a 13 dB gain in sensitivity with respect to the 0.5 μsec pulse mode. While the FM pulse mode offers improved sensitivity to high clouds, this mode cannot measure targets closer than 2km, and range-sidelobes, which are not present in the standard 0.5 μsec pulse mode, sometimes introduce artifacts.

Data from the new system and from the University of Massachusetts Cloud Profiling Radar System (CPRS) are presented from a side-by-side comparison. The purpose of this test is to compare system sensitivities, calibrations, and to assess the effects of range-sidelobes from the USAF system compression mode on different Doppler moments.

F3-9
1640

EXTRACTION OF RAIN PARAMETERS FROM CLUTTER ECHOES

David A. de Wolf*)
International Research Centre for Telecommunications-transmission and Radar
Dept. of Information Technology & Systems
Delft University of Technology
The Netherlands

The purpose of this work is to determine the extent to which the rainfall rate can be determined by a radar with good Doppler- and polarization-discerning capabilities from pre-determined clutter echoes. Such echoes are to be measured before and during intervening rainfall. The signal received after reflections then is weakened by cumulative attenuation through the rain, and it is modified by inextricable volume backscatter from rain drops in the range cell containing the clutter echo. The rain backscatter is treated as noise

A simulation study, specifically tailored to the TU Delft Solidar radar (L.P.Ligthart, L.R.Nieuwkerk, *IEE Proceedings-F,* 418-426, 1990) calculates the errors caused by neglect of incoherent volume backscatter from the rain drops in a range cell located at the clutter target in estimating rainfall rates between 5 and 120 mm/hr from a 1-5 km attenuation and phase change. A modified Marshall-Palmer rain drop-size distribution has been applied to draw numerical conclusions. The study concludes that both attenuation and phase change of the total received signal are required to draw conclusions about the rainfall rate. Use of both polarization and Doppler capabilities is necessary to suppress the rain backscatter "noise" and thus to ensure the desired accuracy. Meteorological conditions that enhance the possibilities will be discussed.

*) *The above work was a joint project of the guest institution noted above, and the author's home institution:* Bradley Dept. of Electrical & Computer Engineering, Virginia Tech, Blacksburg, VA 24061-0111, U.S.A.

F3-10
1700

COMPUTER MODELING OF THE OCEAN CURRENT VELOCITY MONITORING IN THE COMPLEX ENVIRONMENT

K. Naugolnykh* E. C. Shang Y. Y. Wang
University of Colorado, CIRES/
NOAA, Environmental Technology Lab.
Boulder, CO,80303

The sound signal propagation in a medium is influenced by the current what allows to extract the information on the current features as a result of the inverse problem solution. Some aspects of this problem including the different features of the acoustic monitoring of the current are considered in the present paper. The horizontal refraction, Doppler, and scintillation method are outlined and compared. The numerical simulation of the transverse current monitoring in the complex environment such as the Fram Strait is performed using the Horizontal Refraction Modal Tomography (HRMT). The simplified model of the West Spitsbergen Current profile is constructed in the framework of geostrophic approach and several empirical current profiles across the Fram Strait are considered. The sound signal propagation in such an environment transverse to the direction of the current is simulated numerically. The calculation of the modal phase difference between signals arriving along the two the paths of an acoustic interferometer due to horizontal refraction of the sound in the presence of the water current is made for the sound signal frequencies 20-200 Hz and different sound source depth. It was demonstrated that the measurable modal phase difference in a range of 80 -160 degrees can be expected for the averaged current velocity of 0.3 m/s. At a higher frequency of the sound signal the sensitivity of the HRTM increases but the space coherency decreases so the optimal frequency has to be chosen. The strong mode coupling effect presented in such a complex environment when only the well-excited mode used could be diminished by using the signals propagating along the closed paths.

Session G/H4, 1335-Wed., ECCR265
RADAR OBSERVATIONS OF METEORS
Chairperson: John Mathews (Pennsylvania State Univ.)

G/H4-1
1340

THREE-DIMENSIONAL HEAD ECHO CROSS SECTIONS AT 931 MHZ MEASURED BY EISCAT

G. Wannberg*
EISCAT Scientific Association
Box 812, S-981 28 Kiruna, Sweden
A. Westman A. Pellinen-Wannberg
Swedish Institute of Space Physics
Box 812, S-981 28 Kiruna, Sweden

The EISCAT UHF (931 MHz) incoherent scatter radar is at present the world's only radar capable of observing a volume of ionosphere from three directions simultaneously. It thus offers a unique possibility to determine the scattering cross sections of individual meteor head echo events as seen from three different look angles, and eventually to construct 3-D "images" of the cross section spatial distribution. By directing the two remote receiver antenna beams to intersect the vertically pointing Troms=F6 beam at a suitable altitude in= the E region, a common 2 km^3 meteor-atmosphere interaction volume, 1 km wide at the -3 dB points in the horizontal plane, is established. 13*2 μs Barker coded transmitter pulses are used to improve the SNR. Pulsing the radar at a $\geq$ 200 Hz rate ensures that any target traversing the interaction volume at a velocity $\leq$ 200 kms^{-1} will be illuminated at least once. Thus, many interstellar particles should in principle be observable. For targets on planetary orbits, the detection duty cycle approaches 100 %.

To determine a target trajectory, three components of its Doppler velocity must be measured. So far, the velocity information has been extracted by applying an inversion method to the distorted shapes of Doppler-shifted Barker coded echoes (G. Wannberg et al., Radio Sci., 31, 497-518, 1996). However, the= large number of steep gradients found in high velocity echoes makes the fitting of weak returns problematic and not very robust. For the 1998 Leonids EISCAT observations, a new raw data recording system will therefore be employed. The radar receiver second i.f. signal at 7.5 $\pm$ 1.9 MHz is digitized to 12 bits at 10 MHz sampling rate. The data stream is recorded by two DLT= drives running in parallel. Full bandwidth amplitude information from the 65 - 120= km altitude range can be recorded at PRFs of up to 300 Hz. As the ADC has two synchronous channels, the i.f. signals from both the UHF and the VHF (224= MHz) radars are recorded simultaneously, thus allowing direct comparisons of= echoes from the same target at two different **k**-vectors.

The target Doppler velocities and echo powers are determined from the raw amplitude data by an adaptive matched filter technique, thus eliminating most of the problems associated with the earlier power-domain method while lowering the system noise floor by a factor of four as compared to earlier. Some examples of time-resolved, three-dimensional head echoes derived in this manner will be presented and the implications of the observed cross section distributions for some head echo models will be highlighted.

G/H4-2
1400

A QUANTITATIVE THEORY OF RADIO-METEOR HEAD ECHO SCATTERING CROSS-SECTIONS

J. Jones and A.R. Webster,
The University of Western Ontario,
London, Ontario. N6A 5B9.

The cause of the meteor head echo has remained a puzzle for almost five decades. The most common radar echo from a meteor train is the so-called "body" echo from one or more specular reflecting points somewhere along the cylindrical ionised train. In the case of short-lived underdense echoes the reflection is from a single specular point but for long duration echoes several such reflecting points may form as the result of distortion of the train by upper atmospheric winds. Occasionally another kind of echo is observed which appears to arise from a moving ball of ionisation surrounding the meteoroid. This "head" echo which normally precedes a more usual long-enduring echo by a fraction of a second, has historical significance in that it was used by Hey et al (1947) at the birth of radar meteor astronomy to determine the speed of a meteor belonging to the 1946 Giacobinid shower.

A Monte-Carlo simulation of the evaporation of atoms from the meteoroid combined with the latest estimates of ionizing probability of those atoms enables the size of the plasma cloud at the head of a meteor train to be estimated. The scattering cross-section of this cloud is calculated and is shown to be in good agreement with both VHF reported by Jones and Webster (1991) and UHF observations by Mathews et al(1997).

We are optimistic about the essential validity of the theory but recognise that there are many details to be sorted out. One very important task is to determine the scattering cross-sections for the tear-drop-shaped critically dense region which develops at the lower heights. We need also to explain the significant differences between showers over and above what would be expected on the basis of speed

G/H4-3
1420

THE RADAR METEOR SCATTERING PROCESS RE-EXAMINED: PLASMA PROCESSES AND RECENT ARECIBO RESULTS

J. D. Mathews* D. Janches
Communication and Space Sciences Laboratory
316 EE East
The Pennsylvania State University
University Park, PA, 16802
Q. -H. Zhou
Arecibo Observatory
Box 995
Arecibo, Puerto Rico, 00613
D. D. Meisel
Department of Physics and Astronomy
1 College Circle
SUNY Geneseo
Geneseo, NY, 16802

The traditional interpretation of HF/VHF radar scattering from meteor trails, that are oriented perpendicular to the radar beam-axis at closest approach, has been in terms of under/overdense scattering conceptually paralleling optical thin or thick regimes, respectively. This traditional geometry yields a large scattering cross-section across the Fresnel zone as that segment of the trail scatters nearly in-phase while under/overdense trails are largely distinguished by trail lifetime with overdense trails having a relatively long duration [Meisel and Richardson, Statistical properties of meteors from a simple, passive forward scatter system, Planet. Space Sci., in press, 1998]. Localized scattering from the immediate region of the meteoroid – the enigmatic head-echo – is occasionally seen by the classical meteor radars and has never been satisfactorily explained except to conclude that the head-echo moves at expected meteoroid speeds and its radar visibility is substantially different from that of the trail-echo. Recent V/UHF radar observations of head/trail-echoes at Arecibo Observatory have provided new insight into the scattering mechanism. Doppler studies of nearly "down-the-beam" meteors using the UHF (430 MHz) radar demonstrates that the head-echo radar scattering region (the electrons, that scatter the incident radar signal, and associated ions) is moving with the speed of the meteoroid as determined by the range/time trajectory of the meteor. The VHF (46.8 MHz) radar sees both head-echoes and non-classical (the meteor trajectory is clearly not perpendicular to the beam-axis) trail-echoes. Given the Doppler results, we conclude that the meteoroid interaction with the atmosphere generates a (non-equilibrium) plasma that initially travels with the meteoroid (a plasma beam) but through interaction with the atmosphere slows and becomes the (thermalized) plasma-trail while undergoing progressive diffusion and recombination. Within this scenario we discuss various plasma issues including under/overdense interpretation of trail/head-echoes. We also discuss the head-echo scattering mechanism and conclude that the UHF radar head-echo arises from coherent scattering from the N electrons in the immediate vicinity of the meteoroid giving rise to a backscattering cross-section equal to $4\pi N^2 r_e$ where r_e is the classical electron radius. The UHF radar result is then extended to the VHF and HF radar cases. Finally, we discuss possible observational approaches to resolving the issues raised.

G/H4-4
1440

ANTENNA POLARIZATION EFFECTS ON METEOR FORWARD SCATTER PERFORMANCE

A.R. Webster, J. Jones, K.J. Ellis and S-R Chung,
The University of Western Ontario,
London, Ontario. N6A 5B9.

Meteor forward-scatter has been, and is being, used as a means of communication in which "bursts" of information are sent between fixed points separated by distances in the order of several hundred kilometres up to a maximum of about 2000 km. Additionally, such systems can be used to study the statistics of such things as the rate of influx of meteoroids into the atmosphere and the physics of the meteor formation process.

In most instances, Yagi type antennas are used and the preference seems to have been for horizontal orientation of the elements comprising the antenna. In some applications, there is a practical advantage in using antennas which have their elements arranged vertically.

An experimental study of the performance of a long range forward scatter system using both horizontally and vertically oriented antennas has been conducted. This link spanned a distance of 1343 km between Sackville NB and London ON in Canada and the system operated at a frequency of 49.88 MHz. The results obtained so far suggest that there is no inherent disadvantage in the use of vertical rather than horizontal antennas in terms of echo rates, durations or signal strength statistics. Further, there are significant cross-polarization effects resulting from the geometry of the system and these are discussed. Although Faraday rotation can cause such cross polarization effects, depending on the time of day and the layout of the system, it is not felt to be a major cause here. Nevertheless, consideration does have to be given to this process especially at lower frequencies and during day-time operation.

G/H4-5
1500

ARECIBO 430 MHZ RADAR INSTANTANEOUS DOPPLER VELOCITY MEASUREMENTS OF MICROMETEORS

D. Janches* J. D. Mathews
Communication and Space Sciences Laboratory
301 EE East
The Pennsylvania State University
University Park, PA, 16802
Q. -H. Zhou
Arecibo Observatory
Box 995
Arecibo, Puerto Rico, 00613
V. S. Getman
Communication and Space Sciences Laboratory
301 EE East
The Pennsylvania State University
University Park, PA, 16802
D. D. Meisel
Department of Physics and Astronomy
1 College Circle
SUNY Geneseo
Geneseo, NY, 16802

The 430 MHz narrow-beam radar located at Arecibo Observatory (AO) in Puerto Rico has been routinely used in the multi-pulse, high-resolution (150 m and 1 ms range and time resolutions, respectively) meteor observation mode since 1995 to study the November Leonids shower period [Janches et al., URSI, January 1998]. Velocities from the altitude-time trajectory of the head-echo – the leading edge of the nearly down-the-beam meteor return – are obtained when the trajectories have sufficent duration and magnitude. Additionally, in-phase and quadrature voltages are recorded allowing instantaneous pulse-to-pulse Doppler speed estimates of the head-echo (Janches et al., Science, submitted, 1998). The trajectory-based and Doppler velocities are found to agree very well thus proving that the head-echo originates from scattering from electrons within the plasma traveling with the meteoroid. In many cases, decelarations can also be measured and hence masses can be inferred for the case of low mass loss. These masses – of order 1 microgram – agree with those obtained by considering the flux of meteors with the small-volume Arecibo beam [Mathews et al., ICARUS, 126, 157-169, 1997]. These detections represent the first direct and accurate Doppler measurements of radar micrometeor radial velocities and micrometeor decelerations.

We present the Dopper speed/deceleration results from the observations performed during the 1995 and 1997 Leonids shower period as well as (hopefully) preliminary results from the 1998 Leonids period. During the 1995/97 observations more than 1000 events were detected each night yielding of order of 6-10 events per minute at the peak of the observation over the 88-102/105 km altitude region. The velocities detected range between a few kilometers per sec for those events with large components of their velocity across the beam to maximum speeds of the order of 70 km/sec. Decelerations ranging between 0-60 km/sec^2 were measured resulting in meteoroid mass estimates of order of 10-100 micrograms.

G/H4-6
1540

NARROW BEAM METEOR RADAR RESULTS FROM CHRISTMAS ISLAND

S.K. Avery* J. L. Chang D. Thorsen
CIRES
University of Colorado
Boulder, CO 80309

The Christmas Island meteor radar is a narrow beam system that utilizes a wind profiler combined with a meteor echo detection and collection system (MEDAC). In 1993 the wind profiler was upgraded to include five antenna beam directions in a coplanar configuration. This new configuration allowed for the determination of horizontal and vertical motions without making any assumptions about the magnitude of the vertical motions as was done in past calculations. First results demonstrated that the vertical motion deduced from the co-planar beams had a large diurnal component that signficantly contaminated the horizontal wind calculation. When this vertical motion was taken into account, the horizontal wind calculations were more in agreement with co-located MF wind measurements.

The analysis of the vertical motions has now been extended to a full year of data. Results demonstrate that the diurnal vertical motion is robust and consistent throughout the year. It has been suggested that the vertical motion is due to the influence of strong electric fields on the ionized meteor trails. In particular, two-stream plasma instabilities may be triggered that propagate along the meteor trail and that the vertical motions are associated with the movement of these instabilities. The preferred scale of these instabilities seems to correspond to the Bragg scatter wavelength of the radar which reinforces the arguement for the instability theory. The presence of strong electric fields in the mesopause region is still open to question, particularly since the antenna beams are not directed perpendicular to the electrojet at Christmas Island.

This presentation will show the latest results from the co-planar beam analysis as well as discuss potential sources for the observed vertical motions. Future Christmas Island work would ideally include the installation of an interferometer in order to more precisely locate the echo returns.

G/H4-7
1600

A STUDY OF METEOR ECHOES AT HF USING THE BEAR LAKE DYNASONDE*

F. T. Berkey* C. S. Fish M. J. Taylor L. C. Gardner
Space Dynamics Laboratory
Utah State University
Logan, UT 84322-4245

The occurrence of short-lived sporadic E (Es) events at rates up to several per hour have been observed in ionograms recorded by the NOAA dynasonde operated at Utah State University's Bear Lake Observatory (41.9=B0N, 111.4=B0W). Because these Es events tend to occur predominantly between local midnight and early afternoon, have a wide radio bandwidth, and occur at ranges ¡150 km, a meteoric origin is assumed. The database from which this study has been derived is comprised of synoptic ionospheric soundings recorded in the dynasonde B-mode (J.W. Wright and M.L.V. Pitteway, *Radio Sci.*, **14**, 815-825, 1979), acquired at five minute intervals. The soundings sample discrete frequencies over a radio bandwidth of 1.6 to 12 MHz (8 MHz) during daytime (nighttime). Our B-mode sounding pattern is configured such that the ionogram is acquired over an interval of =89100 sec. While many Es events are very short-lived and detected only over a narrow frequency range, numerous events exhibiting wide radio bandwidths (4-5 MHz) have been observed.

Conventional meteor radar systems typically operate in the VHF range, although several studies have been conducted using HF radars, where the duration of the echoes is much longer (D.L. Steel and W.G. Elford,*J. Atmos. Terr. Phys.*,**53** 409-417, 1991). While direct reflections from individual meteor ionization trains are not uncommon in vertical incidence HF sounding, relatively few reports have appeared in the literature. The variation of Es activity with meteoric flux has been studied using ionosonde data from three sites (J.W. Wright, *J. Geophys. Res.*,**72**, 4821-4829, 1967).

In this paper, we utilize the full vector capabilities of the dynasonde to derive meteor echo amplitude, spatial location, height distribution, and temporal duration as a function of radio frequency. We will also present examples of meteors detected concurrently with a multispectral airglow imager also operated at the Bear Lake Observatory. In at least one case, the vapor trail created by a meteor was visible for =8930 min (in the sodium emission).

* Supported by the National Science Foundation, Office of Polar Programs and Division of Atmospheric Sciences.

G/H4-8 1620 KWAJALEIN MISSILE RANGE VHF METEOR SHOWER CHARACTERIZATION

S. Close, S. M. Hunt, M. J. Minardi
MIT Lincoln Laboratory
244 Wood Street
Lexington MA, 02173

F. M. McKeen
Raytheon Range Systems Engineering
P.O. Box 1706
APO AP 96555

During the peak hours of the Perseids meteor shower, which occurred August 13, 1998, the ARPA Long Range Tracking and Instrumentation Radar's (ALTAIR) high sensitivity and VHF operating frequency were utilized to determine the capability of collecting meteor data. Both head echoes and ionized trail data were collected. The Perseids data collection was very successful (Figure 1), and provided a good characterization of the attainable data products using present ALTAIR capabilities. Analysis and reduction of the Perseids data proved the ALTAIR system capable of detecting both meteor head and ionized trail phenomena in the E-region of the ionosphere. An explanation of the techniques used to collect the data for the Perseids meteor shower will be presented. The determination of position, velocity, and radar cross section of both meteor head and ionized trail data will also be presented.

ALTAIR's principal function is to act as a contributing sensor in the US Space Command satellite tracking network. The ALTAIR VHF (158 MHz) radar system has high-power (5 MW peak, 60 kW average), a narrow beam (2.5° half-power beam width), and a 150' diameter mechanically steered dish. For the Perseids measurements, ALTAIR transmitted right circular polarized energy and recorded left circular with a range resolution of 75 meters. Azimuth and elevation difference channel data were also measured, which allow the determination of target position in three dimensions. ALTAIR has a dual frequency capability and also operates in the UHF band (422 MHz). ALTAIR can reliably detect a –70 dBsm VHF target and a –80 dBsm UHF target at a range of 100 km.

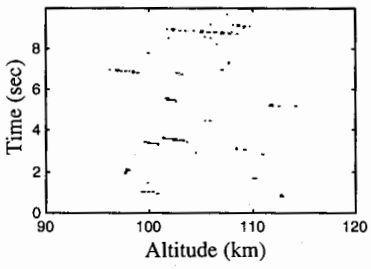

Figure 1. A 10 second sample of ALTAIR data illustrating several meteor head echoes observed during the Perseids meteor shower.

Prepared for the Department of the Army under Air Force Contract F19628-95-C-0002. Opinions, interpretations, conclusions, and recommendations are those of the authors and are not necessarily endorsed by the United States Air Force or Army.

G/H4-9
1640

INCOHERENT SCATTER RADAR STUDY OF IMPACT OF METEORIC INFLUX OF E-REGION INIOZATION

Q. H. Zhou*
Arecibo Observatory
HC3 Box 53995
Arecibo, PR 00612
J. D. Mathews Q. N. Zhou
Communications and Space Sciences Laboratory
The Pennsylvania State University
Unversity Park, PA 16802

The nocturnal E-region are mainly composed of metallic ions, which are known to originate from meteoric deposition. However, whether meteor showers have a significant effect on the E-region ionization remains open. Baggaley and Steel [Planet. Spa. Sci., 32, 1533-1539, 1984], using over thirty-year ionosonde data, found there were no significant correlation between meteor influx and sporadic E occurrence in the southern hemisphere. On the other hand, Grebowsky et al. [J. Atmos. Terr. Phys., 60, 607-615, 1998], using 40 rocket flight data, found that meteor showers do have a significant impact on the average ionosphere composition. Further, these authors found that the metallic layer peak altitude depends on the specific shower. We present Arecibo incoherent scatter radar data collected over the past 12 years totaling around 250 days to examine possible meteor shower effect on E-region column content as well as on layer characteristics. Although most of the 250 days come from the World Day observations and th us are more or less randomly distributed throughout the year, observations have also been made for a few particularly strong meteor showers such as the 1993 Perseids and the 1997 Leonids. The Arecibo electron density data typically covers all the altitudes from 60 km to 500 km with a height resolution of 600 m or 150 m and a time resolution of about one minute. Preliminary analysis indicates that strong causal relation between meteoric influx and nocturnal E-region ionization does not exist. We hope to be able to present results from the much anticipated 1998 Leonids as well.

G/H4-10
1700

THE INFLUENCE OF AURORA ON METEORIC METAL CHEMISTRY

C. J. Heinselman
Radio Science and Engineering Division
SRI International
Menlo Park, CA 94025

Improved models of the gas phase chemistry of metallic species of meteoric origin have recently been published. In particular, a model of the chemistry of iron was presented by Helmer et al (*J. Geophys Res*, **103**, 10913-10925, 1998), and models for sodium chemistry were published by Cox and Plane (*J. Geophys Res*, **103**, 6349-6359, 1998) and Plane et al (*J. Geophys Res*, **103**, 6381-6389, 1998). These models describe the reactions and reaction rates that distribute the available metallic atoms among various chemical species. They include the chemistry involving a number of minor consituents (e.g., O_3, H_2O, and CO_2) but specifically exclude heterogeneous chemistry involving dust particles. None the less, the chemical models do a good job of reproducing measured altitude profiles of Fe and Na.

Utilizing these chemical models, we make a number of specific time-resolved predictions about the influence of auroral ionization on the balance of the various constituents. In particular, we consider the impact of high time-varying concentrations of NO^+ and O_2^+ on the concentrations of Fe, Fe^+, and Na. These species are particularly important because their concentrations are readily measurable by available techniques. NO^+ and O_2^+ can be measured in a range and time resolved manner with the use of an incoherent scatter radar (ISR). The neutral iron and sodium concentrations have, similarly, long been measured by resonance lidar systems. The concentration of Fe^+ can also be inferred from ISR measurements. It should thus be possible to test aspects of the chemical models from a high latitude location.

In addition to the model predictions, several examples of measurements of these processes will be presented. The Sondrestrom Facility, at 74 degrees invariant latitude, includes both an incoherent scatter radar and a resonance sodium lidar. These instruments have been operated for a number of campaigns during the past year and several events have been observed by both instruments. Specific measurements to be presented include the apparent ionization of recently deposited neutral material in a meteor trail. Data will also be presented indicating the ionization of neutral sodium via charge exchange with auroral ionization products.

J5-1
1340

THE LARGE MILLIMETER TELESCOPE (LMT)

Jacob W.M. Baars
LMT Project - 815 Lederle Graduate Research Center
University of Massachusetts, Amherst, MA 01003

The LMT is a 50 m diameter telescope for operation in the wavelength range of 1 to 4 mm from a high mountain site in central Mexico. The telescope is designed to address fundamental questions about the origin and formation of galaxies, clusters of galaxies as well as stars and planets. It is a joint project of the Mexican Instituto Nacional de Astrofisica, Optica y Electronica (INAOE) in Tonantzintla, Puebla and the University of Massachusetts at Amherst, MA, USA. The telescope is in the Detailed Design phase and completion of the installation at the site is scheduled for the middle of 2001. The Design Contractor is MAN Technologie of Gustavsburg, Germany.

The alt-azimuth telescope employs a paraboloidal reflector, composed of 5 rings of panel units, the positions of which can be actively controlled by actuators and a real-time measuring system. The reflector specification under operational conditions is 75 micrometer. The pointing will use a laser based active control system to achieve the specified pointing and tracking accuracy of 0.6". The subreflector of 2.6 m diameter will be capable of beam chopping and will also be adjusted in position for fast pointing corrections. The telescope has a large Nasmyth receiver room, directly behind the main reflector. The flexibility of this room will be exploited to create an observing environment in which easy and remotely controlled change of receivers will enable us to apply queue observing scheduling, thereby taking full advantage of the best observing conditions and providing the largest number of scientific programs with good data.

The LMT will have powerful initial facility instrumentation. A 32-pixel array of MMIC amplifiers covers the 85-115 GHz band with an instantaneous bandwidth of 15 GHz, followed by a large digital correlator. The first half of this system is presently in use at the =46CRAO 14 m telescope in Massachusetts. At 1.2 mm there will be a 144-pixel Bolometer array for high sensitivity continuum mapping. A partial version of this system will be used on the CSO in Hawaii this winter. These Systems are being developed at the UMass. An SJS-receiver for the 1.3 mm band will be built at INAOE, as well as the equipment for the holographic measurement of the primary surface.

The site for the LMT is Cerro la Negra, a 4680 m high extinct volcano in central Mexico, less than two hours drive from the offices of INAOE. Weather monitoring and opacity measurements with a 230 GHz radiometer indicate excellent conditions for millimeter wavelength observations during most of the year. The latitude of 19 degrees is favourable for viewing the Southern sky.

We shall present the basic performance parameters of the LMT, the current status of the Design Effort and the planning for construction.

J5-2
1400

ATMOSPHERIC EFFECTS ON THE METROLOGY SYSTEM FOR THE LARGE MILLIMETER TELESCOPE

Read Predmore*
Five College Radio Astronomy Observatory
619 Lederle GRC
University of Massachusetts
Amherst, MA 01003

The Large Millimeter Telescope (LMT) is a $50m$ diameter astronomical instrument for use primarily at $\lambda 1300\ \mu m$ (230 GHz). The resulting technical specifications for observations at these wavelengths are very stringent. The overall rms surface specification is $74\mu m$ in winds up to $10m/s$, with a goal of $69\mu m$.

At a wavelength of $1300\mu m$, the LMT beamwidth is 6 arcsec. The rms pointing specification for the LMT contractor is < 2 arcsec for absolute pointing. The LMT Project is responsible for the Precision Pointing System with a stability of < 0.6 arcsec over 2 hours, within $10°$ of an astronomical calibration source.

The metrology system to achieve the 0.6 arcsec pointing stability has four major components. The first laser system measures the overall figure of the $50m$ diameter primary to determine its orientation and deformations from the desired parabola. The orientation of the parabola will be determined to < 0.4 arcsec or < 2 parts-per-million. The second laser system aligns the $2.5m$ diameter secondary and the receiver optics with respect to the primary. In order to limit the contribution of the secondary misalignments to the pointing error budget, the secondary must be laterally positioned to $\pm 17\mu m$ and the tilt of the secondary restricted to ± 1.7 arcsec. The third system is an optical and near-infrared guide telescope for use at night and possibly during the day on the brightest stars. The fourth system is a laser system to relate the primary orientation with respect to the ground and would be used when the guide telescope is not usable.

Atmospheric effects such turbulence and temperature gradients will limit the effectiveness of these laser metrology systems. Measurements of these atmospheric effects and an analysis of their influence on the overall pointing error budget, as well as preliminary evaluations of the guide telescope concept will be presented.

J5-3
1420

PREDICTING THE EFFECTS OF ANOMALOUS REFRACTION ON THE TELESCOPE POINT SPREAD FUNCTION: A POSSIBLE COMPENSATING TECHNIQUE

L. Olmi
LMT/GTM Project and FCRAO
630 LGRC, University of Massachusetts
Amherst, MA 01003, USA

Radio seeing effects on cm and mm wavelength interferometers are now reasonably well known. These are a consequence of the inhomogeneously distributed atmospheric water vapor which can cause spatial and temporal variations in the optical path length of radio waves. Therefore, phase fluctuations on a two-element interferometer occurr whenever the columns of water vapor above them are different.

On the other hand, radio seeing shows up on filled-aperture telescopes as an "Anomalous Refraction" (AR), i.e. an apparent displacement of a radio source from its true position, with varying pointing shifts (a few arcsec to $> 10'' - 30''$) and time scales (a few sec to $\sim$ 30 sec). However, little is known, from both an experimental and theoretical standpoint, about how the pathlength differences across the aperture plane of a *radio* telescope distort the incoming wavefront, thus affecting the angular resolution and sensitivity of astronomical observations.

In fact, if for small- to medium-size ($D < 20$ m) mm-wave antennas the main AR effect is a pointing shift, this may no longer be entirely true for large telescopes ($D > 30$ m), where the diameter to Fried parameter ratio, $D/r_\circ(\lambda)$, may become close to or larger than 1. This is the case, e.g., of the *"Large Millimeter Telescope"* (LMT), a 50 m diameter Cassegrain telescope that will be working in the $1-3$ mm wavelength range. Because the LMT will be using focal-plane arrays, it is of interest to study the atmospherically distorted shape of the telescopic Point Spread Function (PSF) and the resulting "cross-talk" among adjacent pixels.

The atmospherically aberrated PSF can be studied by assuming that the effects of the irregular medium above the telescope are equivalent and can be modeled by a two-dimensional phase screen located in the aperture plane of the antenna. Simulations of the corrupted wavefront can be made in several ways but, following a technique in use at optical wavelengths, the polynomials of Zernike can be used to represent the wavefront within a circular aperture. Phase screens can be generated that contain the correct statistical (Kolmogorov) distribution and can then be moved past the aperture plane at a given velocity, namely the wind speed component parallel to the aperture plane. Several examples of phase screens and aberrated PSFs are shown and a possible compensating scheme making use of an *aperture-plane* array is proposed.

J/E1-1
1440

CURRENT ISSUES IN SPECTRUM MANAGEMENT AFFECTING RADIO ASTRONOMY AND REMOTE SENSING

P. G. Steffes
School of Electrical and Computer Engineering
Georgia Institute of Technology
Atlanta, GA 30332-0250

The National Research Council Committee on Radio Frequencies (NRC/CORF) serves to coordinate and define the U.S. research community's needs for passive radio frequency allocations and assignments in areas such as space science, radio astronomy, meteorology, oceanography life sciences, and remote sensing. Over the past year, CORF has considered a number of frequency allocation issues which involve potential interference to the passive services, including proposals by the FCC to allocate frequencies in the 47.2-48.2 GHz band for use by a new communications service involving stratospheric balloons, or high altitude platforms (HAP's), and proposals for new allocations for downlinks from LEO satellites in frequency bands from 6700-7075 MHz and 15.43-15.63 GHz. Since all of these allocations are adjacent to frequencies currently allocated to the Radio Astronomy Service (RAS), the potential for harmful interference to radio astronomy from relatively weak out-of-band emissions from these spaceborne transmitters will be very substantial. While new technological approaches may reduce the level of spurious emissions from space-qualified transmitters in the future, the required suppression (more than 90 dB over a few MHz) will be hard to achieve, or even accurately measure.

Further rulemaking in the millimeter-wavelength spectrum has continued to present risks for potential harmful interference at frequencies above 40 GHz. Studies of systems such as 77 GHz vehicle radar collision avoidance systems have shown potential harmful interference to radio telescopes operating at their third harmonic, a strongly used radio astronomy band.

Results of these studies will be presented, in addition to a general discussion of topics of concern to scientific users of passive allocations.

J/E1-2
1500

NRAO OBSERVATIONS OF AN IRIDIUM SATELLITE AT 1610.6 - 1613.8 MHz

M. M. McKinnon
National Radio Astronomy Observatory
Green Bank, WV 24944

The National Radio Astronomy Observatory (NRAO) made observations of an Iridium satellite in February and March of 1998 to measure the spectral power flux density (SPFD) of the spurious emissions produced by the satellite downlink within the radio astronomy observing band at 1610.6 - 1613.8 MHz. The results of the observations were compared with the interference thresholds that are defined in Recommendation ITU-R RA.769 and agreed upon in a memorandum of understanding between NRAO and Motorola, the satellite operator.

The observations were made with a 3.6 meter antenna in Tucson, Arizona, one of the 25 meter antennas in the Very Large Array (VLA) near Socorro, New Mexico, and the 140-Foot Telescope in Green Bank, West Virginia. The small antenna was able to track the satellite, but the two large antennas were set for beam transit observations because they could not move fast enough to track the satellite. The receivers for the large antennas were modified to avoid amplifier saturation by the satellite downlink, and special observing techniques and data analysis methods were developed to minimize the contribution to the SPFD from other sources of interference.

Spurious emissions attributed to satellite-intrinsic intermodulations of the frequency channels in the downlink were detected in the radio astronomy band during the observations. The spurious emissions produced with the downlink's voice channels appear as a continuum of emission across the radio astronomy band. The measured SPFDs of these emissions do not exceed the interference thresholds agreed upon in the NRAO/Motorola memorandum of understanding. The spurious emissions produced with the downlink's broadcast channels are a series of sharp spectral peaks spaced at 330 kHz intervals. The SPFDs of these emissions exceed the interference threshold for the Green Bank site.

J/E1-3
1540

EXCISION OF RADIO INTERFERENCE FROM OBSERVATIONS OF HYDROGEN ABSORPTION LINES FROM HIGHLY REDSHIFTED QUASARS

M.C. Aller*
Beebe Hall, Wellesley College
106 Central Street
Wellesley, MA 02481-8281
M. Davis T. Ghosh C. Salter
Arecibo Observatory
HC3 Box 53995
Arecibo, PR 00612

An observational program at the Arecibo Radio Observatory to detect HI absorption in the host galaxies of quasars with redshifts between 2.25 and 2.37 was hampered by significant man-made interference. The large frequency shift places the observing frequency near 430 MHz, an unprotected radio band. This presentation describes the results of applying an interference removal algorithm which depends upon the temporal variability of the received interference. Observations using primarily the 430 MHz line-feed of the Arecibo telescope were conducted on three days during July 1998. Nine radio-loud quasars were observed in two polarizations in a series of 4 one-minute integrations on-source alternated with 4 one-minute integrations off-source tracking along the same section of the sky. Observations were obtained with a 2048 channel spectrometer using a wide bandwidth of 12.5 MHZ and a narrow bandwidth of 3.125 MHz.

The radio frequency interference (RFI) found in the spectra had one or more of three characteristics: narrow-band rapid frequency gradients, time variability or polarization. Preliminary calculations indicate that for the individual one-minute integrations on the 430 MHz line feed,only 10 to 15 percent of the spectra exhibit RFI. Following the preliminary removal of narrow-band spikes, the remaining data were examined for time variability, which should not exist in HI absorption. Finally, the spectra were examined for polarization features where an apparent absorption feature existed in only one polarization. Since the HI absorption should not be polarized, such features can be assumed to be RFI. Preliminary calculations indicate that despite large amounts of RFI in the raw data, the noise per channel in the excised data was reduced by a factor of 10 and is within 30 percent of what is theoretically predicted from the system noise. Approximately 90 percent of the spectral bins are free of RFI. Although no hydrogen absorption was detected in these initial observations, we expect that longer periods of integration coupled with this interference excision method will lead to a good probability for the detection of high redshift hydrogen absorption lines.

J/E1-4
1600

RFI EXCISION USING THE DISCRETE WAVELET TRANSFORM

I. R. Linscott, S. Maslakovic, M. Oslick, and J. D. Twicken
STARLab, Radioscience Group
Stanford University
Stanford, CA 94305

We have developed a library based method for the selection of optimum wavelet bases for the representation and subsequent excision of common types of RFI. The method involves prior construction of a library of wavelets with minimum mutual projections as well as compact representation of RFI, based on minimum entropy measures. A strength of this approach is the ability to design wavelets that produce compact representations for whole classes of RFI waveforms. By collecting together a group of such wavelets, each associated with a common type of RFI, into a library then waveforms that are contaminated with common forms of interference can be treated. The treatment consists of taking the discrete wavelet transform (DWT) of an RFI contaminated signal, using a wavelet selected from the library. Next the largest DWT coefficients are eliminated and then the inverse DWT is computed. A version of the original signal is thus obtained with the RFI contaminant excised. If the original signal is not in the same waveform class as the RFI, and the selected wavelet is a good match to the RFI, then the excised version obtained by these means is a high fidelity estimate of the original signal. The success of this method depends on a strategy for selecting a wavelet that is a good match to the RFI but not a good match to the original signal. For if the original signal is not represented with any small subset of wavelet domain coefficients it will therefore not suffer significant degradation in the excision process. This presentation will discuss wavelet and library design with particular attention to optimization for compact RFI representation and wavelet selection strategies. In addition, the performance of this method will be illustrated using RFI contaminated waveforms recorded at Stanford's 45-m diameter radio telescope.

5J/E1-1620

RECENT PROGRESS IN DIGITAL ADAPTIVE INTERFERENCE CANCELING FOR RADIO ASTRONOMY

Richard F. Bradley*
NRAO
Charlottesville, VA 22903-1733
J. Richard Fisher
NRAO
Green Bank, WV 24944

Over the past few years, we have been experimenting with a temporal-based adaptive canceling technique applied to the problem of RF interference in radio astronomy. Our proof-of-concept, 12-bit digital system operates at baseband (0-1 MHz bandwidth) in the signal path between the telescope radiometer and the spectral processor. A separate antenna and receiver reference channel is processed by an adjustable-weight, nine-tap digital filter and subtracted from the primary radiometer channel to form the system output. The least-mean square (LMS) algorithm adjusts the filter tap weights in order to minimize the total power out of the canceling system thereby improving the signal-to-interference ratio. The system operates in real-time and can alter itself in response to slowly-varying changes in the characteristics of the interference.

On the Green Bank 140 foot in June 1997, we evaluated the performance of this basic system in response to actual interference consisting of well-characterized, FM broadcast signals. The canceling performance was compromised by the use of only one reference channel and a few problems related to RF shielding and analog filtering. Despite these limitations, measured interference attenuation as high as 25 dB was demonstrated.

The encouraging results from the telescope run has lead to number of recent laboratory experiments to verify the linearity and intrinsic dynamic range of our adaptive system. Canceling effectiveness was studied as a function of reference channel interference-to-noise ratio (INR) for various FM signal characteristics (power level, modulation index, etc.). Weak signal recovery in the presence of severe interference and the tracking capability of the algorithm under non-stationary conditions was explored. Based upon these measurements and corresponding software simulations, some general trends are developing that will govern the designs of future interference canceling systems. A summary of these results will be presented (see also C. Barnbaum and R. F. Bradley, *Astronomical Journal*, in press, Nov. 1998).

We are currently in the process of building a four reference channel system with the improvements suggested above. With this system we plan to study the effects of spatial polarization on interference canceling through a series of field experiments set for Fall of 1998. A progress report and initial results will be presented.

J/E1-6
1640

RADIO INTERFERENCE REDUCTION USING A CONICAL SHIELD AT THE PRIME FOCUS OF A PARABOLOID

H. D. Aller* G.E. Latimer
Department of Astronomy
830 Dennison Bldg.
University of Michigan
Ann Arbor, MI 48109-1090

This is a report on the initial results of using a truncated cone to shield the primary-focus feed horns of the University of Michigan 26-meter radio telescope in an attempt to reduce radio interference. The major function of this shield is to redirect the off-antenna response of the feed horn (which usually causes significant back side lobes, 'spill over') onto the sky in the general direction in which the antenna is pointed. The truncated cone, with a diameter of 1.25 meters at its larger end, is mounted so that the line of sight from the focus which strikes the edge of the cone hits the reflector surface approximately 20 cm from the outer edge of the reflector. In our implementation the cone extends 30 cm toward the primary reflector from the focal surface; this distance is determined by the F/D ratio of the paraboloid. The opening angle of the cone is determined by the criterion that rays entering from beyond the edge of the primary reflector are not reflected back to the primary focus. Diffraction effects blur the shadowing effect of the cone; the reduction of the feed horn response at the edge of the reflector (measured at 8 GHz) is a factor of 0.34. The performance costs of this shield, expressed as relative aperture efficiencies, are measured to be 0.93, 0.96, and 0.97 at 4.8, 8.0 and 14.5 GHz respectively. However, the reductions in aperture efficiencies are off set by the very significant reductionsin system temperature (measured to be 22°K at 8 GHz) resulting from the removal of ground emission associated with spillover entering the feed horn. Although this shield has very significantly reduced 'spill over' and hence reduced our system temperatures, it has apparently not, (based upon observations of control radio sources for nearly a year), dramatically reduced the sensitivity of the instrument to radio interference. We thus confirm the conclusion reached at other Radio Astronomy facilities which operate in high interference environments that signals, scattering from feed support structures, are a major origin of the interference entering the feed horn.

J/E1-7
1700

WORLDWIDE MAP OF RF BACKGROUND RADIATION AS DETECTED BY FORTE

R. S. Zuelsdorf*
Institute of Geophysics and Planetary Physics
University of California, Los Angeles
405 Hilgard Ave.
Los Angeles, CA 90024
A. Jacobson
Los Alamos National Laboratory
NIS-1
Los Alamos, NM 87545
R. J. Strangeway C. T. Russell
Institute of Geophysics and Planetary Physics
University of California, Los Angeles
405 Hilgard Ave.
Los Angeles, CA 90024

Continuous observation by the FORTE spacecraft has allowed for the production of worldwide maps displaying the background radiation emitted by RF sources in 16 different frequencies. FORTE is an 800-km orbit at 70 degrees inclination and has a 40 degree half-angle 3 dB footprint. For the greater part of 1 November 1997 to 31 March 1998, FORTE has been configured to detect radio emissions in two separate 20 MHz bands: one centered at 38 MHz, the other at 130 MHz. Here we provide maps derived from data recorded in the 8 1-MHz sub-bands in each of these 20 MHz bands. Data are based upon results recorded in the FORTE state of health. The power recorded in each of the sub-bands is reported over a period of 4 seconds (data from each band returned 2 sub-bands at a time) with every band being updated every 4 seconds. The recorded power is based upon an average of the instantaneous power received over 2.2 ms. The recorded power is affected by the attenuation setting at time of reception as well as upon the one of two antennas used to receive the signal. Data have been converted from the power received to the incident electric-field in mV/m upon the receiving antenna. The results indicate which of these 16 bands is dominated by carriers and at what strengths for the various regions of the world. For most of the bands, emissions from Europe and the eastern U.S. dominate, although the strongest sources vary with frequency.

J/E1-8
1720

ADVANCED INTERFEROMETRY APPLIED TO PRACTICAL DIRECTION FINDING AND RADIOLOCATION SYSTEMS

William A. Luther
Chief, Radiocommunication Policy Branch
International Bureau
Federal Communications Commission
2000 M Street, NW.
Washington, D.C. 20554

After a number of years of interferometry research, coupled with new advances in digital signal processing, U.S. government engineers have developed a new direction finder antenna array configuration and signal radiolocation system. Successfully applying advanced techniques, a new civilian-service, long-range interferometer network was installed in 1996 and 1997 at fourteen sites dispersed throughout the United States, including Alaska, Hawaii, and Puerto Rico. The new interferometer completely replaces all previously-used direction finders designed for use over the last eight decades by the only national, civilian radiolocation network in the United States. The new and improved interferometric system uses a number of techniques based both on a unique, minimum-element design for the desired frequency range, and on simultaneous digital signal processing in a phase-matched receiving system having eleven separate channels, one for each of the eleven elements of the antenna array. This paper explains the many improvements the new system offers over direction finders previously available, including increased reliability, as well as significant hardware, installation, and personnel resource efficiencies. The paper begins with the theory used to derive the interferometric system, leading to a description of the design chosen by the U.S. government for its LF, MF, and HF civil radiolocation purposes. Both radio frequency and processed statistical data taken using the advanced system are presented and analyzed. Bearing data is compared to that taken from the previous generation (Wullenweber) civil direction finding system. The data shows significant improvement in accuracy of signal bearing results. A patent on the advanced interferometer is pending before the United States Patent and Trademark Office.

Session B4, 0835-Thurs., ECCR151
NUMERICAL METHODS
Chairperson: S.L. Dvorak (Univ. of Arizona)

B4-1
0840

3-D Conducting Object Scattering by Using On-Surface Measured Equation of Invariance Method

Y. W. Liu*, Y. B. Gong, and K. K. Mei
Department of Electronic Engineering
City University of Hong Kong,
Tat Chee Avenue, Kowloon, Hong Kong
eeliuy@cityu.edu.hk

Since measured equation of invariance (MEI) method (K. K. Mei et al., IEEE Trans. on Ant. & Propagat., v42, 320~327, 1994) has been extended to on-surface level (J. M. Rius et al., IEEE Trans. on Magnetics, V32, 962~967, 1996, and Y. W. Liu, IEEE Microwave and Guided Wave Letters, v8, 99 - 101, 1998), problems solved is limited to 2-D conducting structures. In this summary, 2-D conducting scattering is extended to 3-D problems by means of new on-surface MEI formulations. The numerical results of a metal square plate scattering under a TM plane wave incidence is used in demonstrating the validness of the formulations.

For deriving the formulations, we start with Maxwell's equations, and obtains the simplest on-surface relations between the components of tangential scattered scalar magnetic potential and magnetic field. Therefore, the final system matrix is highly sparse in comparing with the previous on-surface MEI formulations. The highly sparse matrix allows us to save a lot of computational time and memory usage in comparing with method of moments (MoM), finite difference (FD), and finite element method (FEM). It is so important to 3-D fast electromagnetic computational problems.

In order to prove the validity of the on-surface MEI method, the 3-D scattering problem of a square perfectly conducting plate is regarded as an example to be solved. The results obtained are in good agreement with that of the MoM.

B4-2
0900

A COMPARISON OF THE ACCURACY OF THE PATH INTEGRAL TIME-DOMAIN AND FINITE-DIFFERENCE TIME-DOMAIN METHODS

Robert Nevels* Jeffrey Miller
Texas A&M University
Department of Electrical Engineering
College Station, TX 77843-3128

The Path Integral Time-Domain (PITD) method is a new numerical method for electromagnetic scattering based on a state variable propagator solution to the time domain differential form of Maxwell's equations (R. Nevels, J. Miller, and R. Miller, "The Path Integral Time-Domain Method: A New Numerical Method for Electromagnetic Scattering," *AP-S/URSI International Symposium*, Montreal, Canada, July 1997, p. 263). The similarities between PITD and the Finite-Difference Time-Domain (FDTD) methods are that both are full domain propagator methods characterized by an initial field propagating through a numerical lattice. An unusual aspect of the path integral time-domain method is that a field propagating in a homogeneous region can be simulated in the numerical lattice without error or numerical dispersion and it is unconditionally stable. For the same propagation conditions, these properties are not in general shared by the FDTD method.

In this paper we will present a comparison of the PITD, FDTD and exact scattered fields when two types of two-dimensional objects, a circular dielectric cylinder and a dielectric half-plane, are illuminated by a plane wave. In each case the numerical region will be composed of a square numerical lattice and the lattice spacing will be the same for both methods. In a square numerical lattice, curved scattering objects are not smooth but rather have a perimeter that is stair-stepped in appearance. This is because the location of all objects in the numerical region is determined by material parameters which are specified only at the individual lattice points. Even a planar object appears to be stair stepped when its surfaces do not lie in a coordinate plane of the numerical grid. Results will be presented which will show the effect of rotating the planar dielectric half-space in the numerical grid.

It will be shown that the PITD method scattering results are much more accurate than those obtained by the FDTD method. It is speculated that this is due to the nature of the equations upon which each of these numerical methods is based. The PITD method requires numerical integration while FDTD is grounded upon numerical differentiation. Differentiation tends to amplify discontinuities whereas integration is a smoothing process. The PITD method tends to smooth stair-stepped surfaces produced by numerical gridding, thus giving a more accurate scattered field.

B4-3
0920

THE EFFECT OF DIELECTRIC LOSS IN FDTD SIMULATIONS OF MICROSTRIP STRUCTURES

David C. Wittwer* Richard W. Ziolkowski
Electromagnetics Laboratory
Department of Electrical and Computer Engineering
University of Arizona
Tucson, Arizona 85721-0104

The importance of dielectric losses in planar microstrip structures is evaluated with the finite-difference time-domain (FDTD) method. This analysis was previously not possible in many FDTD simulators due to a lack of absorbing boundary conditions (ABCs) which appropriately terminate air/dielectric interfaces for which the dielectric is lossy. The newly proposed lossy two-time derivative Lorentzian material (L2TDLM) model ABC allows for these terminations and is presented and implemented here for 3D FDTD simulations.

A summary of the generalized formulation for the lossy two time-derivative Lorentz material (L2TDLM) model and its coupling to Maxwell's equations is given. To achieve a complete ABC we introduce the requisite formulation for a corner depending on three independent loss profile parameters. A formulation is introduced which reduces to the lossless case when the conductivity of the media becomes zero and which further reduces to Maxwell's equations in free space as the permittivity goes to unity and, hence, recovers the 3D TDLM ABC developed in (R. W. Ziolkowski, "Maxwellian Material Based Absorbing Boundary Conditions," to appear in a Special Issue of CMAME, Summer, 1998). It is highly desirable from a numerical implementation point of view to arrive at a formulation that has these properties. Furthermore, it is also highly convenient from an implementation point of view to have a formulation for a corner which reduces uniquely to the correct edge formulation and which further reduces uniquely to the correct face formulation with the appropriate selection of parameters. This avoids having separate formulations for each region, hence, makes the ABC very efficient to implement algorithmically and reduces the coding complexity.

The resulting FDTD simulator has been applied to several microwave structures including a microstrip low-pass filter, a microstrip branch line coupler, and a microstrip line-fed rectangular patch antenna. A summary of these simulations is given and compared with measurements. Comparisons between cases in which the substrates associated with each these structures are lossless, slightly lossy, and very lossy are made. The importance of including the loss in the prediction of the performance of these microstrip structures is emphasized.

B4-4
0940

INTEGRATING LUMPED CIRCUIT MODELS INTO FDTD SIMULATIONS

Ian Rumsey* Jason Mix Melinda Piket-May
Department of Electrical and Computer Engineering
Campus Box 425
University of Colorado
Boulder, CO 80309

As high speed systems place greater demands on electronic packaging and interconnects, numerical simulation at the package and circuit board levels before prototyping is needed to produce designs which meet stringent EMI, EMC, and signal integrity requirements. In order to model these complex systems, lumped circuit elements must be included in the electromagnetic simulation. In the FDTD method, auxiliary update equations may be used to model circuit components within the simulation space (Ciampolini et.al., *IEEE Trans. on Microwave Theory Tech.*, **vol. 44**, no. 12, Dec. 1996). Another attractive method of accomplishing this goal is to link the FDTD engine with an external circuit simulator such as SPICE. Such an interface has been developed for LC, a 3-D FDTD simulator being developed by Silicon Graphics and the University of Colorado.

The basic method for exchanging electromagnetic field quantities with circuit voltages and currents will be discussed in detail. The impact of this method on the implementation of practical circuits will be illustrated with examples of SPICE circuits fed by FDTD transmission lines. These examples will be compared with lumped circuits modeled within the FDTD simulation space where possible.

Potential applications of this technique include passive filters, transmission line matching networks, and including active elements and amplifiers in full-wave simulations. Another area of current research using this interface is the study of the electrical performance of integrated circuit packaging. The real performance of a device can be predicted by placing a SPICE model within an FDTD model of the IC package and the surrounding circuitry. Particular interest is being paid to signal integrity and feedback into the integrated circuit due to line coupling in high speed designs.

B4-5
1000

RADIATION FROM A CIRCULAR LOOP NEAR SYMMETRICALLY PLACED CONDUCTING SPHERICAL CAPS

Hakan P. Partal, Joseph R. Mautz and Ercument Arvas
Department of Electrical Engineering and Computer Science
Syracuse University, Syracuse, NY 13244

The problem considered here is that of finding the electromagnetic field produced by a circular loop antenna when it is placed near one or two perfectly conducting spherical caps. The antenna of radius a, carrying a current I is placed in the xy plane with its center located at the origin. A spherical cap of radius $b < a$ centered at the origin is placed symmetrically near the loop. This cap occupies the region defined by $\theta_b \leq \theta \leq \pi$. When $\theta_b = 0$, the cap becomes a complete sphere centered at the origin and when $\theta_b = \pi/2$, the cap is an empty hemisphere with its south pole at $z = -b$ and its rim lying in the xy plane. Similarly, we may have another spherical cap of radius $c > a$ occupying the region defined by $0 \leq \theta \leq \theta_c$. When $\theta_c = \pi$, this cap becomes a complete sphere surrounding the loop and no radiation is possible. In general, the fields in various regions are expressed in terms of infinite series and the coefficients are determined by satisfying boundary conditions at various boundaries. For the case of one complete sphere of radius $b < a$, the coefficients can be found exactly. Otherwise a point matching technique is used to find the coefficients using a simple MATLAB program. Computed results include the far-field pattern, the current distribution on the caps and the total near field. The computed fields for the case of very small caps ($\theta_b \approx \pi$ and $\theta_c \approx 0$) agree very well with the fields of the isolated loop antenna. The computed far-field results for the general case are compared with a Moment solution of the problem where the caps are approximated by triangular patches, and good agreement was observed.

B4-6
1040

RAPID ELECTROMAGNETIC ANALYSIS OF THREE-DIMENSIONAL CIRCUITS

S. Tuomey D. L. Heckmann S. L. Dvorak*
Department of Electrical and Computer Engineering
The University of Arizona, Tucson, AZ 85749

Recent advances in multi-layer insulating substrates have motivated novel designs of RF/microwave passive components which attempt to take advantage of the third dimension in order to reduce component size. An important enabling technology for the realization of such systems is an electromagnetic modeling tool capable of providing the computational efficiency necessary for design iteration in a three-dimensional conductor layout. We present a novel approach to the frequency-domain integral equation modeling of conducting structures which are embedded in a homogeneous dielectric and shielded by two perfectly-conducting ground planes. The Method of Moments (MoM) is applied to the integral equation to obtain an approximate solution.

A significant portion of the computational effort in the MoM is associated with the calculation of the elements in the impedance matrix. These elements can be represented as Sommerfeld-type integrals, which are often highly oscillatory and slowly convergent. Due to the oscillatory nature of the integrands, the integrals are very difficult to directly integrate numerically. We present a closed-form solution to these integrals, expressed in terms of rapidly-computable special functions, free from any numerical integration.

The impedance matrix elements are evaluated by writing the two-dimensional integral in polar coordinates. It has been shown that the resulting angular integral can be decomposed into terms which contain incomplete Lipschitz-Hankel integrals (ILHIs) and Bessel functions of the first kind (S.L. Dvorak and E.F. Kuester, *Int. J. Micro. and Millimeter-Wave Computer-Aided Eng.*, 1, 333-345, 1991). The ILHIs are special functions which are closely related to Bessel functions, and can be rapidly calculated using convergent and asymptotic series expansions (S.L. Dvorak and E.F. Kuester, *J. Comput. Phys.* , 87, 301-327, 1990; M.M. Mechaik and S.L. Dvorak, *Radio Sci.*, 31, 409-422, 1996). Next, the lower limit of integration on the semi-infinite integral is extended to negative infinity. The presence of the shielding conductors eliminates all branch cuts in the integrand except those associated with the Hankel functions. This allows us to solve the infinite integral using contour integration techniques (D. Heckmann, S.L. Dvorak, and A.C. Cangellaris, *6th Topical Meeting on Electrical Performance of Electronic Packaging (EPEP '97)*, San Jose, CA, October, 1997).

This novel closed-form expression for the impedance matrix elements results in matrix fill times which are orders of magnitude smaller than those associated with direct numerical integration. In this presentation, applications from its use in the design of three-dimensional circuits will be used to demonstrate its accuracy and computational efficiency.

B4-7
1100

EFFICIENT MODELING OF THE INDUCTION TOOL RESPONSE IN DEVIATED BOREHOLES AND ANISOTROPIC FORMATIONS

K. A. Michalski
Department of Electrical Engineering
Texas A & M University
College Station, TX 77843-3128

Induction logging is one of the techniques employed to obtain the conductivity profile along an oil borehole. From early 1960s, the industry-standard induction tool has been the so-called 6FF40 coil array, which comprises three receivers and three transmitters operating at 20 kHz. Many wells drilled nowadays are deviated from the direction perpendicular to the formation beds and an increasing number of them eventually approach a horizontal direction. Also, the conductivity of some earth formations, such as shale, is often uniaxially anisotropic, due to their internal microscopic layer structure.

In this paper, an efficient algorithm is described for the computation of the induction tool response in deviated wells and multilayered uniaxial formations. Attention is limited to the so-called one-dimensional model, in which the effects of the borehole and of the invasion of borehole fluids into the permeable formations is neglected. The 6FF40 coils are modeled in terms of the equivalent magnetic dipoles.

It is essential that the analysis, or forward modeling, be very efficient, because it is invoked iteratively in the induction log data inversion process. The approach described in this paper is based on the transmission line model of the layered medium (K. A. Michalski and J. R. Mosig, *IEEE Trans. Antennas Propagat.*, **45**, 508-519, 1997). The Hankel transforms that arise are efficiently computed by a numerical quadrature along the steepest descent path in the transverse wavenumber plane (P. Cornille, *J. Math. Anal. Appl.*, **38**, 633-639, 1972). Sample numerical results are presented for both vertical and deviated wells, and are shown to compare favorably with published data.

B4-8
1120

COMPARISON OF THE DISCRETE WAVELET TRANSFORM AND THE PYRAMID ALGORITHM FOR SEMI-ORTHOGONAL SPLINE WAVELETS IN THE SOLUTION OF INTEGRAL EQUATIONS BY THE MOMENT METHOD

Richard Miller Robert Nevels*
Texas A&M University
Department of Electrical Engineering
College Station, TX 77843-3128

The discrete wavelet transform (DWT) has been shown to generate a moment impedance matrix that can be converted from a dense matrix to a sparse form with controlled error. Orthogonal wavelets have typically been chosen to perform the DWT since they form an orthogonal transformation. This guarantees that the matrix condition number is not changed.

Recently the DWT with semi-orthogonal wavelets has been reported. The DWT formed with these wavelets do not form an orthogonal transformation and do change the matrix condition number. The semi-orthogonal DWT produces a sparser matrix than orthogonal DWTs. The sparsification of the new matrix by thresholding does not significantly change the matrix condition number.

The DWT is a modified version of the two-dimensional wavelet transform used in image processing. This pyramid algorithm, which is also a discrete wavelet transform, is not an orthogonal transformation regardless of the orthogonality of the wavelets. The only difference between the two transforms is how the wavelet decomposition is applied.

The DWT produces a matrix where only the lowest frequency (or resolution level) scaling functions are used as part of the basis/testing functions. These scaling functions then interact with wavelet functions at all resolution levels. The wavelets also interact with wavelets from other resolution levels. The pyramid algorithm instead yields a matrix with scaling functions at each resolution level but only interacting with scaling functions or wavelets at the same resolution level. The wavelets also only interact with wavelets at the same resolution level.

The impedance matrices generated by a transverse magnetic plane wave excitation of a two-dimensional finite width flat plate will be used to compare the DWT to the pyramid algorithm. The matrix condition number and sparsity will be presented for the wavelet transforms generated with semi-orthogonal wavelets.

B4-9
1140

RESONANT CONFOCAL IMAGING (RCI) OF RESONANT SPATIAL CURRENT MODES OF STRUCTURES IN THE RESONANT REGION

J. D. Rockway, Y. Kuga, and A. Ishimaru
Department of Electrical Engineering, Box 352500
University of Washington, Seattle, Washington 98195.2500
email: kuga@ee.washington.edu

S. T. Li, C. W. Manry, and J.W. Rockway
SPAWAR System Center in San Diego

Abstract

Recently, studies have been conducted to determine the resonant and low frequency response of structures. In this frequency range the major contributor to the radiated or scattered far-field response of a structure is resonant spatial current modes. Identification and location of these resonant spatial current modes provide a means of understanding the effect of a structure on radiation or scattering. For canonical problems, the identification and positioning of these spatial modes may be computed analytically. For more complicated structures, a structure may be computed numerically. Harrington and Mautz [1971] characteristic mode formulation may then be used to determine these spatial modes via an eigenvalue formulation. From the far-field response of a structure, we have recently developed an inverse technique called Resonance Confocal Imaging (**RCI**) which effectively images the resonant current spatial modes for a given structure. For electrically small and intermediate sized structures $\sim \lambda$, only a few spatial modes are needed to characterize the radiation and scattering over the frequency band of interest. By considering the far-field scattering of a structure, the resonant frequency can be determined from the peak response of a structure. At the resonant frequency the response will be the result of only a minimal number of spatial modes. By imaging the far-field spectrum at a peak response, (i.e., resonant frequency), the spatial modes contributing to the far-field are imaged. The **RCI** imaging technique was verified by comparison to the resonant current spatial modes identified by the characteristic mode eigenvalue equation at a resonant frequency. This **RCI** imaging technique enables a direct ability to determine the resonant spatial current modes from far-field scattered response.

F4-1
0920

ON THE NATURE OF INSAR MEASURE OF OCEAN SURFACE CURRENT SOURCES

D. B. Trizna*
Remote Sensing Division
Code 7252
Washington, DC 20375-5351

The ocean surface velocity measured by an along-track interferometric SAR (INSAR) is proportional to the mean Doppler velocity of the surface within a cell, and thus depends on the mean flow, surface wind drift, the orbital motions of the long waves, and the velocity of the approach and recede components of the short wave roughness dominating the backscatter. The latter contribution can be particularly troublesome, as it can consist of linear waves, bound waves, and breaking wave features. The linear Bragg wave contribution can be significant (up to 23 cm/s for an X-band radar), and it can vary with azimuthal look with weights that are proportional to the approach and reced component spectral amplitudes (e.g., zero for cross wind look, maximum for upwind look). For arbitrary look angles, the weights are determined by the spreading function of short wave energy, which is not well known and which may in fact vary versus position on the dominant gravity wave. In this work we simulate these effects in a linear model to determine a current error estimate due to short waves with a variety of assumptions on small scale roughness directional spreading and relative contributions due to the three sources identified above.

F4-2
0940

ACTIVE AND PASSIVE SENSING OF SEA SURFACE FRICTION VELOCITY

David E. Weissman
Department of Engineering
Hofstra University
Hempstead, New York 11549

Vladimir G. Irisov
Environmental Research Laboratories/NOAA
Boulder, CO 80303

William J. Plant
William Keller
Applied Physics Laboratory
University of Washington
Seattle, WA 98195

The capability of airborne polarimetric microwave radiometers for the measurement of sea surface winds is being extended to include the estimation of sea surface friction velocity. This development is being advanced when microwave radar scatterometers are operated coincidently with polarimetric radiometers during aircraft experimental operations. The scatterometer radar cross section can be converted into friction velocity using new algorithms for Ku-band, X-band and C-band measurements. This is supplemented with in-situ data from meteorological instruments. The approach here includes the development of anisotropic ocean emissivity models by synthesizing what is known about sea surface processes as observed by the microwave radar cross section dependence on incidence and azimuthal angles.

The coincident measurements of the X-band radar scatterometer and the 37 Ghz polarimetric radiometer during the COPE Experiment (Sept - Oct '95) were used to determine the dependence of the radiometers' azimuthal parameters on friction velocity (and incidence angle). The radar measurement provides the in-situ sensing of surface winds and stress (friction velocity), to support the development of model functions for the first and second harmonic coefficients of the 2^{nd} and 3^{rd} Stokes parameters("Q" and "U").

Additional data from the Labrador Sea Experiment (March 1997) is being analyzed to extend the data set. It includes 37 Ghz polarimetric radiometer data at a variety of incidence angles, C-band scatterometer data and in-situ flux measurements from the R.V. Knorr.

F4-3
1000

POLARIZATION DEPENDENT RADAR BACKSCATTER CALCULATIONS FROM CRESTING OCEAN WAVES

D. J. Donohue* H.-C. Ku D. R. Thompson
Applied Physics Laboratory
Johns Hopkins Road
Laurel, MD 20723

¿From a recent study on the statistics of ocean radar backscatter, we have collected theoretically modeled backscatter cross section information from tens of thousands of random ocean surface realizations. Sarting from these results, we have identified specific realizations giving rise to the largest backscatter returns for both HH and VV polarizations. In general, we find that for low grazing angles, sharply crested waves are the dominant scatterering features in the numerical realizations. This has been verified by integrating the backscattered power from numerous small sections of the wave, and subsequently identifying the regions of greatest contribution to the total power. Interestingly, when examining the relationship between incident field, induced surface current, and localized scattering cross section, some surprising differences are found between the two polarizations. For example, the results clearly show that for HH polarization, the surface current and dominant scattering centers are concentrated over a small region near the crest of the wave. A deep shadow is often observed on the backside of the wave. For VV polarization, however, surface currents tend to be more uniformly distributed over the entire extent of the wave, and strong scattering centers are rarely observed. These differences support the well-known hypothesis that horizontal polarization is considerably more sensitive to wave cresting, potentially explaining the so-called super-events, where HH/VV ratios exceed one. The results also illustrate the substantial contribution of non-linear wave steepening to the surprisingly large variance of HH backscatter at low grazing angles.

The intermediate and high grazing angle results support the classical mechanisms of long-wave tilt modulation of small-scale Bragg scatterers and specular facets. An examination of surface currents at the higher grazing angles offers little additional information, that is, the relationship between surface current and scattered power appears to be highly chaotic. Previous calculations have been limited to two spatial dimensions. For this talk, we describe a new 3-dimensional implementation of our previously-developed multi-grid iterative method.

F4-4
1040

A WIND SPEED THRESHOLD IN MICROWAVE SCATTERING FROM THE OCEAN

W.J. Plant* W.C. Keller
Applied Physics Laboratory
University of Washington
Seattle, WA 98105
M.A. Donelan
Rosenstiel School of Marine and Atmospheric Sciences
University of Miami
Miami, FL 33149
D.E. Weissman
Hofstra University
Hempstead, NY 11550

In 1982, the Naval Research Laboratory carried out a field program called SEBEX at Nantucket Shoals, largely as a result of the efforts of Gaspar Valenzuela. The experiment was designed to try to explain the pattern of bathymetric features observed on the ocean surface in this area by the synthetic aperture radar on SEASAT in 1978. One result of this experiment was the observation by an airborne X-band radar of abrupt changes in backscattering cross section of as much as 20 dB (Valenzuela et al, *Journal of Geophys. Res.*, **90**, 4931-4942, 1985). Many of these changes were highly localized and have subsequently been explained by Gaspar's colleagues as due to current gradients, in this case caused by tidal flow over bottom topography. Some of the changes, however, were not highly locallized and were therefore difficult to explain on the basis of shear currents in the water.

In SEBEX, it was observed that the sudden changes in cross section occurred at low wind speeds but not at high. In recent years, experiments both at sea and in wind wavetanks have provided an explanation for such sudden increases in cross section. In this paper we will show data taken in a wind wavetank at Ku band which clearly show that microwave backscattering cross sections rise abruptly as the wind speed increases above a threshold level. We will also present Ku band data taken from an airship in conjunction with meteorological measurements which verify that the same increase occurs on the ocean. We suggest that the existence of this threshold is in agreement with the prediction made several years ago by Donelan and Pierson (Donelan and Pierson, *Journal of Geophys. Res.*, **92**, 4971-5029, 1987) that the short waves which scatter microwaves grow very rapidly at a wind speed which is just sufficient to overcome viscous damping. We will discuss some of the remaining discrepancies between the observations and Donelan and Pierson's predictions. Finally we will examine the implications of this threshold wind speed for spacebased scatterometry.

F4-5
1100

THEORETICAL STUDY OF THE SMALL PERTURBATION METHOD FOR OCEAN POLARIMETRIC THERMAL EMISSION

J. T. Johnson* M. Zhang
Department of Electrical Engineering and
ElectroScience Laboratory
The Ohio State University
205 Dreese Laboratories, 2015 Neil Ave
Columbus, OH 43210

Analytical models for ocean surface polarimetric thermal emission based on the small perturbation method (SPM) have shown success in matching brightness temperature azimuthal variations from aircraft based measurements. It has also been shown that use of the small perturbation method for calculation of surface emissivity results in a series in surface slope, not surface height, so that the method remains accurate for large height surface emission even when it fails for the corresponding scattering calculations. In this presentation, a detailed analysis of the SPM/small slope approximation (SPM/SSA) for ocean surface polarimetric thermal emission is performed, and the extent to which varying ocean surface length scales contribute to brightness temperature zeroth and second azimuthal harmonics is investigated. SPM/SSA predictions of brightness temperature azimuthal harmonics are simplified and expressed as an integration of a distinct "weighting" function for each azimuthal harmonic and polarimetric quantity multiplied by the corresponding ocean curvature spectrum azimuthal harmonic. An examination of the weighting functions typically shows that ocean waves of lengths both comparable to and much greater than the electromagnetic wavelength can significantly contribute to brightness temperature azimuthal harmonics, depending on the extent to which the ocean surface spectral model places asymmetry in these length scales. In addition, the SPM/SSA is approximated for the contributions of both very long and very short ocean length scales compared to the electromagnetic wavelength, and it is found that both long and short wave contributions can be expressed in simple equations involving either standard or modified ocean surface slope variances. The analysis presented eliminates uncertainties in the azimuthal properties of the ocean wave directional spectrum, thereby clarifying the physics of the emission process predicted by the SPM/SSA.

F4-6
1120

SIMULATION OF THE DOPPLER SPECTRUM OF THE SIGNAL SCATTERED BY A TIME-VARYING ROUGH SURFACE USING MOMI

J. V. Toporkov* G. S. Brown
The Bradley Department of Electrical and Computer Engineering
340 Whittemore Hall
Virginia Tech
Blacksburg, VA 24061-0111

Calculations of the temporal evolution of the signals scattered by time-varying ocean-like rough surfaces and their power spectral density (the "Doppler spectrum") have been receiving considerable attention in recent years. Such calculations are based on approximate analytical models (D. R. Thompson, in *Radar Scattering from Modulated Wind Waves*, 27-40, 1989) and numerical simulations (Rino et al, *Radio Science*, **26**, 51-71, 1991). The emergence in recent years of powerful and robust numerical techniques for rough surface scattering like the Method of Ordered Multiple Interactions (MOMI) allows one to extend such simulations to much lower grazing angles.

As in the works cited above, the temporal evolution of the surface is obtained by letting each surface harmonic propagate in accordance with the dispersion relation (surfaces with non-linear behavior can be obtained from such a model as well). In simulations, the evolving surface is considered at discrete time moments separated by a certain time interval. At each such moment, the surface is assumed to be "frozen" and scattering of a time-harmonic incident field is calculated using, for example, MOMI. The results of these calculations form time samples of a complex time-varying envelope of the scattered signal. We will discuss limitations of this approach, the region of its validity and the choice of simulation parameters such as temporal resolution.

Sample simulation results for scattering from 1-D perfectly conducting time-evolving surfaces for both vertical (TM) and horizontal (TE) polarizations will be presented and discussed. Incident angles in these simulations vary from 0 (normal incidence) to 85 degrees. In particular, for linear surfaces the Doppler spectrum of the backscattered signals at low grazing angles turns out to be very narrow and centered at the Bragg frequency (i.e. the angular frequency of Bragg components that is obtained from a dispersion relation for surface waves). The computing task and the actual amount of time such simulations take will be addressed. Future plans for simulations using this approach will be discussed.

F4-7
1140

AN EXTENDED BISTATIC MODEL FOR EM SCATTERING FROM PERFECTLY-CONDUCTING RANDOM SURFACES

D. R. Thompson* T. M. Elfouhaily
Johns Hopkins University
Applied Physics Laboratory
Laurel, MD 20723 USA
D. Vandemark
NASA/Goddard Space Flight Center
Wallops Flight Facility
Wallops Island, VA 23337 USA
B. Chapron
Institut Francais de Recherche pour l'Exploitation de la MER
IFREMER Centre de Brest
29280 Plouzane, France

An article written by Gaspar Valenzuela over 20 years ago (*Boundary-Layer Meteor.*, 13, 61-85, 1978) entitled "Theories for the Interaction of Electromagnetic and Oceanic Waves - A Review" is still one of the most frequently referenced papers in fields concerned with microwave scattering from rough surfaces. In this article, Valenzuela describes the backscattering cross section in terms of a generalized version of the composite model proposed earlier by Wright (1968), and gives expressions for the tilting of the "Bragg facets" in terms of the slope probability of the longer surface waves. One drawback of the composite-model approach is that the surface-wave spectrum must be divided into long- and short-wave portions such that the rms height of the short waves is small compared to the microwave wavelength; the so-called Small Perturbation (SP) limit. The well-known Kirchhoff approximation does not suffer from this drawback, but does not yield the proper polarization sensitivity in the SP limit. For the case of backscattering, Holliday (1987) showed how the Kirchhoff method can be extended to yield the proper SP polarization dependence. In our presentation, we expand Holliday's approach to include the more general bistatic scattering problem. To accomplish this, we solve the surface-current integral equation retaining all terms through first order in the surface slope, and derive expressions for the scattered field that exhibit the proper polarization sensitivity. Local tilting by longer waves is also considered in a manner analogous to that used by Valenzuela (1978). In the present case however, the long-wave facet size is determined by the radar footprint rather than by the SP limit discussed above. We require in our computation that terms of second-order in the surface slope are small (See e.g. Voronovich, 1993). A vector notation is introduced that greatly simplifies the treatment of the polarization effects; especially for bistatic scattering. A clarification of the expressions for the local tilting as given in Valenzuela (1978) is also presented. We believe that our technique provides a convenient new method to study both passive and active microwave scattering from random rough surfaces.

G4-1
0920

THE MID-LATITUDE *F*-REGION TURBULENT UPWELLING OF FEBRUARY 17. 1998

M. C. Kelley* W. E. Swartz F. Garcia J. Makela
School of Electrical Engineering
Cornell University
Ithaca, NY 14853
E. Kudeki S. J. Franke
School of Electrical and Computer Engineering
University of Illinois
Urbana, IL
M. Sulzer
Arecibo Observatory, Arecibo, PR

A violent ionospheric upwelling was observed over Puerto Rico during the geomagnetically disturbed evening of February 17, 1998. The event caused strong coherent scatter with Doppler shifts exceeding 300 m/s and fine filamentary echoes as observed both by the Cornell University Portable Radar Interferometer located near Isabela, PR, and by the University of Illinois VHF radar at Salinas, PR. The incoherent scatter radar at the Arecibo Observatory recorded a high velocity upward motion of the *F*-region that moved the peak to over 400-km altitude. Finally the Cornell All-sky imager showed bands oriented northwest to southeast that moved rapidly from one horizon to the other. GPS data show the airglow minima to be co-located with plasma depletions.

Similar events have been previously observed over Puerto Rico and Japan (R. A. Behnke, *J. Geophys. Res.*, **90**, 4448, 1979; S. Fukao *et al.*, *Geophys. Res. Lett.*, **15**, 768-771, 1988; S. Fukao *et al.*, *J. Geophys. Res.*, **96**, 3725-3746, 1991; M. C. Kelley and C. A. Miller, *J. Atmos. and Solar-Terr. Phys.*, **59**(13), 1643-1654, 1997), but never before have both coherent scatter and incoherent scatter data of the same event been obtained with good optical data. Features of previous events have provided evidence that southwest propagating TID's are amplified by the Perkin's instability (C. A. Miller *et al.*, 1997; M. C. Kelley and S. Fukao, *J. Geophys. Res.*, **96**, 3747-3754, 1991) with only one more e-fold of growth required to produce the violent upwellings. The February 1998 event, however, seems to have had additional unique driving forces leading to the spectacular 3-meter scatter. Several features of this and other related events will be explored.

G4-2
0940

OBSERVATIONS WITH THE ARECIBO RADAR DURING THE GEOMAGNETICALLY DISTURBED CONDITIONS IN FEBRUARY AND JUNE, 1998

M. P. Sulzer*
Arecibo Observatory, Arecibo, PR 00612
S. González
Arecibo Observatory, Arecibo, PR 00612
M. C. Kelley
School of Electrical Engineering
Cornell University, Ithaca, NY 14853

The Arecibo incoherent scatter radar has observed impressive and sometimes spectacular disturbances in the F region during a campaign directed at geomagnetically disturbed conditions. A set of instrumentation was assembled in Puerto Rico, including coherent scatter radars, GPS receivers, and an all-sky imager, in order to study such disturbances. We present primarily incoherent scatter radar results for the events of the nights of February 17-18 and June 25-26, 1998.

Both nights show large ion temperature enhancements near local midnight, but the observations differ in other aspects. During the February event, the line of sight ion velocity component is at times greatly enhanced upward, and the peak of the F layer moved to a correspondingly high altitude. The radar pointing direction was fixed due to operational limitations and no vector velocities are available.

Vector velocities are available during the June event; although they are somewhat disturbed, line of sight components are not as large as in February. However, power profile measurements sometimes show very large disturbances, similar to those seen when a powerful HF wave interacts with the F region of the ionosphere. There is no significant electron temperature enhancement and so these disturbances are to the electron density alone.

The time history of the profile disturbances suggests that they are propagating in a way that is consistent with the propagation of the airglow disturbances seen by the imager in February. The coherent radars saw 3 meter structure in February, but not in June, suggesting that the June observations captured the event in a later, less active phase.

G4-3
1000

OVERVIEW OF A YEAR-LONG STUDY OF *E*- AND *F*-REGION COHERENT SCATTER FROM PUERTO RICO

W. E. Swartz* M. C. Kelly
School of Electrical Engineering
Cornell University
Ithaca, NY 14853
E. Kudeki S. J. Franke J. Urbina
School of Electrical and Computer Engineering
University of Illinois
Urbana, IL

From July, 1997 through July, 1998 the Cornell University Portable Radar Interferometer (CUPRI) made regular (although not continuous) observations of the *E*- and *F*-regions of the ionosphere from a site near Isabela, Puerto Rico. During some of the observations supporting data was supplied by the incoherent scatter radar and optical facilities at the Arecibo Observatory and by the University of Illinois radar at Salinas, PR. The characteristics of the echoes varied considerably throughout the year and exhibited marked differences with those we might have expected based on similar radar measurements in the Japanese sector and from previous CUPRI observations from the island of St. Croix. During this period, only two *F*-region coherent scattering events were observed, one during a quiet period and the other during a very geomagnetically disturbed period. The spectral characteristics of these two events differed considerably. The quiet period echoes possessed little Doppler shift while the disturbed echoes had Doppler velocities ranging from a few tens of meters per second to 340 m/s depending on the evolution in time and space of the event. *E*-region echoes were obtained during almost half of the evening periods from sunset to midnight, but only during about 20% of the midnight to sunrise periods. None of the *E*-region echoes exhibited large Dopplers, even though significant Dopplers were not unusual for our other CUPRI mid-latitude measurements. Quasi-Periodic echoes were rare.

G4-4
1040

IRKUTSK INCOHERENT SCATTER RADAR INVESTIGATIONS OF THE MID-LATITUDE IONOSPHERE

O. I. Berngardt* A. P. Potekhin
Institute for Solar-Terrestrial Physics
664033 Irkutsk, Russia
P. J. Erickson J. C. Foster
Atmospheric Sciences Group
MIT Haystack Observatory
Route 40
Westford, MA 01886

The Institute for Solar-Terrestrial Physics (ISTP) and MIT Haystack Observatory have been awarded a two-year CRDF grant to support technical development of the Irkutsk radar facility and to expand collaboration between Russian and American research groups in studies of the mid- latitude ionosphere. The ISTP incoherent scatter facility is based on a former military radar system, located 75 miles northwest of Irkutsk, Siberia. Beginning in 1988, a preliminary incoherent scatter capability has been developed and World Day data have been acquired since 1992 within the limits imposed by the existing equipment, software, and analysis capabilities. The Irkutsk system is a monostatic pulsed radar operating in the frequency range 154-162 MHz, with frequency-controlled beam steering over an angular region +/-30 degrees from zenith. The facility consists of six 1.5 MW UHF transmitters (150 MHz), a sectorial horn antenna with opening size 246 m x 12.2 m, receiving systems and radar service equipment. The horn antenna is able to transmit and receive only a single linear polarization, which complicates derivation of plasma density profiles from the received signal. The current system is able to use the spectral method to measure both electron and ion temperatures and bulk plasma drift velocity, as well as recovering density profiles by the Faraday method. Radar analysis algorithms have been cross checked between the Irkutsk and Millstone Hill facilities, and two years of World Day observations of mid-latitude plasma altitude profiles have been produced in the NCAR/ISR database format and intercompared with simultaneous observations from Millstone Hill. Results of these initial investigations and the techniques being employed in the Irkutsk radar experiments and analyses will be discussed. The application of the Faraday rotation technique for the recovery of density/altitude profiles from the linearly-polarized system will also be described.

G4-5
1100

SMALL HORIZONTAL SCALE COUPLED E/F REGION ELECTRODYNAMICS AT ARECIBO

J. D. Mathews*
Communications and Space Sciences Laboratory
316 EE East
Penn State University
University Park, PA 16802
D. W. Machuga
Northrup Grumman
PO Box 746
Mail Stop 55, Baltimore, MD 21203
Q. Zhou
Communications and Space Sciences Laboratory
316 EE East
Penn State University
University Park, PA 16802
Q. -H. Zhou
Arecibo Observatory, Box 995
Arecibo, Puerto Rico, 00613

High resolution ISR observations of the evening and nighttime E and F regions at Arecibo suggest that E/F region electrodynamic coupling down to horizontal scales as small as a few kilometers is present most evenings and likely through the night. This coupling is manifested most clearly in the intermediate and tidal ion layers as "ion rain" and sporadic E events and less often as bottomside spread-F all of which show structure at apparent periods as short as a few minutes. Active spread-F events clearly reveal electrodynamic links between the low-lying layers, ion-rain, and the spread-F instability process. These processes are observed as the ionosphere is advected through the Arecibo beam that is fixed thus avoiding time/horizontal-structure "aliasing" inherent to "beam-swinging." We present several examples of the various events. Additionally, we suggest that these structures are a manifestation of polarization electric fields that "map" into the E-region and are of order 1 mV/m except for the most intense spread-F events that appear to be characterized by significantly larger E-fields. These E-fields are hypothesized to be generated in a "field" of linear and/or non-linear Perkins instabilities and are of relatively small horizontal-scales but occur over large horizontal-scales in the bottom-side of the nighttime F region. We present numerical simulations of 3-dimensional ion trajectories in wind and electric field structures similar to those implied by these observations. These simulations give insight into formation of the ion rain, sporadic E, and spread-F structures. We also discuss instrumentation – including the Arecibo dual-beam radar system – and observational modes needed to further study electrodynamics on the suggested small scales.

G4-6
1120

SIMULTANEOUS OBSERVATION OF ELECTRIC FIELD MAGNITUDE AND E-REGION COHERENT PHASE VELOCITY WITH THE MILLSTONE HILL UHF RADAR

P. J. Erickson* J. C. Foster
Atmospheric Sciences Group
MIT Haystack Observatory
Route 40
Westford, MA 01886

During an interval of intense, steady enhancement of the auroral convection electric field, simultaneous observations of E-region coherent backscatter properties and the magnitude of the causative electric field were obtained with fixed beam positions of the 440 MHz Millstone Hill radar. The experiment was performed on 27 August, 1998 between 18 UT and 24 UT (13 MLT - 19 MLT) in response to an interval of relatively steady southward IMF (Bz $\approx$ -10 nT until 21 UT). The narrow (1 deg fwhm) radar beam was directed approximately parallel to the $\vec{E} \times \vec{B}$ direction and line of sight F-region convection (integrated over 20-s intervals) in excess of 3000 m/s was observed. Simultaneously, E-region coherent echo amplitude and line of sight phase speed were observed in the lower-altitude range gates. Both coherent echo amplitude and echo source location are determined by a combination of magnetic aspect angle sensitivity, off-axis radar beam sensitivity, and the altitude and latitude extent of the E-region perturbation. Knowledge of the off-axis antenna sensitivity function and the magnetic aspect angle sensitivity for the coherent echoes permits the calculation of the off-axis contribution to the coherent signal at each sampling gate (range). Coherent phase velocity can be measured both in the region of amplitude (receiver) saturation in the main radar beam at E-region heights, and in the side-lobe echoes which appear at greater ranges.

During the interval 21 UT - 24 UT the F and E-region gates were aligned to sample nearly the same invariant latitude (61 deg invariant) and the simultaneous observations of E-region coherent backscatter properties and the electric field were obtained. A $\approx$ 20 mV/m electric field threshold for the onset of the coherent echoes was observed with $\approx$380 m/s coherent phase speed. Coherent phase speed increased linearly with increasing electric field strength at the rate 8.5 m/s per mV over the electric field range 20 mV/m - 60 mV/m. The logarithm of the coherent backscatter amplitude (in dB) increased linearly with the electric field magnitude at the rate 25 dB per 30 mV/m.

G4-7
1140

NEW RESULTS CONCERNING THE EFFECTS OF ELECTRON COLLISIONS ON THE INCOHERENT SCATTER SPECTRUM AT JICAMARCA RADIO OBSERVATORY

M. P. Sulzer*
Arecibo Observatory, Arecibo, PR 00612
S. González
Arecibo Observatory, Arecibo, PR 00612

Our recent efforts to fit incoherent scatter spectra taken in the lower topside ionosphere nearly perpendicular to the magnetic field over the Jicamarca Radio Observatory have suggested the possibility that an additional unexpected effect needs to be included in the model spectra. Others have encountered similar problems; in fact the best evidence that an unexplained physical effect alters the shape of the spectra is from Kudeki (private communication, 1998) who has fitted spectra taken with the beam pointing very close to perpendicular to the field. The angular size of the radar beam covers a sufficient range of angles to the field so that the spectral shape of the scatter changes significantly, and so it is necessary to construct a model which sums spectra over a range of angles. The fitted temperatures are too low, implying that the spectra are narrower than predicted. Aponte (private communication, 1998) has used spectra taken at several angles to the field in his thermal balance work. He has found that the apparent ratio of electron temperature to ion temperature varies with the angle to the field for angles close to perpendicular, but this effect dissappears as the angle from perpendicular increases.

We describe recent theoretical results, and show how measurements at various heights are affected. Coulomb collisions affecting the motion of the electrons are responsible for the spectral narrowing. We have carried out very accurate simulations of electron motion resulting in incoherent scatter spectra which are qualitatively similar to spectra resulting from other types of collisions, and to those predicted in an analytic solution for the Coulomb case (R. F. Woodman, *Incoherent Scattering of Electromagnetic Waves by a Plasma*, Doctoral Thesis, Harvard University, Cambridge, Massachusetts, 1967). However, the effects extend to somewhat shorter scale lengths, or further from perpendicular to the magnetic field, than in these other cases because the spectrum of the velocity component in the radar line of sight departs significantly from the usual Lorentzian, especially at the higher frequencies.

H2-1
0900

F-REGION ION HEATING OBSERVED WITH INCOHERENT-SCATTER RADAR

J. D. Kelly
Radio Science and Engineering Division
SRI Internaitonal
Menlo Park, CA 94025

One of the outstanding questions in Magnetosphere-Ionosphere coupling is how do the heavy (O^+) ions escape from the ionosphere to populate the magnetosphere in such large numbers? Indeed, the fluxes that are often needed to explain the magnetospheric population suggest that an upward transport mechanism must be operating at quite low ionospheric altitudes, where the number densities are sufficiently high. Perpendicular ion heating resulting from velocity shear-driven ion cyclotron waves has been suggested as a possible mechanism to energize the ions (Ganguli et al *J. Geophys Res*, **99**, 8873-8889, 1994).

The incoherent-scatter radar in Sondrestrom, Greenland, frequently measures F-region ionospheric parameters in the dayside auroral oval, polar cap, and poleward edge of the nightside oval. Phenomena exist within these regions, such as electric fields and shear convection reversals, which may also produce enhanced ion temperatures through frictional heating.

The radar directly measures electron density, line-of-sight ion velocity, and ion and electron temperature. Depending on the antenna pointing sequence, line-of-sight ion velocities can yield the horizontal and vertical (field aligned) velocities. From these ionospheric parameters, we can derive other terms including large-scale electric fields, conductivity, and joule heating rates. These derived parameters, when correlated with the directly measured ion temperature, can be used to investigate ion heating mechanisms. It is important to note that ion frictional heating is dependent on the differential velocity of the ions and the neutrals, consequently the neutral wind speed and direction need to be considered along with the electric field.

We present a data set that examines the effects of these sources of ion heating and we characterize their relative contributions.

H2-2
0920

COHERENT STRUCTURES AND OSCILLATIONS DUE TO INHOMOGENEOUS PARALLEL FLOWS [1]

V.V. Gavrishchaka*
Science Applications International Corporation
McLean, Virginia
G.I. Ganguli
Plasma Physics Division, Naval Research Laboratory
Washington, D.C.

Electrostatic fluctuations in a magnetized plasma with a structured field-aligned flow are investigated. It is found that a transverse gradient in parallel flow can significantly reduce critical value of the relative ion-electron field-aligned drift for both the current-driven electrostatic ion acoustic and ion-cyclotron modes. The shear-modified ion acoustic and ion-cyclotron modes can be also excited without any relative field-aligned drift provided that flow gradient is sufficiently strong. The new shear-modified ion-acoustic and ion-cyclotron modes are shown to be different from both the nonresonant mode due to a velocity shear in the parallel flow [*D'Angelo*, 1965] and the resonant classical current-driven ion acoustic and ion cyclotron modes [*Fried and Gould*, 1961,*Drummond and Rosenbluth*, 1962]. Linear and nonlinear regimes of coherent oscillations and spatial structure formation due to parallel-flow inhomogeneity are observed in 2D Particle-In-Cell simulations. The new modes can be excited for typical ionospheric conditions and wide range of ion/electron temperature ratios. The reported results may explain ionospheric observations of low-frequency ion-acoustic and ion-cyclotron waves and associated macroscopic effects (particle energization, anomalous transport, etc.), especially for ion/electron temperature ratios of the order of unity and larger when the critical current for the classical current-driven modes is significantly above the observed values. Other possible applications of our results to space and laboratory plasmas are also discussed.

[1] Work supported by the National Aeronautics and Space Administration and the Office of Naval Research

H2-3
0940

EXPERIMENTAL INVESTIGATION OF THE PARALLEL VELOCITY SHEAR INSTABILITY

J. Willig N. D'Angelo R. L. Merlino*
Department of Physics and Astronomy
The University of Iowa
Iowa City, IA 52242 USA

The parallel velocity shear instability may be excited in a magnetized plasma if the streaming velocity of the ions along the magnetic field, **B**, varies from point to point, in a direction perpendicular to **B**. This instability was analyzed theoretically by D'Angelo (*Phys. Fluids, 8*, 1748, 1965), and investigated experimentally, in a cesium plasma, by D'Angelo and von Geoler (*Phys. Fluids, 9*, 309, 1966). Parallel ion flow with shear across **B** is also a common occurrence in space plasmas. Examples include: solar wind flow at the outer magnetospheric boundary, entry of plasma into the earth's polar cusp, auroral arcs, and comet tails. In this talk we discuss recent laboratory work, performed in a double-ended Q machine, on the parallel velocity shear instability.

Two arrangements are used to produce velocity shear. The first is the so-called 'ring + disk' setup (N. D'Angelo and S. v. Goeler, *Phys. Fluids, 9*, 309, 1966) in which shear occurs at the boundary between two counterstreaming plasmas. In the second case a nonuniform magnetic field configuration is used to produce a plasma column with an inner core of nearly stationary plasma surrounded by an outer annular region of flowing plasma. The presence of shear and the value of the shear parameter (dv_z/dx, the variation of the axial ion flow velocity with the coordinate perpendicular to **B**) are determined from probe measurements.

The effect of neutral-particle collisions on this instability was also studied. This is of some interest, since it has been argued (B. Basu and B. Coppi, *J. Geophys. Res., 94*, 5316, 1989) that a collisional version of the parallel velocity shear instability might provide a means of explaining plasma density and electric field fluctuation spectra near auroral arcs at F region altitudes where ion-neutral collisions are important.

Work supported by the U.S. Office of Naval Research.

H2-4
1000

THEORY OF VELOCITY SHEAR-DRIVEN INSTABILITIES IN A ROTATING PLASMA LAYER: APPLICATION TO NRL SPACE PHYSICS SIMULATION CHAMBER[1]

J.R. Peñano[2]* G. Ganguli W.E. Amatucci D.N. Walker
Plasma Physics Division, Naval Research Laboratory
V. Gavrishchaka
Science Applications International Corporation

A theoretical model in cylindrical geometry has been developed to investigate the linear stability of a uniformly magnetized plasma to the sheared flow induced by a radially directed, radially localized dc electric field. The model is based on an eigenvalue equation describing the electric potential associated with electrostatic fluctuations. The ion and electron response perpendicular to the magnetic field is assumed to be that of a cold collisionless fluid while, parallel to the magnetic field, the collisionless kinetic electron response is retained.

When the local $\mathbf{E} \times \mathbf{B}$ velocity is comparable to the product $r_0\Omega_\alpha$, where r_0 is the radius about which the electric field is localized and Ω_α is the cyclotron frequency of plasma species α, the azimuthal flow velocity differs significantly from the $\mathbf{E} \times \mathbf{B}$ velocity. Instabilities arise from the free energy associated with the sheared flow. Additionally, since the azimuthal flow velocity is mass dependent, the large difference between the ion and electron masses can lead to an azimuthal current which can also drive unstable eigenmodes. Four types of instabilities are found. The dominant instabilities for long wavelength fluctuations have been identified as type-A and type-B Kelvin-Helmholtz modes (Jassby, *Phys. Fluids*, **15**, 1590, 1972) and a transverse current-driven instability. For shorter wavelengths, where these modes are damped, the inhomogeneous energy density driven instability (IEDDI) (Ganguli, *Phys. Plasmas*, **4**, 1544, 1997) can be excited.

The model is applied to a parameter regime characteristic of the Space Physics Simulation Chamber (SPSC) experiments (Amatucci *et al.*, *Phys. Rev. Lett.*, **77**, 1978, 1996) at the Naval Research Laboratory. A quantitative comparison between theory and experiment indicates that an experimentally observed fluctuation localized within a rotating plasma layer is an IEDDI.

[1] Work supported by the Office of Naval Research

[2] National Research Council-NRL Research Associate

H2-5
1040

BEAM-DRIVEN LOCALIZED WAVE STRUCTURES: SIMULATIONS AND CONNECTION TO FAST E-FIELD MEASUREMENTS

M. Oppenheim*
Astronomy Department
Boston University
725 Commonwealth Ave.
Boston MA 02215 D. Newman M. Goldman
Center for Integrated Plasma Studies
Campus Box 390
University of Colorado
Boulder, CO 80309

The FAST spacecraft has recently reported measuring spatially localized bipolar electric fields in the downward current region of the auroral ionosphere (see, Ergun, R. E., et. al., *Phys. Rev. Lett.*, **81**, 826, 1998). Our two-dimensional kinetic simulations of the nonlinear stage of the two-stream instability in a magnetized plasma show the development of bipolar electric fields with amplitudes, spatial extent, and phase velocities similar to those measured. We initiate these massively-parallel, 2-D, periodic, particle-in-cell (PIC) simulations with an electron distribution consisting of a stationary component and a drifting component. We also include an initially stationary kinetic ion component (nominally hydrogen). A two-stream instability drives perturbations in the electron distribution which quickly saturate due to trapping. The trapped electrons form hollow vortices in x-v_x phase-space, where $x||B$. While these structures are localized to only a few tens of Debye-lengths parallel to the magnetic field, they extend over hundreds of Debye lengths in the y direction (i.e., perpendicular to B). Thus, they form elongated hollow *tubes* in x–v_x–y space. In 1-D simulations, two vortices merge when they collide, leaving a single vortex with a somewhat different velocity and electric field amplitude. The situation is more complicated in 2-D where the phase-space tubes break, reconnect, and merge but often with differing behaviors at different locations in y. In addition, the 2-D simulations allow the development of oblique magnetized modes such as electrostatic whistlers.

In this talk, we will show movies depicting the evolution of the electric field energy generated by our massively-parallel, PIC code. These movies show the formation and nonlinear evolution of bipolar wave structures. Among the features seen are merging events, the development of perpendicular modulations, the growth of electrostatic whistlers, and the eventual decay of the structures. We will discuss the role of dynamic ions and will explore the effects of varying system parameters such as beam energy, temperature, and density, on the formation and longevity of the structures.

Supported by NASA and NSF.

H2-6
1100

VLF WAVE COUPLING TO FIELD-ALIGNED IONIZATION ENHANCEMENT DUCTS IN THE MAGNETOSPHERE

R. A. Helliwell
Durand 325, STAR Lab
Stanford University
Stanford CA, 94304

Field aligned "whistler" ducts play important roles in cold plasma diagnostics and hot plasma wave-particle interactions at VLF. To understand how VLF energy is coupled into and out of such ducts we propose a simple model of duct coupling based on a numerical simulation of the end points of ducts which terminate at altitudes from 300 to 2000km, depending on local time and season [Bernhardt, P. A. and C. G. Park, JGR, 82(32), 5222-5229,1977]. Since the refractive index in the ionosphere is generally very high at VLF, the waves excited in this region by ground sources are close to the vertical, assuming horizontal stratification of the ionosphere. Then we can derive a simple relation between duct enhancement and the trapping in the duct of upward propagating waves as follows.

Assuming a dipole approximation for the Earth's magnetic field we let γ be the dip angle of the duct axis. Then for a trapping angle θ_T, defined as the maximum value of the angle between the wave normal of a trapped wave and the duct axis [Helliwell, R. A., Whistlers and Related Ionospheric Phenomena, Stanford University Press, 1965], the condition for trapping of any part of an upgoing wave is given by $\theta_T > (\pi/2 - \gamma)$, where γ = dip angle of duct axis at its end point = $\tan^{-1}[2 \tan \phi]$, ϕ = geomagnetic latitude. Thus at the geomagnetic poles, where $\gamma = \pi/2$, $\theta_T = 0$, all incident energy is trapped, whereas at the equator where $\theta_T = 90°$ there is no trapping. If for example $\theta_T = 25°$, the above condition for trapping gives $\phi = 50°$ geomagnetic latitude ($\sim 40°$ North geographic latitude on East Coast of U. S. A.). In this case, all trapping is cutoff at lower latitudes, while at higher latitudes the fraction of the available input energy that is trapped (called the "trapping cross section") is less than unity. The only way to achieve a ducting cross section of unity at middle latitudes is by introducing horizontal gradients that will tilt the input wave normals so that they are aligned with the duct axis (H. G. James, Refraction of whistler mode waves by large scale gradients in the middle latitude ionosphere, Ann. Geophys, 28, 301, 1972).

At the output of a duct those output rays whose wave normals fall within the "transmission cone" will excite waves in the earth-ionosphere waveguide while those that fall outside this cone will be reflected upwards and can be seen on satellites as nonducted rays. Those reflected rays that reach the source duct will be re-trapped and may echo back and forth in the same duct, giving rise to phenomena such as "periodic emissions". Other reflected rays may enter adjacent ducts creating the so-called "mixed path" echoes.

H2-7
1120

A LABORATORY INVESTIGATION OF LOWER HYBRID WAVE INTERACTIONS WITH A DENSITY STRIATION

S. I. Rosenberg* W. Gekelman
Department of Physics
15-70 Rehab
University of California, Los Angeles
Los Angeles, CA 90095

For decades, rockets and satellites have observed localized bursts of intense lower hybrid wave radiation in conjunction with density depletions; these have been termed lower hybrid solitary structures (LHSS). With recent improvements in the temporal resolution of rocket measurements, and the corresponding increase in spatial resolution, research on LHSS has focused on their internal structure. As rockets and satellites pass through the ionosphere, they can only record data along a line through LHSS. Using just these data, one can not completely understand the electric field and density patterns. We are conducting laboratory experiments at the Large Plasma Device (LAPD) at UCLA in order to do just that. By working in a laboratory experiment, we are able to scale the key experimental parameters ($1 < f/f_{lh} < 6$; $1 < d/\rho_{ci} < 7$; $d/\lambda_{lh,\perp} \leq 3$; $1 < d/(\delta = c/\omega_{pe}) < 5$; where d is the the size of the striation) to be relevant to ionoshperic physics and make the high-resolution spatial and temporal measurements necessary to understanding LHSS patterns. In our laboratory experiments, we launch lower hybrid wave radiation into a field aligned density striation ($3 < dn/n < 7$). We then use a dipole electric field probe to map the pattern of the wave electric field in time and space. Our results correlate well to ionospheric observations of electric fields near density depletions. This paper investigates the structures' dependence on several factors: striation geometry, including its shape (cylindrical or slab) and transverse size (scaled to the collisionless skin depth) and the wave frequency. Data characterizing the background plasma and the striation will be presented along with high-resolution electric field data. In addition, we will compare our results with those from recent souding rocket flights.

H2-8
1140

THE ROLE OF SELF-ORGANIZED CRITICALITY IN AURORAL PLASMA PROCESSES

Tom Chang
MIT Center for Space Research
Room 37-261
77 Massachusetts Avenue
Cambridge, MA 02139

Observations indicate that plasma processes in the auroral zone are generally sporadic, localized and nonlinear. The wave turbulence there is usually intermittent and inhomogeneous, and the associated wave-particle interactions are commonly nonlocal. These are the general characteristics of global dynamical systems near "self-organized criticality (SOC)".

The concept of self-organized criticality was first introduced by Bak et al. (*Phys. Rev. Lett.*, **59**, 381, 1987) to explain the invariant properties of complex dynamical systems far from equilibrium. They demonstrated that for inhomogeneous dissipative driven systems with many metastable states, the natural outcome would be a self-organized critical state without intrinsic length or time scales. It was suggested by Chang (*IEEE Trans. Plasma Science*, **20**, 691, 1992) that global-multiscale space plasma processes generally would display the scale-invariant properties of self-organized criticality. In addition, such systems generally would exhibit low-dimensional behavior with nonlinear, chaotic, multifractal signatures. (See also, Tom Chang, *AGU Monograph*, **104**, 193, 1998).

In this talk, we shall employ numerical simulation results, scaling laws, and renormalization-group arguments (Tom Chang et al., *Physics Reports*, **217**, 279, 1992) to demonstrate that most of the sporadic, localized space plasma processes in the auroral zone are manifestations of stochastic dynamical systems at self-organized criticality. Specific examples to be discussed are the weak auroral double layers in the acceleration region, the randomly distributed fast electron holes in the return current region and elswhere, the strong spiky lower hybrid turbulence, the strong Langmuir turbulence, and associated wave-particle interactions.

J6-1
0900

ADVANCES IN RADIO OCCULTATION STUDIES

B. Ahmad G. L. Tyler*
Center for Radar Astronomy
Stanford University
Stanford, CA 94305-9515

Radio occultation is a remote sensing method for 'sounding' planetary atmospheres. Since its inception in the early 1960's, this methodology has been used to obtain high vertical resolution profiles of atmospheric temperature and pressure for most of the planets of the solar-system, and for Titan, the largest moon of Saturn. Radio occultation also has been used to obtain total electron content profiles of planetary ionospheres. Recent application of this method to the study of Earth's atmosphere has generated wide interest in further understanding of its potential and limitations. We present findings in two areas: quantitative definition of resolution, and errors due to large-scale horizontal gradients.

The original formulation of the radio occultation method in terms of the Abel transform (Fjeldbo et al., *Astron. J.*, **76**, 123–140, 1971) assumes the atmosphere to be spherically symmetric for the forward as well as the inverse problems. This formulation makes it difficult to assess the 2-D or 3-D resolution when perfect spherical symmetry does not exist. We model the radio occultation experiment as a tomography experiment in which only one parallel projection of the object is available (Ahmad and Tyler, *Radio Sci.*, **33**, 129–142, 1998). This eliminates the need to assume spherical symmetry for the forward problem. For the inverse problem spherical symmetry is assumed, consistent with the standard approach to handling occultation data. This process yields the 2-D resolution kernel for Abel inversion. The 3-D resolution kernel can be obtained easily if geometrical rays are replaced by a more accurate representation of radio wave propagation, e.g., Fresnel tubes.

Large-scale horizontal gradients are not analyzed accurately with the kernel approach because the ray paths are altered substantially from the zeroth order approximation. We analyze errors in atmospheric profiles due to large- scale departures from spherical symmetry using a first-order perturbation approach (Ahmad and Tyler, *submitted to J. Geophys. Res.—Atmos.*, 1998). Our analysis is general in that no particular occultation geometry is assumed. Moreover, the analysis is applicable to tenuous as well as dense atmospheres. The results of the perturbation analysis are compared with those obtained from simulated occultations of the atmospheres of Mars and Earth, representing tenuous and dense atmospheres, and subsequent Abel inversion. The two approaches are in close agreement.

J6-2
0920

AN UPDATE ON THE LONG-TERM VARIATIONS OF JUPITER'S SYNCHROTRON EMISSION

Michael J. Klein and Scott J. Bolton
Jet Propulsion Laboratory
California Institute of Technology
Pasadena CA 91109

Time variability in the synchrotron radio emission from Jupiter's magnetosphere has been widely reported in the literature (e.g., I. dePater and M. J. Klein, *NASA SP 494*, 139-150, 1989). Attempts to correlate the variations with solar wind parameters (Bolton et. al. *JGR 94* 121-128, January 1, 1989) showed promising results with the recognition that the microwave observations spanned only about two cycles of solar activity. Additional observations to extend the time base were clearly needed.

The data base of 13-cm observations that constitute the NASA-JPL Jupiter Patrol, begun in 1971, has been extended to 1998. When combined with published observations made in the 1960's, the Jupiter observations at wavelengths near 13 cm span more than three solar cycles. Moreover, the precision of the data has been improved through the use of larger apertures and better techniques to minimize the effects of confusion with weak background radio sources.

In this paper we report new observations made with the 34-m and 70-m antennas at NASA's Goldstone Deep Space Network complex. The new data show that the Jovian synchrotron flux is increasing once again, thereby reversing the seven-year trend of steadily falling integrated flux density from 1991 through May of 1998 (with the obvious exception of the large outburst following the Comet SL-9 impacts). We also report progress on a synchrotron radiation model and compare the early results with the observations

Observations by Bolton using the 26-m Hat Creek radio telescope in the period 1988-1991 are compared with the Jupiter Patrol data. Fortuitously, the Hat Creek data fills in a gap in the Goldstone data that happened to coincide with a sharp rise in the Jovian synchrotron flux that began in November 1989.

The research reported in this paper was performed by the Jet Propulsion Laboratory, California Institute of Technology, under contract with the National Aeronautics and Space Administration

J6-3
0940

NEAR-NADIR SCATTERING FROM A FRACTAL SURFACE.

Michael K. Shepard
Dept. of Geography and Earth Science
400 E. Second St.
Bloomsburg University
Bloomsburg, PA 17815
Bruce A. Campbell
CEPS, MRC 315
National Air and Space Museum
Washington, D. C. 20560

Numerous studies have demonstrated that natural surfaces, including those found on other planets, are better described by non-stationary fractal statistics than by the stationary statistics commonly assumed in current radar scattering models [cf. Shepard and Campbell, Icarus, 134, 279-291, 1998]. The major difference is that quantities such as the surface root-mean-square (RMS) height, RMS slope, and autocorrelation length are functions of the sample size of the surface, *i.e.*, these quantities cannot be considered constants. Therefore, we have developed a near-nadir (incidence/backscattering angles <25°) scattering model applicable to self-affine fractal surfaces. Because fractals are not differentiable at any given point, we utilize a Huygen's wavelet approach instead of a direct electromagnetic field boundary value solution. In essence, each point on the surface is modeled as an independent source of a spherical scattered wave. The contribution to the far-zone electromagnetic field from any given point is found by superposing all wavelets. Each wavelet is assumed to have the same magnitude (dependent upon the composition of the surface), but a phase which depends upon it's height relative to it's neighbors.

A number of interesting insights and predictions are provided by this model approach. For instance, we find that a surface will have a finite area around each point which coherently contributes to the wavelet scattered from that point. We refer to this area as the "effective aperture", since it approximates the behavior of a diffracting aperture or radiating antenna. Additionally, the model predicts a family of angular scattering functions that mimic and smoothly transition between the commonly utilized Hagfors [J. Geophys. Res., 69, 3779-3784, 1964], Gaussian [Hagfors, 1964], and exponential surface models [e.g., Tyler *et al.*, J. Geophys. Res., 97, 13115-13139, 1992]. Further, the model predicts that near-nadir scattering behavior is determined by the wavelength-scaled surface roughness, *i.e.*, the roughness (RMS height or RMS slope) that would be measured by a field worker using a ruler one wavelength in size, and the surface scaling behavior described by the fractal dimension or Hurst exponent. Finally, the model predicts that the scattering behavior from such a surface will scale with wavelength in a self-affine manner, *i.e.*, a power law. The scattering behavior predicted by the model is consistent with that observed for Venus by the Magellan altimeter experiment [Tyler *et al.*, 1992].

J6-4
1000

IMAGING MERCURY'S NORTH POLE WITH THE UPGRADED ARECIBO S-BAND RADAR

J. K. Harmon*
Arecibo Observatory
HC3 Box 53995
Arecibo, PR 00612
M. A. Slade
Jet Propulsion Lab.
MS 238-420
Pasadena, CA 91109-8099

We report results from recent observations of Mercury using the new S-band (λ=12.6 cm) radar on the upgraded Arecibo telescope. The primary objective of the observations was to obtain improved radar images of the planet's north polar region, where earlier radar observations had revealed bright spots attributable to deposits of cold-trapped volatiles (probably water ice) in permanently shaded crater floors.

The observations were made in mid-August 1998, when Mercury was at inferior conjunction with it's north pole tipped toward Earth for favorable viewing. Also, at this time the sub-Earth longitude was on the opposite side of the planet from that of the 1991-92 Arecibo observations, which afforded the possibility of observing certain parts of the polar region at a much more favorable aspect than before. The 850-KW transmissions were modulated using a 1023-length pseudorandom phase code with a 20 μs baud. From this we were able to generate high-quality delay-Doppler images of the pole with a surface resolution of 3 km, which represents a considerable improvement over the 15-km resolution of the pre-upgrade Arecibo images. Although the use of a conventional repeating-code (rather than a coded-long-pulse) waveform resulted in some Doppler aliasing of the overspread echo, the resultant degradation of the depolarized images at the pole was negligible.

All of the previously known "ice" features were easily seen even in single-run (10-min) images, except for a couple of features that were now too close to the radar horizon. In addition, more than a dozen new, small features were found. All of these new features that are located in the Mariner-10-imaged hemisphere could be identified with known craters. Also, some new features could be seen at relatively low latitudes (down to 75 degrees). The biggest surprise was that feature K, which appeared oblong in the old images, was found to be simply the permanently shaded portion (protected by the equatorward section of crater rim) of a much larger crater. Also, interior structures could be resolved in the floors of all of the larger crater features (D, E, H, J, and K) suggestive of central peaks or smaller superimposed craters.

J6-5
1040

PRELIMINARY RESULTS OF LABORATORY MEASUREMENTS OF THE CENTIMETER WAVELENGTH PROPERTIES OF PHOSPHINE UNDER SIMULATED CONDITIONS FOR THE OUTER PLANETS

J. P. Hoffman* P. G. Steffes
School of Electrical and Computer Engineering
Georgia Institute of Technology
Atlanta, GA 30332-0250

It has been suggested that phosphine (PH_3) may contribute significantly to the microwave emission spectrum of Neptune, and to the centimeter-wavelength opacity measured by the Voyager 2 spacecraft at Neptune (D. R. DeBoer and P. G. Steffes, *ICARUS*, **123**, 324-335, 1996). As a result, laboratory measurements of the microwave opacity and refractivity of PH_3 in an H_2/He atmosphere are being conducted at 1.5 GHz (20 cm), 2.2 GHz (13.3 cm), 8.3 GHz (3.6 cm), 13.3 GHz (2.3 cm), and 21.6 GHz (1.4 cm) at pressures of 1, 3, and 5 bars at room temperature. The experimental approach is similar to that previously used by DeBoer and Steffes (D. R. DeBoer and P.G. Steffes, *Astrophys. and Space Sci.*, **236**, 111-124, 1996) utilizing the Georgia Tech high sensitivity microwave measurement system. Preliminary results at room temperature indicate current theories significantly understate the centimeter-wavelength opacity of PH_3. This appears to be most drasti! c at longer wavelengths (13.3 and 20 cm).

This higher-than-expected opacity will further elucidate the interpretation of centimeter-wavelength microwave observations from radio telescopes and previous spacecraft (Voyager) radio occultation measurements of the atmospheres of all four Jovian planets. Specifically, previous analysis of Voyager 2 radio science data at Neptune (G. F. Lindal, *Astronomical Journal*, **103**, 967-982, 1992) requires reassessment. These data will also serve to aid future interpretation of entry probe signal attenuation measurements from the Galileo probe, and from Cassini radio science studies at Saturn. Future experiments will be conducted at ambient, 213 K and 173 K, at the same frequencies and pressures.

This work is being supported by the NASA Planetary Atmospheres Program under grant NAG5-4190.

J6-6
1100

HIGH RESOLUTION TOPOGRAPHIC MAPS OF THE LUNAR POLAR REGIONS FROM EARTH-BASED RADAR INTERFEROMETRY

J. L. Margot* D. B. Campbell
Cornell University
Ithaca, NY 14853
R. F. Jurgens M. A. Slade
JPL/Caltech
Pasadena, CA 91109

Earth-based radar interferometry has been used to map the radar backscatter cross-section and measure the topography of the lunar polar regions as well as a few other areas of interest. Absolute elevation data and radar imagery at high spatial (~100 m) and height (~50 m) resolutions were obtained over ~300 km by ~1000 km regions at each pole, where the topography was previously largely unknown. Compared to existing topographic data sets at lower latitudes, the radar observations provide digital elevation models with denser horizontal spacing and better height resolution.

Elevation data for the lunar polar regions may refine global models of lunar topography (D. E. Smith *et al.*, *J. Geophys. Res.*, **102**, 1591, 1997) which currently rely on interpolation over these areas. The digital elevation models for high-latitude regions will also contribute to lunar ice investigations (W. C. Feldman *et al.*, *Science*, **281**, 1495-1500, 1998) by facilitating the determination of areas which are in permanent shadow. Topographic maps for other parts of the Moon allow detailed morphometry of impact craters (Margot *et al.*, submitted to *J. Geophys. Res.*, 1998).

Our three-dimensional mapping was accomplished with an Earth-based radar interferometer using essentially the same techniques as Shapiro *et al.* (*Science*, **178**, 939, 1972), but with ten times higher spatial and height resolutions. The NASA/JPL Goldstone 70 m antenna was used to transmit at 3.5 cm wavelength while two nearby 34 m antennas were used to form a receive interferometer. Elevation measurements were derived from the relative phase between the two radar echoes.

Comparison of the radar-derived topography with Clementine lunar orbiter laser altimetry data (D. E. Smith *et al.*, *J. Geophys. Res.*, **102**, 1591, 1997) shows good agreement between the two techniques. RMS deviations between the radar-derived heights and Clementine altimetry points near 75° latitude are ~100 m. This comparison also allowed us to produce maps of absolute elevations above a known reference ellipsoid. The elevation maps are currently being analyzed to measure the location and extent of permanently shadowed regions which may harbor ice deposits.

J6-7
1120

BISTATIC RADAR ASTRONOMY: RECENT SPACECRAFT RESULTS

R. A. Simpson*
Space, Telecommunications, and Radio Science Laboratory
Department of Electrical Engineering Stanford University
Stanford, CA 94305-9515

In the five years since the review of spacecraft bistatic radar was published (Simpson, *IEEE Trans.*, **GRS-31**, 465-482, 1993) additional experiments have been conducted at Venus, the Moon, and Mars.

Venus echoes were detected as the Magellan spacecraft overflew Maxwell Montes in 1994. Although the incident signal was highly dispersed during scattering from the rough terrain, polarization of the echo was consistent with reflection from a surface with electrical properties of a semiconductor. Elemental tellurium, a trace component of terrestrial volcanic gases, would provide a remarkably good match ($\sigma \simeq 2000$ mho/m) to the observed properties (13 mho/m) if present as a thin layer (Pettengill et al., *Science*, **272**, 1628-1631, 1996).

Clementine conducted both quasi-specular and spotlight observations during its short visit to the Moon in 1994. The spotlight experiments were targeted toward the north and south lunar poles in a search for enhanced backscatter from postulated deposits of relatively pure water ice, perhaps in permanently shaded craters. Nozette et al. (*Science*, **274**, 1495-1498, 1996) claimed a detection near the south pole, but their conclusions have been challenged using high-resolution Arecibo radar images. Stacy et al. (*Science*, **276**, 1527-1530, 1997) argued that the distribution of pixel brightness near the south pole is no different from elsewhere on the Moon. We are conducting an independent analysis of the Clementine data; although incomplete at the time this abstract was written, we have been unable to provide any additional support for the Nozette detection. Its magnitude is within the range expected from a heterogeneously scattering surface; but we cannot rule out ice as a cause.

Atmospheric radio occultations began in January 1998 using the Mars Global Surveyor spacecraft. In a parallel investigation, we are searching for transient echoes from the surface at or near the occultation time. Although the narrow X-band antenna beam ($\sim 1°$) limits quasi-specular scattering to incidence angles greater than 89° on the surface, highly oblique echoes were detected previously using Mariners 6 and 7 (Fjeldbo et al., *Icarus*, **16**, 502-508, 1972). Preliminary examination of part of the new MGS data set has shown no signals that can be unambiguously identified as arising from surface scattering.

J6-8
1140

INTERPLANETARY SCINTILLATION POLARIMETRY AND CORONAL FARADAY ROTATION

S. R. Spangler
Department of Physics and Astronomy
University of Iowa
Iowa City, IA 52242

Measurement of Faraday rotation of radio waves which have propagated through the corona is a valuable observational technique for determining the plasma properties of the corona. Such measurements can yield information on the large scale magnetohydrodynamic structure of the corona, smaller scale plasma structures, and turbulent fluctuations. Faraday rotation observations of extragalactic radio sources viewed through the corona have been made with the Very Large Array of the National Radio Astronomy Observatory (T. Sakurai and S. R. Spangler, *Astrophysical Journal*, **434**, 774-785, 1994). VLA observations have the disadvantage that full mapping must be done at the required time resolution, solar active regions can contaminate the short baseline data, and elevated system temperature (T_{sys}) values begin to be a problem at solar elongations of interest. Polarization observations with a large single dish possessing a small beam would have less of a T_{sys} problem and offer simplified data processing. However, polarized solar inferference would seem to render such observations impossible. These difficulties could be circumvented by combining polarimetric and interplanetary scintillation (IPS) observations. Radio sources with compact components less than a few tenths of an arcsecond in angular size show intensity scintillations on timescales of less than a second. A significant fraction of sources selected at decimetric wavelengths display IPS, due to compact hot spots in the source structures. These fluctuations may be accurately measured even in close proximity to the Sun. The IPS process essentially turns a single dish into an interferometer, and offers the prospect of polarimetric observations close to the Sun in the inner solar wind and outer corona. Test observations at a frequency of 850 MHz were made with a polarimeter at the NRAO 300 foot radio telescope in June and July, 1977. Good results were obtained for sources with as little as 0.1 Jy of scintillating flux, and the technique appears to have worked satisfactorily in measuring the polarization characteristics of 3C138. This technique is worth exploring with current large radiotelescopes, such as the upgraded Arecibo antenna and the Green Bank Telescope.

J6-9
1200

RADIO SCIENCE WITH MARS GLOBAL SURVEYOR

G. L. Tyler* D. P. Hinson R. A. Simpson
Space, Telecommunications, and Radio Science Laboratory
Department of Electrical Engineering
Stanford, CA 94305-9515

The MGS Radio Science Investigation is one of five experiments associated with Mars Global Surveyor spacecraft, expected to achieve a low circular orbit about Mars in March, 1999. Objectives of this investigation are observation and study of the atmosphere over a martian year, and determination of a precise model for the gravity field. MGS radio science builds on advances first achieved with the Voyager mission to the outer planets. Among these are the use of very high stability quartz oscillators as on-board frequency reference sources, attention to spacecraft and ground systems and to mission detail affecting radiometric performance, and advances in algorithms and software for data reduction and analysis. Frequency stabilities $\Delta f/f \sim 1\text{–}4 \times 10^{-13}$ are achieved with one- and two-way links used for radio occultation and tracking. The downlink SNR $\sim$ 70 dB near opposition. Corresponding tracking accuracies are 2–3 m in range, and 10–30 μm s^{-1} in range rate.

Atmospheric occultations carried out from an intermediate orbit in 1998 have yielded more than 100 soundings of the atmosphere and the shape of Mars. The accuracies of retrieved surface pressure and temperature are in the range of a few pascals, and one kelvin, respectively. Atmospheric structure is obtained with a vertical resolution of about 0.8 km; recent advances in understanding diffraction effects in occultation observations are expected to lead to an order of magnitude improvement, however. These observations reveal a number of interesting features including, a near-Chapman ionosphere controlled by solar zenith angle, strong diurnal variations in the lowest 2 km of the summer boundary layer, dynamically forced inversions in the lowest scale height in the northern winter hemisphere, and prominent atmospheric wave structures. Observations are accurately located in planetary radius, allowing study of thermal tides, the thermal wind, and the seasonal cycling of gas between the atmosphere and the polar caps.

Study of the gravity field is based on perturbations to the motion of MGS observed along the line of sight from Earth. Preliminary results provide new, very high quality observations of the northern hemisphere. Early analyses of the tracking data show that they support spherical harmonic models of degree and order 75 with sensitivities of $1\text{–}10 \times 10^{-6}$ m s^{-2}. Direct observation of the seasonal change in mass of the polar cap is a distinct possibility.

A proposed ancillary experiment for late in the mission would use the radio system for bistatic radar studies of the surface of Mars.

Session B5, 1355-Thurs., ECCR151
ANTENNAS AND GUIDED WAVES
Chairperson: M. Piket-May (Univ. of Colorado)

B5-1
1400

OPTIMIZATION OF AN ARRAY CONFIGURATION MINIMIZING SIDE LOBES

L. Kogan
National Radio Astronomy Observatory
PO Box 0
Socorro, NM 87801

The analytical expression for the first derivative of the array beam as a function of the position of the given element has been derived. The required shift of the given element towards the given direction to minimize the value of the array beam for this direction in the sky is proportional to the value of the first derivative . This idea has been applied to optimize an array configuration minimizing the side lobes of the array beam. Many iterations are used to find the final configuration. For each iteration, the direction of the worst side lobe at the area of optimization is determined. Then each element is shifted in accordance to the derivative. Only a small portion of the required shift is applied to save the first derivative value for other elements. The portion of the shift should be rather small ($\sim 0.00001 - 0.001$) and should be found empirically. For each iteration, the array configuration is normalized to the unit size to conserve the area of optimization in the sky. The relevant software is written in the NRAO Astronomical Image Processing System (*AIPS*) enviroment. The initial configuration can be taken from an input file or as an evenly distributed configuration on one, two, or three circumferences. The software produces the plots of the initial and final configurations with the relevant worst side lobe value and its location given in the header. The optimization can be carried out under different constraints including the topographical constraint of the site, donuts, one or two circumferences, minimum spacing between the antennas. Other constraints can be added.

The minimum achieved level of the side lobes depends on the area of optimization in the sky. The smaller this area is, the lower side lobes can be achieved as the result of the optimization. The nearest side lobes can be minimized better then the grating side lobes. Examples of the optimization are presented for different constraints.

The method and the software have been developed for the *MilliMeter Array (MMA)*, the radio telescope of new generation being created by the National Radio Astronomy Observatory (*NRAO*). But they can be useful for the design of any array.

B5-2
1420

CIRCULARLY POLARIZED CPW FED SLOT ANTENNA

Alpesh Bhobe* Melinda Piket-May
Department of Electrical and Computer Engineering
Campus Box 425
University of Colorado
Boulder, CO 80309

Coplanar waveguide (CPW) transmission lines have been studied by many investigators mainly because of their easy adaptation to both parallel and series insertion of both active and passive components eliminating the need for via holes for connections. They have low radiation leakages. In addition the substrate can be made relatively thick.

Radiation behavior of the CPW transmission line and slot are used to create antenna structures. These antennas have operating bandwith of 10-15%, while the traditional microstrip patch element has a typical bandwidth of 5%. This wider bandwidth may make them a more popular design then microstrip patch antennas in future. Much research has been devoted to characterize microstrip patch antennas but very little research has been done to determine their CPW counter part either theoretically or experimentally. There is a need for practical models of CPW slot antenna configurations and their design algorithms.

Many applications in communications and radar require circular or dual-linear polarization. In this paper we propose a practical design methodology for designing circularly polarized CPW fed slot antenna. The circular polarized design is investigated using method of moments (MOM) and finite difference time domain (FDTD) method. Prototype antenna will be fabricated and the return loss and radiation patterns will be shown.

B5-3
1440

DESIGN OF A WIDEBAND CPW FED SLOT ANTENNA

Alpesh Bhobe* Martin Haeusler K.C.Gupta
Melinda Piket-May
Department of Electrical and Computer Engineering
Campus Box 425
University of Colorado
Boulder, CO 80309

Coplanar waveguide (CPW) circuits offer several advantages over the traditional microstrip circuits. Advantages of CPW circuits includes ease of shunt and series connections, low parasitic radiation, low dispersion, and avoidance of the need to for thin fragile substrates. Radiation behavior of slot and CPW transmission lines can be used to create antenna structures. Slot antenna structures have much wider bandwidth as compared to microstrip patch antennas. This wider band- width may make them a more popular design than a microstrip patch antennas in future. Unfortunately, until now, compared to microstrip patch antennas very little research has been undertaken regarding CPW antennas and slot antennas. There is a need for practical models of CPW antenna and slot antenna configurations and their design algorithms.

In this paper we will show a practical method for bandwidth improvement of slot antennas. Several new CPW fed slot antenna structures are proposed and investigated using method of moments (MOM) and finite difference and time domain (FDTD) method. Prototype antennas will be fabricated and the return loss and radiation patterns will be measured to verify the modeled results.

B5-4
1500

RECENT DEVELOPMENTS IN THE CHARACTERIZATION OF REDUCED SURFACE WAVE MICROSTRIP ANTENNAS

Michael Amin Khayat* Jeffery T. Williams David R. Jackson
Stuart A. Long
Department of Electrical and Computer Engineering
University of Houston, Houston, TX 77204-4793

During the past few years a new class of microstrip patch antennas, known as Reduced Surface Wave (RSW) antennas, has been developed. These microstrip antennas produce only a small amount of surface wave radiation. In addition, if printed on electrically thin substrates, these antennas only weakly excite lateral waves. As a result, these antennas do not suffer from the deleterious effects of surface and lateral wave scattering or from the mutual coupling normally associated with the surface and lateral waves. These characteristics make the RSW antenna ideal for applications where the supporting substrate or ground plane of the antenna is small, in which case diffraction of the surface and lateral waves from the edges of the structure may be quite significant for conventional microstrip antennas. These RSW antennas also show promise for array applications, where the presence of surface and lateral waves produce significant mutual coupling and lead to scan blindness. To date, the most promising RSW design is the Shorted Annular Ring Reduced Surface Wave antenna (SAR-RSW), which is a conventional annular ring microstrip antenna with the inner boundary short-circuited to the conducting ground plane. The dimension of the outer radius is chosen to eliminate surface-wave excitation from the magnetic current of the dominant mode at the outer edge, while the inner radius is chosen to make the patch resonant at the design frequency. Most of the previous investigations of the SAR-RSW antenna concentrated on one particular design (called "design 2") that utilized the TM_{012} mode of the annular ring as the dominant mode (D. R. Jackson, J. T. Williams, A. K. Bhattacharyya, R. Smith, S. J. Buchheit, and S. A. Long, IEEE Trans. Antennas Propagat., 41, 1026-1037, Aug. 1993). Although good performance was obtained from this design, this design requires that the relative permittivity of the substrate be greater than approximately 8.4. Another design (called "design 1"), which is based on the TM_{011} mode, has not been thoroughly investigated. Design 1 does not have any permittivity restriction for the substrate material, and also has an inherently larger bandwidth than design 2.

In this presentation we will summarize our study of the design 1 SAR-RSW antenna. We will present numerical results from a theoretical analysis of this antenna, along with a complete set of experimental results. These results include input impedance, bandwidth, radiation patterns, and mutual coupling between a pair of SAR-RSW antenna elements. The results verify that extremely low surface-wave and lateral-wave excitation can be achieved with this design, resulting in negligible diffraction of the surface and lateral waves from the substrate edges and very small mutual coupling between elements.

B5-5
1540

PATCH ANTENNAS WITH EXTERNAL SUBSTRATE PERFORATION

J. S. Colburn Y. Rahmat-Samii*
Department of Electrical Engineering
University of California, Los Angeles
405 Hilgard Ave.
Los Angeles, CA 90095-1594

Patch antennas are useful in a very broad range of application due to their simplicity, in both operation and fabrication, conformability and integrability with planar circuitry. In order to reduce size and weight, compact microwave circuit designs are achieved by using high dielectric constant substrates, but patch antennas don't perform well on this type of material. Patch antennas suffer performance degradation due to strong surface wave excitation in high dielectric materials, which lowers efficiency, degrades far-field radiation patterns and increases coupling between elements in arrays. Also, high dielectric constant substrates reduce the bandwidth of the patch resonance.

One approach to overcome these drawbacks of patch antennas on high dielectric materials is to use micromaching techniques to remove a portion of the dielectric material from under the patch (Gauthier *et al.*, *IEEE Trans. on Antennas and Propagation*, pp. 1310–1314, Aug. 1997). Removing a portion of the material under patch, results in a lower effective dielectric constant thus reducing the degradations caused by high dielectric substrates. Although this approach does allow integration of the antenna directly on the monolithic microwave integrated circuit substrate, it does not allow one to take advantage of the high dielectic constant substrate to reduce the size of the patch. Also, fabrication is quite difficult.

The approach suggested in this paper is not to affect the dielectric region under the patch but to introduce an array of holes just outside the patch, which is termed external substrate perforation. By placing the holes outside the patch, the effective dielectric constant of the surrounding substrate can be lowered. The change in dielectric constant between under the patch and the rest of the substrate helps suppress surface wave.

In the research to be presented, the Finite-Difference Time-Domain (FDTD) technique was used to study external substrate perforation. Using this numerical method, a patch antenna was simulated on finite sized ground planes of two different substrate thicknesses, with and without external substrate perforation. The computations showed the directivity drop in the radiation pattern caused by substrate propagation was noticeably improved by introducing the substrate perforation external to the patch for the case of a patch antenna on a relative thick substrate without any loss of bandwidth.

B5-6
1600

TWO DIMENSIONAL PHASED ARRAY BEAMSTEERING VIA PERIMETER DETUNING OF COUPLED OSCILLATOR ARRAYS

R. J. Pogorzelski
Mail Stop 138-307
Jet Propulsion Laboratory
Calif. Institute of Technology
4800 Oak Grove Drive
Pasadena, CA 91109

Linear arrays of coupled electronic oscillators have been used in experiments designed to control the aperture phase of a one dimensional phased array antenna. The linear phase progressions across the aperture necessary to produce steering of the beam may be induced by merely detuning the end oscillators in the array in an antisymmetric manner. [R. A. York, IEEE Trans., MTT-41, pp.1799-1809][P. Liao and R. A. York, IEEE Trans., MTT-41, pp. 1810-1815] A continuum model of the dynamics of such an array has been developed in which the aperture phase is governed by a second order partial differential equation of diffusion type. Solution of this equation yields considerable insight into the behavior of the array. [R. J. Pogorzelski, P. F. Maccarini, and R. A. York, IEEE AP-S Symposium Digest, Atlanta, GA, June 1998, pp. 462-465.]

The present work concerns extension of the continuum model to two dimensions. The resulting two dimensional diffusion equation is solved via the Laplace transform to yield an analysis of the dynamics of a two dimensional phased array controlled by a two dimensional array of coupled voltage controlled oscillators (VCOs). It is shown that the beam of the array can be steered in two dimensions by appropriate tuning of the oscillators on the perimeter of the array. This represents a considerable simplification of the beam steering electronics in that, for an M by N array, one need only control 2M+2N-4 oscillators as opposed to the usual MN. Moreover, no phase shifters are required. One need only control the voltages applied to the tuning ports of the perimeter oscillators. A convenient way to do this is to use a computer controlled digital to analog converter board which provides a programmable voltage for each of the oscillators on the perimeter. Computed examples illustrate the dynamic; i.e., time varying, behavior of the far field during the beam steering transient as predicted by the two dimensional continuum model.

B5-7
1620

INTRINSIC LOCALIZED MODES IN NONLINEAR PHOTONIC CRYSTAL WAVEGUIDES

A. R. McGurn*
Department of Physics
Western Michigan University
Kalamazoo, MI 49009

A discussion is given of the theory of intrinsic localized modes for nonlinear waveguide impurities in photonic crystals. A waveguide type impurity is formed in a photonic crystal by creating an infinite line of single site impurities in an otherwise perfect photonic crystal, and associated with the infinite line of impurities are a series of traveling wave impurity modes. Waveguide impurities can act as channels to conduct electromagnetic energy through photonic crystals just as optical fibers conduct electromagnetic energy through space. In our treatment we consider waveguide impurities which are formed of Kerr nonlinear media and are created in photonic crystals which are otherwise composed of linear optical media. The Kerr media allows for some of the modes associated with the waveguide impurities to become intrinsic localized modes (localizied in space) rather than extended propagating impurity wave modes. Conditions are determined for the existance of even- and odd-parity intrinsic localized modes and kink intrinsic localizied modes. A full solution is given for the electromagnetic fields associated with these different types of intrinsic localized modes. The theory is illustrated by an application to a photonic crystal formed from a square lattice array of dielectric rods. In addition, we study a two- dimensional array of Kerr impurities which are created in a two-dimensional photonic crystal which is otherwise composed of linear dielectric media. In this structure intrinsic localized modes are found with impurity mode frequencies in the stop bands of the photonic crystals. Results are present for the electromagnetic fields of these modes as well as for the necessary conditions for the existence of these intrinsic localized modes. These theories are readily generalizable to treat similar impurity structures in one- and three- dimensional photonic crystals.

B5-8
1640

MICROSTRIP AND STRIPLINE DESIGN FOR NOVEL STRUCTURES

Ian Rumsey* Todd Lammers Melinda Piket-May
Department of Electrical and Computer Engineering
Campus Box 425
University of Colorado
Boulder, CO 80309
P. Keith Kelly
Ball Aerospace and Technologies Corp.
P.O. Box 1538
Broomfield, CO 80038-1538

Understanding interconnect behavior in electronic packages is of critical importance to successful package level and system level design. Physical and electrical trade-offs can be understood and optimal performance can be achieved if the performance characteristics for various structures are studied before commitment to hardware. The application of Maxwell's equations within a finite-difference time-domain engine accounts for the structure's electrical behavior. The results presented in this paper will help determine the optimal physical parameters of a given system while staying within electrically and physically dictated thresholds that accompany a variety of case studies.

We will first present novel transmission line structures along with their performance characteristics. We will present a study of microstrips and striplines over meshed ground planes. There are a number of reasons a meshed ground plane may exist. Sometimes the structures are periodic and can exhibit photonic bandgap behavior, while at other times there simply needs to be a slot in the ground plane, again changing the performance of the line. (Piket-May et.al.,*APS/URSI Proceedings*, June, 1995, p260) We will be expanding on earlier work (Radisic et.al.,*IEEE Microwave and Guided Wave Letters*,**vol. 8**, Feb, 1998, pp.69-71) in the analysis of novel transmission line configurations.

It has been shown that microstrip photonic band gap (PBG) structures may be designed to minimize unwanted frequency propagation (Radisic et. al.,*URSI Proceedings*, Jan 7, 1998, p192),(Rumsey et.al., accepted to *IEEE Microwave and Guided Wave Letters*). We will present several configurations for using photonic band gap dielectrics in microstrip and stripline structures. We will compare these results to those obtained using a periodic meshed ground plane. Once again we will present a systematic study for a number of packaging and signal integrity specifications. Where possible, case studies using other numerical techniques as well as measured data will be used for verification.

CFGJ-1
1340

COMPENSATING REFLECTIVITY ESTIMATES BIASED BY GROUND CLUTTER FILTERS

Scott Ellis and Charles L. Frush
National Center for Atmospheric Research (NCAR)
Boulder, CO 80307-3000

Numerous studies have recently shown the usefulness of radar data for estimating rainfall rates and amounts. The presence of anomalous propagation (AP) ground clutter presents serious problems for radar precipitation estimation. The high reflectivity values of the ground echoes are misinterpreted as rainfall by reflectivity based estimation algorithms. Clutter filters are able to effectively cancel AP clutter in most situations. However, it is well known that clutter filters introduce a negative reflectivity bias in weather echoes near zero velocity. In order to alleviate the clutter without biasing reflectivity, several methods for identifying AP clutter have been developed, which will allow selective application of clutter filters based on the location of AP. In situations of mixed AP and weather it is impossible to avoid clutter filter reflectivity bias. It is desirable to correct for this bias. A simple Gaussian correction model (SGCM) was developed at NCAR for this purpose.

The SGCM uses the (filtered) Doppler velocity and spectrum width values to approximate the Doppler spectrum as a Gaussian distribution. Next, a filter designed to emulate the WSR-88D clutter filters is applied to the Gaussian approximation to obtain a filtered spectrum. The power is then estimated for both the filtered and unfiltered Gaussian spectra using classical moment calculations. Finally, the correction factor is computed as the ratio of the approximate unfiltered power to the approximate filtered power.

The SGCM has been tested on both simulated and real radar data. For the simulated data, the Doppler spectrum is approximated by a Gaussian distribution. For the tests with real data, we use archive I data recorded at the Memphis WSR-88D radar using NCAR's A1DA data recorder. In this case, auto-correlation calculations are performed on the in-phase and quadrature data to obtain estimates of the first three moments for both the filtered and unfiltered data. Next, the simple Gaussian correction model is used to obtain the corrected reflectivity. In this way, we are able to evaluate the original reflectivity, the filtered reflectivity and the compensated reflectivity. In the absence of clutter, we are able to quantitatively determine the severity of the bias introduced by the clutter filter, as well as the effectiveness of the SGCM to remove this bias. We can also evaluate the performance of the system on ground clutter targets. It should be noted that the uncertainty of reflectivity estimates in clutter mixed with weather near zero velocity is still high after compensation, however, removing the bias should yield significant improvements in precipitation estimation.

The modeling study suggests reflectivity may not be recoverable when using a high suppression filter at zero velocity. Using the low suppression filter seems to be a workable solution. At this time our archive I data results are very preliminary, and we are currently developing the ability to compute meaningful statistics for a quantitative analysis of the real data tests. Visually examining the data plots suggests that reflectivity bias from filtering clutter is reduced, but not completely removed, by the SGCM technique in regions free of ground clutter with velocity very close to zero. Further, in regions where the magnitude of the velocity is higher, but still small enough to be biased by the filter, the SGCM can actually over-estimate the reflectivity. Overall, the SGCM significantly reduces clutter filter bias, thus improving precipitation estimates.

CFGJ-2
1400

DETECTION OF ANOMALOUSLY-PROPAGATED GROUND CLUTTER USING FUZZY LOGIC

Cathy Kessinger, Scott Ellis and Joseph VanAndel
National Center for Atmospheric Research [1]
Boulder, CO 80307-3000

An algorithm to detect anomalously-propagated (AP) ground clutter contamination for the National Weather Service (NWS) Weather Surveillance Radar-88D (WSR-88D) system has been under development for several years. This work is being done with the cooperation of the WSR-88D Operational Support Facility (OSF) and the National Center for Atmospheric Research (NCAR). Detection of AP contamination will augment the detection of ground clutter from stationary targets (i.e., normally-propagated ground clutter) that is currently contained within the WSR-88D system. This augmentation is necessary since AP contamination varies depending on atmospheric conditions and, when present, adversely effects data quality. This algorithm is planned to be a pre-processor of the WSR-88D base data fields prior to input into the Precipitation Processing System (PPS), a hydrological analysis package that derives precipitation amounts from radar reflectivity return.

Using fuzzy logic techniques, an AP detection algorithm has been developed using multiple radar-derived input variables (R.J. Keeler, et al., *Preprints, 14th Int'l Conf. on Interactive Info. and Proc. Sys. for Meteor., Ocean. and Hydro.*, Amer. Meteor. Soc., 296-300, 1998). Other techniques were evaluated, but the fuzzy logic technique was selected due to the ease of implementation and the small differences in statistical performance when compared to the other two techniques. Piece-wise linear membership functions have been developed and optimized for each variable that is input into the fuzzy logic classifier. Input variables consist of the mean radial velocity, the mean spectrum width, the standard deviation of the radial velocity, the "texture" of the signal-to-noise ratio, and the difference in reflectivity values between the 0.5^{o} and the 1.5^{o} elevation angles. Texture is similar to the standard deviation of a field, and is a measure of the amount of change occurring over a specified region.

Selected cases from the WSR-88D archives have been input into the AP detection algorithm for evaluation. A human "expert" has defined the regions of AP contamination (i.e., the "truth" regions) by drawing polygons. These "truth" regions are used to statistically score algorithm performance. A total of 60 elevation angles have been truthed and used to evaluate the algorithm. Data from nine WSR-88D radars, located across the country, were used.

Results from the fuzzy logic classifier show that the AP detection algorithm has considerable skill in detecting AP contamination.

CFGJ-3 1420

NEXRAD AP CLUTTER RECOGNITION AND SUPPRESSION

R. Jeffrey Keeler, Cathy Kessinger, Scott Ellis, Joe VanAndel
National Center for Atmospheric Research
Atmospheric Technology Division/Research Applications Program
PO Box 3000
Boulder, CO 80307

NCAR has developed an automatic Anomalous Propagation (AP) ground clutter recognition and suppression scheme based on "fuzzy logic" for the WSR-88D. AP clutter is an unpredictable radar echo that contaminates precipitation measurements generating erroneous hydrology products and confounds operational application of the radar data. It is caused by changing propagation characteristics in the atmospheric boundary layer. In our algorithm AP clutter is first recognized using a robust "fuzzy" inference system, then suppressed with standard clutter filters automatically applied, and the biased radar reflectivities are compensated to yield accurate rainfall rates. As the AP clutter field changes, the filter processing adapts to accommodate.

We plan a phased two-stage implementation – first, in the evolution to the "Open Systems Radar Product Generator (RPG)" and later in the "Open Systems Radar Data Acquisition (RDA)" upgrade. We plan to generate a new "AP clutter" and "precip" product set that can be used within the Open RPG architecture in ~2001. The enhanced precipitation estimation algorithm (PPS) (and possibly air traffic control products) will make direct use of this AP product. Fuzzy logic membership functions based on WSR-88D base data will discriminate AP clutter from precipitation regions. The AP product can automatically control application of clutter filters by enhancement of the standard clutter map. Reflectivity compensation and clutter residue removal will be integral components of this automated processing. Additional RDA processing and access to both the filtered and unfiltered base data streams will allow a higher performance algorithm in the 2005-10 era. Beyond this date the advanced Open RDA processor system will allow Doppler spectral processing to combine new AP and precipitation recognition schemes with operational range velocity ambiguity mitigation techniques.

We describe scientific justification for improving the Nexrad precipitation estimation, the atmospheric conditions producing AP clutter, the signal processing employing "Sugeno-style" fuzzy logic processing to recognize both AP clutter and precipitation, and an implementation plan for Nexrad.

CFGJ-4
1440

REDUCTION OF RADAR RANGE AMBIGUITY: PERFORMANCE EVALUATION USING PHASE CODED TRANSMISSIONS ON A NEXRAD RADAR

Charles L. Frush and J. Daughenbaugh
National Center for Atmospheric Research (NCAR)
Boulder, CO 80307-3000

A search for better methods to reduce range and velocity ambiguity in NEXRAD (WSR-88D) radar data has resulted in the discovery by the National Severe Storms Laboratory in Norman, OK of a set of "optimal" systematic phase code sequences known as SZ codes. These sequences evolved from codes designed for communications applications having the property of zero cyclic autocorrelation for all lags except zero. (Chu, D. C., 1972: Polyphase codes with good periodic correlation properties. *IEEE Trans. On Information Theory*, vol. **IT-18**, 531-532.) The SZ codes are designed to be short, symmetrical, and periodic. These sequences split out-of-trip (or lag n) spectra into evenly spaced replicas of equal amplitude across the unambiguous frequency interval. This effectively whitens radar signal returns from trips that are not phase cohered. The principal aim of the SZ code is to allow retrieval of mean velocity estimates from weak spectra in one trip, when overlaid with strong signal returns from other trips. In many instances, spectrum width can be determined with little contamination from the competing echoes.

NCAR has equipped a testbed WSR-88D radar (KOUN) located in Norman, Oklahoma and the NCAR S-Pol 10cm radar located in Boulder, Colorado with the necessary hardware to transmit these SZ phase coded pulse sequences and to record the I and Q time series signal returns. A particularly useful sequence is the SZ (8/64) code, that minimizes the correlation of adjacent-trip return echoes, using a sequence that repeats every 32 hits. This code sequence splits the N+1 or N-1 trip echo into eight, evenly-spaced spectra, of equal amplitude over the radar unambiguous Nyquist interval. The desired Nth trip echo is "cohered" for normal Doppler processing, and is not whitened by the code after cohering.

This paper will describe tests of echo separation, using I and Q time series data collected with the two radars. The KOUN data include a squall line at long range that produces overlaid echoes at shorter ranges. Using the described separation technique, a good separation of 1st and 2nd-trip echoes is usually obtained. The measured separation routinely exceeds 30db, and often exceeds 40dB.

We will discuss performance of this technique using a variety of data containing first and second-trip echoes as input. Some of the data contain target signatures quite different from the theoretical data used to predict the performance of the SZ code. We will discuss algorithm considerations that help make the method more robust to these situations.

CFGJ-5
1500

PHASE CODING FOR RESOLUTION OF RANGE AMBIGUITIES IN DOPPLER WEATHER RADAR

D.S. Zrnic[1], M. Sachidananda[2], and R.J. Doviak[1]

(1) National Severe Storms Laboratory, USA
(2) Cooperative Institute for Mesoscale Meteorological Studies / University of Oklahoma, USA

Resolution of range and velocity ambiguities has been a long standing problem in pulsed Doppler weather radars. To have a large unambiguous range a long pulse repetition time (PRT) is needed which opposes the requirement for a sufficiently high unambiguous velocity. One compromise solution allows some ambiguities in both velocity and range. The velocity ambiguities can then be sorted by considering the continuity of the fields. But, to recover velocities in presence of overlaid echoes in range, some type of transmitter signal coding is required. Random and systematic phase codes have been proposed. A new systematic phase code and an algorithm for estimating the mean velocities of 1st and 2nd trip signals when they are overlaid, is presented in this paper. The transmitted pulses are phase shifted in this code sequence to modify the spectrum of the overlaid signals. The return samples are phase corrected to cohere 1st or the 2nd trip signal leaving the other signal power spread in a deterministic manner across the spectrum. A new algorithm has been developed which enables one to recover the velocity of the weaker signal even if the overlaid power ratio is as large as 40 dB, for spectrum widths 4m/s or less and an unambiguous velocity of 32 m/s. Thus, the procedure to retrieve spectral moments of the weak signal involves spectral and time domain processing. It has been tested on simulated weather signals, and the test results indicate that the method can be employed in a Doppler radar to effectively double the unambiguous range without sacrifice of the unambiguous velocity interval.

CFGJ-6 1540

ENHANCEMENTS IN SIGNAL PROCESSING FOR THE NEXT GENERATION OF RADAR WIND PROFILERS

Timothy L. Wilfong[1], David A. Merritt[2], Richard A. Lataitis[2], Madison J. Post[2], and Bob L. Weber[2]

[1]Science and Technology Corporation at the NOAA Environmental Technology Laboratory 325 Broadway; Boulder, CO 80303 USA

[2]NOAA Environmental Technology Laboratory 325 Broadway; Boulder, CO 80303 USA

Over a decade of experience with a variety of UHF and VHF Doppler wind profilers is available for judging their performance. The technology has proven to be of notable value to numerous operations including severe weather forecasting, numerical modeling, pollution monitoring and space launch support. Individual profilers or networks of profilers can provide continuous measurements, economically and automatically, with high time resolution and high spatial resolution, which are necessary for the observation of many important synoptic scale, mesoscale, and smaller scale phenomena. In recent years, however, improvements in the reliability and the accuracy of meteorological products derived from profiler measurements have reached a plateau short of the needs of many operational users. Continued integration of wind profiling technology into operations and research requires continued improvement in the reliability and accuracy of the derived meteorological products. In particular, extracting measurements of meteorological quantities in the presence of interfering signals and quantifying the error in the measurements introduced by lack of homogeneity and other limiting meteorological conditions must be addressed.

While quite useful, winds measured by wind profilers (and virtual temperatures measured using an additional sound source) are only part of the information required for many studies of the atmosphere. Air pollution or dispersion models may require velocity variances, momentum and scalar fluxes, and convective mixed-layer depth. With improved on-line signal processing, it is possible to monitor atmospheric turbulence parameters and reflectivity gradients in real time; however, many of the same problems that affect the performance of profilers for wind profiling also pertain to turbulence applications, because both make use of the moments generated from the Doppler spectrum.

The advent of powerful, inexpensive digital computers has enabled significant improvements in real time signal processing for wind profilers. An advanced data acquisition and signal processing system is being developed and tested at the NOAA Environmental Technology Laboratory. Five major steps are implemented as well defined modules: (1) enhanced data acquisition and time domain filtering, (2) adaptable spectral filtering including both band-pass and in-band filtering, (3) detection of multiple signals and robust moment estimation, (4) identification of the atmospheric signals using pattern recognition and simple models, and (5) generation of meteorological products using robust interpolation to a time/height grid. In addition to being field deployable, the system is also designed to facilitate algorithm development and assessment. The current system will be discussed concentrating on the details of underlying algorithms. Comparisons showing the results of conventional and enhanced processing applied to both real and simulated data will be presented.

CFGJ-7
1600

WEATHER RADAR MEASUREMENTS OF DOPPLER SHIFT

R. G. Strauch* R. G. Frehlich
CIRES
University of Colorado
Boulder, CO 80309

Atmospheric LIDAR and SODAR systems measure the radial velocity of the scatterers by measuring the Doppler shift of the backscattered radiation. However, 'Doppler' weather radars do not measure Doppler shifts; they measure the radial velocity of the scatterers by measuring the pulse-to-pulse change in the amplitude and phase of the backscattered signal, a measure of the pulse-to-pulse change in the two-way rf path to the scatterers. The reason for this difference in the way the velocity is measured is that the echo coherence time for radar exceeds the time between pulses while LIDAR or SODAR echo coherence time does not. A simple example shows that the radial velocity measured by a 'Doppler' weather radar has nothing whatever to do with the Doppler shift of the backscattered radiation. This fundamental difference in the way that a LIDAR or SODAR measures velocity and the way that a weather radar measures velocity leads to the troublesome range-velocity ambiguity in weather radar while LIDAR and SODAR have a range resolution-velocity resolution limitation not found in weather radar data. It is possible to obtain a measurement of the Doppler shift with a weather radar, albeit a measurement with a very large expected velocity error even when the signal-to-noise ratio is very high. Averaging of the Doppler measurements in range and time reduces the velocity error to values that may be useful for special applications. This presentation discusses the differences in LIDAR or SODAR and radar velocity measurements and the possible use of weather radar measurement of Doppler shifts.

CFGJ-8
1620

MAXIMUM LIKELIHOOD ESTIMATORS FOR DOPPLER RADAR AND LIDAR

Rod Frehlich
CIRES Campus Box 216
University of Colorado
Boulder, CO 80309

The maximum likelihood (ML) estimator of unknown parameters Θ is the value of these parameters that maximize the likelihood function of the data. This estimator is one of the most attractive choices for paramter estimation because it is asymptotically efficient, i.e., in the limit of a large number of samples the bias approaches zero and the standard deviation approaches the theoretical minimum predicted by the Cramer Rao lower bound. However, the functional form of the likelihood function must be known a priori and when many parameters are unknown, the numerical effort is large. For many estimation problems in Doppler radar and lidar, these limitations are not severe and the ML estimator has the best performance. The performance of an estimator is described by it's bias and standard deviation.

Data from Doppler radar and lidar is well approximated as a zero-mean Gaussian random process. The joint probability density function and therefore the likelihood function are described by the covariance matrix of the data. Generally, there are three unknown parameters: the mean radial velocity v, the signal power (signal to noise ratio SNR), and the spectral width w or equivalently, the correlation time of the signal. Data from solid-state Doppler lidar is typically described by two parameters: the radial velocity v and the SNR. This is the case for space-based Doppler lidar measurements and the results can also be applied to Doppler radar operating in lidar processing mode for polarimetric measurements of differential phase and differential reflectivety. The performance of the ML estimator is presented and compared with the theoretical limit of the Cramer Rao bound and with the performance of the ML estimator when signal power and spectral width are known a priori. The performance of the ML estimates for mean velocity are insensitive to knowledge of the spectral width. The ML estimator for signal power has a smaller standard deviation than traditional estimators but also a small bias.

The ML estimator for signal power has a simple form in the limit of infinite SNR and a priori knowledge of spectral width and mean velocity. However, very large SNR is required for this limiting case because the smallest eigenvalues of the covariance matrix are affected by extremely little additive receiver noise.

CFGJ-9
1640

DOPPLER RESISTANT WAVEFORMS FOR SPACEBORNE IMAGING RADAR

D. M. Haines* B. W. Reinisch K. Bibl G. P. Cheney
UMASS Lowell Center for Atmospheric Research
600 Suffolk St, 3rd Floor
Lowell, MA 01854

Remote Sensing from space, or in space, is made more difficult by the high speed of the space vehicle, which may cause a large Doppler shift of the echo signals. The rapidly changing signal phase complicates the task of coherent signal processing, and since only coherent signals can be detected under conditions of negative signal-to-noise ratio, it is of great interest to design signals which do not lose their coherent properties under conditions of high Doppler shifts. The paper presents methods for determining the coherence intervals (spatial and temporal), as well as deriving the limits of range and Doppler ambiguity values. It then moves on to describe two waveforms which allow a maximum signal processing gain while resolving the Doppler frequencies without ambiguity up to very high velocities.

The two waveforms described are FM Chirp pulses, and what we call a Staggered Pulse sequence, which is also known as a Minimum Redundancy sequence. This name differentiates the new sequences from previous practice, in that they are much longer than previously reported designs. The Chirp pulses are very resistant to high Doppler shifts, but will eventually produce a range error when the Doppler shift is a significant percentage of the signal bandwidth. However, a pulse stream of Doppler shifted Chirp pulses can be integrated with significant advantage over a period approaching the coherence interval as defined by the medium.

While these techniques apply to any high Doppler environment we will illustrate their implementation in the Radio Plasma Imager, or RPI instrument to be flown on NASA's IMAGE satellite. IMAGE is NASA's first Medium-size Explorer mission for the year 2000, to be launched in January 2000.

CFGJ-10
1700

SIGNAL PROCESSING IMPLEMENTATION FOR A DIGITAL-BEAMFORMING PHASED ARRAY RADAR

J. Li* J. Eshbaugh S.J. Frasier
Department of Electrical and Computer Engineering
Box 34410
University of Massachusetts
Amherst, MA 01003-4410

A second-generation Focused Phased Array Imaging Radar, FOPAIR-II, has been developed at the University of Massachusetts for high-resolution, high-speed imaging of the ocean surface at X-band. Using direct digital chirp synthesis combined with a digital receiver and DSP, the new instrument improves on the design of it's predecessor (R.E. McIntosh et al., *IEEE Trans. Geosci. & Rem. Sensing*, **33(1)**, 115-124, 1995). The primary improvement achieved with the new system is variable range resolution: as coarse as 10 m and as fine as 40 cm. Coarse resolutions support large area mapping applications (e.g. surface current mapping, air-sea interaction studies) while the finest resolutions support detailed investigation of microwave scattering mechanisms from real ocean surfaces. This paper outlines the signal processing implementation used for calibration and imaging with FOPAIR-II and presents sample measurements with the new system.

The radar consists of a linear-FM chirp transmitter, a 128-element receiving antenna array, and a stretch-processor receiver that mixes radar echoes with a delayed replica of the transmitted waveform. The stretch-processor is a hybrid of conventional chirp radar and FM-CW radar. The mixing process converts, or deramps, chirp echoes into constant-frequency sinusoids whose frequency indicates range. A high-speed A/D converter samples the deramped echoes at IF, and a digital in-phase and quadrature receiver is implemented through bandpass sampling and FIR digital filtering. Following the receiver, a pair of vector signal processors based on the Sharp LH9124 (Butterfly DSP) chip implement range compression, near-field focusing, and azimuthal beamforming for all the array elements. The Butterfly DSP is a block-floating-point processor optimized for FFT operations. Each vector signal processor includes high-speed FIFO memories and a TI'C40 DSP chip that manages the LH9124s. Following beamforming, a pulse-pair algorithm computes images of the first two moments of the Doppler spectrum at each pixel. Resulting images of received power and mean Doppler velocity are then streamed through a third 'C40 DSP board that interfaces with a fast-wide SCSI adaptor to 8mm tape or to disk. Typical image sizes are 64x64 or 128x128 pixels, and the system is capable of capturing radar images at rates over 80 frames/second.

CFGJ-11
1720

A NEW DATA ACQUISITION CONCEPT FOR DIGITAL IONOSONDES: PHASE-BASED ECHO RECOGNITION AND REAL-TIME PARAMETERIZATION

J. W. Wright
Svavelgatan 6
S-59338 Vastervik, Sweden
F. T. Berkey*
CASS, Utah State University
Logan Utah, 84322-4405

The problem of identifying echoes in digital ionosonde observations is discussed starting with an off-line simulation of the procedure long used in real time by the Dynasonde. In that method, echoes are defined as amplitude-modulus peaks from rapid (10 microsecond) sampling of receiver quadrature outputs; coincidence of peak time among a small number of repeated pulses (4 to 8) has served well to reject impulsive noise, while identifying the time sample of the complex-amplitudes to be retained for off-line analyses. Early work (J. W. Wright and M. L. V. Pitteway, *Radio Science*, **14**, 815-825, 1979) showed that the probability of accepting a noise impulse falsely as an "echo" by this method was typically less than 1/1000.

This paper presents a new method dependent on all of the signal phase information contained in the same rapid sampling. No change is made in basic sounding function, but conversion to physical parameters is done first, for all 10 microsecond samples. The consistency of these parameters in 5 dimensions over at least 4 samples defines "an echo", or at least a partial "glint". There is no surviving requirement that distinct echo "peaks" of amplitude modulus be present. Because of the over-determined nature of the phase analysis, error parameters are available to characterize 'wavefront curvatures' and other consequences of overlapping glint interference.

In an example recording, the new method recognizes about 60and glints than the earlier method, giving better trace continuity. Measurement resolution among proximate echoing regions is improved. Weighted means of the physical parameters within their defining samples yields better accuracy; almost incidentally, these will be available immediately in a real-time implementation of the method. For research ionosondes in particular, these improvements will contribute to studies of kilometer-scale plasma irregularities and of radiowave scattering processes. For monitoring ionosondes they should at least permit obtaining more ionospheric information with less sounding activity and consequent RFI.

CFGJ-12 1740 **DETECTING METEORS AND SPACE DEBRIS USING ACOUSTICS: SIGNAL PROCESSING TECHNIQUES AND OPPORTUNITIES FOR COMPARISONS WITH OTHER REMOTE SENSING APPROACHES**

Alfred J. Bedard Jr.
National Oceanic and Atmospheric Administration
Environmental Technology Laboratory
Mail Code R/E/ET4
325 Broadway
Boulder, CO 80303

Atmospheric infrasonic signals detected from meteors, space debris, and space shuttle re-entries provide information valuable for comparison with optical, radar, and satellite systems. The low-frequency acoustic signals can travel for great distances (1000's of kilometers), are not obstructed by clouds or weather, and may have the potential to provide information on location, trajectory, height, and ablation rates (A.J.Bedard Jr and R. Bloemker, *Proc. SPIE*,3116, 177-191,1997). A review of potential uses emphasizes opportunities for comparisons with other remote sensing methods. An overview of the acoustic data processing techniques applied also defines the system capabilities. Based upon phased array processing, such quantities as correlation coefficient, signal bearing, elevation angle, and dominant frequency are obtained (F.Einaudi, A.J.Bedard Jr, and J.J.Finnigan, *J. Atmos.Sci.*,46,303-329, 1989). A variety of weighting techniques are applied to enhance detection of different classes of signals and various geophysical sources can be identified from their acoustic signatures alone. The potential uses of infrasonic systems for the detection, identification, and study of meteors and space debris include: monitoring the number and trajectories of objects, identifying the type of atmospheric interaction occurring (e.g. shock wave or explosive interaction), possibly infer object size and type, and possibly provide a tool for studying meteor ablation rates. A review of key observations will provide examples of the various types of detections, as well as highlight some aspects of acoustic meteor detection that are not understood. For example, although traveling at high Mach numbers some meteors seem to radiate sound isotropically for the length of their paths.

F5-1
1420

COMPARISON OF MUSIC DIRECTION FINDING AND BEAM FORMATION FOR HF MULTIFREQUENCY RADAR

C. C. Teague*
STAR Laboratory, Stanford University
Stanford, CA 94305
K. E. Laws
Dept. of Physics, Univ. of California
Santa Cruz, CA 95064

The University of Michigan/ERIM/Stanford Multifrequency Coastal Radar (MCR) was used along with two other high-frequency (HF) radar systems during the third Chesapeake Bay Outflow Plume Experiment (COPE-3) conducted during September–October 1997. The MCR measures ocean surface currents by delay-Doppler processing of first-order Bragg-resonant ocean-wave backscatter signals received from different locations on the ocean surface. Multiple radar operating frequencies are used to estimate the vertical current shear over the top two meters of the ocean surface. A narrow pulse provides range resolution. Angular resolution is provided by the receive antenna composed of a linear array of eight wideband loop antennas equally spaced one-half wavelength apart at the highest operating frequency (21.8 MHz). While this provides optimum performance at the highest frequency, the resulting 48 m aperture limits the angular resolution using conventional beam formation at lower frequencies (4.8, 6.8 and 13.4 MHz). As an alternative to beam formation, the Multiple Signal Characterization (MUSIC) direction-finding algorithm of R. O. Schmidt (*IEEE Trans. Antennas & Prop.*, **AP-34**, 276–280, 1986) can be applied to the ocean echoes.

The antenna system was calibrated by processing the signals returned by a low-power transponder carried on a small boat about 1 km from the antenna. After an average set of phase corrections was calculated, subsequent processing of the transponder signals using MUSIC direction finding indicated bearing errors on the order of 5° or less.

Ocean current estimates were made using both beam formation and MUSIC direction finding, and the current vectors were resolved into eastward and northward components. Typically the time-varying current values over a period of several weeks were larger when using MUSIC than when using beam formation, particularly in the northward (along-shore) direction, and narrow features in the current patterns were better resolved using MUSIC. However, simulations of various current patterns indicate that RMS errors between radar measurements and simulation inputs sometimes are lower using beam formation, particularly in the case of current patterns which have slow azimuthal variation and for which beam formation effectively averages over more samples to smooth out noise in the measurements. Conversely, the simulation results also indicate that the RMS errors using MUSIC are lower for current patterns which have narrow azimuthal features, such as coastal current jets.

F5-2
1440 EMMISIVITY OF RANDOM DIELECTRIC ROUGH SURFACES: A COMPARISON BETWEEN THE SECOND ORDER SMALL PERTURBATION METHOD AND THREE-DIMENSIONAL MONTE-CARLO SIMULATIONS

Q. Li, L. Tsang, C.H. Chan, K. Pak (Univ. of Washington)

F5-3
1500

AN IMPEDANCE BOUNDARY CONDITION AND WIDE-ANGLE PIECEWISE-LINEAR SHIFT MAP FOR THE EM PARABOLIC WAVE EQUATION

D. J. Donohue* J. R. Kuttler
Applied Physics Laboratory
Johns Hopkins Road
Laurel, MD 20723

The parabolic wave equation (PWE) has been widely used to model the propagation of radar at low grazing angle over ocean and terrain. However, until recently only approximate methods existed to model the effect of a rough boundary. For example, within the Fourier/split-step solution method, one approach, called terrain masking, models the terrain by a series of knife-edge diffractors. A more rigorous approach based on a transformation of the coordinate system and PWE was introduced in 1979 by Beilis and Tappert (*J. Acoust. Soc. Am.*, **66**, 811-826, 1979). This approach, which involves locally flattening the boundary at each range step, is now extended to the more general rough boundary. A self-consistent wide angle form of the PWE is derived to accommodate larger terrain slopes, and a new polarization-dependent impedance boundary condition is developed for finitely conducting terrain. The new impedance boundary condition and an improved shift map for piecewise linear surfaces allow the PWE to be marched in range using the previously-developed mixed Fourier transform (Kuttler and Dockery, *Radio Science*, **26**, 381-393, 1991).

In this presentation, calculations based on the extended method are compared with exact analytical solutions for selected benchmark problems. For example, the numerical solution is compared with an exact analytical calculation of point source radiation reflecting from a tilted flat plane. The application of the method to discretely sampled terrain is also demonstrated by making use of the piecewise linear shift map. The extended method is found to be a considerable improvement over existing approximations including terrain masking, image methods, and conformal mapping. However, the solution is also found to be incomplete and several sources of error are identified. The principal limitations are in the maximum slope or slope change of the piecwise linear surface. These errors, and suggestions for an improved model, will be discussed.

F5-4
1540

A COMPARISON BETWEEN MODELLED SIGNATURES OF AN ESTUARY FRONT

S. R. Chubb* A. L. Cooper
Remote Sensing Division
Code 7252
Washington, DC 20375-5351
G. M. Nedlin
Department of Physics
Worcester Polytechnic Institute
100 Institute Road
Worcester, MA 01609-2280

Considerable progress has been made in full-spectral modelling of radar signatures of fronts. Specifically, Jansen et al (*J Geophys Res*, **103**, 18723-18743, 1998) and Chubb et al (*Trans Geos and Rem Sen, in press*, 1998) have quantitatively modelled radar signatures of Gulf Stream fronts, but only by including wave-breaking (WB) effects in an approximate manner. However, these studies used the composite scattering (CS) model at a frequency (X-band), where simulations of internal waves previously have indicated that this model may be deficient (Lyzenga, D.R. and J.W. Bennett, *J Geophys Res*, **93**, 12345-12354, 1988). For this reason, questions have remained concerning the importance of WB effects in the studies by Jansen et al and Chubb et al. Also, the CS model is limited to intermediate incident angles. These factors have provided the motivation for the present study. Here, we compare simulations of radar signatures from a front using three different radar models, applied to the common wave spectrum that results from a full-spectral treatment of wave-current interaction. These simulations have been carried out with and without incorporation of WB effects. The comparison involves: 1.) the CS model, 2.) the model due to Holliday (D. Holliday, *IEEE Trans. Ant. Prop.*, **Vol. AP-35**, 120-122 (1987)) and Thompson (D. R. Thompson et al, *J. Geophys. Res.*, **96**, 4947-4955, 1991), and 3.) a new model that extends this last model to the case involving a finite dielectric constant appropriate for water. These models are used to simulate a prominent radar signature of the buoyant plume associated with the efflux of fresh water from the Chesapeake Bay that was observed in X-band imagery during the COPE-2 experiment (M.A. Sletten, G.O. Marmorino, T.F. Donato, *IGARSS'98*, **IV**, 2198-2200, 1998).

F5-5
1600

USE OF TWO SCALE MODELS IN ROUGH SURFACE SCATTERING

Ezekiel Bahar and Paul Crittenden
Electrical Engineering Department
University of Nebraska-Lincoln
Lincoln, NE 68588-0511

It is well known that both familiar theories (physical optics and small perturbation) associated with scattering from random rough surface are restricted to surfaces that are characterized by a limited range of mean square heights, mean square slopes and/or correlation lengths. In an attempt to derive solutions to the problems of electromagnetic scattering that were valid over a broader range of rough surface parameters Wright and Valenzuela were amongst the first to introduce a hybrid physical optics-perturbation solution based on a two scale model of the rough surface. Thus the rough surface was viewed as a filtered large scale surface (exhibiting all the characteristics of specular point scattering predicted by physical optics) upon which a small scale (perturbed) surface is superimposed. Since the small scale surface was subject to the small perturbation restriction; namely $\beta = 4k_o^2\langle h^2 \rangle << 1$ (where k_o is the free space wavenumber and $\langle h^2 \rangle$ is the mean square height) there was little flexibility in the choice of the wavenumber k_d at which spectral splitting of the rough surface was assumed to occur. Moreover Brown had shown that even with this limited choice of the Raleigh roughness parameter β, the values for the radar scatter cross sections depended critically upon the choice of the spatial wavenumber k_d.

The purpose of this paper is to examine the manor in which the spectral splitting can be performed on adopting the two scale model, such that the evaluation of the cross sections remain stationary over a wide range of the parameter k_d. The fully polarimetric full wave solutions, which unlike the small perturbation solutions are not restricted to surfaces with small Raleigh roughness parameters, are used in the analysis.

F5-6
1620

ELECTROMAGNETIC SCATTERING FROM CONDUCTING OBJECTS ABOVE A RANDOMLY ROUGH SURFACE

Y. Zhang* Y . E. Yang H. Braunisch J. A. Kong
Research Laboratory of Electronics and Department of EECS
Massachusetts Institute of Technology
Cambridge, MA 02139

Although extensive literature exists on EM scattering from discrete objects as well as randomly rough surfaces, little has been reported on the interaction of electromagnetic waves between discrete objects and rough surfaces. Standard numerical algorithms can be applied to the complete environment of discrete objects with rough surface, yet it would be difficult to separate individual scattering mechanisms from the total return. Furthermore, discretization over the rough surface can greatly increase the computational resource requirement compared to the problem with discrete objects only, especially when the object surfaces are small to the illuminated area of the rough surface.

This paper presents a hybrid SPM (Small Perturbation Method) /MoM (Method of Moments) solution that requires a smaller number of unknowns in the matrix equations. As in the SPM formulation, we expand the Green's function and field quantities in terms of the surface height function on the mean surface, followed by decomposing the electric integral equations, which are based on the extinction theorem and the surface boundary conditions, into different orders. It was found that higher order equations are of the same form as the zeroth order with equivalent source terms that can be evaluated by integration on the mean surface using lower order solutions. Therefore we only have to develop the solution algorithm for the zeroth order equations with arbitrary incident field. Because the zeroth order equations are identical to the ones with objects above a flat interface, the solution algorithm can be simplified by introducing the dyadic Green's function for a half-space. This allows us to avoid solving for tangential fields on the rough surface and the mean surface as well, leaving only unknowns on the conducting objects. The separation of the solution into different orders also helps us identify the individual interaction terms between the object and the rough surface.

Several configurations have been studied using the hybrid technique to the first order and the standard MoM algorithm. The total returns show good agreement between the two methods, however the hybrid technique requires only a fraction of the CPU time. The speed-up is especially dramatic in Monte Carlo simulations. The impedance matrix in the hybrid technique can be used for all realizations. Only the equivalent source terms on the mean surface for the higher-order equations need to be re-evaluated. As a result, what may take several days with the standard MoM simulation can be done in a matter of hours with the hybrid technique.

Session H3, 1355-Thurs., ECCR1B40
WAVES AND ENGIZATION IN PLASMAS: MERGING OF SPACEBASED AND LABORATORY TECHNIQUES (II)
Chairpersons: G. Ganguli and W. Amatucci (Naval Research Laboratory)

H3-1
1400 LABORATORY STUDIES OF ION AND NEUTRAL DYNAMICS OF THE IONOSPHERE

A.Y. Wong, G. Rosenthal, R.F. Wuerker, P. Cheung, M. McFarland, N. Hicks, G. Howes, J. Pau and W. Huhn

HIPAS Observatory, Department of Physics and Astronomy, UCLA.

We are in the process of producing a laboratory plasma with similar charge and neutral density and composition as the natural ionosphere, complete with UV radiation, particulate and neutral circulation. This plasma allows us to investigate the physics of positive and negative ion plasmas and the coupling between charged particles and neutrals in the presence of neutral flows.

We will present experiments relevant to the lower ionosphere where ion-neutral collisions are high and the upper ionosphere where collisions are infrequent. We will show that wave processes are important at all altitudes. Secondly ion acoustic waves become less damped when collisions disrupt the Landau damping. Thirdly the motion of neutrals can be inferred by tracking the motion of ions when ion-neutral coupling is strong.

Special exciters will be used to couple to ion acoustic wave and neutral sound waves and detectors are developed to monitor both. The exchange of momentum between particles and waves will be investigated through the use of very sensitive detectors of impulses.

This paper will discuss the use of Laser Induced Fluorescence technique to monitor the motion of ions and neutrals. The use of lasers to produce plasmas in the ionosphere by laser-dust interactions will be described.

Research supported by ONR.

H3-2
1420

LABORATORY STUDIES OF THE EFFECT OF NEUTRAL GAS RELEASE ON SPACE VEHICLE CHARGING: ELECTRODE GEOMETRY EFFECTS ON MINIMUM BREAKDOWN POTENTIAL[1]

D.N. Walker* W.E. Amatucci R.F. Fernsler C.L. Siefring M.J. Keskinen
Plasma Physics Division, Naval Research Laboratory

The laboratory investigation we describe has the intent of investigating the feasibility of using neutral gas release to ameliorate the effects of spacecraft charging, whether produced naturally or artificially. The program began as a continuation of the SPEAR (Space Power Experiments Aboard Rockets) program which was sponsored by the Ballistic Missile Defense Organization (BMDO) in the late 1980's. The SPEAR III series of experiments were carried out both in a large chamber environment and in a rocket experiment in space. The current laboratory experimental series at NRL uses the pulsing electronics from the laboratory portion of that program and involves the release of neutral gas from a highly negatively charged aluminum cylinder. The original experimental arrangement consisted of the aluminum cylinder which holds a neutral gas release valve designed for millisec release times, a pressure regulated neutral gas reservoir, and nozzles with various mach numbers. After the cylinder is charged to high voltage, the neutral gas is released, inducing breakdown of the gas in the strong electric field about the cylinder. Collection of ions from the dense plasma near the cylinder, in addition to secondary electron emission, provide the return current required to ground the body. The experimental focus has been on determining the parameter combinations that most effectively ground the body and gaining an understanding of the physics of the discharge mechanism. We have recently completed an experimental series in which we vary the geometry and size of the release electrode to determine the effect on minimum breakdown potential. Theory based on a simple linear model of Townsend discharge will be presented. Various breakdown dependencies predicted by this model in comparison to experimental results will also be presented.

[1] Work supported by the Office of Naval Research

H3-3
1440

HIGH-VOLTAGE PULSE PROPAGATION ON ELECTRODYNAMIC-TETHER TRANSMISSION LINES

Sven G. Bilén* and Brian E. Gilchrist
Radiation Laboratory
Electrical Engineering and Computer Science Department
University of Michigan
Ann Arbor, MI 48109

This research characterizes the general propagation behavior of high-voltage electromagnetic pulses along electrodynamic tethers in the ionosphere. Electromagnetic pulses are produced along the tether-plasma system as it transitions from open- to closed-circuited states and as it is driven by radio-frequency voltage sources. These perturbations take a finite amount of time to propagate along the tether and, as they do so, they affect the surrounding ionospheric plasma. This interaction in turn affects the tether's transmission-line characteristics. The dynamic evolution of the sheath is examined as the pulse front travels past a given section of tether and disturbs the local sheath.

Present tether transmission-line models assume, as a first-order approximation, that the plasma-sheathed tether can be modeled as a simple rigid coaxial transmission line. This has proven acceptable for tethers with low induced or driven voltages. An improved model is needed, however, when steady-state plasma-sheath dynamics cannot be assumed, such as for longer deployed tether lengths, which have higher induced *emf*, or higher driven voltages.

A dynamic circuit model of the plasma-sheathed tether is developed with knowledge gained from theoretical analyses, experimental results, and particle-in-cell simulations. Using this dynamic-sheath model as their basis, lumped-element transmission-line parameters for capacitance and inductance per unit length are derived for the plasma-immersed tether where it was found that capacitance is a function of voltage but inductance is approximately constant. These parameters are included with per-unit-length resistance and induced-*emf* elements to form the complete lumped-parameter model. The tether circuit model is implemented in the SPICE circuit simulation program. This implementation allows examination of the tether's transmission-line characteristics as well as pulse propagation and morphology. Previously developed models of satellite and Orbiter interactions with the plasma based on Tethered Satellite System mission data (S. G. Bilén *et al.*, *Radio Science*, **30**, 1519-1535, 1995; S. G. Bilén *et al.*, *Journal of Spacecraft and Rockets*, **34**, 655-661, 1997) can be used with this circuit model as the endpoints of the complete electrodynamic-tether system.

H3-4
1500

SURVEY OF AKR FINE-STRUCTURE STRIATIONS OBSERVED BY THE POLAR PLASMA WAVE INSTRUMENT

J. D. Menietti, A. M. Persoon, J. S. Pickett, and
D. A. Gurnett
Physics & Astronomy, University of Iowa, Iowa City IA 52242; 319-335-1919; email: jdm@space.physics.uiowa.edu

Auroral kilometric radiation (AKR) has been observed by the plasma wave instrument on board Polar on almost every northern hemisphere pass. High-spectral resolution plots of the AKR obtained by the wideband receiver of the plasma wave instrument on board the spacecraft sometimes show discrete, negative-slope striations each extending over a period of several seconds. A preliminary survey of over 5000 spectrograms (each covering 48 seconds) indicates that the striations are seen in the northern hemisphere near apogee in a frequency range of 40 kHz $< f <$ 100 kHz. A few observations of the signatures have been made at higher frequency ($f <$ 200 kHz). If the wideband instrument is in the 90-kHz bandwidth mode, the occurrence frequency may exceed 50%. The frequency drift rates, R, are similar ranging from -9.0 kHz/sec $< R <$ -1.0 kHz/sec. The paucity of positive-slope features may be due to the location of the satellite at altitudes well above the AKR source region. Past studies have suggested these features may be due to AKR wave growth stimulated by the propagation of electromagnetic ion cyclotron waves travelling up (-R) or down (+R) the field line, through the source region. High-resolution waveform data from Polar shows the presence of solitary waves in the auroral region that may also be a source of these striations.

H3-5
1540

EVIDENCE THAT THE FINE STRUCTURE OF AURORAL KILOMETRIC RADIATION IS NOT INTRINSIC TO THE SOURCE MECHANISM

R. J. Strangeway*
Institute of Geophysics and Planetary Physics
University of California at Los Angeles
Los Angeles, CA 90095
P. L. Pritchett
Department of Physics
University of California at Los Angeles
Los Angeles, CA 90095
R. E. Ergun C. W. Carlson J. P. McFadden G. T. Delory
Space Sciences Laboratory
University of California
Berkeley, CA 94720

The Fast Auroral SnapshoT Explorer (FAST) has made detailed observations within the source region of Auroral Kilometric Radiation (AKR). FAST has demonstrated that the waves are generated below the cold electron gyro-frequency, and further that ionospheric and secondary electrons are almost completed excluded from the auroral cavity. In addition, the wave electric field is often polarized perpendicular to the ambient magnetic field, while the magnetic field is polarized parallel to the ambient field. This sense of polarization is consistent with X-mode waves propagating nearly perpendicularly with respect to the ambient field. These results confirm that AKR is generated by the cyclotron maser instability, but with the proviso that the wave dispersion is also modified by relativistic effects. This allows for wave generation by the precipitating and mirroring auroral electrons; a population whose free energy for wave instabilities is replenished by the parallel electric field.

FAST is also able to resolve the detailed structure of the waves within the source region. AKR is highly structured within the source region. On occasion AKR does show falling and rising tones, usually referred to as "fine structure." More typically, however, AKR within the source region tends to be bursty and packet-like. Inspection of the wave forms shows packets with a few ms duration, a result inconsistent with lasing through reflection within the cavity. The narrower tones cited as evidence of lasing are usually observed some distance away from the source region, indicating that narrow tones are a consequence of refraction, rather than intrinsic to the source.

H3-6
1600

LABORATORY STUDIES OF SPACE PLASMA MICROPHYSICS AT HIGH BETA

Earl E. Scime*
Department of Physics
Box 6315
West Virginia University
Morgantown, WV 26506

Anisotropic temperatures or asymmetric velocity distributions can drive electromagnetic instabilities in high beta space plasmas. Such microphysical instabilities can in turn modify the macroscopic properties of the plasma system by affecting the distribution of energy among the various components of the system, e.g., fields and particles. The Large Experiment on Instabilities and Anisotropies (LEIA) was constructed at West Virginia University in order to study high beta electromagnetic instabilities. Two instabilities of particular interest are electromagnetic ion temperature anisotropy (EMITA) driven instabilities and electron heat flux instabilities. Based on their theoretical properties, EMITA instabilities have been used to explain the observed correlation of ion temperature anisotropy and plasma beta in the terrestrial magnetosheath [Anderson et. al., *J. Geophys. Res. 99*, 5877 (1994)]. This relationship is believed to be a signature of plasma processes crucial to the equilibrium and dynamics of this boundary layer, across which solar energy is transferred to the Earth environment. Electron heat flux driven instabilities have been suggested as a possible explanation for the observed dissipation of electron heat flux in the expanding solar wind [Scime et al., *J. Geophys. Res., 99*, 23,401 (1994)]. We will present initial results from experiments in LEIA designed to excite ion temperature anisotropy driven instabilities. Ion temperature anisotropy profile measurements will be compared to the profiles of electrostatic and electromagnetic fluctuations as a function of plasma beta. Work supported by the National Science Foundation and the US Department of Energy.

*in collaboration with M. Balkey, R. Boivin, P. Keiter, J. Kline, A. Badeau Jr., and B. Inman

H3-7
1620

EXPERIMENTAL VERIFICATION OF SWEET-PARKER CHARACTERISTICS IN TWO-DIMENSIONAL MAGNETIC RECONNECTION

Hantao Ji, Masaaki Yamada, and Scott Hsu
Princeton Plasma Physics Laboratory
Princeton University
P.O. Box 451
Princeton, NJ 08543

Magnetic reconnection plays a crucial role in determining the topology of magnetic fields in solar flares, magnetospheric substorms, and relaxation processes in laboratory plasmas. The first quantitative model of magnetic reconnection was proposed by Sweet and Parker more than 40 years ago. A key element of this model is the existence of a rectangular "diffusion region" whose length is of macroscopic scale and whose width is determined by the Spitzer resistivity. Since then, however, the validity of the Sweet-Parker model has been questioned because its predicted reconnection rate is too slow to explain explosive solar flares. Instead, the attention has shifted to Petschek's model which predicted faster reconnection rates and is based on a much smaller diffusion region and standing shock waves. Nonetheless, the debates have continued since neither model has been verified or disproved in a real plasma. In MRX (Magnetic Reconnection Experiment) (M. Yamada, et al., *Phys. Rev. Lett., 78*, 3117, 1997, M. Yamada, et al., *Phys. Plasmas, 4*, 1936, 1997) the first quantitative tests of reconnection models have been carried out (H. Ji, et al., *Phys. Rev. Lett. 80*, 3256, 1998) in well-controlled MHD plasmas ($S = 10^2$-10^3, $L/\rho_i = 10^1$-10^2). Detailed structures and key plasma parameters of magnetic reconnection in two-dimensional geometry have been measured by extensive diagnostics in the case with no third magnetic field component (null-helicity). The shape of the diffusion region in MRX was observed to correspond to the Sweet-Parker model (a rectangular box) rather than the Petschek model (much smaller box with standing shock waves) in our experimental regimes. However, the measured width of this diffusion region is on the order of the ion gyro-radius ρ_i and the ion skin-depth c/ω_{pi}, much larger than values predicted by the Sweet-Parker model in the collisionless regime. This observation is consistent with the measured resistivity which is enhanced over the Spitzer value, possibly due to electric field fluctuations driven by microinstabilities. Using this measured effective resistivity, the observed reconnection rates can be well explained by a generalized Sweet-Parker model which also incorporates finite compressibility and downstream pressure. An attempt to extend this model to reconnection with a sizable third component (co-helicity) will be reported. Other recent highlights from MRX, including ion heating, fluctuation measurements, and magnetic helicity dissipation will also be presented.

INDEX

Backscatter – Vegetation, Targets